THE QUANTIFICATION OF RATES OF TOTAL SEDIMENT INFLUX TO LLYN GODDIONDUON, GWYNEDD.

Thesis submitted in accordance with the requirements of the University of Liverpool for the degree of Doctor in Philosophy, by

Jan Bloemendal (30/8/82)

THE QUANTIFICATION OF RATES OF TOTAL SEDIMENT INFLUX TO LLYN GODDIONDUON, GWYNEDD

J. BLOEMENDAL

ABSTRACT

(i) This study uses mineral magnetic parameters (e.g. magnetic susceptibility, saturation isothermal remanence and anhysteretic remanence) and lithostratigraphical description to correlate a suite of sediment cores sampled from a closely-meshed grid network covering the whole of a small upland lake basin in Gwynedd, North Wales.
(ii) The core correlations are used to define three horizons within the lake sediment deposits: (1) the Loch Lomond Stadial clay - early Flandrian clay-mud contact, at the base of the Post-glacial sediment sequence. (2) A peak in magnetic susceptibility which is identified as a concentration of paramagnetic iron and manganese which are tentatively assumed to have entered the lake basin in solution. (3) A peak in magnetic susceptibility and magnetic remanence in the uppermost sections of the cores which is identified as a concentration of ferrimagnetic material. The correlated horizons define three contiguous layers of sediment within the lake basin. Contour maps of the thicknesses of the sediment layers are constructed and used to estimate the volume of each layer.
(iii) Radiometric dating (C-14 and Cs-137) is used to estimate the ages of the boundaries of the sediment layers, thereby enabling rates of total sediment influx and sediment yield per unit area of the terrestrial part of the watershed to be obtained. Sediment yield estimates of 36 kg/ha/yr, 126 kg/ha/yr and 263-326 kg/ha/yr were obtained for the periods (representing the duration of the deposition times of the sediment layers) 10 400-800 bp; 800 bp-AD 1951 and AD 1951-1977, respectively.
(iv) Pollen analyses are used together with documented regional and local environmental history to provide a context for the evaluation of the estimated rates of sediment yield. During the majority of the 10 400-800 bp period the watershed is likely to have been occupied by relatively undisturbed deciduous woodland, and during the 800 bp-AD 1951 period by grazed and possibly burnt-over moorland. The sediment yield for the AD 1951-1977 period is ascribed predominantly to soil erosion resulting from a forest fire within the watershed in AD 1951. Comparison of the estimates of sediment yield with those obtained using conventional geomorphological techniques in watersheds under comparable forms of land-use suggests some accordance.
(v) The core correlations and sediment thickness contour maps depict the history of the spatial pattern of sediment accumulation within the lake basin. The lake basin appears to have infilled asymmetrically, with the focus of sediment accumulation having moved progressively northwards with time. Marked variations in rates of sediment accumulation over short distances (tens of metres) are also evident. In contrast to the results obtained from other lake basins, the currently deepest part of the lake basin is virtually devoid of sediment. The observed patterns of sediment accumulation are tentatively assumed to be a response to wind stress.

ERRATUM

The pages of this thesis are numbered from 1-187 and from 189-275.

There is no page 188.

LIST OF CONTENTS PAGE NO.

LIST OF TABLES PAGE NO.

LIST OF FIGURES PAGE NO.

PAGE NO.

PAGE NO.

LIST OF APPENDICES

ACKNOWLEDGEMENTS

I wish to express my sincere thanks to the following persons:- My supervisor Frank Oldfield for assistance and advice at all stages of the work; Tim Rummery, John Dearing, Alec and Jennifer Jackson, Roy Thompson, Norman Towler, Frank Oldfield, Sandra Higgitt, John Smith, Ann Baron, Ann Worsley, Margaret Wray and my father for help with field-work. John Smith for the XRF results; Rick Nelms for the diatom analyses; David Owen for invaluable computing assistance; Dominic Dickson for the Mössbauer spectroscopy results and Roy Thompson for assistance and advice regarding the magnetic measurements. Tim Rummery, Brian Arkell and Margaret Wray for proof-reading; Sandra Mather and Julie Isaacs for help with the diagrams; Ian Qualtrough and Chris Roberts for photographing the diagrams and Mary Main for typing the text.

Finally, I recall with pleasure the comradeship of Tim, John, Ann, Ann and Sandra over the last few years.

CHAPTER 1 INTRODUCTION

1.1 The problem of sediment flux

Human activity tends to increase the rate of sediment flux in ecosystems (Sears, 1956). Increasing the rate of sediment flux may have considerable economic and aesthetic repercussions in terms of the effects on both the source and recipient (both temporary and ultimate) of the transported materials. Erosion of sediment (together with adsorbed nutrients) may represent a serious drain on the nutrient reservoir of an ecosystem, with consequent implications in terms of biological productivity, if firstly the rate of nutrient loss exceeds the rate of input from atmospheric sources and weathering and secondly if capital inputs are not readily available to make up the loss, as in the context of agricultural systems in many underdeveloped countries (cf. Oldfield, 1975). In the developed world, estimates are available of the economic cost of soil erosion: in the U.S.A., for example, rural erosion and sediment problems amount to over $1 billion per annum (cited in Gregory and Walling, 1973). Since in many environments sediment flux is effected predominantly by flowing water, increases in flux rates may also be accompanied by problems such as altered depositional patterns in rivers, rapid loss of reservoir storage capacity and river and lake eutrophication (e.g. Strahler, 1956; Dendy, 1968; Likens, 1972).

1.2 Approaches to the quantification of sediment flux

Assessment and evaluation of the magnitude of human impact on rates of sediment flux require the accurate quantification of flux rates both in undisturbed and disturbed ecosystems. This kind of knowledge provides the basis for the prediction of the effects on sediment flux rates of various kinds of human land exploitation, and ultimately for the formulation of the most economic means of

implementing control measures. A substantial quantity of data relating to current rates of sediment flux is now available for the northern temperate zone - largely from substantially man-modified ecosystems but also from undisturbed woodland ecosystems. These data have been obtained principally by the application of two broad kinds of approach: continuous process monitoring and the determination of the volumes of sediment accumulated within reservoirs. These approaches are briefly described below.

Continuous process monitoring

Soil erosion rates have been measured more or less at the source using techniques such as erosion pins, field traps and volumetric determinations of channels (e.g. Imeson, 1971; Morgan, 1977). More usually, however, the mass of suspended sediment (and in some cases bedload and solutes) leaving a watershed has been measured and the results expressed in terms of sediment yield per unit area of the watershed per unit time. A watershed-based approach to the quantification of sediment flux has several advantages: for example, the watershed ecosystem concept as developed by Bormann and Likens and others (e.g. Likens and Bormann, 1974) is available to provide a conceptual basis for empirical studies of particulate (and solute) flux within inter-linked terrestrial and aquatic ecosystems. Also, watersheds are systems with boundary conditions suitable for systems analysis (Loucks, 1975), facilitating the use of systems modelling in order to aid the identification of control strategies for the improvement of environmental management technique (e.g. Scavia and Robertson, 1979). A disadvantage is that in large watersheds there are likely to be problems of local deposition and temporary storage of sediment (Trimble, 1977). The approach is exemplified by the Hubbard Brook ecosystem study, in which sediment and solute yield in small upland forested ecosystems have been monitored continuously since 1963

(Likens et al., 1977). In this case, the small size of the study watersheds has enabled the adoption of an experimental approach in which the response of the system in terms of the output of water, solutes and sediment to perturbations such as forest clearance has been studied (e.g. Bormann et al., 1968).

One of the principal drawbacks of the continuous monitoring approach is the problem of temporal representivity: the lifespan of most projects may be insufficient to identify accurately the long-term trends of sediment yield. For example in the case of the Hubbard Brook study, analysis of four years of data showed that 86% of the total particulate output was exported in only 1.6% of the total time, the magnitude of the output being highly correlated with individual storms (Bormann et al., 1974).

Reservoir accumulation studies

Rates of watershed sediment yield may also be obtained by estimating the volume of sediment accumulated within a reservoir and adjusting the result to allow for reservoir trapping efficiency and sediment density. A value for the average rate of sediment yield during the life of the reservoir is thereby obtained. This technique has been extensively applied in the U.S.A. (e.g. Megahan, 1975) and has the advantage of eliminating the problem of temporal representivity in continuous monitoring studies. However, it is impossible to use this approach for monitoring solute yield.

1.3 The use of lake basins to estimate sediment yield

The use of natural lake basins to estimate rates of watershed sediment yield represents a development of the reservoir accumulation technique. The history of many lakes spans the entire Post-glacial period and providing the sediment record can be dated, the potential exists for obtaining a continuous record of sediment yield covering the period (in the northern temperate zone) prior to significant

human influence and extending right up to the present day. The possibility of being able to relate current rates of sediment yield to 'natural' rates within the same watershed is extremely attractive, since such comparisons have usually had to be made by comparing 'disturbed' and 'wilderness' watersheds: watersheds that are completely uninfluenced by man are rare (and are becoming rarer); moreover, a large number of variables influences sediment yield (Leopold, 1956) and this kind of inter-comparison may be difficult. Two factors may operate to increase the value of a lake basin - based approach: firstly, a variety of palaeoecological techniques (e.g. Birks and Birks, 1980; Oldfield, 1977; 1981) may be used for palaeoenvironmental reconstruction in order to aid the interpretation of 'fossil' rates of sediment yield. Secondly, continuous monitoring studies may profitably be carried out within lake watersheds, enabling the results to be compared with, and used to aid the interpretation of 'fossil' rates of sediment yield obtained from the lake sediment record; Likens and Davis (1975) have already gone some way towards approaching this ideal.

Despite their advantages, lake basins have been used only infrequently for studies of sediment yield. This is largely the result of practical difficulties. Obtaining a continuous record of sediment yield from a lake basin requires firstly, a set of sediment cores sufficiently large to be representative of sediment accumulation throughout the basin and secondly, some means of establishing a series of synchronous horizons within the set. Given both requirements then the volume of sediment accumulated within the lake basin during known time intervals can be calculated and using estimates of sediment density (and assuming that all of the sediment has originated from without the lake basin) converted to sediment yield per unit watershed area per unit time. Detailed sediment isopach contour maps based on

lithostratigraphical core correlations have been constructed for several Swedish lakes (e.g. Digerfeldt, 1969; Bengtsson, 1975; Bengtsson and Persson, 1978) and could be used to obtain estimates of sediment yield. In the absence of synchronous visual stratigraphic markers then time-consuming and/or expensive techniques (such as microfossil analyses) are normally required to transfer a series of dates (e.g. radiocarbon) from a single master core to the rest of the cores in the set. This problem of core correlation has tended to limit the number of cores that has been used to estimate rates of sediment yield in lake watersheds. Likens and Davis (op. cit.) and Edwards and Rowntree (1980) have inferred relative changes in sediment yield from changes in sediment accumulation rates recorded in a single core from a lake basin; and it has been suggested (Lehman, 1975) that such data when obtained from lake basins of regular morphometry may be used in conjunction with theoretical models of sediment accumulation to obtain absolute estimates of sediment influx to the whole of a lake basin. However, such attempts are unconvincing because of the large number of unverifiable assumptions upon which they depend. In order to obtain estimates of sediment yield in small lake watersheds in Southern Michigan, Davis (1976) has successfully used pollen analyses and X-radiography to correlate relatively small core suites. However, in the absence of cheap and rapid methods of correlating large numbers of cores such attempts have been exceptional.

The recent application of mineral magnetic measurements to problems in environmental science has enabled considerable progress to be made in overcoming this problem. The relevant magnetic parameters are indicative of the quantity and types of magnetic minerals in samples and have the advantage of being easily and rapidly measured in comparison with conventional core correlation techniques: for example, magnetic susceptibility measurements (see section 1.8) may be performed on whole unextruded cores of sediment. These techniques also

have the advantage of being indicative of sediment source. This follows directly from the sensitivity of iron minerals to influences such as burning and cultivation and to more general pedological processes such as gleying. The action of such processes tends to produce variations in the type and concentration of magnetic minerals within different parts of the solum thereby potentially enabling the identification of lake sediment sources.

1.4 Nature of the present study

The aims of the present study are as follows:

i) To use magnetic measurements and other techniques to correlate sediment cores obtained from a closely-meshed grid network covering the whole of a small upland lake basin in North Wales.

ii) To use the core correlations to estimate total volumes of sediment accumulated within the lake basin.

iii) To obtain a chronology of sediment accumulation, thereby enabling rates of total sediment influx and sediment yield to be obtained.

iv) To interpret the changes in sediment yield, using standard methods of palaeoenvironmental reconstruction such as pollen analysis and by reference to the magnetic parameters themselves. It was hoped that the latter would aid the identification of lake sediment sources.

Two additional themes were of interest:

v) Following from (iv), to make a contribution to continuing efforts to interpret variations in the mineral magnetic properties of lake sediments. (See Chapter 7, section 7.2).

vi) To reconstruct the history of sediment accumulation within the whole of the lake basin. In view of the increasing use of lake sediments for the study of environmental change (see Oldfield, 1977) it is becoming increasingly important to ascertain the extent to which inferences derived from the study of the small

number of sediment cores commonly employed in such studies are valid for the sedimentary record contained within the whole of a lake basin.

Since the application of mineral magnetic measurements to environmental science is a relatively recent development, the remainder of this chapter describes the history of their use in this field, describes the principles of their interpretation and, since soils are important lake sediment sources, gives a brief account of soil magnetism.

1.5 Palaeomagnetism and mineral magnetism

Palaeomagnetism is the study of the history of the geomagnetic field as recorded in the permanent magnetization of rocks and sediments. Palaeomagnetic studies are based on the natural remanent magnetization (NRM) properties of samples and have been widely applied in such fields of study as sea-floor spreading, continental drift and the stratigraphy of marine and continental sequences (McElhinny, 1973; Thompson, 1974). As a result of the construction of geomagnetic secular variation master curves calibrated with observatory, archaeomagnetic and radiocarbon dates (Turner and Thompson, 1981) NRM measurements are being increasingly applied to the problem of the dating of lake sediment sequences (Oldfield, 1977; 1981).

The application of magnetic measurements to environmental science is a relatively new field of investigation, differing from palaeomagnetic studies by the emphasis it places on mineral magnetic, or non-naturally remanent and non-directional, properties. The main magnetic properties used have been induced in artificially-applied low and high strength magnetic fields. Thompson et al. (1980) give examples of environmental applications of mineral magnetic measurements to problems in geophysics, meterology, climatology, hydrology, limnology, oceanography, sedimentology, pedology and land-use studies.

Mineral magnetic measurements have been used for the magnetic fingerprinting of suspended stream sediments (Oldfield et al., 1979a), thereby enabling the identification of the sediment type, source areas and the relative contribution each area makes to the suspended load during a flood event (Walling et al., 1979). Stream bedload-tracing using natural material magnetically-enhanced artificially in ovens (Oldfield et al.,1981a) has been demonstrated by Rummery et al. (1979) and Arkell et al. (unpublished). They have shown that the technique may yield insight into the storage and delivery rates of stream

bedload, thereby making a significant contribution to studies in fluvial geomorphology and hydrology.

Dearing (1979) has demonstrated the application of mineral magnetic measurements to pedological and land-use studies in contrasting magnetic environments, while Oldfield and collaborators (Oldfield et al., 1978a; Oldfield et al., 1981b) have utilised the distinctive magnetic properties of industrial and domestic atmospheric particulates in order (i) to permit the volume of the post-1840 influx of magnetic particulates to ombrotrophic peat deposits to be determined; (ii) to identify the source areas of the particulates and (iii) to calculate the variations in the post-1840 atmospheric magnetic flux density.

Following the pioneering work of Radhakrishnamurty et al. (1968) in the field of marine sedimentology, stratigraphic variations in the mineral magnetic properties of marine sediment cores have been interpreted as reflecting variations in palaeocurrent intensity (Bloemendal, in press), glacial-interglacial climatic fluctuations and episodes of sediment diagenesis (Robinson, unpublished); while the potential of these techniques for continental shelf placer exploration has been demonstrated by Currie and Bornhold (unpublished).

Of principal concern for the present study, in lake watersheds mineral magnetic measurements have been used for multiple core correlation (e.g. Thompson et al., 1975; Dearing et al., in press) and for the establishment of sediment source - lake sediment linkages (Dearing, 1979). Their potential for lake sediment core correlation was first demonstrated in a study of cores from Lough Neagh, Northern Ireland, in which the synchroneity of maxima and minima in the concentration of magnetic minerals in cores with widely varying accumulation rates and separated by distances of up to 8 km was confirmed independently by comparison with the diatom biostratigraphy (Thompson et al., op. cit.). Subsequently, the synchroneity of variations in

the magnetic concentration of cores from several lakes has been demonstrated by reference to independent parameters: e.g. radiometric dating in Loch Frisa, Scotland, and Lac d' Annecy, France (Dearing, op. cit.) and palaeomagnetic declination and inclination in Llyn Geirionydd, Wales; Loch Lomond, Scotland, and Lake Windermere, England (Turner, 1979).

1.6 Principles of Magnetism

Diamagnetism and paramagnetism

The atoms of any substance possess an electronic structure in which electrons move in orbits about a central nucleus. Since electrons possess an electrical charge this motion constitutes an electrical current and results in each electron producing a magnetic moment. In addition, all electrons possess magnetic moments due to their spin. The atoms of many elements possess zero magnetic moment because the various orbital and spin components cancel out. However, when such atoms are placed in a magnetic field there is a rearrangement of the spin and orbital motions of their electrons resulting in a net magnetic moment in the opposite direction to the field. This type of behaviour is called diamagnetism and is exhibited for example by quartz, calcite, water and organic matter. When the atoms or molecules of a substance each have a magnetic moment, the application of a magnetic field causes each moment to align itself in the field direction. This type of behaviour is called paramagnetism and is exhibited for example by clay minerals, pyroxenes and amphiboles. Both the diamagnetic and paramagnetic effects are weak and disappear with the removal of the field. Figure 1.1 shows the variation of magnetization with the strength of an applied magnetic field for diamagnetic and paramagnetic substances.

Ferro-, ferri- and antiferromagnetism

Substances such as iron, cobalt and nickel exhibit strong magnetic effects called ferromagnetism. In this case, exchange forces between the valence electrons cause their spins to become aligned even in the absence of an applied magnetic field. Ferromagnets therefore exhibit spontaneous magnetization. Antiferromagnetic and ferrimagnetic substances exhibit somewhat similar behaviour but are characterised by

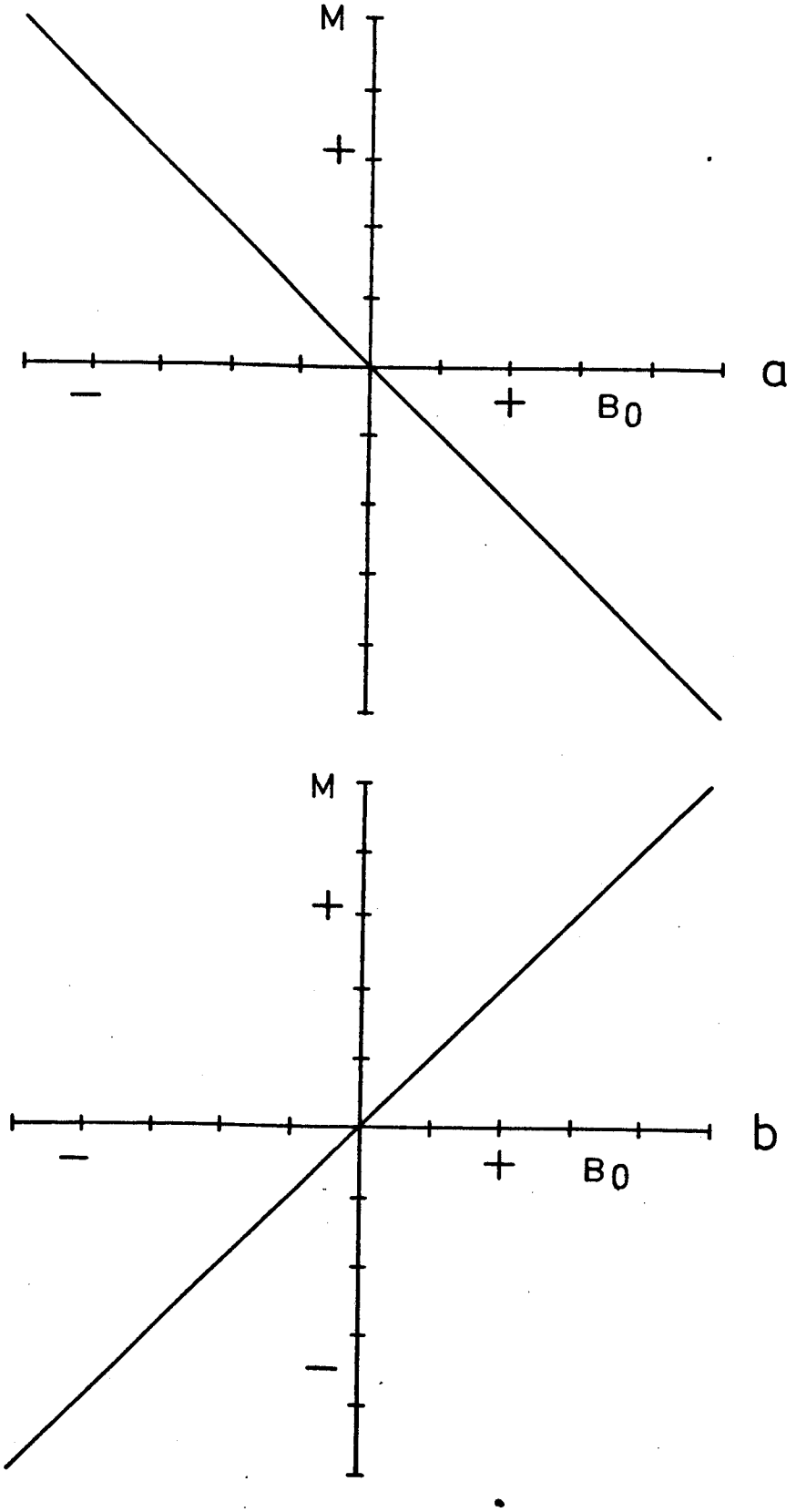

Figure 1.1 Variation of magnetization with the strength of an applied magnetic field for diamagnetic and paramagnetic substances

two crystal sublattices, A and B. In antiferromagnets the atomic moments of the A and B sublattices are aligned antiparallel to one another; the ferromagnetic effects cancel each other out and there is no net magnetic moment. If the atomic moments of the A and B sublattices are unequal then there is a net spontaneous magnetization known as ferrimagnetism. If the equal atomic moments in the two sublattices are not exactly antiparallel then the net spontaneous magnetization is known as canted antiferromagnetism. The common soil magnetic minerals magnetite and hematite exhibit ferrimagnetic and canted antiferromagnetic effects, respectively.

In the case of ferro-, ferri- and canted antiferromagnets as the temperature is increased, thermal agitation may destroy the magnetic alignment process and their magnetic behaviour reverts to paramagnetism. This occurs at a critical temperature for each substance, called the Curie point. The Curie points of magnetite and hematite are 580°C and 680°C, respectively.

Whether a substance exhibits ferro-, ferri- or antiferromagnetic behaviour depends upon its crystal structure. A cubic spinel structure as in magnetite consists of alternating layers of anions and cations but due to an imbalance of Fe^{2+} ions in the B lattice the crystal acts a ferrimagnet. In contrast, hematite and ilmenite have hexagonal, corundum-type crystal structures which allow a balance of Fe^{3+} ions to occur in both sublattices. In hematite the imperfect antiparallel alignment of the spin moments in the sublattices results in the crystal behaving as a canted antiferromagnet; in ilmenite the perfect antiparallelism results in antiferromagnetic behaviour (Stacey and Banerjee, 1974).

Domain theory

When the magnetization of a body gives rise to an external field (i.e. exhibits a remanent magnetization, or remanence) it

possesses a magnetostatic energy, or energy of self-demagnetization. This arises from the shape of the body, because it is more easily magnetized in some directions than in others. A long thin rod, for example, is preferentially magnetized along its length rather than across its width (McElhinny, 1973). Ferro-, ferri- and canted antiferromagnetic grains attempt to minimise their magnetostatic energy by subdividing into two or more regions which are magnetized in different directions. The regions are called magnetic domains and they are separated by domain walls through which there is a progressive rotation of atomic magnetic moments. Some magnetic grains are so small that they only possess a single domain; larger grains are multi-domained. Dunlop (1973) deduced that the single domain - multidomain boundary for equant magnetite grains lies between 0.035 and 0.05 μm. However, the value is greatly influenced by factors such as the presence of impurities and by grain shape: for example, the boundary rises with increasing grain elongation. In the case of hematite the boundary is much larger, ca. 0.15 cm (McElhinny, op. cit.).

In a large multidomain grain the domain walls can usually find suitable positions so that the magnetostatic energy is zero; therefore, it can be demagnetized so as to have no net magnetization. This contrasts with single domain grains whose moments may be reversed but cannot be destroyed. In very small multidomain grains the domain walls may be unable to occupy the exact positions necessary to give the grain zero magnetic moment; therefore, the moments of these grains can be reversed but not demagnetized. Such grains behave in a similar manner to single domain grains and are called pseudo single domain grains (McElhinny, op. cit.). The critical boundary for true multidomain behaviour in equant magnetite grains is ca. 17 μm (Stacey and Banerjee, op. cit.).

The domain state of a magnetic grain greatly influences its magnetic properties. In single domain grains greater than superparamagnetic size (see definition, below) a large energy barrier separating the easy directions of magnetization must be overcome in order to change the direction of the remanence; and relatively high magnetic fields are required to achieve this. In contrast, in multidomain grains domain wall movements may occur in relatively low fields; therefore, their magnetic stability is lower than that of stable single domain grains (Lowrie and Fuller, 1971).

Superparamagnetism and magnetic viscosity

At any particular temperature below the Curie point a single domain ferrimagnetic grain may be sufficiently small so that it undergoes frequent (relative to the observation time) thermally-excited spontaneous reversals of the direction of magnetization. However, in the presence of a magnetic field the moment of the grain will spend relatively longer lengths of time aligned within the field. This behaviour is the same as that for a paramagnetic material; however, since the atomic moments are much larger than for normal paramagnetics the alignment in the field is much stronger. Hence, this behaviour is termed superparamagnetism. Dunlop (op. cit.) estimated the threshold size for superparamagnetism of equant magnetite grains at room temperature as 0.03-0.035 μm. This value will rise with increasing grain elongation.

Magnetic grains on the superparamagnetic-stable single domain boundary exhibit behaviour known as magnetic viscosity, or time-dependent magnetization. This may be demonstrated, for example, by measuring the rate of decay of an artificially-induced remanent magnetization with time. Such measurements of magnetic viscosity almost always yield a log (time) relationship (Stacey and Banerjee, op. cit.).

Multidomain grains also display magnetic viscosity due to thermally-activated domain wall movements; however, this is usually some two orders of magnitude less than the viscosity of single domain grains (Mullins and Tite, 1973).

The hysteresis loop

Most of the magnetic parameters used in the present study can be defined with reference to the hysteresis loop. The loop is the plot of induced magnetization versus the strength of the applied field. Figure 1.2 shows the hysteresis loop for an assemblage of randomly oriented ferrimagnetic grains of sizes varying from super-paramagnetic (thermally unstable at room temperature) (SPM) through stable single domain (SD) and multidomain (MD). The intensity of magnetization (M) is plotted on the ordinate and the strength of the applied field (B_0) on the abscissa.

As B_0 is increased from zero, $M(B_0)$ rises linearly from the origin as indicated by portion 'a' of the curve. The increase in M is caused by three kinds of effect: (i) the alignment of SPM grains in the field; (ii) in SD grains, a slight rotation of the grain magnetic moments in alignment with the field; (iii) in MD grains, a slight rotation of the moments of individual domains towards the field, together with the enlargement of domains whose moments are aligned more or less parallel with the field, at the expense of domains with antiparallel moments. At this point in the process all three effects are reversible and $M(B_0)$ will return to the origin along path 'a' if B_0 is reduced to zero. The slope of the curve 'a' gives the initial (low field) apparent reversible susceptibility (usually referred to simply as susceptibility) of the assemblage.

If B_0 is increased further, $M(B_0)$ increases in the region 'b' on the curve. The process is now no longer reversible. With the reduction of B_0 to zero, $M(B_0)$ does not follow the path 'b' but

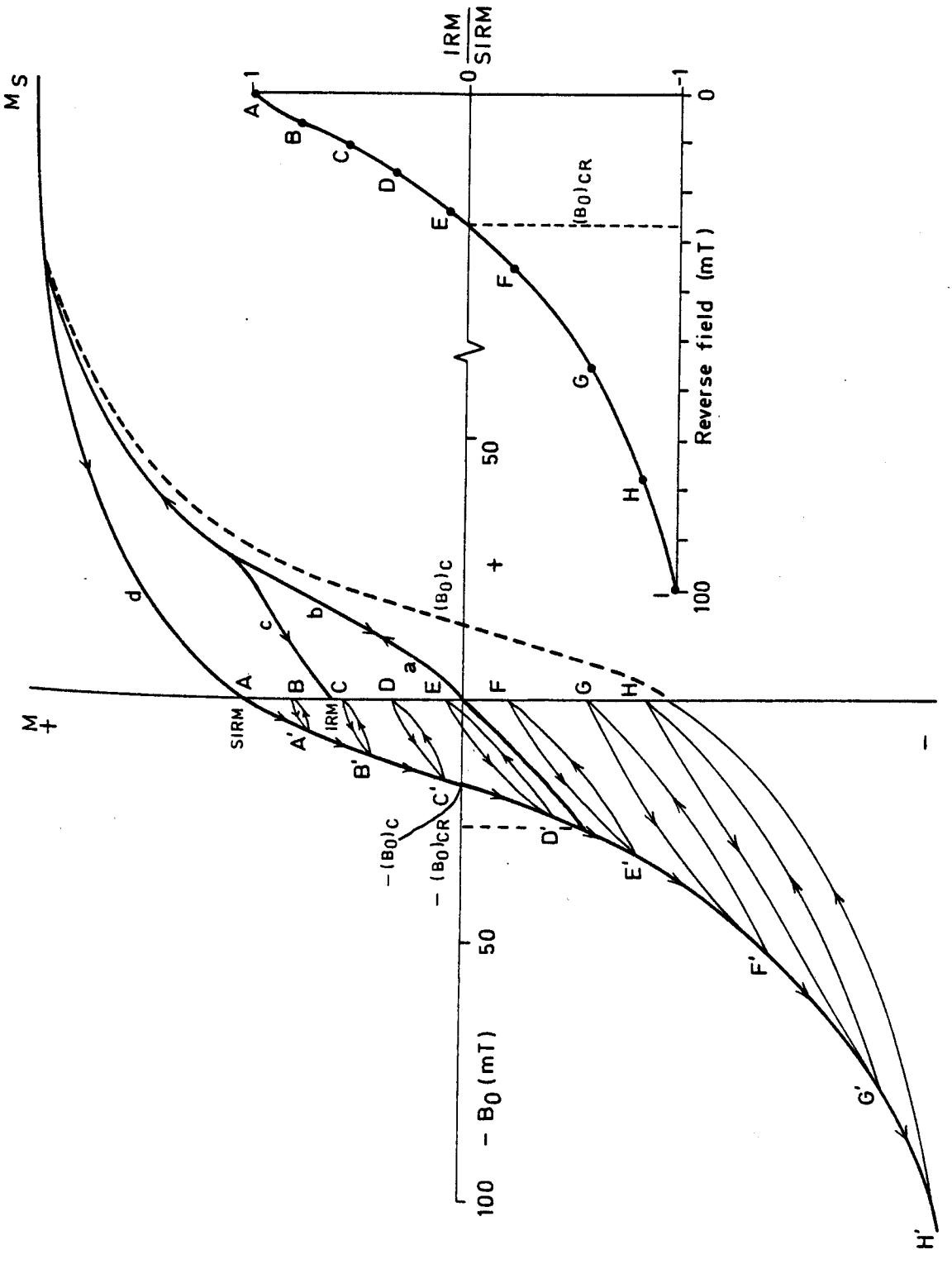

Figure 1.2 The hysteresis loop

follows the curve 'c', producing an isothermal remanent magnetization (IRM) given by the point IRM. Two kinds of effect contribute to give the assemblage a remanence: (i) each individual SD grain is characterised by a critical magnetic field strength (known as its intrinsic coercivity) which at room temperature is sufficient to overcome the energy barrier separating the easy directions of magnetization. In Figure 1.2 the value of B_0 at the junction of curves 'b' and 'c' exceeds the intrinsic coercivities of some of the SD grains with moments aligned more or less antiparallel to the field, causing the moments to flip irreversibly through 180^o to align with the field. (ii) Similarly, individual domains in MD grains have coercivities corresponding to the field strength required to force the domain walls over energy barriers represented by crystal imperfections in the grain. At junction 'b'-'c', B_0 is sufficient to overcome some of these energy barriers.

Subsequent increases in B_0 take $M(B_0)$ upto point M_S, beyond which any further increases produce no further increase in M. The magnetization at this point is called the saturation magnetization (M_S) of the assemblage. This is the largest magnetization that the assemblage can possess. The moments of all of the SD grains have flipped round and/or rotated, and the domain walls in MD grains have been forced over high energy barriers, to achieve the maximum alignment of domain moments in the field.

When B_0 is reduced to zero, $M(B_0)$ follows the path 'd' to point A which corresponds to the saturation isothermal remanent magnetization (SIRM or M_{RS}). This is the largest isothermal remanence that the assemblage can possess. SIRM is lower than M_S because with the removal of the field (i) the alignment of SPM grains is destroyed by thermal disturbance and (ii) in order to minimise magnetostatic energy, in SD grains there is a rotation of magnetic moments to align with

the easy axes of magnetization and in MD grains a readjustment of the domain configuration.

The application of a reversed magnetic field at this point leads to the growth of a reverse magnetization that is plotted 'downwards' on the M axis. From A to A' the assemblage is in the field. The net magnetization of the assemblage is the resultant of (i) SPM grains temporarily aligned in the reversed field; the alignment in the reversed field of the moments of stable domains whose intrinsic coercivities have been exceeded by the field at point A'; the reversible alignment in the field of the moments of SD grains and reversible changes in the domain configuration of MD grains allowing more of each grain to be magnetized in the reversed field direction. (ii) Domains, whose coercivities have not been exceeded, which are still aligned in the directions which obtained before the reversal of the field.

If B_0 is now reduced to zero, $M(B_0)$ will follow the path from A' to B with a loss of 'downwards' magnetization resulting from the randomization of the alignment of SPM grains together with reversible movements of domain moments in SD and MD grains in order to minimise magnetostatic energy. Therefore, the arrow goes up to B.

If the strength of the reversed field is increased still further, the coercivities of more stable domains are exceeded, the SPM grains realign and reversible movements of magnetic moments occur in SD and MD grains so that the intensity of 'downward' magnetization follows the path from B to B'. If B_0 were reduced to zero at this point, M (B_0) would follow the path to C. Eventually point $(B_0)_c$ is reached, at which the forward and reversed in-field magnetizations cancel each other out and the net assemblage magnetization is zero. The field at which this occurs defines the coercive force $((B_0)_c)$ of the assemblage.

At a point on the hysteresis loop approximately mid-way between

points D' and E', $M(B_0)$ will return to the origin if B_0 is reduced to zero. This point defines the coercivity of SIRM ($(B_0)_{CR}$) of the assemblage. With the reduction of B_0 to zero the forward and reversed remanent (out-of-field) magnetizations would cancel each other out and the net assemblage remanence would be zero.

If the reversed field is increased in steps until H, increases in M will follow the path from E' to F upto G' to H. At all times there is a decrease in M on removal of the field. At H' the assemblage is completely saturated in the reversed direction. At this point, if the direction of the field is again reversed the hysteresis loop will follow the course shown by the broken line and will exhibit the same changes in M on removal of the field.

Points A-H (plotted separately in Figure 1.2) define the coercivity of SIRM curve for the assemblage.

The shape of the hysteresis loop is characteristic of different magnetic mineral types and grain sizes. Figure 1.3 shows hysteresis loops typical of 'soft' (e.g. magnetite) and 'hard' (e.g. hematite) magnetic materials.

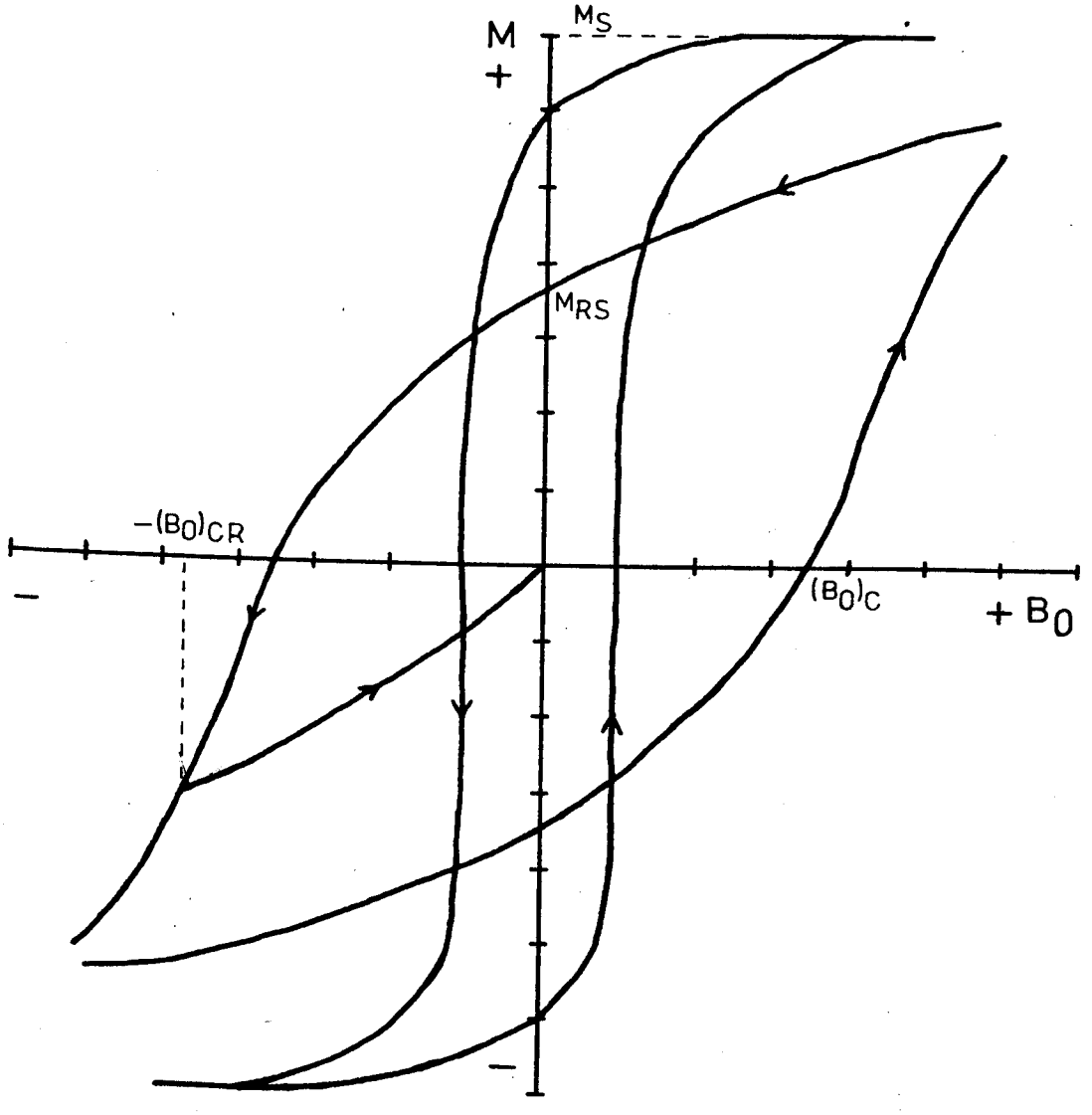

Figure 1.3 Hysteresis loops for 'soft' and 'hard' magnetic materials

1.7 Units of measurement

S.I. units are used throughout. The units, together with factors for conversion to c.g.s. units, are shown in Table 1.1.

Parameter	Symbol	S.I. unit	c.g.s. unit	Conversion to c.g.s.
Volume susceptibility	k	dimensionless	Gcm^3Oe^{-1}	X 0.0796
Specific susceptibility	χ	m^3kg^{-1}	$Gcm^3g^{-1}Oe^{-1}$	X 79.6
Volume magnetization	M	Am^{-1}	Gcm^{-3}	X 0.001
Specific magnetization	σ	Am^2kg^{-1}	Gcm^3g^{-1}	X 1.0
Magnetization/ susceptibility	-	Am^{-1}	Oe	X 0.0126
Magnetic field strength	B_0	T	Oe	X 10 000

Table 1.1. S.I. and c.g.s. units

1.8 Interpretation of magnetic parameters

Methods of measurement are given in Chapter 3 (section 3.4).

Saturation magnetization (M_S)

M_S is indicative of the volume concentration of magnetic minerals in a sample. It is largely independent of grain size and shape. Magnetite and hematite have values of M_S of ca. 90 and ca. 0.4 Am^2kg^{-1}, respectively.

Initial (low field) apparent reversible susceptibility (K, χ)

Susceptibility is also indicative of the volume concentration of magnetic minerals in a sample; however, in addition to the intrinsic susceptibility of different magnetic minerals the measured (apparent) susceptibility depends on magnetic grain size and shape, internal stress and other non-intrinsic parameters (Thompson et al., op. cit.). Mullins (1977) discusses in detail the circumstances under which susceptibility can be considered to be directly proportional to the quantity of magnetic material in a sample.

Table 1.2 shows the results of magnetic measurements of dispersed, sized magnetic powders. Grain size and domain status vary from coarse multidomain to fine multidomain and single domain. The grains are more or less equidimensional. No results for superparamagnetic magnetite grains are shown. A slight decrease in susceptibility with decreasing grain size is apparent. Theory predicts a very high susceptibility for a well-dispersed assemblage of superparamagnetic magnetite grains and Stacey and Banerjee (op. cit.) state that such an assemblage may have a much greater susceptibility than an assemblage with the same concentration of normal ferrimagnetic grains.

Saturation isothermal remanent magnetization (SIRM)

SIRM is also indicative of the volume concentration of magnetic minerals in a sample. Thompson et al. (op. cit.) show that in a suite of samples in which a single type of magnetic mineral is

Grain size (μm)	Susceptibility ($m m^3 kg^{-1}$)	SIRM ($Am^2 kg^{-1}$)	SIRM/ susceptibility ($k Am^{-1}$)	$(B_o)_{CR}$ (mT)	Source
Magnetite					
220	0.752	0.483	0.642	12	2
120	0.582	1.41	2.42	17	1
100	0.728	1.16	1.59	14	2
88	0.509	1.49	2.92	18	1
58	0.534	1.47	2.75	19	1
37	0.534	1.85	3.47	20	1
37	0.728	1.29	1.78	20	2
37	0.631	1.04	1.65	20	2
37	0.703	1.14	1.62	19	2
21	0.509	1.74	3.41	23	1
19	0.461	2.32	5.03	22	1
15	0.679	3.48	5.12	25	1
12	-	2.70	-	23	1
6	0.461	4.05	8.79	23	1
4.5	0.655	6.95	10.6	30	2
1.5	0.388	5.85	15.1	32	1
1.5	0.461	5.79	12.6	34	1
1.5	0.485	11.2	23.1	38	2
0.22	0.708	10.2	14.4	-	3
0.10	0.679	17.9	26.4	-	3
0.076	0.650	21.8	33.5	-	3
0.037	0.572	26.0	45.5	-	3
0.03x0.2 (Single domain)	0.451	41.8	92.6	-	3
Hematite					
100	0.0003	0.075	250	500	4

Sources: 1. Parry, 1965; 2. Parry, 1980; 3. Dunlop, 1972; 4. Thompson and Morton, 1979.

Table 1.2. Values of susceptibility, SIRM, SIRM/susceptibility and $(B_o)_{CR}$ for magnetite and hematite.

dominant or in which the magnetic minerals present occur throughout in constant proportions, there will be a direct linear relationship between susceptibility and SIRM.

Reference to Table 1.2 shows that the SIRM of magnetite rises significantly with decreasing grain size and is at a maximum in stable single domain grains. However, grains smaller than this, exhibiting viscosity and superparamagnetism, will exhibit negligible SIRM.

SIRM may be used to indicate trends in magnetic grain size and mineralogy in several ways:

i) Calculation of the ratio of SIRM to susceptibility. Since SIRM exhibits a significantly greater variation with ferrimagnetic grain size than does susceptibility, SIRM/susceptibility is indicative of grain size variations (see Table 1.2). Maximum SIRM/susceptibility occurs in stable single domain grains; low values occur in superparamagnetic and coarse multidomain grains. SIRM/susceptibility in samples dominated by ferrimagnetic minerals is usually $\ll 100$ kAm^{-1} and > 100 kAm^{-1} in samples dominated by hematite. Samples with a very high concentration of paramagnetic material (with weak positive susceptibility but no remanence) and a low concentration of ferrimagnetic material may have values of SIRM/susceptibility < 1 kAm^{-1}.

ii) The ratio M_{RS}/M_S is indicative of grain size and domain status. In an assemblage of stable single domain magnetite M_{RS}/M_S is ca. 0.5; assemblages with values lower than this will contain multidomain, pseudo single domain or superparamagnetic grains (Levi and Merrill, 1978).

iii) The minimum (saturating) field required to induce SIRM is indicative of magnetic mineral types: magnetite saturates in fields less than 0.2 T, while fine-grained hematite may require fields greater than 1.5 T.

Coercivity of SIRM curves

Reference to Figure 1.4 shows that the overall shape of the coercivity of SIRM curve is indicative of magnetic mineral types and grain sizes (and shapes). Samples dominated by coarse-grained or viscous/superparamagnetic ferrimagnetic components have 'soft' concave $(B_O)_{CR}$ curves; samples dominated by fine-grained multidomain and stable single domain ferrimagnetic material an intermediate sigmoid-shaped curve and samples dominated by fine-grained hematite a 'hard' convex curve. In soil and sediment samples composite curves are common. Oldfield et al. (1978b) note that coercivity of SIRM curves appear to differentiate between such samples very sensitively without however permitting more than general, non-quantitative estimates of the basis of the variation.

One or a combination of individual parameters may be used to characterise a coercivity of SIRM curve. Usually the $(B_O)_{CR}$ value itself is given. Table 1.2 shows the variation of $(B_O)_{CR}$ with grain size for multidomain equant magnetite grains within the size range ca. 200-1 μm. Multidomain grains less than 1 μm, and stable single domain grains, may have $(B_O)_{CR}$ values of ca. 40-60 mT. $(B_O)_{CR}$ is considerably reduced by the presence of viscous/superparamagnetic grains. The single value for fine-grained hematite in Table 1.2 shows that $(B_O)_{CR}$ may be around one order of magnitude higher.

'S' values are obtained by calculating the ratio of the minus IRM at a particular reverse field (often 100 mT) to the SIRM. If 100 mT is used then S is usually greater than zero in ferrimagnetic-dominated assemblages and less than zero in hematite-dominated assemblages. S values enable some indication of ferrimagnetic versus canted antiferromagnetic contrasts within a suite of samples to be obtained by two simple and rapid measurements.

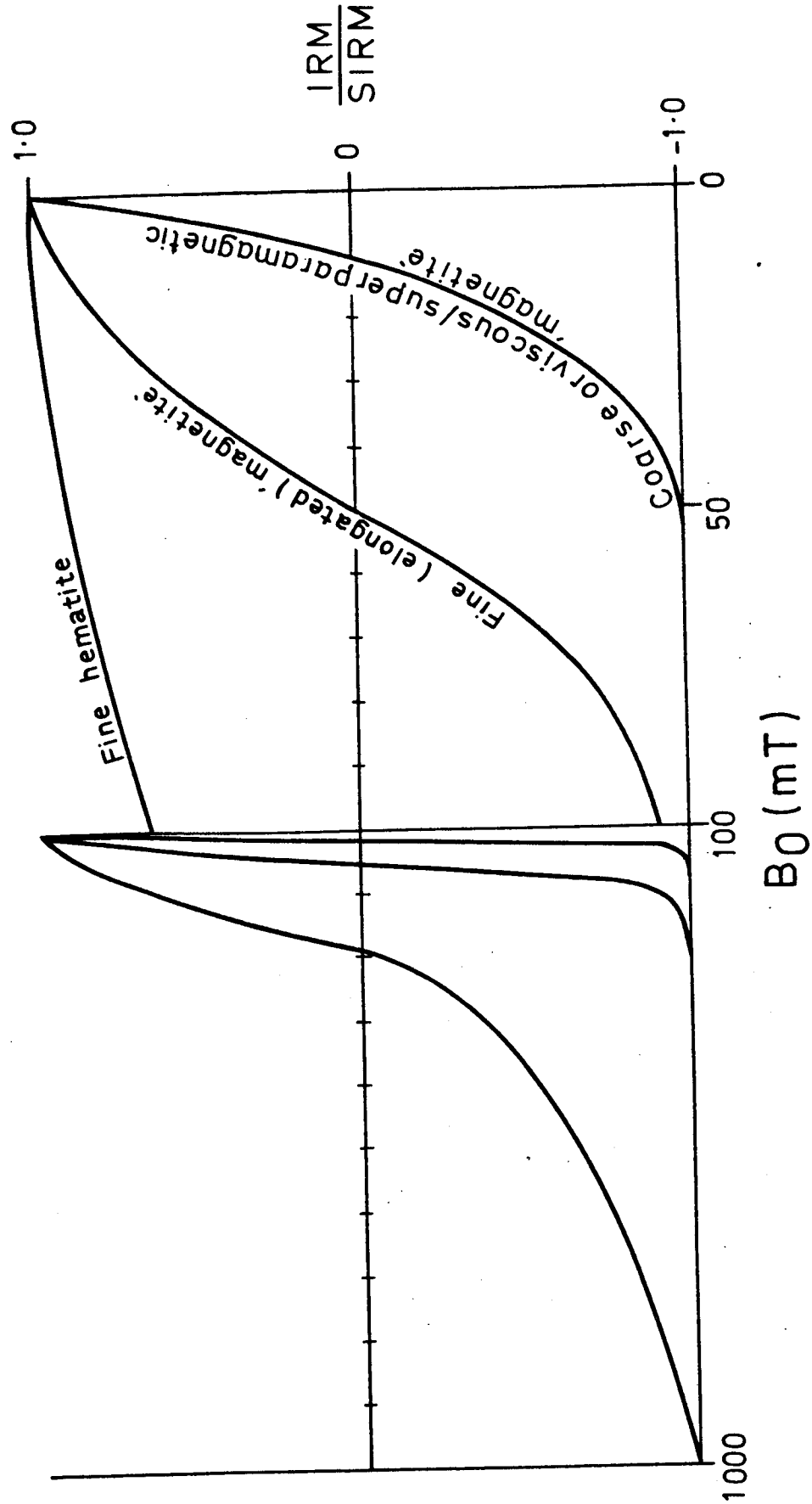

Figure 1.4 Coercivity of SIRM curves for magnetite and hematite

Coercive force ($(B_0)_C$)

$(B_0)_C$ is also indicative of the magnetic hardness of a sample. Parry (1980) gives experimental values of $(B_0)_C$ ranging from 0.7-16.0 mT for equant multidomain magnetite grains of varying sizes, $(B_0)_C$ increasing with decreasing grain size. For multidomain and stable single domain grains the ratio $(B_0)_{CR}/(B_0)_C$ decreases with decreasing grain size (Parry, op. cit.). $(B_0)_C$ is greatly reduced by the presence of superparamagnetic grains (which have a relatively large susceptibility), while $(B_0)_{CR}$ (an out-of-field measurement) is only characteristic of the stable magnetic fraction, so that in a sample with a large proportion of superparamagnetic grains $(B_0)_{CR}/(B_0)_C$ becomes large (Mullins, 1974).

Anhysteretic Remanent Magnetization (ARM)

If a sample is subjected to a decreasing alternating field with a small steady field superimposed it acquires a remanent magnetization approximately proportional to the steady field. This is called an ARM and is indicative of the volume concentration of magnetic minerals in a sample. The ratio SIRM/ARM may be used to indicate stable single domain versus multidomain contrasts in ferrimagnetic grain assemblages (R. Thompson, personal communication).

Many of the parameters described above are considerably influenced by factors such as variations in magnetic grain shape, variations in the Ti content of titanomagnetites and non-homogeneity of grain composition. For example in magnetite, increasing grain elongation will result in higher SIRM, SIRM/susceptibility, $(B_0)_C$, $(B_0)_{CR}$ and S in comparison with equidimensional grains of the same volume; while in titanomagnetite grains either an increase in Ti content or the presence of exsolved ilmenite lamellae (thereby effectively decreasing the size of the grain) will have the same effect (Larson et al., 1969). Moreover, soil and especially sediment

samples usually contain complex assemblages of magnetic grains of varying mineralogy, grain size and grain shape. Consequently, precise identification of the various magnetic phases in a sample is rarely possible by magnetic measurements alone. Normally, only generalised trends in magnetic mineralogy/grain size/grain shape may be inferred.

1.9 Magnetic minerals and the soil

The mineral magnetic properties of soils are frequently dominated by ferrimagnetic minerals of the following solid solution series: magnetite (Fe_3O_4) - ulvöspinel ($FeTiO_4$) (the titanomagnetites, frequently referred to simply as magnetites) and magnetite - maghemite ($\gamma\ Fe_2O_3$) (including the titanomaghemites). It is only where these are absent or present in very low concentrations that antiferromagnetic components, such as the hematite (αFe_2O_3) - ilmenite ($FeTiO_3$) solid solution series, the iron oxyhydroxides, goethite (α FeOOH) and lepidocrocite (γ FeOOH), and dia- and paramagnetic components can make a significant contribution. For example, the magnetite content of a sample need be only 0.5-1% of the hematite content for the two minerals to contribute equally to the susceptibility. Table 1.3 lists some common soil magnetic minerals and gives typical susceptibility values. The magnetic properties of these minerals are discussed in detail in Stacey and Banerjee (1974) and O'Reilly (1976).

Basalt and andesite, and to a lesser extent other igneous rocks, contain relatively high concentrations of primary magnetite. Both within the rocks themselves and in the soils developed from them, the magnetite occurs predominantly as sand and silt-sized equidimensional grains (Mullins, 1977). In sedimentary rocks and in soils derived from them primary ferrimagnetic minerals usually occur in much lower concentrations. However, the magnetic properties of the soils may be significantly influenced by the occurrence of secondary ferrimagnetic minerals formed by a variety of pedogenic processes and usually present in the clay-sized fraction. This magnetic 'enhancement', primarily occurring in the topsoil, was first observed by Le Borgne (1955, 1960) who attributed it to the formation of maghemite. Maghemite has very similar magnetic properties to magnetite.

Mineral	Formula	Magnetic property	Typical susceptibility ($\mu m^3 Kg^{-1}$)	Crystal System
Ilmenite	$FeTiO_3$	Antiferromagnetic	1.7	hexagonal
Hematite	αFe_2O_3	Antiferromagnetic	0.27 - 0.63	hexagonal
Goethite	$\alpha FeOOH$	Antiferromagnetic	0.125- 1.26	orthorhombic
Lepidocrocite	$\gamma FeOOH$	Antiferromagnetic	0.5 - 0.75	hexagonal
Pyrrhotite	Fe_7S_8	Ferrimagnetic	53	hexagonal
Magnetite	Fe_3O_4	Ferrimagnetic	390-1 000	cubic spinel
Maghemite	γFe_2O_3	Ferrimagnetic	410- 440	cubic spinel

Table 1.3. Some soil magnetic minerals (after Mullins, 1977).

Mullins (1977) lists four different ways in which maghemite can be formed:

i) By the low temperature (150-250°C) oxidation of magnetite.

ii) By the dehydration (at 275-410°C) of lepidocrocite.

iii) Via a reduction-oxidation cycle ('fermentation') occurring during normal pedogenic conditions in which weakly magnetic iron oxides and hydroxides are converted to secondary maghemite. Experimental work by Taylor and Schwertmann (1974) indicates that this enhancement mechanism is likely to be favoured by relatively high temperatures, pH values and total Fe concentrations.

iv) As a result of burning. This mechanism has now been widely demonstrated. On the basis of controlled laboratory and field experiments Le Borgne (1955) suggested the following process during burning:

$$\underset{(\alpha Fe_2O_3)}{\text{hematite}} \xrightarrow{\text{reduction}} \underset{(Fe_3O_4)}{\text{magnetite}} \xrightarrow{\text{oxidation}} \underset{(\gamma Fe_2O_3)}{\text{maghemite}}$$

Subsequently, Tite and Mullins (1971) showed that heating soils in nitrogen-then-air was an extremely effective enhancement mechanism, and assumed the mineral responsible to be maghemite. Longworth et al., (1977), using Mössbauer spectroscopy, demonstrated that non-stoichiometric magnetite with the formula $Fe_{2.9}O_4$ was produced after the accidental burning of both hematite-rich substrates and substrates poor in both ferri- and antiferromagnetic minerals. Oldfield et al. (1981a) have shown experimentally that manipulation of various heating procedures may be used to grow distinctive assemblages of secondary magnetic minerals in initially paramagnetic shales and mudstones. Depending upon rates of heating and cooling, assemblages consisting predominently of hematite and superparamagnetic magnetite; stable single domain magnetite; or stable single domain and superparamagnetic magnetite may be grown.

Two sets of pedogenic processes act in opposition to the enhancement mechanisms described above: gleying and podsolization both effect the chemical breakdown of ferrimagnetic minerals. Several workers have noted that gleyed profiles always exhibit very low values of susceptibility (e.g. Vadyunina and Babanin, 1972 ; Mullins, 1974; Dearing, op. cit.). In podsolized profiles, the decomposition of ferrimagnetic minerals occurs principally in the eluvial horizons, while slight increases in the susceptibility of the illuvial horizons may result from the precipitation of paramagnetic iron (Mullins, 1974).

Figure 1.5 summarises the role of magnetic minerals in the soil iron cycle. Fuller accounts of soil magnetism are given in Mullins (1974; 1977) and Dearing (op. cit.), while the genesis and properties of soil iron oxides, including magnetic forms, are described in detail in Schwertmann and Taylor (1976).

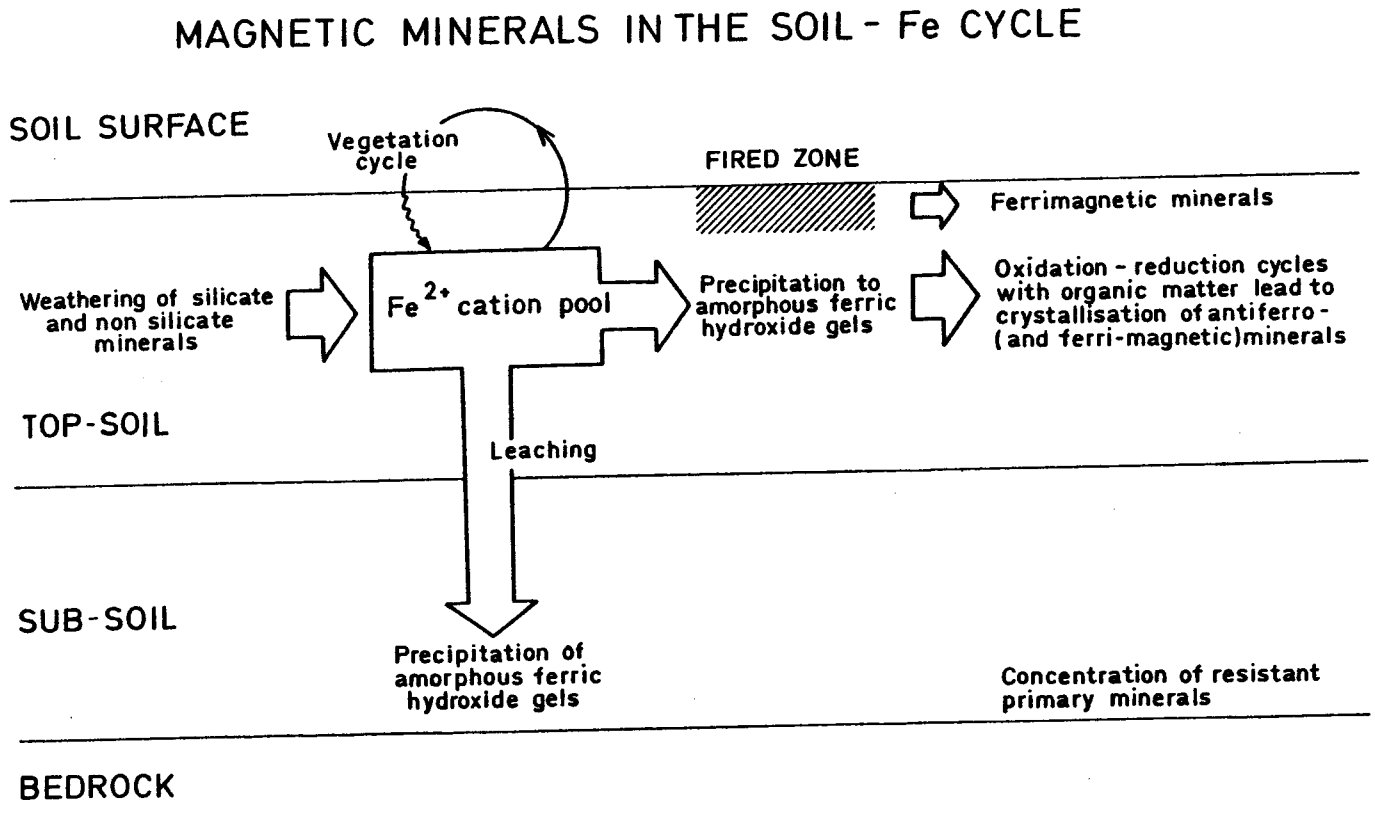

Figure 1.5 Magnetic minerals and the soil Fe-cycle (from Dearing, 1979)

CHAPTER 2. THE STUDY SITE.

2.1 Introduction

The site chosen for the study was Llyn Goddionduon, in the Gwydyr Forest area of North Wales. Preliminary studies of five sediment cores from the lake basin indicated the occurrence of correlatable changes in magnetic susceptibility associated with a major disturbance in the watershed in the recent past (Bloemendal, 1977). In addition, the site had several logistical advantages: in terms of size, accessibility by road and the availability nearby of accommodation and laboratory facilities at the Rhyd-y-Creau Drapers' Field Centre, Betws-y-Coed.

2.2 Location and physical characteristics of the watershed

Llyn Goddionduon lies at an altitude of 244 m above O.D. in the Gwydyr Forest area of Gwynedd, North Wales. The centre of the lake basin is located at Grid Ref. SH753586; Latitude $53^{\circ}\ 6'\ 40''$ N, Longitude $3^{\circ}\ 51'\ 30''$ W. Figure 2.1 illustrates the topography of the area together with its location in Wales (also included are the locations of soil profiles and stream bedload samples referenced in Chapter 7, section 7.5). The watershed is situated on a broken and undulating plateau known as the 'Glyn', predominantly an area of high moorland utilised mainly for sheep grazing and afforestation. Table 2.1 shows various data for the Goddionduon watershed.

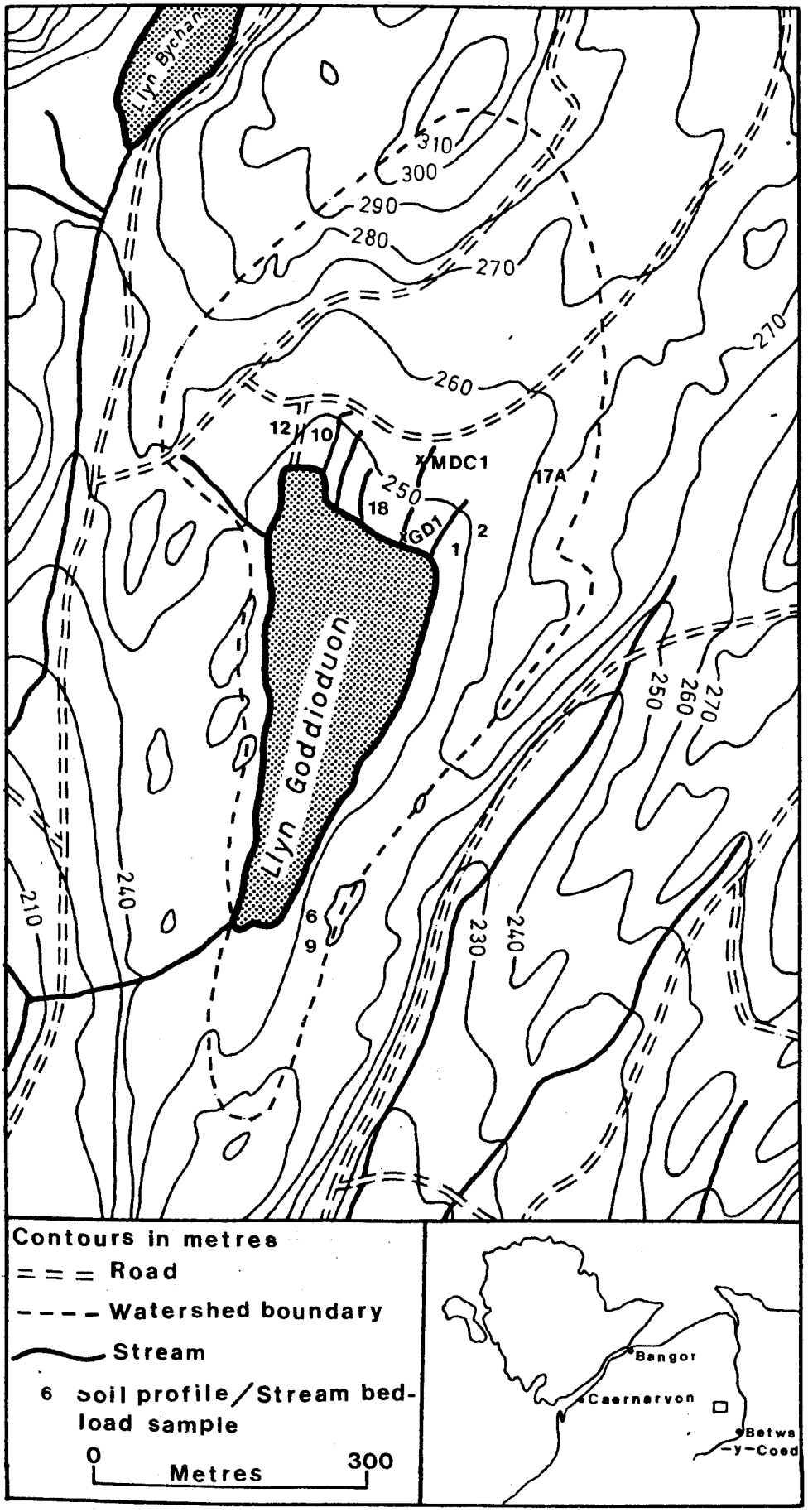

Figure 2.1 Location, topography and drainage of the Llyn Goddionduon area

Size of watershed (ha)	31
Rainfall (cm/yr)	191
Percentage of forestry	80
Percentage of lake surface	20
Turnover time (days)	57.6

Table 2.1. Watershed data

(Source: Liddle, unpublished)

Figure 2.2 illustrates the geology of the area. The following account of the geology was obtained from Davies (1936) and Howells et al. (1978). The whole of the geological sequence exposed within the area falls within the Caradoc and Ashgill series of the Ordovician. During the late Caradoc, the deposition of siltstones and mudstones was interrupted by rapid incursions of acid volcanic deposits generated largely by submarine eruptions (represented by the Crafnant Volcanic Group). During and subsequent to these incursions, the establishment of a deeper water environment signalled the onset of black graptolitic mudstone deposition. The rocks underlying the Goddionduon watershed itself consist of tuffite (Upper Crafnant Volcanic Formation) and slates (Llanrhychwyn Slates). The tuffite is composed of a heterogeneous mixture of pyroclastic and epiclastic material. The former consists of cuspate shards of variable form, together with crystals of sodic feldspar and pumice fragments; the latter consists of an aggregate of chlorite, sericite, carbonaceous material and iron ore. The proportions of the various constituents of the tuffite are highly variable: around Llyn Goddionduon itself the rocks are largely tuffaceous mudstones. The Llanrhychwyn Slates,

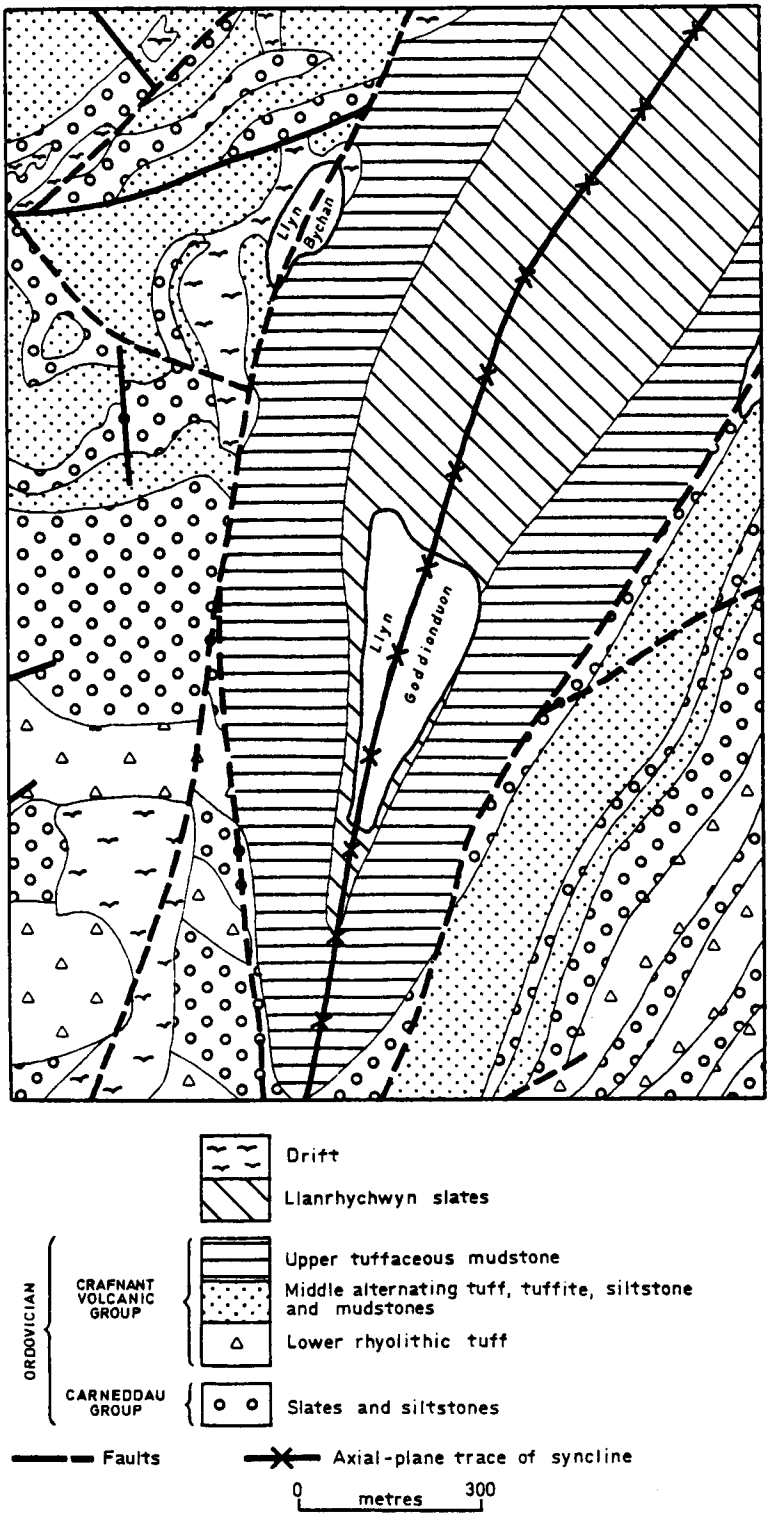

Figure 2.2 Geology of the Llyn Goddionduon area

dominating the northern part of the watershed, are graptolitic, well-cleaved and with frequent iron-rich bands (principally pyrite).

Structurally, the Glyn forms part of the eastward dipping monocline of eastern Gwynedd, upon which is superimposed a succession of northeast-southwest folds pitching at low angles to the northeast. The axial-plane trace of a fault-bounded synclinal structure is more or less coincident with the long axis of the Goddionduon watershed and lake basin.

During the Pleistocene, the area was severely glaciated; however, the glacial drift deposits are relatively thin and of restricted extent. They consist typically of grey to greyish brown clay with a high proportion of pebbles and boulders, all of local origin. Field observations suggest that there is a relatively thin (less than 1 m deep) mantle of drift principally in the northern part of the watershed.

On the O.S. Soils Sheet 106 the Goddionduon watershed is mapped as part of the Hiraethog-Bodafon soil complex, consisting of shallow phase peaty podzolic soils. Analytical data and profile descriptions in Ball (1963) indicate that these soils have relatively low pH values (less than 5.0) and sandy loam or silty loam textures. Soils of this type occur in the northwestern and eastern parts of the watershed; however, peaty gleyed soils with organic horizons upto ca. 1 m deep also occur over most of the western and northern parts of the watershed.

2.3 Vegetation and recent history of the watershed

The following account is based on information supplied by D.L. Shaw (personal communication and unpublished) and R. Hughes (personal communication). Prior to Forestry Commission acquistion in 1920, the watershed had for several hundred years formed part of an extensive sheep walk of low productivity, a density of no more than 1 animal to ca. 1.2 ha being possible. At the time of acquisition the vegetation

was dominated by Calluna vulgaris[1] together with Myrica gale, Molinia caerulea, Erica tetralix, Trichophorum cespitosum, Eriophorum angustifolium and Juncus spp. in the wetter areas; and Ulex spp. and Vaccinium myrtillus in the drier areas. Following the enclosure of the area (for afforestation) and the exclusion of sheep, there followed a considerable increase in the vigour and density of grasses, gorse and heather, to the extent that from 1928 until the development of a more or less continuous crown cover an annual weeding and cutting program was required.

Ground preparation prior to planting was carried out in 1925 and involved the digging by hand of drainage ditches and the cutting and spreading of the peat turves into lines ca. 2 m apart into which the seedlings were planted. Figure 2.3 shows the main constituents of the plantations at the present day. Picea abies and P. sitchensis, particularly the latter, are the dominant species in the low-lying peaty hollows that occur along the northern and western shores. Pinus sylvestris and Pinus contorta are dominant in the more steeply-sloping and better drained areas along the eastern shore. Small plantations of Larix kaempferi also occur within the watershed and there are occasional individuals of other species: e.g. Sorbus aucuparia, Tsuga heterophylla, Quercus petraea, Betula sp. and Chamaecyparis lawsoniana. With the exception of the largely unforested area represented by the mire adjacent to the southern end of the present lake basin (see section 2.4, below), together with the fire line extending eastwards from the southeastern shore, the remnants of the former heath and bog vegetation are confined to a zone of a few

---

[1]Throughout the following, nomenclature of vascular plants follows Clapham et al. (1962).

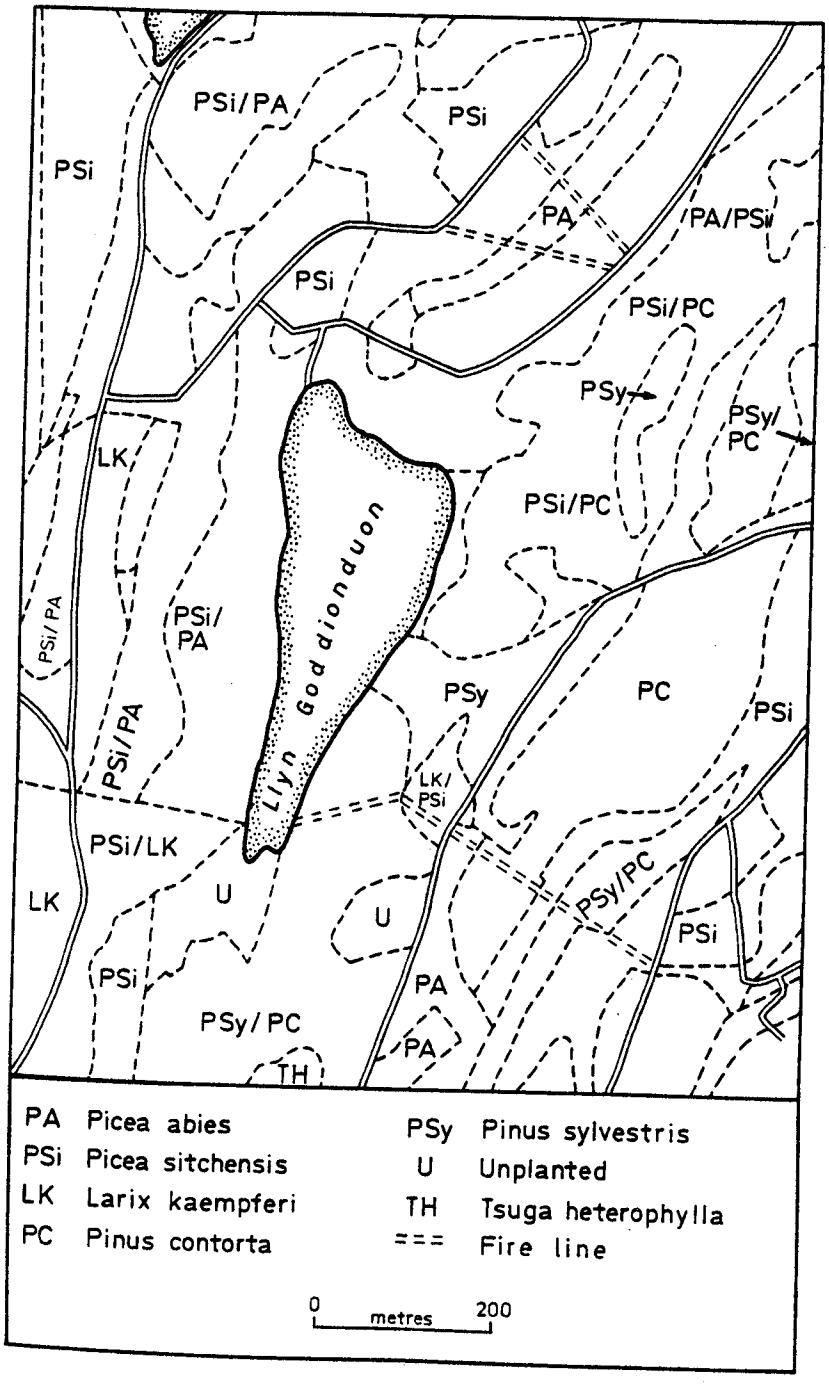

Figure 2.3 Forest composition of the Llyn Goddionduon area

metres width fringing the lake.

On 12th May 1951, a major forest fire started along the south-eastern shore of Llyn Bodgynydd, ca. 500 m northeast of Goddionduon. Due to the limited extent of the forest road network at that time, control of the fire proved difficult and it eventually affected over 50 ha, including part of the Goddionduon watershed. The lake itself was used by the fire fighters as a water source. There are no accurate maps available indicating the precise extent of the affected area; however, within the Goddionduon watershed this largely corresponds to the Pinus sylvestris and P. contorta plantations in the southeastern part of the watershed (Figure 2.3). These areas were only replanted in 1966-67. In order to facilitate extraction of the timber crop and to improve accessibility in the event of future fires, an enlargement of the forest road network was carried out from 1954 onwards. In the Goddionduon watershed this had the effect of blocking an inflow (see section 2.4, below) from the stream draining Llyn Bychan, ca. 500 m. to the north of Goddionduon, and effectively reducing the size of the watershed. The forest road network in the northern part of the watershed (shown in Figure 2.3) was constructed in 1960-61, although this was to some extent an enlargement of pre-existing tracks.

2.4 Lake basin morphometry and drainage

Figure 2.4 shows the bathymetry of the lake basin and the axes of the grid network described in Chapter 3 (section 3.1). Figure 2.5 shows a SYMVU plot (Muxworthy, 1977) of the basin morphometry; data points were obtained by echo-sounding, depth probing with a ranging pole and plumb-lining. Table 2.2 shows morphometric parameters for the lake basin.

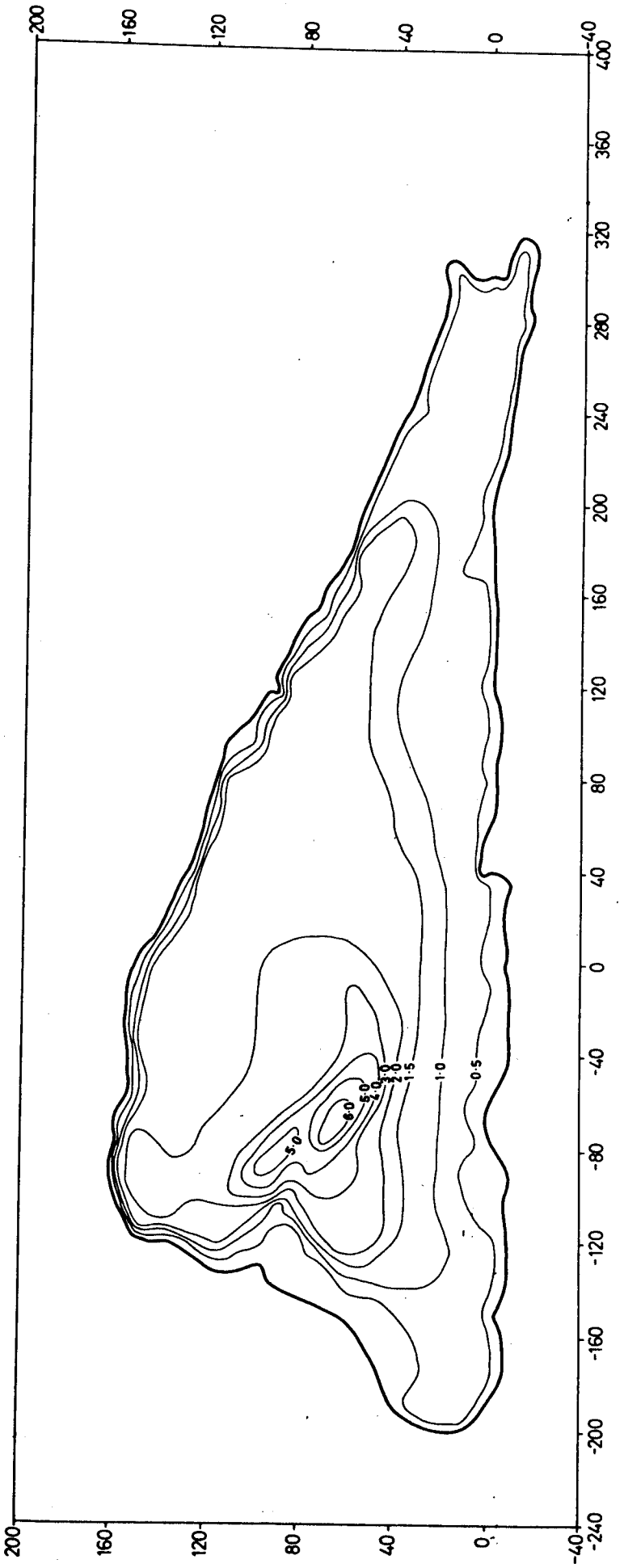

Figure 2.4 Llyn Goddionduon: bathymetry and grid axes

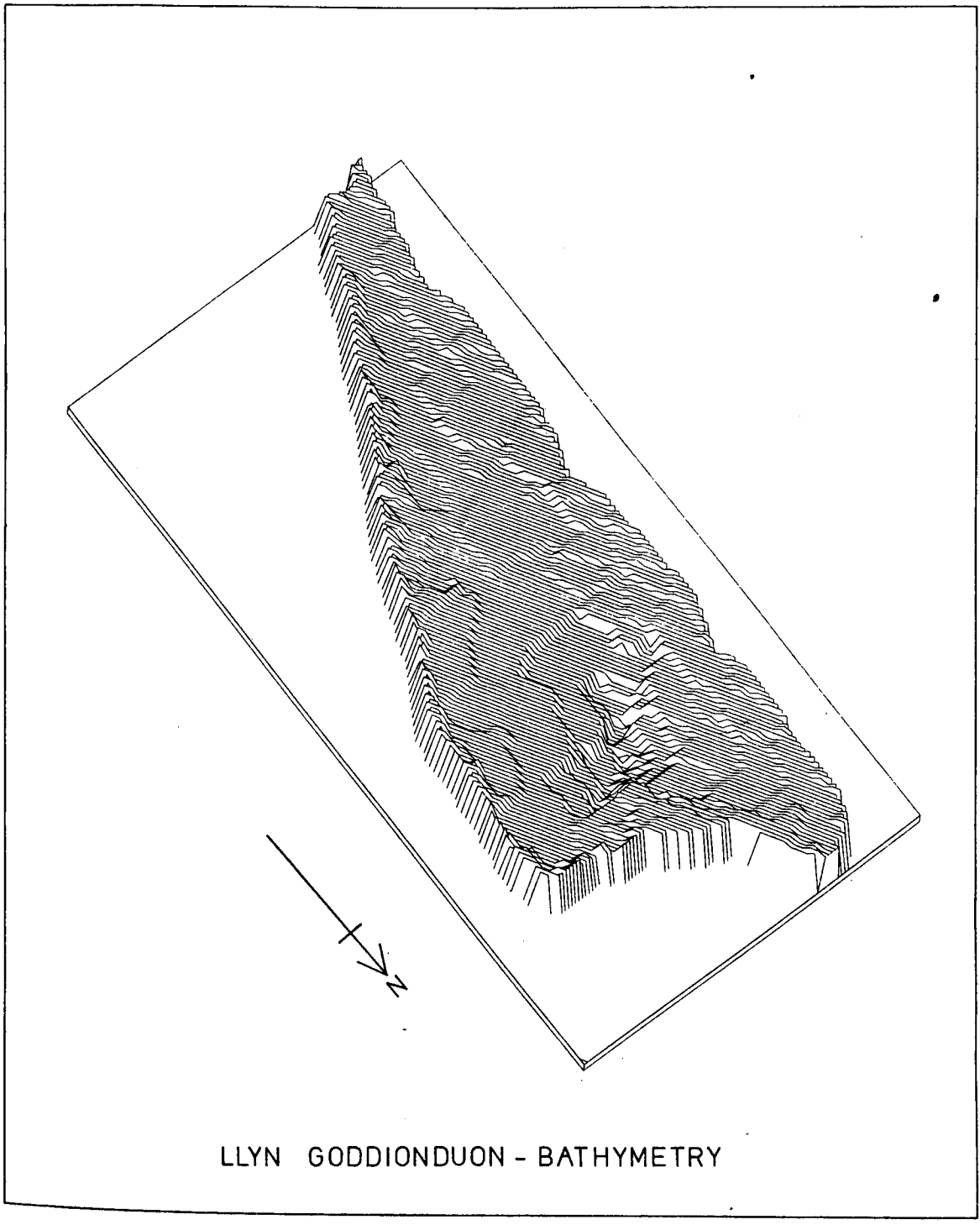

Figure 2.5 Llyn Goddionduon: SYMVU plot of the bathymetry

Length of shoreline (L) (m)	1 260
Maximum length (l) (m)	519
Maximum width (b) (m)	170
Area (A) (m^2)	51 400
Volume (V) (m^3)	73 130
Maximum depth (Zm) (m)	6.5
Mean depth ($\bar{Z}$) (m)	1.42
Shoreline development[1] (Dl)	1.57

[1] $Dl = L/2 \sqrt{Ao}$, where Ao is the area of a circle equivalent to the area of the lake basin (Wetzel, 1975).

Table 2.2 Morphometric parameters for the Goddionduon lake basin

The lake basin is likely to have originated at the end of the last (Devension) glaciation as a kettle hole (Liddle, unpublished). Maximum water depth occurs in the small 'trench' area in the northern part of the basin, occupying less than 5 percent of the basin area. Reference to Table 2.2 shows that the mean depth is shallow: less than 1.5 m. A small mire of ca. 6 000 m^2 in area adjacent to the southern end of the basin represents overgrowth of telmatic peat on marginal lake sediments. The lake basin receives drainage from six channels (see Figure 2.1), all of which are less than 1 m in width: five Forestry Commission drainage ditches (excavated during the early 1920's) enter from the north, and one other stream enters from the northwest; the latter was constructed during the Victorian period, and prior to road construction in 1960-61 was connected with the stream draining Llyn Bychan; it was intended to facilitate the passage of trout between the two watersheds. A small

outflowing stream in the southwestern corner of the basin drains ultimately into the Afon Llugwy; a small weir at its proximal end was constructed during the 1920's.

2.5 Water chemistry and physical properties

The chemistry and physical properties of the Goddionduon lake, inflow[1] and outflow waters were investigated during a survey of twelve lakes in the Gwydyr Forest area. Methods and full results are given in Liddle (op. cit.). Field-work and sample collection were carried out during June and July, 1973. The very low light extinction coefficients obtained using four different filters underlined the exceptional clarity of the lake water. Temperature varied from 19°C at a depth of 0 m to 15.5°C at a depth of 4-5 m, indicating some degree of thermal stratification, and oxygen saturation from ca. 85-80 percent over the same depth range. Table 2.3 shows the results of the chemical analyses. As would be expected from its elevation and situation in an environment of low productivity, the lake has oligotrophic characteristics: low pH, alkalinity and conductivity and a low concentration of solutes. The only unexpected features were the high levels of N and P in the inflow, suggesting a local source of decomposing organic material (Liddle, op. cit.). The lake water also had a high level of P in the surface waters.

---

[1] Liddle (op. cit.) does not specify which inflow was used for sample collection.

		Inflow	Lake	Outflow
Alkalinity	S	0.05	0.05	0.19
1	B	-	0.22	-
Conductivity	S	60	61	52
2	B	-	52	-
Total N	S	27.7	9.9	2.4
3	B	-	2.4	-
N as NH_3	S	10.6	5.9	1.4
3	B	-	1.4	-
N as NO_2	S	0.11	0	0
3	B	-	0	-
N as NO_3	S	17	4	1
3	B	-	1	-
Total P	S	2.09	0.7	0.25
3	B	-	0.26	-
P as PO_4	S	0.1	0.11	0.06
3	B	-	0.11	-
Si	S	17	2	1
3	B	-	1	-
Na	S	5.2	6.3	5.9
4	B	-	5.9	-
K	S	0.8	0.42	0.14
4	B	-	1.22	-
Mg	S	2.0	1.5	1.2
4	B	-	1.3	-
Ca	S	3.3	3.1	2.7
4	B	-	2.4	-
Cu	S	-	2.8	-
3	B	-	-	-
Zn	S	-	60	-
3	B	-	-	-
Fe	S	-	7	-
3	B	-	-	-
pH		5.8		
5				

Notes: 1. m.eq/l 2. mhos/cm at 20°C 3. µg/l
4. ppm 5. Mean of surface, inflow and outflow samples S = Surface B = Bottom

Table 2.3. Llyn Goddionduon: water chemistry (Source: Liddle, unpublished)

2.6 Macrophytic vegetation

The macrophytic vegetation was also investigated by Liddle (op. cit.) and Table 2.4 summarises some of the results. Figure 2.6 shows the distribution of emergent and floating-leaved macrophytes. Over most of the area of the lake basin occupied by emergent and floating-leaved macrophytes, the vegetation takes the form of a fringing reedswamp with Schoenoplectus lacustris, Phragmites communis and Equisetum fluviatile as the dominant species. The restriction of the reedswamp to the northwestern, western and southern areas of the lake basin reflects the more extensive littoral area available for plant colonisation. Floating-leaved macrophytes (Nymphaea alba and Potamogeton natans) are largely confined to the southernmost area of the basin. Small areas of Carex rostrata and Eleocharis palustris reedswamp, together with occasional individual specimens of Sparganium angustifolium, are also present. Littorella uniflora and Lobelia dortmanna (principally in water of less than 0.5 m depth) and Isoetes lacustris (principally in water of greater than 1.5 m depth) are the dominant submerged macrophytes. At the present time, much of the sediment surface of ca. 1-3 m depth is covered by a dense Isoetes sward. In summary, although many of the macrophytes recorded in Goddionduon are

Area occupied by emergent vegetation (m^2)	12 354
Area occupied by floating-leaved vegetation (m^2)	2 344
Percentage of lake area occupied by emergent vegetation	20
Percentage of lake area occupied by floating-leaved vegetation	4

Table 2.4. Llyn Goddionduon: areas occupied by emergent and floating-leaved macrophytes. (Source: Liddle, unpublished).

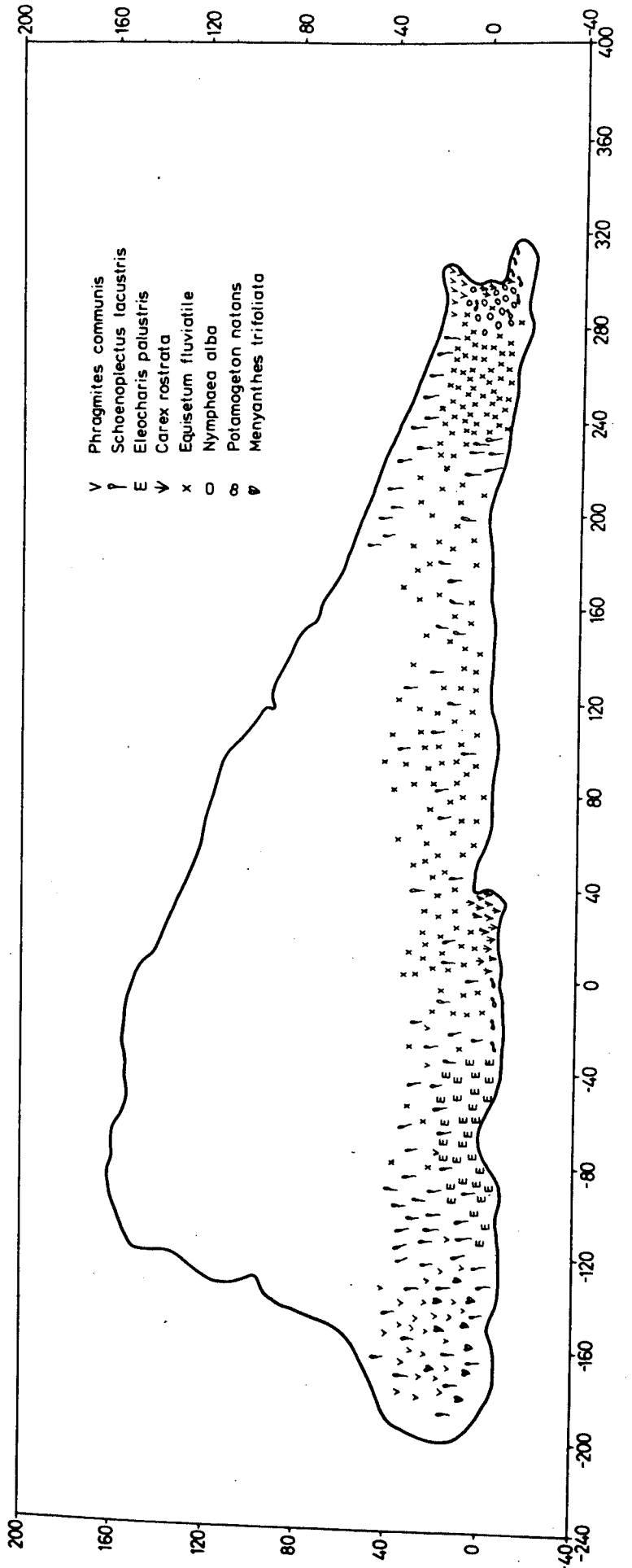

Figure 2.6 Llyn Goddionduon: map of the emergent and floating-leaved macrophytes

characterised by tolerance of a broad range of trophic and substrate conditions, the occurrence of such species as Lobelia, Littorella and Isoetes would be considered characteristic of clear, acid and unproductive lakes such as this.

2.7 Phytoplankton and productivity

These were also investigated by Liddle (op. cit.). Over 50 percent of the recorded phytoplankton taxa were members of the Chlorophyta, most of which were Desmids. This latter group is characteristic of unproductive waters (Macan and Worthington, 1972). Calculation of Nygaard's phytoplankton coefficient produced a value of 0.64; lakes with values below 0.8 are classed as oligotrophic (Liddle, op. cit.). Estimation of the numbers of organisms per m^3 of water, together with measurement of the chlorophyll concentration also indicated that Goddionduon currently has a very low level of productivity.

CHAPTER 3 FIELD AND LABORATORY METHODS

3.1 Core location

In order to obtain a fully representative record of sediment accumulation over the whole of the lake basin it was anticipated that, in the context of most lake sediment studies, a very large number of cores would need to be sampled. This in turn required an accurate method of core location. The system selected involved constructing a base-line marked out with ranging poles at 10 m intervals along the western shore. Once this had been achieved, a quick-set level was used to sight across the lake at 90 degree angles to the base-line in order to locate the positions of a second line of ranging poles at 10 m intervals along the eastern shore. Therefore, by stretching ropes marked off in 10 m intervals across the lake between the two lines it was possible to obtain cores along a series of parallel lines approximately at 90 degree angles to the long axis of the lake. The grid axes established by this system are illustrated in Figure 2.4 (Chapter 2, section 2.4)[1]. All of the cores obtained during the course of this study are referenced by the grid co-ordinates of the site from which they were obtained: for example the code 40/-120 refers to the core obtained from the point defined by longitudinal (parallel to the base line) grid-line 40 and transverse grid-line -120. The units are metres.

---

[1] This simple scheme of core location is well suited to lakes of moderate dimensions; however, in the case of larger lakes more sophisticated methods would be required. One possible technique is laser-beam tacheometry, successfully used in a similar, although smaller-scale exercise on Lough Augher, Co. Tyrone, Northern Ireland (R.W. Batterbee, personal communication). However, accuracy of core location would probably best be achieved by working from a frozen lake surface.

3.2 Lake sediment sampling

The cores from the Goddionduon lake basin were obtained during two main periods of field-work: 131 ca. 0.5-1.1 m-long cores were taken during a two week period in July 1977, by a team varying from five to nine people, operating two Mackereth pneumatic minicorers (Mackereth, 1969) from two inflatable dinghies. This corer obtains a near-perfect mud/water interface. Cores were obtained at 20 x 20 m grid-line intersections over the whole of the lake basin, barring those areas with an impenetrable substrate, in which case intermediate cores were taken. For reasons given in Chapter 4 (section 4.3.1) it was considered that the small 'trench' area would have been subject to rates of sediment accumulation substantially higher than over the remainder of the lake basin. Therefore, in order to permit detailed monitoring of sedimentological changes in the trench, cores were obtained at 5 m intervals along three lines arranged parallel to its long axis. A second set of 11 ca. 1.8 m long cores was obtained during July 1979 from the central area of the lake basin by a team of three people using the corer described in Appendix A. These longer cores are referenced subsequently by the letter 'L' (e.g. 60/60L).

After being brought into the boat, the cores were immediately sealed at the top either with a screw-on brass cap or rubber bung and at the base with a rubber bung and electrical tape. Care was taken to ensure that the cores were transported to the laboratory in a vertical position. Upon arrival, the cores were prepared for whole core susceptibility measurements (section 3.4.1, below) by siphoning the surplus water from the top and pushing a rubber bung down to the upper mud surface.

A Russian corer (Jowsey, 1966) with a 50 cm-long, 5 cm-diameter chamber, was used for lithostratigraphical investigations and for collection of samples for ^{14}C dating. On open water, the corer was

operated from an inflatable dinghy; in order to provide a sufficiently stable platform for coring it was found to be necessary to tie-up to two ropes arranged transversely across the lake and pulled as taught as possible. Coring was limited to shallow (less than 3 m deep) water. When working from the dinghy it was found to be physically impossible to push the corer below sediment depths of ca. 5 m.

3.3 Extrusion

The sediment was extruded from the core tubes by inserting a rubber bung, of appropriate diameter, attached to a wooden pole into the bottom of the tube. By holding the tube vertical and exerting slight downward pressure, the top of the sediment column was forced upwards into a perspex ring of either 1 cm, 2 cm or 5 cm depth, held firmly to the top of the tube. The sediment was then sliced off using a thin perspex sheet. In most cases the top 4 cm of each core was sliced into 1 cm-thick discs, and the rest into 2-cm thick discs. These were stored in petri dishes or in sealable plastic bags. For some of the cores, the top 10-20 cm were extruded as described above, the remainder then being extruded directly into polythene-lined 'V'-shaped wooden troughs. These were sealed in polythene 'tubes' and stored until required.

3.4 Magnetic measurements

Definitions of the magnetic parameters referenced below are given in Chapter 1 (section 1.6).

3.4.1 Whole core susceptibility measurements

Whole core susceptibility measurements were carried out on the bridge described by Molyneux and Thompson (1973). The air-cored coil system has a cylindrical sample head of 8.5 cm diameter through which the core is passed. As it does so the core tube passes over a roller attached to a slotted disc and photocell arrangement, which causes

measurements to be taken at approximately 2.7 cm intervals along the core. The sensor signal drops to 66 percent at about 3 cm from the end of the sample, and therefore the measurements obtained represent a smoothed version of the true susceptibility record, features closer than about 6 cm being unresolved; in addition, susceptibility peaks at the extremities of cores are considerably reduced in magnitude. The measurement procedure is extremely rapid, taking about 1 minute to measure a 1 m core. In operation, the instrument is interfaced with a mini-computer which lists the measurements on a teletype and onto paper tape; the latter can subsequently be used as data input for graph-plotting computer programs.

Whole core volume susceptibility (k) measurements of all the cores obtained during July 1977 were carried out during the same two-week period of field-work using the equipment described above installed temporarily in the Drapers' Field Centre, Rhyd-y-Creuad, ca. 3.5 km from the lake. Whole core k versus depth graph plots were produced automatically on a teletype after measurement, making it possible to plan day-to-day field sampling priorities in the light of results obtained within a few hours of taking each set of cores.

Whole core k measurements of the set of 1.8 m-long cores obtained during July 1979 were made at the Department of Geophysics, University of Edinburgh, using identical instrumentation.

3.4.2 Sample preparation for dry-weight specific magnetic measurements (sections 3.4.3-3.4.5, below)

Lake sediment samples were oven-dried overnight at 90°C. Ca. 5-10 g of the dried sediment were then placed in small plastic bags, lightly crushed with a pestle and then transferred to pre-weighed plastic

cylinders of 10 cc volume. The sediment was packed down as tightly as possible and the cylinder sealed with a plastic cap. The weight of cylinder plus sample was then obtained. After weighing, if the sediment did not completely fill the cylinder, clean foam rubber was inserted to prevent movement of material during remanence measurements (section 3.4.4 , below). Soil samples were treated in the same way, except that the greater than 2 mm particle size fraction was removed by dry sieving.

Selected soil and stream bedload samples were subjected to a simple fractionation procedure involving suspension in de-ionised water, followed by wet sieving down to 45 μm. No chemical dispersants were used. The fractioned samples were then treated in the manner described above.

3.4.3 Single-sample susceptibility measurements

The majority of measurements were made on an air-cored bridge similar to that described in section 3.4.1, but with a 3 cm diameter aperture. The noise level is about 2 μ SI units. A small number of measurements were made on a 'Highmoor' variable temperature susceptibility bridge (Highmoor Scientific Instruments Ltd.).

3.4.4 Remanence measurements

The majority of measurements were made on a Digico complete result balanced fluxgate spinner magnetometer, interfaced with a minicomputer (Molyneux, 1971). The noise level is about 0.1 mA m^{-1}. A small number of measurements were made on a parastatic magnetometer at the Department of Geophysics, University of Liverpool; the noise level was at least two orders of magnitude less than the measured remanences.

The instruments described above were used for measuring ARM and SIRM, and for obtaining the coercivity of SIRM $(B_0)_{CR}$ and 'S' values. ARMs were grown in samples in a peak alternating field (AF) of 100 mT with a DC field of 0.05 mT superimposed, the DC field being applied parallel to the axis of the coil generating the AF.

Samples were given an SIRM by placing them in a 1 T DC field generated by a conventional electromagnet. Selected samples were placed in successive reversed fields of increasing strength, and the change in IRM measured at each stage, in order to obtain the $(B_0)_{CR}$. The $(B_0)_{CR}$ was estimated by fitting an approximating cubic spline to the IRM curve and iterating to the point of intersection of the cubic spline function with the zero remanence axis. After measurement of SIRM, selected samples were placed in a reversed field of either 40 or 100 mT to obtain the parameter 'S'. In this study, 'S' values are expressed in terms of 'percentage reverse saturation': for example, an S_{100} value of 100 percent indicates that after growth and measurement of SIRM the magnetization of the sample is completely resaturated in a reverse field of 100 mT.

3.4.5 Magnetization hysteresis loop measurements

The magnetization hysteresis loops of a small number of samples were measured with a vibrating-sample magnetometer at the School of Physics, University of Newcastle. A peak field of 1.05 T was used in constructing the loops. The noise level of the instrument was about 0.2 Am^{-1}.

3.4.6 Data handling

The raw magnetic data were routinely filed on the Liverpool ICL 1906S computer. Subsequently, three kinds of FORTRAN computer program

were used for data handling and presentation: (i) for calculating dry-weight specific magnetic parameters and various susceptibility and remanence ratios and plotting them against depth; (ii) for plotting susceptibility versus SIRM diagrams; (iii) for plotting coercivity of SIRM curves (R. Thompson, personal communication).

3.5 Wet density, percentage water content and percentage weight loss on ignition

The wet density of lake sediment samples was obtained by filling pre-weighed plastic cylinders of known volume with sediment. The weight of cylinder plus sediment was then obtained. Percentage water content was measured by reweighing samples after oven-drying overnight at 90°C. Percentage weight loss on ignition was measured subsequent to percentage water content determination by reweighing samples after ignition at 450° C for 4 hours in a muffle furnace.

3.6 Chemical analyses

The concentrations of Fe, Mn and Al of selected lake sediment samples were measured by two methods: (i) by atomic absorption spectrophotometry (Pye-Unicam SP 190 atomic absorption spectrophotometer) after HNO_3-HF digestion; and (ii) by X-ray fluorescence (XRF) (Philips PW 1410 X-ray spectrometer). Both instruments were calibrated with solutions containing a known concentration of the relevant element. The relative concentrations of additional elements were determined by XRF (see Chapter 7, section 7.4).

3.7 Pollen analyses

Lake sediment and peat samples were prepared for analysis using techniques similar to those described by Faegri and Iversen (1975): removal of humic acids with 10% NaOH; removal of siliceous material with 40% HF and removal of cellulose with a mixture of 9 parts $(CH_3.CO)_2O$ to 1 part concentrated H_2SO_4. Highly minerogenic samples (for example, Late-glacial clay) were dispersed using 5% $Na_4P_2O_7$ and

then subjected to a density separation using a solution of $ZnCl_2$ with a density of 2.0 g cm^{-3} (Björck et al., 1978). Subsequent to chemical treatment, the samples were stained with aqueous safranin and either dehydrated with tertiary butyl alcohol and mounted in silicone oil (viscosity 1000 cSt), or mounted directly in glycerol. A small number of samples were analysed without chemical pretreatment (see Chapter 4, section 4.3.1).

Pollen and spore counts were carried out using Nikon (L-Ke Model) and Leitz 'Dialux' microscopes. A magnification of X400 was used for routine counting, critical identifications being made at X1000 using an oil-immersion objective. For most samples, either 150 tree pollen grains or 500 land pollen grains and spores were counted. Pollen and spore types were identified using a reference slide collection and by reference to pollen keys, descriptions and photographs in Beug (1961); Birks, 1973; Faegri and Iversen (op. cit.) and Moore and Webb (1978).

CHAPTER 4 LITHOSTRATIGRAPHY, MAGNETOSTRATIGRAPHY AND CORE CORRELATION

4.1 Introduction

Section 4.2 presents the results of a series of Russian corer borings which were carried out within the present lake basin and on the small bog (Chapter 2, section 2.4) in order to estimate the total volume of sediment accumulated within the lake basin during the Post-glacial period. It was hoped that this would provide a mean value for the rate of sediment influx for a period of time, a substantial proportion of which was characterised by minimal human activity: i.e. the interval from ca. 10 000 to 5000 bp, corresponding to West's (1970) chronozones I and II. Therefore, this would provide a perspective for the evaluation of more recent rates of sediment influx.

Sections 4.3-4.5 present the results of attempts to define synchronous horizons within 1-2 m-long sediment cores, on the basis of both magnetostratigraphic and lithostratigraphic variations.

The results described in sections 4.2-4.5 are used to construct three sediment isopach contour maps (Chapter 6) and using a chronology of sediment accumulation established in Chapter 5 used to estimate the mean rate of sediment influx and yield for the period of time represented by each contour map.

4.2 Russian corer borings

Because of excessive water depth and since it is possible to elucidate the history of Flandrian sedimentation for the northern part of the lake basin from the records of 1-2 m-long cores (section 4.3, below), Russian coring was restricted to that part of the basin south of the /0 line. One boring transect (A-B) approximately along the long axis of the lake basin and three transects (C-D, E-F,

G-H) perpendicular to A-B are shown in Figure 4.1. Transects A-B and E-F reveal the presence of a ridge lying approximately along the /120 line, and which therefore divides the basin into sub-basins. At site 60/120 the top of the ridge lies ca. 5 m below the present lake level and is covered by ca. 3 m of sediment. In neither sub-basin was it possible to determine the maximum thickness of Post-glacial sediment; the greatest depths penetrated were 5.2 m (site 70/40) in the northern and 7.9 m (site 35/200) in the southern sub-basin.

With the exception of the 'trench' area, the stratigraphy of which is described in section 4.3 (below), both sub-basins contain essentially the same sequence of deposits. At the base of the sequence is solid rock or gravel, overlain by clays, clay-muds and muds of the Devensian Late-glacial period. Proceeding from the base upwards, the Late-glacial sequence typically consists of (i) variously-coloured laminated clays; (ii) clay muds and muds of the Windermere Interstadial period (there is considerable spatial variation in the organic content of this layer, although it appears to be significantly higher in the southern sub-basin); (iii) variously-coloured laminated clays of the Loch Lomond Stadial period. Ince (1980) has obtained three radiocarbon dates for the Late-Devensian and early Flandrian sediments beneath the Goddionduon peat bog. These dates are shown in Table 4.1, together with details of the lithostratigraphic and pollen biostratigraphic contexts of the samples from which they were obtained.

The Devensian Late-glacial deposits are overlain by early Flandrian clay muds, the lowermost sections of which are frequently laminated. These are in turn overlain by fine, and at marginal sites, medium and coarse detritus muds of the middle and late Flandrian. The detritus muds range in colour from dark grey-green

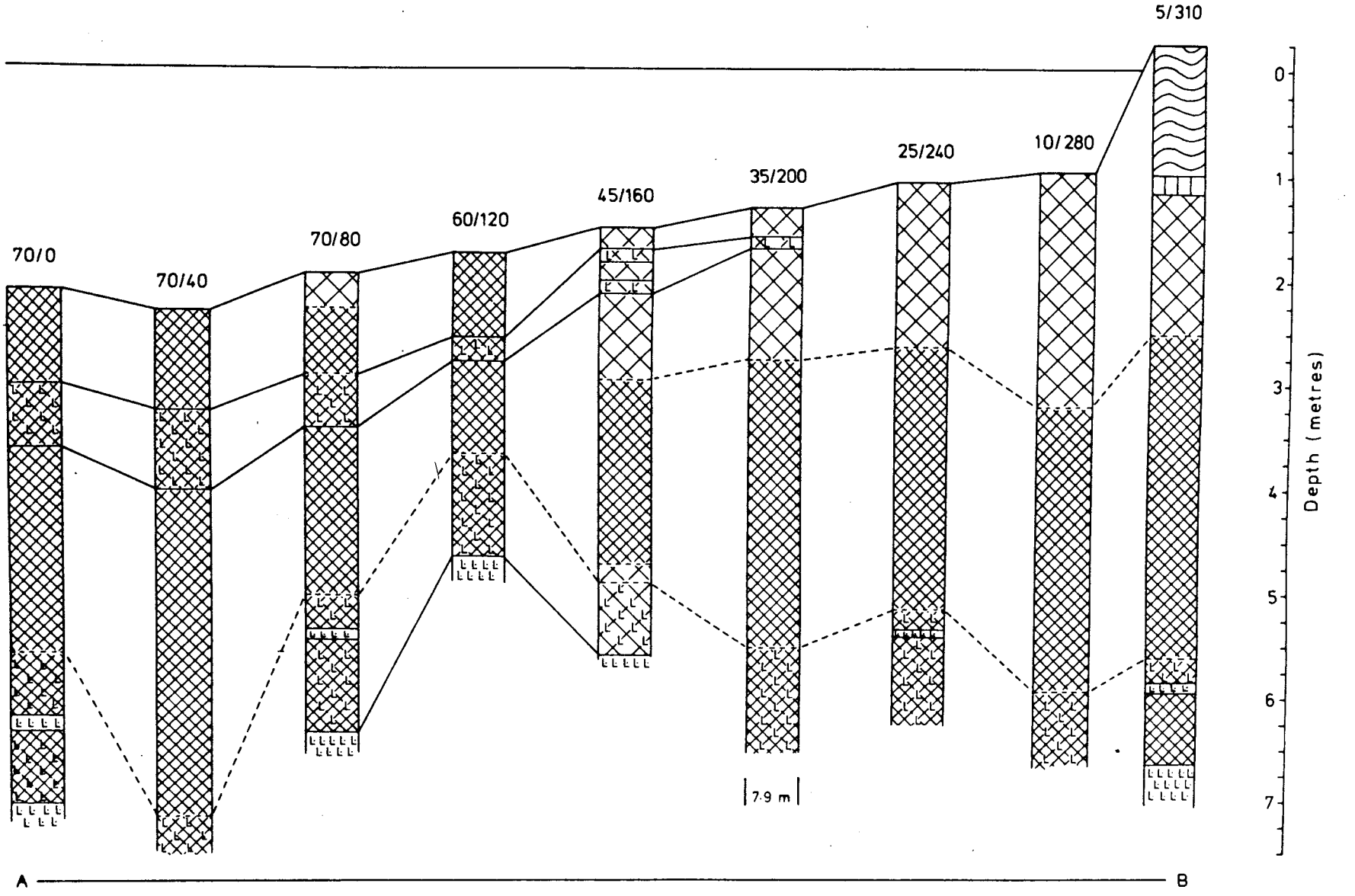

Figure 4.1 Boring transects

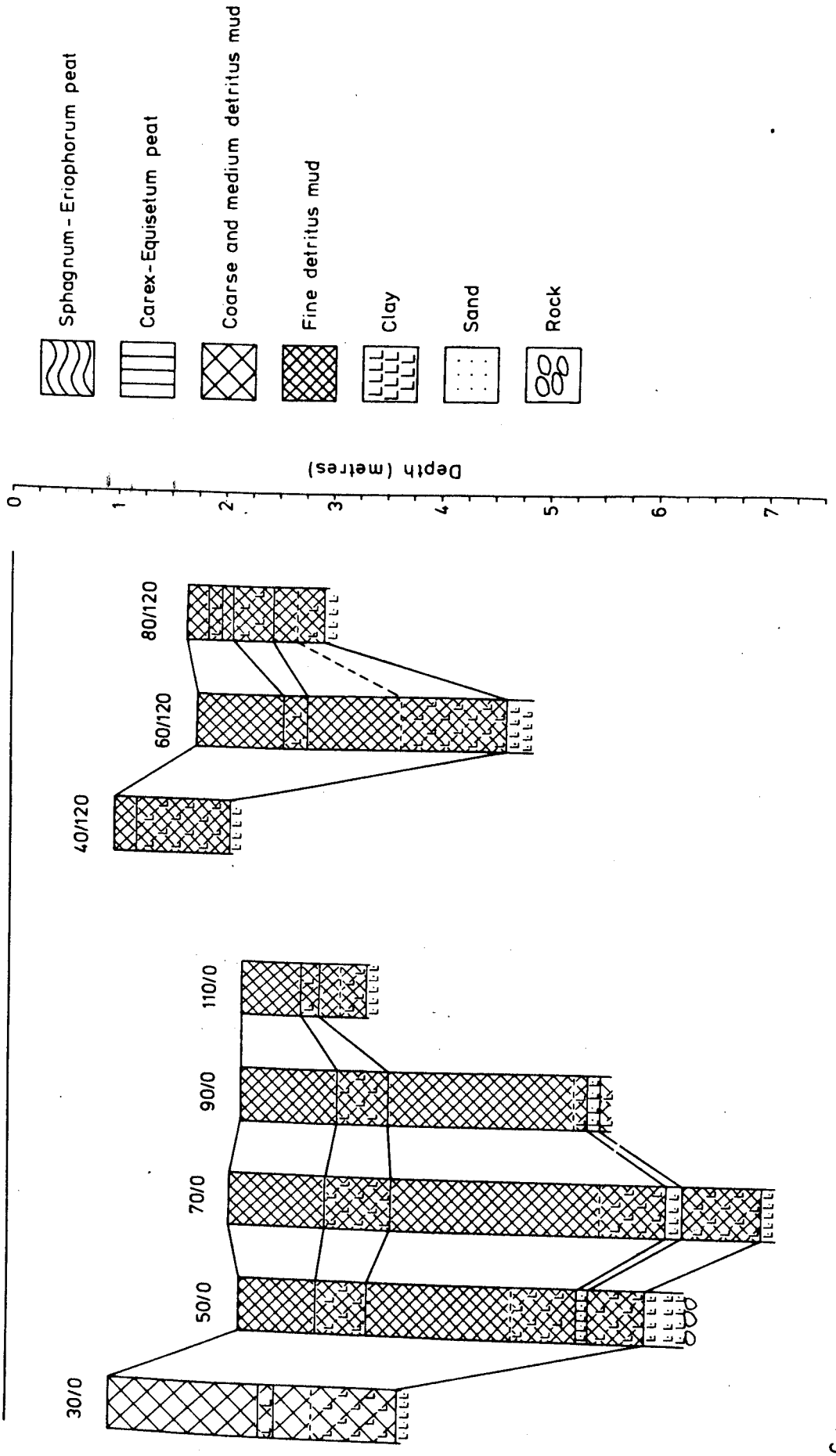

Figure 4.1 continued

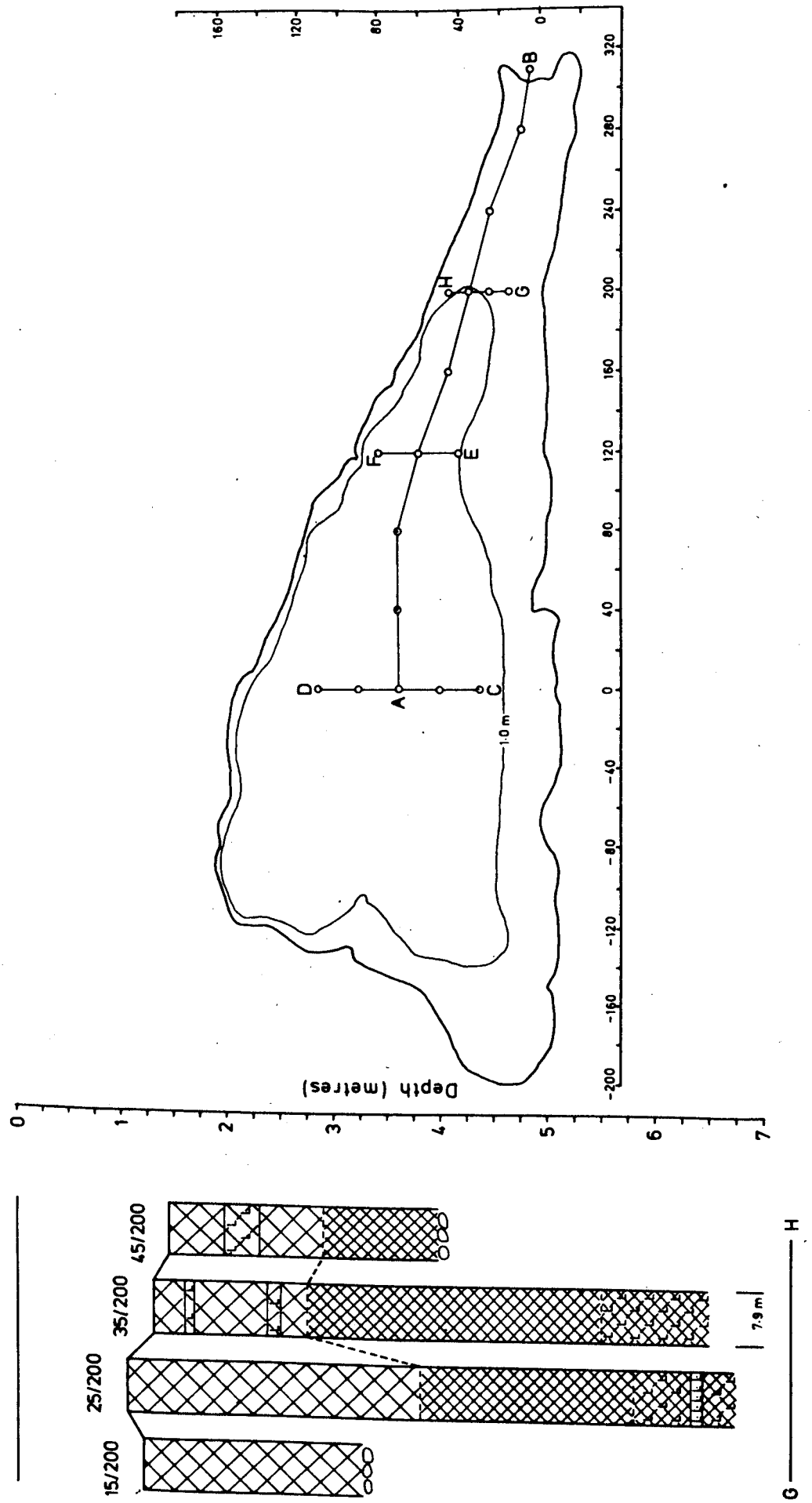

Figure 4.1 continued

Age (^{14}C years bp)	Number	Local Pollen Assemblage Zone (Ince, 1980)	Lithostratigraphic context of sample
10 415±320	GU-1081	LG5. Juniperus-Betula	10 cm sediment slice immediately above contact between Loch Lomond Stadial clays and early Flandrian clay muds.
11 125±265	GU-1080	LG3. Juniperus-Betula-Gramineae	2 cm sediment slice immediately below contact between Windermere Interstadial clay muds and Loch Lomond Stadial clays
13 735±330	GU-1079	LG2. Gramineae-Rumex	3 cm sediment slice at base of Windermere Interstadial clay muds

Table 4.1 Radiocarbon dates for Late-Devensian and early Flandrian sediments from beneath the Llyn Goddionduon peat bog. (Source: Ince, 1980).

to dark brown and are generally homogeneous in composition; however, at almost all of the sites investigated they are interrupted within ca. 2.0-0.2 m of the sediment surface by a zone of pronounced and varied colour changes. The complexity of these is indicated by the following field notes for boring site 70/0 (depths in cm):

20-36	Dark brown fine detritus mud
(36-42)	Slightly clayey mud; colour changes as follows:
36-38.5	Dark green
38.5-39.5	Pale grey
39.5-40.5	Dark green
40.5-41	Pale grey
41 -42	Dark green
42 -87	Dark brown fine detritus mud
(87 -149)	Slightly clayey mud; colour changes as follows:
87 - 88	Pale yellow
88 - 97	Pale grey
97 - 98	Dark green
98 -102	Alternate pale grey and green bands
102 -108	Pale greyish orange
108 -116	Pale green
116 -117	Pale yellow

117-130	Pale grey
130-131	Pale yellow
131-133	Dark orange brown
133-136	Pale grey
136-146	As above, with two ca. 0.5 cm-thick pale yellow bands in upper part of section
146-149	Alternate ca. 0.5 cm-thick dark green and grey bands
149-320	Dark brown fine detritus mud

This zone is also characterised by increased wet density, decreased percentage water content and by increases in magnetic susceptibility (see Appendix B and section 4.3, below).

In addition to the Devensian Late-glacial and Flandrian open-water sediments, the bog immediately adjacent to the southernmost part of the present lake basin contains 10-20 cm of Phragmites-Equisetum reedswamp peat, overlain by 1-2 m of Sphagnum-Eriophorum bog peat. Boring site 5/310 (Figure 4.1) illustrates this succession. The abruptness of the change from lake mud to reedswamp peat implies a relatively sudden change from open water to wet ground rather than a gradual autogenic hydroseral succession. This is in turn implicates a reduction in lake level as the mechanism responsible. There is no evidence at site 5/310 of the near-surface variously-coloured clayey layers present at the open water sites.

A series of additional borings was carried out on the peat bog; at most of these sites only the depth to impenetrable basement was determined. The results are used in the construction of sediment isopach contour maps (Chapter 6).

4.3 Whole core magnetic susceptibility measurements

4.3.1 The 'trench' grid

Figure 4.2 shows plots of whole core volume susceptibility (k) versus depth for 44 cores sampled approximately at 5 x 5 m grid-line intersections from the small 'trench' area in the northern part of the lake basin. The origin of each graph represents the point on the grid network from which the core was obtained. The first tick on the

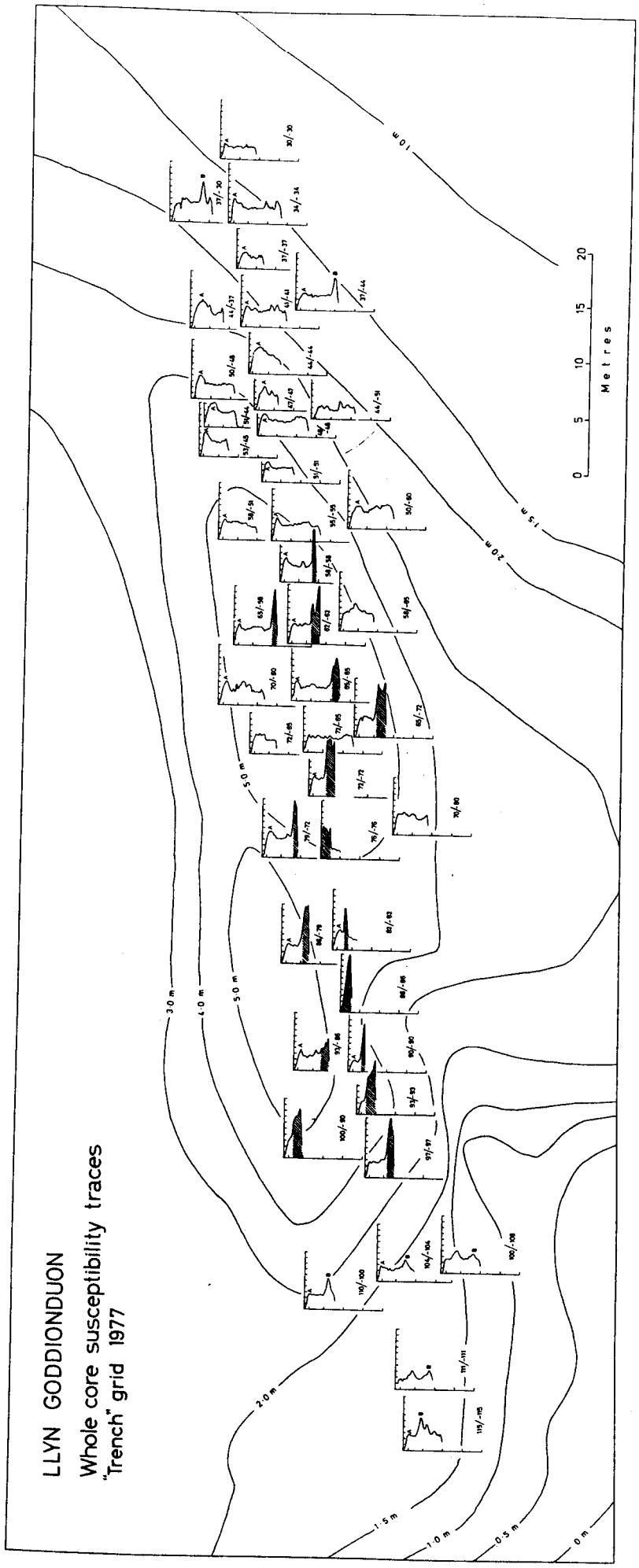

Figure 4.2 Whole core k traces: 'trench' grid

depth (vertical) axis corresponds approximately to the top of the sediment. The increment on the depth axis is 25 cm, and that on the volume susceptibility axis is 5×10^{-6} SI units. Selected isobaths for the sampled area are also shown.

Almost all of the cores from water depths greater than 4 m exhibit pronounced k peaks which correspond to a lithology of clay, interpreted as Late-Devensian in age. In Figure 4.2 the sections of cores containing clay are shaded. At one of the sites (76/-76) a core was retrieved which contained clay layers with no overlying detritus mud. The relatively high k of the clay layers in comparison with the overlying detritus muds is a function of the much higher wet density of the former; when expressed on a dry-weight specific basis the magnetic concentrations of the clays and detritus muds were shown to be much more comparable (see Chapter 7, section 7.5.4).

The occurrence of Devensian Late-glacial deposits within the trench cores clearly implies that there has been negligible sediment accumulation during the Post-glacial period within what is at present the deepest part of the lake basin. Since this contradicts the results of several workers which indicate a tendency for the most rapid accumulation of sediment within small lake basins to occur within the deepest areas (see Chapter 9, section 9.3) it was considered important to confirm that the clay layers are of Late-glacial provenance. With this intention, a number of pollen analyses was carried out on samples from selected trench cores, and an attempt made to tentatively assign the pollen spectra to the local and regional pollen zonation schemes of Walker (1977) and Ince (1980). By this means approximate ages can be assigned to the horizons of the cores from which the samples were obtained. With the exception of core 86/79 the analyses were carried out on unprepared samples. The percentage pollen counts are given in Appendix C. Table 4.2 shows the

Table 4.2 Relationship of the pollen spectra from Goddionduon minicores to the pollen zonation schemes of Walker (1977) and Ince (1980).

Core and sample depth (cm)	^{14}C years bp	Regional Pollen Assemblage Zone (Walker, 1977)	Local Pollen Assemblage Zone (Ince, 1980)
60/-80 58 60/-80 94.5 60/-120 14-16 34/-34 116-118		SN5B Quercus-Alnus-Corylus-Ericales	
	ca. 2150[1]		
34/-34 116-118 41/-41 92-94 50/-43 20-22		SN5A Quercus-Alnus-Corylus	
	2925[2]		
41/-41 92-94 50/-43 20-22 140/-100 52-54		SN4 Quercus-Alnus-Ulmus-Corylus	
	ca. 7150[1]		
50/-43 58-60 48/-48 116-117 55/-55 116-117		SN3 Pinus-Quercus-Ulmus-Corylus	LG7 Betula-Pinus-Corylus
	ca. 8800[1]		
86/-79 140/-100		SN2 Betula-Pinus-Juniperus-Salix	LG6 Betula-Polypodiaceae
			LG5 Betula-Juniperus
	10257[2], 10415[3]		
		SN1 Betula-Pinus Gramineae	LG4 Pinus-Cyperaceae-Artemisia

Notes: 1. Date from Melynllyn, Gwynedd (Walker, 1977) 2. Date from Scaleby Moss, Cumbria (Godwin et al., 1957) 3. Date from Llyn Goddionduon bog (Ince, 1980).

relationship of the spectra to the pollen assemblage zonations, together with the radiocarbon ages of the zone boundaries; if a spectrum could not be assigned unambiguously to a particular assemblage zone it was included in each of the possible alternatives. Table 4.2 includes the results of the analyses of samples from several main grid cores; the significance of these is considered in section 4.3.2, below.

Four pollen analyses were carried out on samples from core 86/-79. The lithostratigraphy of this core was as follows:

0-32 cm	Dark grey-brown fine detritus mud
32-41 cm	Grey clay
41-76 cm	Pale grey clay

No pollen was found in samples from 33-34 cm, 36-37 cm and 39-40 cm; however, they contained small numbers of unidentified trilete microspores, presumably of pre-Quaternary origin. A sample from 30-31 cm yielded a pollen spectrum, which as indicated in Table 4.2 may be assigned to Ince's (1980) early Flandrian pollen assemblage zone LG6 (Betula-Polypodiaceae), thereby confirming the Late-glacial origin of the clay. Samples from cores without clay layers from the southwestern end of the trench (55-/-55, 48/-48, 50/-43, 41/-41) yielded spectra with either early Flandrian or middle Flandrian ages, confirming the paucity of sediment accumulation in this area of the lake basin during Post-glacial time.

In addition to those in the clays, k peaks also occur in the detritus muds. The most consistent of these occurs at the top of the cores and is designated 'A' in Figure 4.2; it is subsequently referred to as k peak A. Figure 4.3 shows a correlation diagram of peak A in cores on a northeast-southwest transect along the long axis of the trench; it is most evident, both in terms of k and vertical extent, in cores near the southwestern end of the trench. (Because whole core measurements mask susceptibility variations at the

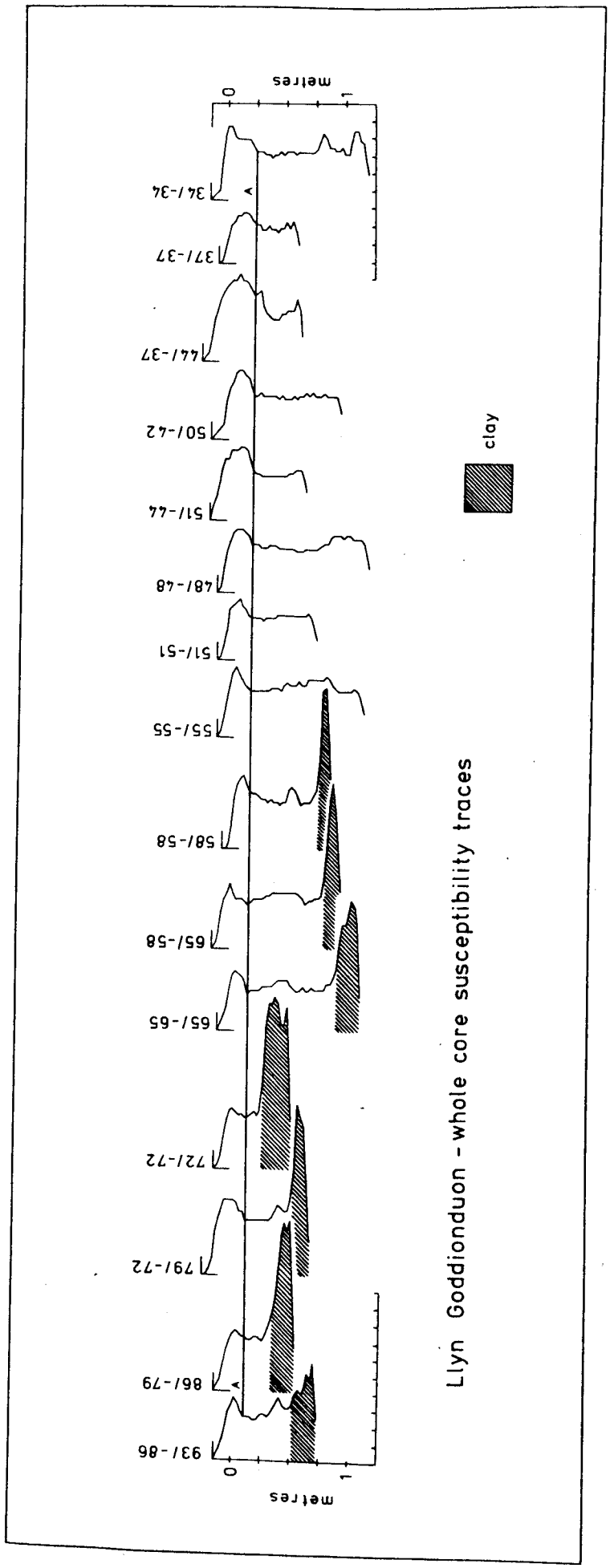

Figure 4.3 Correlation diagram of whole core k traces: 'trench' cores

extremities of cores this feature is much more pronounced when expressed on the basis of dry-weight specific magnetic measurements (section 4.3.2, below)). In many cases there was an association between peak A and the presence of black-coloured sediment at the tops of the cores. This is clearly illustrated in the results of single-sample magnetic measurements of core 50/-43 (Chapter 5, section 5.2).

Several of the cores in Figure 4.2 exhibit major subsurface k variations not attributable to clay layers: 115/-115, 111/-111, 110/-100, 100/-108, 104/-104, 37/-44 and 37/-30 have either one or two major k peaks. The most pronounced of these is designated 'B' and is subsequently referred to as k peak B. All of the cores listed above are marginal to the trench, from depths shallower than 2m.

4.3.2 Main grid

Figure 4.4 shows the k traces for 75 of the minicores obtained during July 1977 approximately at 20 x 20 m grid-line intersections over the whole of the lake basin. The format of the plots is identical to that in Figure 4.2, and again the sections of cores containing basal Late-glacial clay are shaded. Unsampled areas reflect the occurrence of impenetrable substrate. To aid presentation and description of the results the lake has been divided arbitrarily into three sectors: north, central and south. Figures 4.5, 4.6 and 4.8 show enlarged diagrams of the k traces for minicores from the north, central and south sectors respectively, allowing the changes to be seen more clearly. Figure 4.7 shows the k traces for 9 of the 2 m cores taken from the central area of the lake during July 1979. The 1.5 m isobath is shown in Figures 4.5-4.8, while in Figure 4.5 the 4 m isobath is included to show the location of the trench. The pattern of k variations in the three sectors is described below.

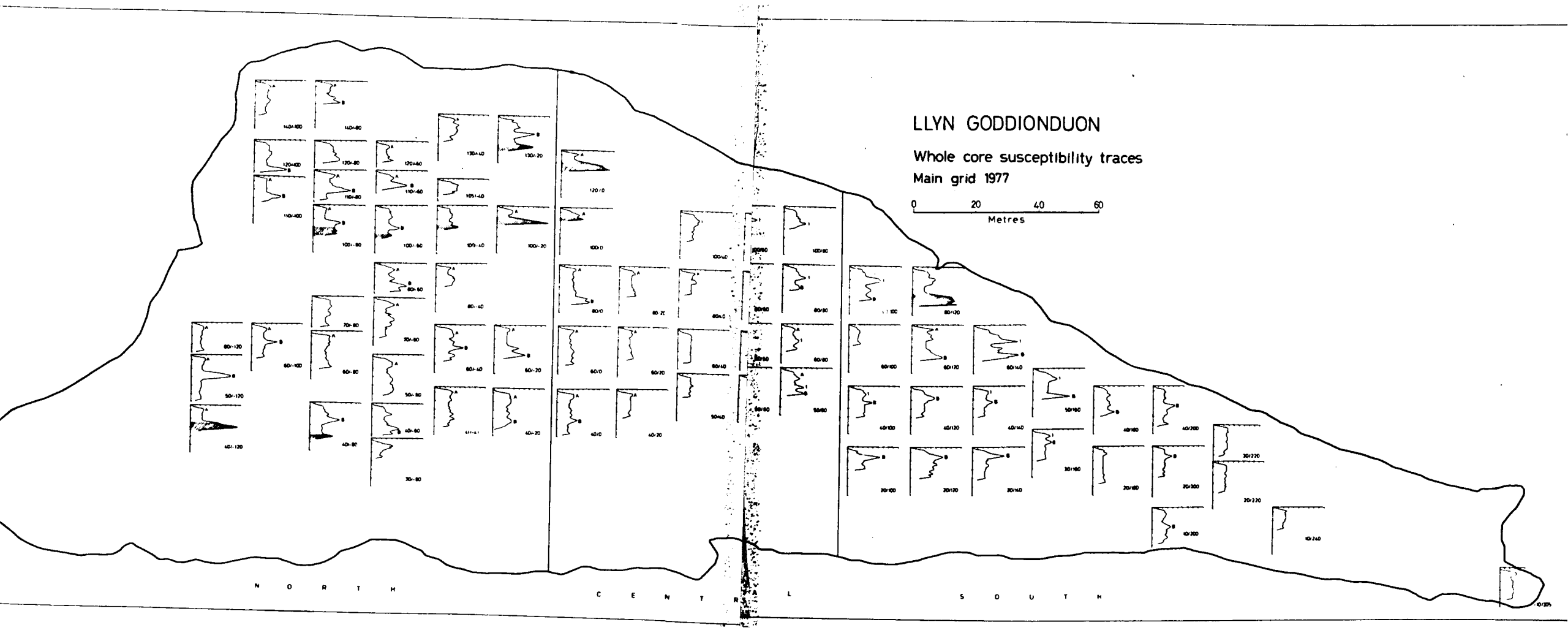

Figure 4.4 Whole core k traces: main grid.

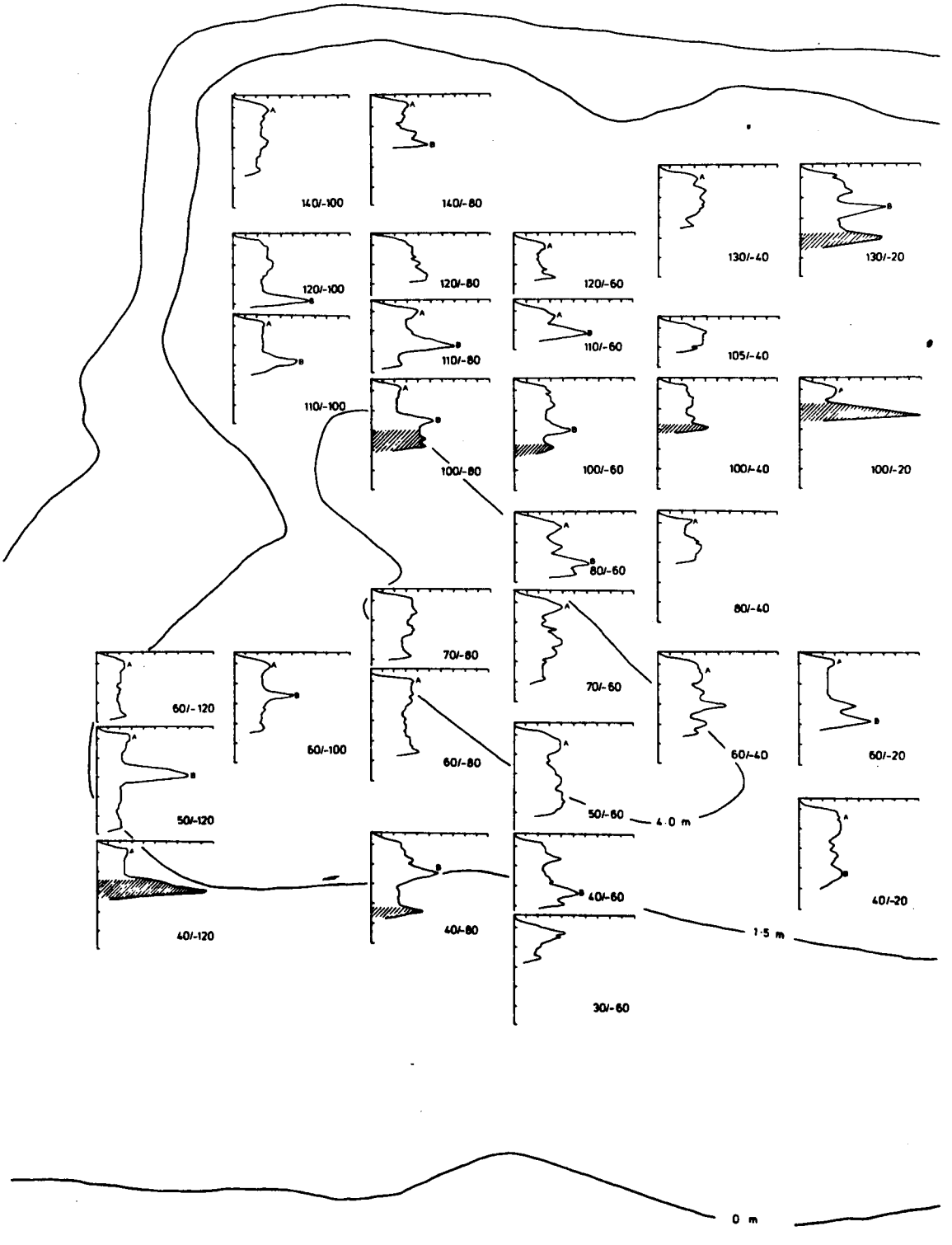

Figure 4.5 Whole core k traces: north sector

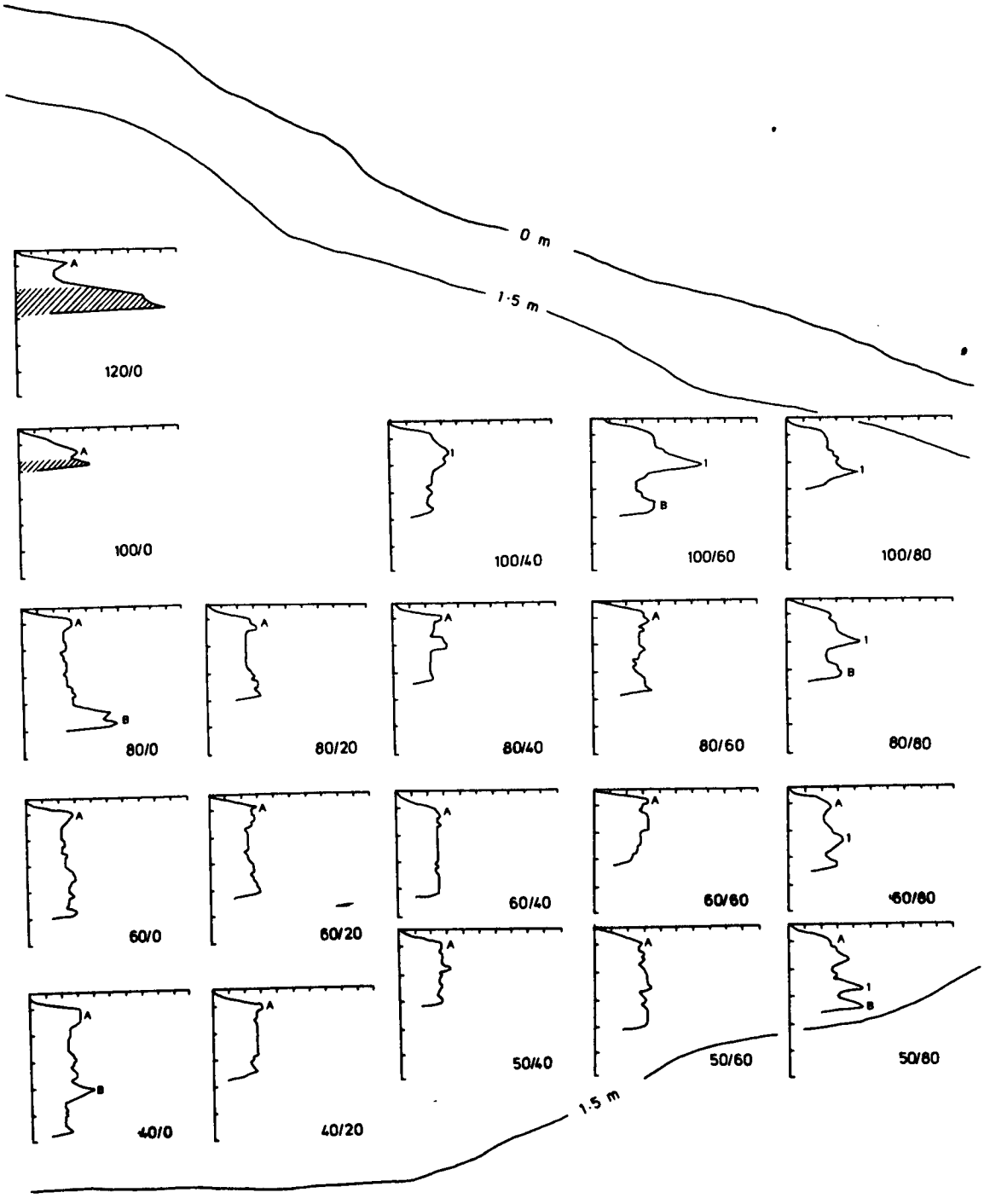

Figure 4.6 Whole core k traces: central sector

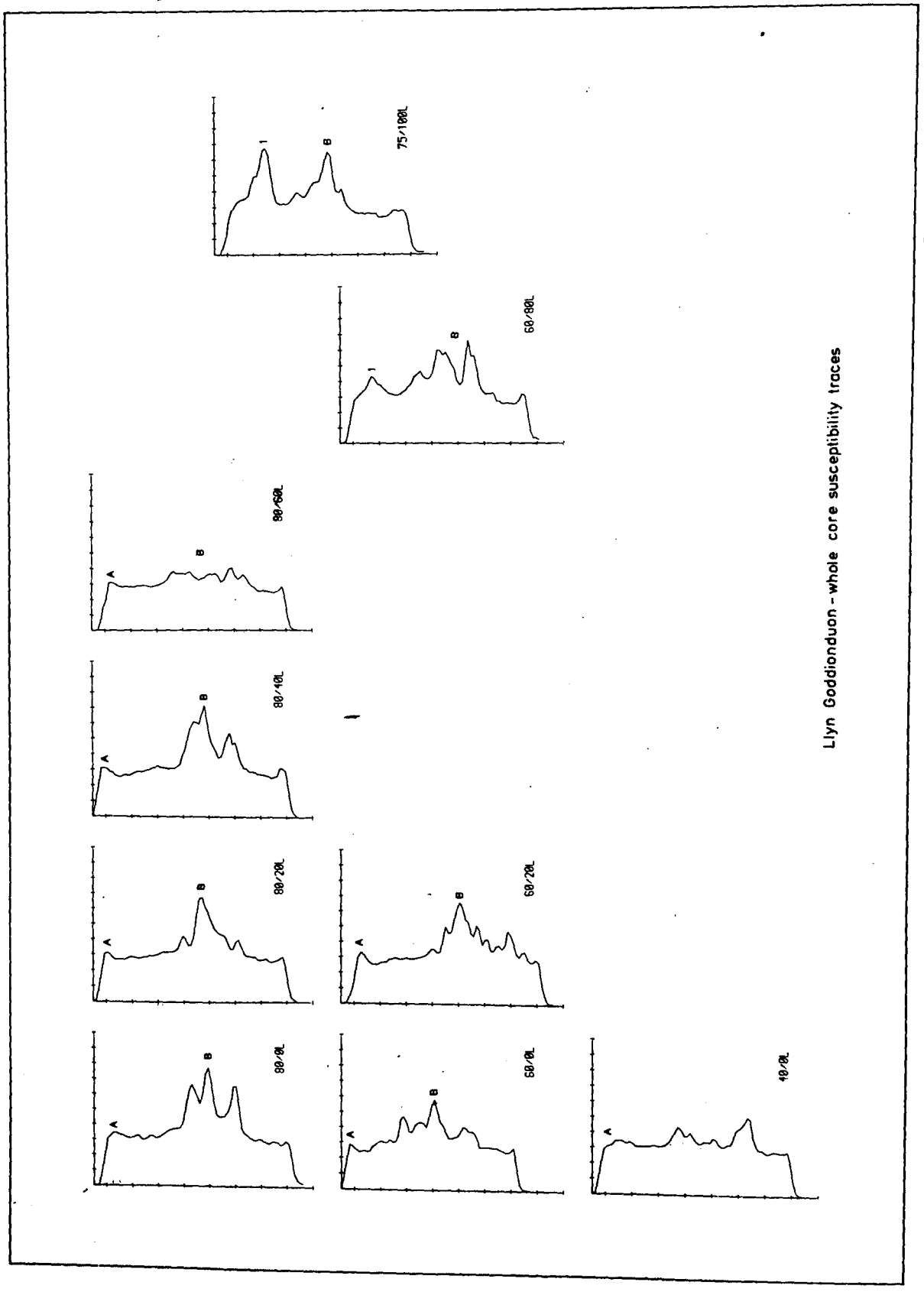

Figure 4.7 Whole core k traces: central sector (2 m cores)

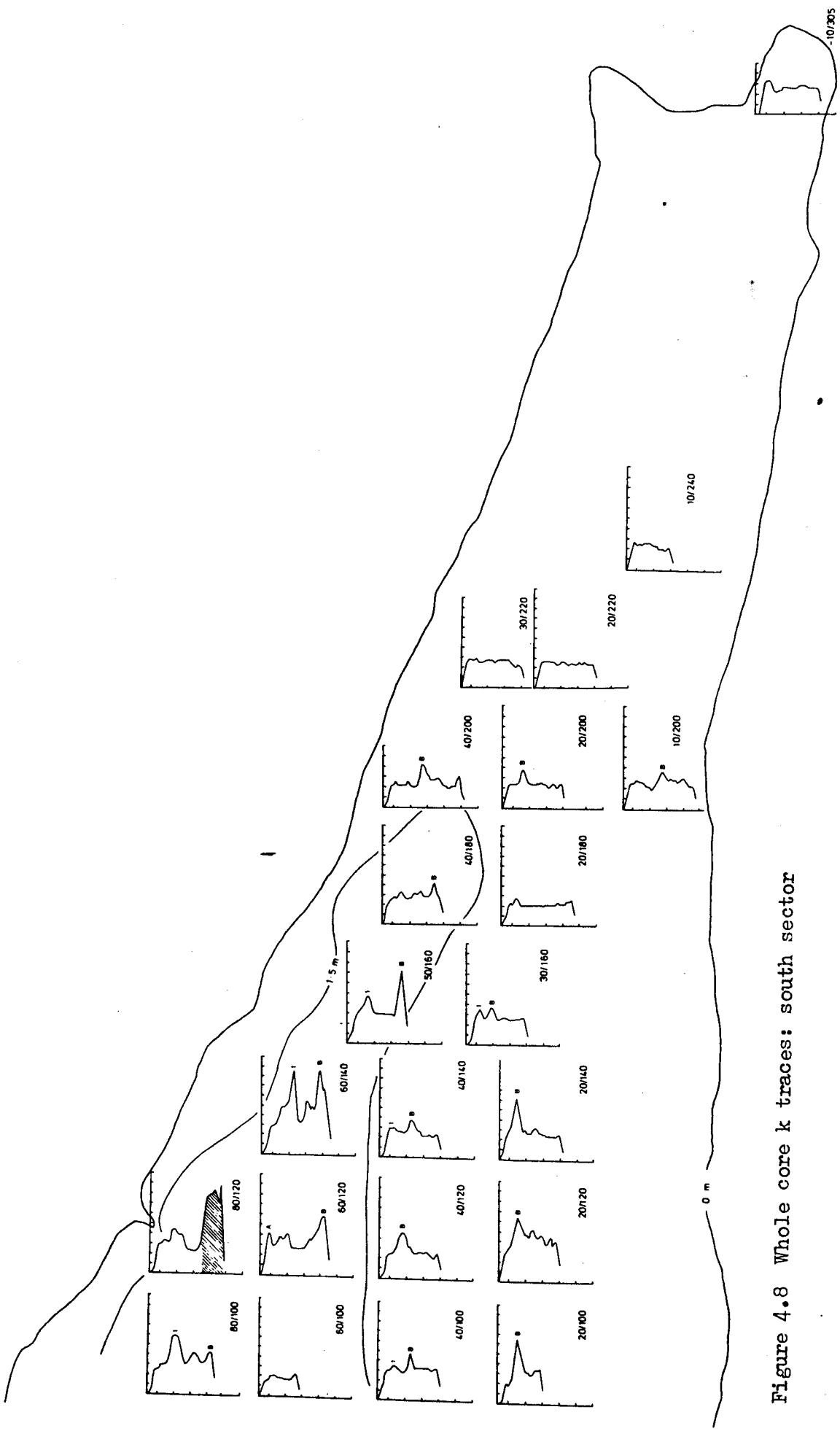

Figure 4.8 Whole core k traces: south sector

Northern sector (Figure 4.5)

Several of the cores have k peaks attributable to basal clay: marginal cores 40/-120, 40/-80 and 130/-20, and the more centrally located cores 100/-20 and 100/-40. The latter were sampled from an area of the lake basin from which several field records were made of occurrences of rocks (sites 110/-40, 115/-40, 120/-40, 120/-20), despite the fact that sites of equivalent or shallower depth in other areas of the lake basin have accumulated substantial depths of sediment.

Many of the cores exhibit the uppermost k peak (A) noted in the trench cores (section 4.3.1); and again the greatest thickness of this horizon may be seen to occur in or near the southwestern end of the trench: for example, in cores 70/-60, 50/-60, 60/-40 and 40/-20. Excluding the basal clay layers, several of the cores have a subsurface horizon of high k, either as a single pronounced peak (as in cores 50/-120, 60/-100, 110/-100 and 120/-100) or as a more extended and complex feature (as in cores 80/-60, 60/-40 and 60/-20). This feature is considered to correlate with k peak B noted in section 4.3 (above) and is designated as such in Figure 4.5. The occurrence of this feature is sporadic: for example, it is present at ca. 40-50 cm in cores 50/-120 and 60/-100, while in adjacent cores 60/-120 and 60/-80, from similar water depths, it is absent. Similarly, it is present in cores 120/-100 and 140/-80, but absent in adjacent core 140/-100.

In order to determine whether its inconsistent occurrence was due to the presence of extensive sedimentary hiatuses, pollen analyses were carried out on selected samples from cores 60/-120, 60/-80 and 140/-100. The percentage pollen counts are given in Appendix C. The relationship of the spectra to local and regional pollen zonations is shown in Table 4.2 (above). The assignment of the spectra from

core 140/-100 to pollen assemblage zones pre-dating 5000 bp clearly indicates a major hiatus. However, the spectra from cores 60/-120 and 60/-80 are of recent age, implying that the absence of k peak B in these cores may be caused by substantial variability in sediment accumulation rates, even between adjacent coring sites.

Several of the k traces in Figure 4.5 are difficult to interpret: cores 120/-80, 120/-60, 130/-40, 105/-40 and 80/-40 appear to be too short to record k peak B; however, the trend of rising k at the base of cores 120/-80, 120/-60 and 130/-40 may suggest that it occurs immediately below the maximum depth that was sampled in these cores. No speculations are made regarding the k fluctuations in cores 70/-80, 70/-60 and 50/-60, since these sites are located close to areas of the trench which have been shown to contain extensive hiatuses (section 4.3, above).

Central sector (Figures 4.6-4.7)

Peak A is apparent in most of the cores in Figure 4.6; however, the only cores exhibiting pronounced subsurface variations in k are 80/0 and 100/60, together with those obtained from along the /80 line. However, reference to Figure 4.7 shows that most of the 2 m-long cores show a pronounced k peak, or peaks, below the maximum sediment depths sampled by the cores in Figure 4.6. This feature is assumed to correlate with k peak B in Figure 4.5. Its occurrence at a significantly greater depth below the sediment surface in the central sector than in the northern sector is consistent with the evidence presented in sections 4.2 and 4.3 (above), which indicates limited Flandrian sediment accumulation over much of the trench area, but in contrast a significant maximum in accumulation in the central sector.

In Figure 4.7, peak B occurs at depths compatible with those of the laminated clayey sediments illustrated in Figure 4.1 and described in section 4.2 (above). This direct correspondence between

lithostratigraphy and magnetostratigraphy is further illustrated in section 4.4.2 (below).

In Figure 4.7, k peak B may be seen to extend over ca. 0.5-1.0 m and in several cases to consist of more than one k peak: core 80/0L has three major adjacent peaks. In addition to peak B, several cores have a major near-surface k peak: this is indicated with the number '1'[1] in Figures 4.6-4.7. It is particularly pronounced in the marginal cores (100/60 and 100/80) and in the southernmost cores in this sector (50/80, 60/80L, 75/100L). Finally, the occurrence of near-surface clay layers in cores 100/0 and 120/0, together with the absence of cores from sites 100/20 and 120/20, reflects limited sediment accumulation in this area.

---

[1]Throughout the following, numbers are used to distinguish k peaks identifiable only over limited areas of the lake basin.

Southern sector (Figure 4.8)

Reference to the 1.5 m depth contour shows that several of the cores from sites along the 20/ and 40/ lines are from shallow water: all are within the present reedswamp zone. Therefore, it is possible that as a result of wind disturbance, and the consequent prevention of sediment accumulation, their sedimentary records may be incomplete. Considering, first, the cores from deeper water (greater than 1.5 m): core 60/100 is too short to interpret, while core 80/120 (closest to the shore) contains a basal clay layer. Cores 60/120, 60/140 and 50/160 exhibit similar k traces: a pronounced upper peak, or series of peaks, extending over ca. 20-30 cm, together with an equally pronounced lower peak. Core 40/180 only contains low amplitude peaks. Cores 60/120 and 60/140 resemble compressed versions of the upper ca. 120 cm of core 75/100L (Figure 4.7); and on this basis the lower peaks in cores 60/120, 60/140 and 50/160 are considered to correlate with peak B, and the upper peaks to correlate with peak 1 in Figures 4.6-4.7. Most of the other cores in this sector exhibit a single major k peak. Assuming that in shallow water, sediment accumulation will continue upto a critical point beyond which the degree of sediment resuspension becomes sufficiently great so as to prevent further accumulation (Pennington et al., 1972), then it is logical to designate this feature peak B rather than peak 1.

With the exception of core -10/305 with a single peak in the uppermost part of the trace, the cores from sites south of the /200 line exhibit little variation in k. An attempt to achieve a lithostratigraphical correlation between sites in this southernmost area of the lake basin is described in section 4.5 (below).

4.3.3 Summary of the results of whole core susceptibility measurements

The results of the k measurements indicate that it is possible to identify two horizons of increased magnetic concentration over large areas of the Goddionduon lake basin. The first of these (peak A) is visible as a small k peak in the uppermost sections of the cores; so far as is discernable from the whole core records, it is largely confined to the northern and central sectors of the lake basin. The second (B) is present either as a single major k peak, or, in cores with higher accumulation rates, more typically as a series of adjacent peaks. Some of the cores exhibit an additional k peak (1) at sediment depths intermediate between peaks A and B. This third feature is especially pronounced in cores from sites adjacent to the eastern margin of the lake in parts of the central and southern sectors. This provisional core correlation scheme is summarised in Figure 4.9.

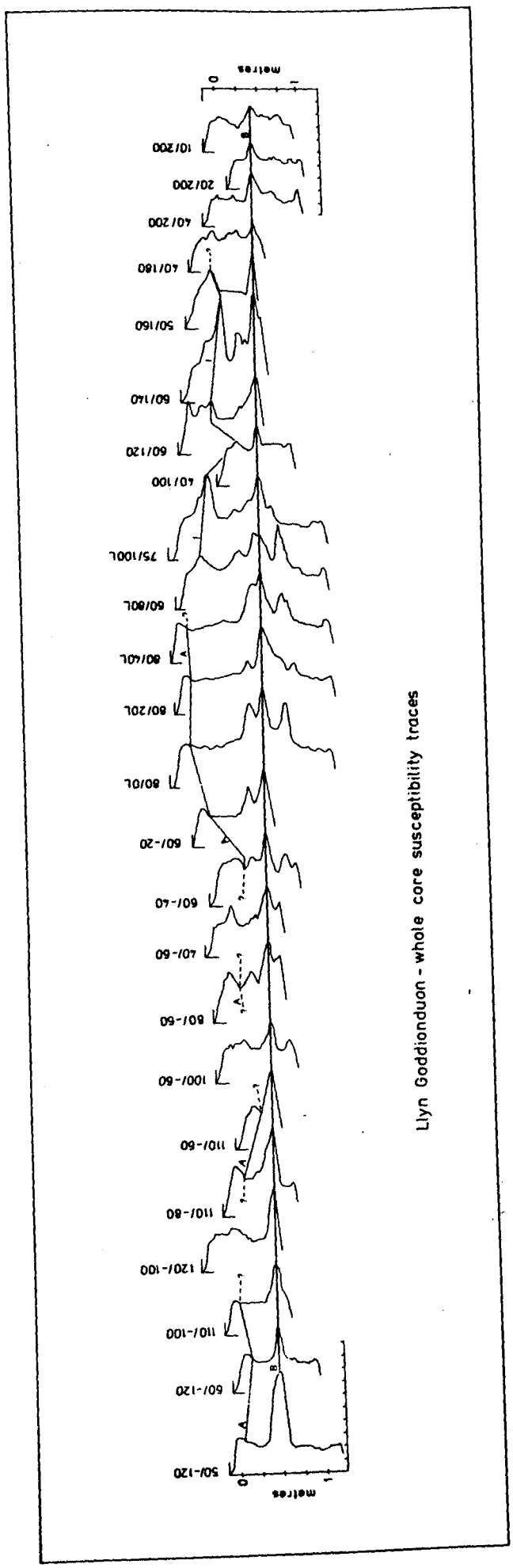

Figure 4.9 Correlation diagram of whole core k traces: main grid cores

4.4. Single-sample magnetic measurements

4.4.1 Introduction

The basis of the core correlation scheme described in section 4.3 (above) and illustrated in Figure 4.9 is the assumption that the lowermost k peak (B) recognisable over the majority of the area of the lake basin represents a synchronous sediment depositional event. Although the association of peak B with lithostratgraphic changes suggested that this was likely to be the case, it was considered necessary to attempt to test the validity of the assumption as rigorously as possible. Several different kinds of analysis could have been carried out for this purpose: for example, a detailed examination could have been made of the relationship between the stratigraphic position of peak B and variations in independent parameters, such as pollen, diatom, or chemical changes (cf. Thompson et al., 1975). Although pollen and chemical analyses are used subsequently in an attempt to reconstruct the environmental history of the lake watershed and to provide additional characterisation of the types of accumulated sediment, emphasis was placed on the use of single-sample magnetic measurements to achieve the aim stated above. This decision was based on the possibility that the changes in magnetic concentration apparent in the k stratigraphy might also reflect changing contributions by different magnetic mineral types or grain sizes, and that measurements of single-sample magnetic parameters diagnostic of such changes (Chapter 1, section 1.8) would permit the characterisation (and consequently the differentiation) of the k peaks. The principal reason for selecting single-sample magnetic measurements in preference to other techniques was that although time consuming in comparison with whole core k measurements, they are still considerably faster than most conventional forms of sediment analysis. However, because of their successful application to the problem of sediment-source tracing in both lacustrine and fluvial situations (Dearing, 1979;

Walling et al., 1979) it was also hoped that comparison of the magnetic properties of the lake sediments with those of potential source materials in the watershed would elucidate possible sediment source-lake sediment linkages.

4.4.2 Down core specific susceptibility, SIRM and ARM

Figures 4.10-4.13 illustrate the variation of various single-sample magnetic parameters down four widely separated cores selected for detailed study. Whole core k traces for three of the cores (120/-100, 40/-20 and 40/200, all of which exhibit k peak B) are shown in Figures 4.5 and 4.8 (above). No whole core k data are available for the fourth core (50/90L); however, the trace would probably closely resemble that for adjacent core 60/80L (Figure 4.7, above). The lithostratigraphy for core 50/90L is included in Figure 4.12. It is possible that the top ca. 2 cm of this core were lost during coring.

Examination of the down-profile variation of the magnetic parameters permits the definition of features (delimited by horizontal lines) with distinctive magnetic properties; three of these correspond to k peaks A, 1 and B and are designated as such on the diagrams.

The magnetic characteristics of the features indicated in Figures 4.10-4.13 are described below. The significance of the absolute values of the magnetic parameters for the interpretation of the magnetic mineralogy of the cores is considered in Chapter 7 (section 7.3).

Peak A (120/-100 0-12 cm; 40/-20 0-22 cm; 50/90L 0-4 cm; 40/200 0-6 cm).

This horizon exhibits relatively high values of specific susceptibility (χ), SIRM and ARM, and intermediate to high values of SIRM/χ and ARM/χ. It exhibits very uniform values of SIRM/ARM in 40/-20, and high S_{40} in 50/90L. (Comparison of the plots for 120/-100, 40/-20 and 40/200 with whole core k plots for these cores (Figures 4.5 and 4.8) clearly illustrates the extent to which whole core measurements depress

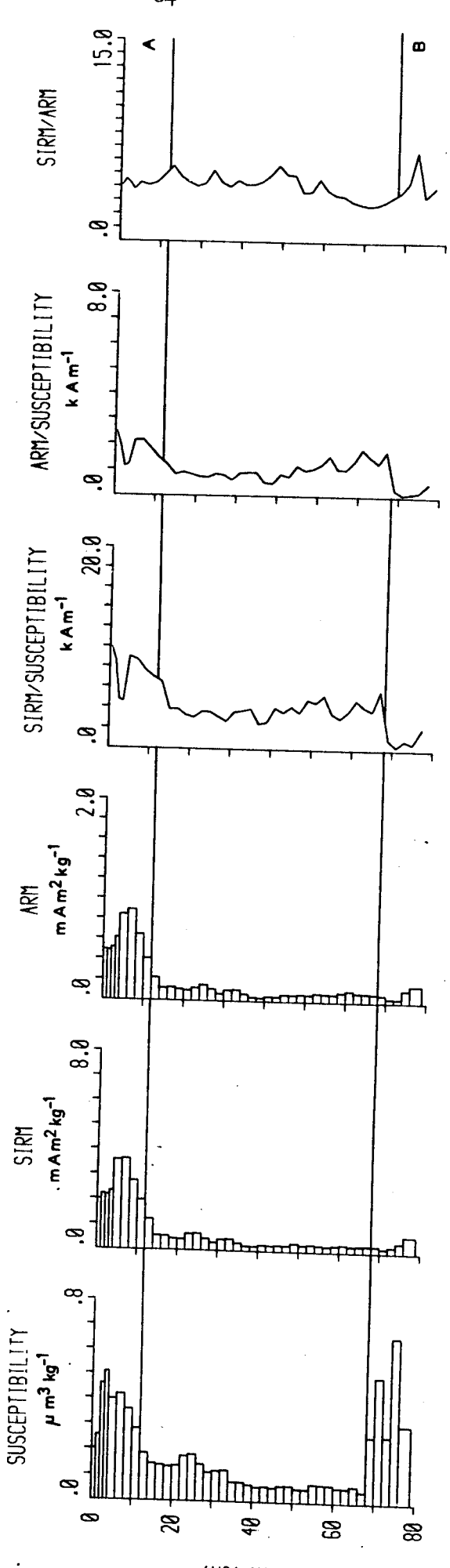

Figure 4.10 Single-sample magnetic measurements for core 120/-100

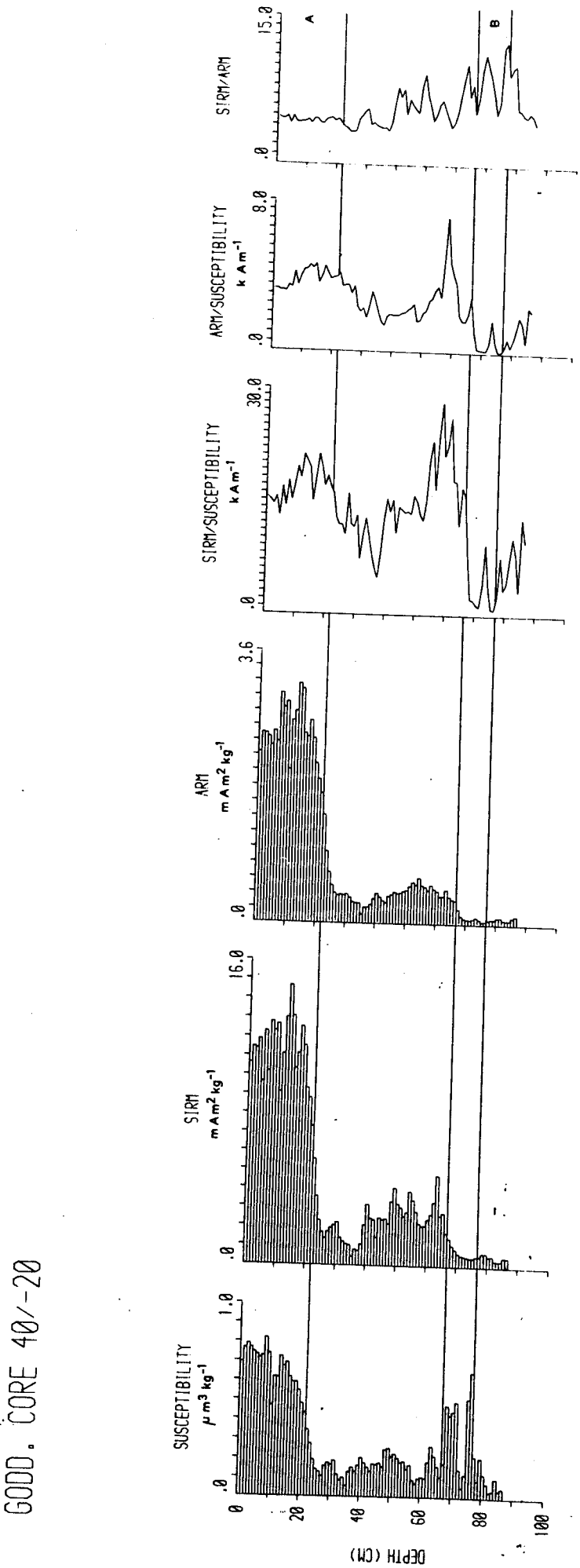

Figure 4.11 Single-sample magnetic measurements for core 40/-20

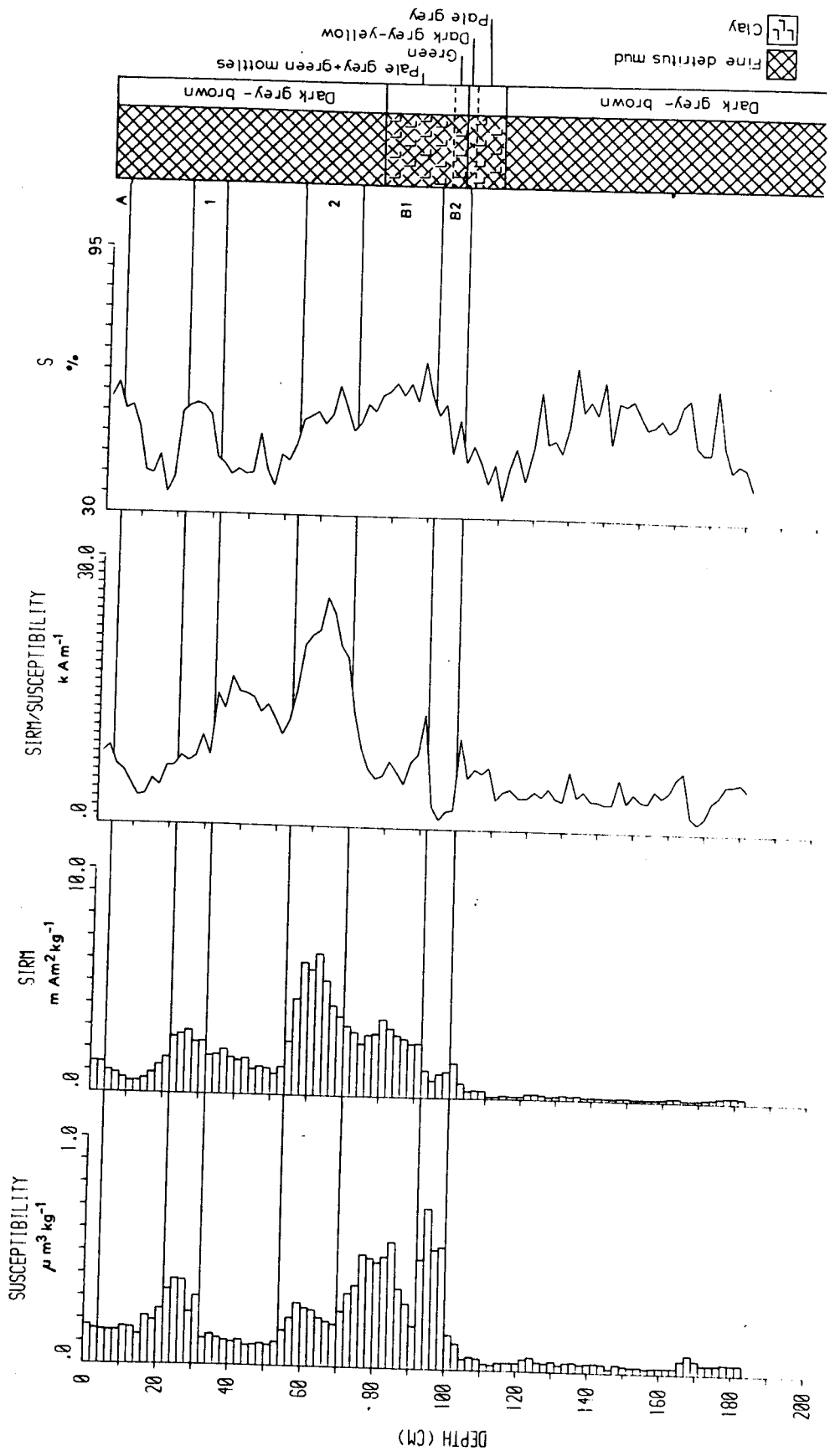

Figure 4.12 Single-sample magnetic measurements for core 50/90L

GODD. CORE 50/90L

GODD. CORE 40/200

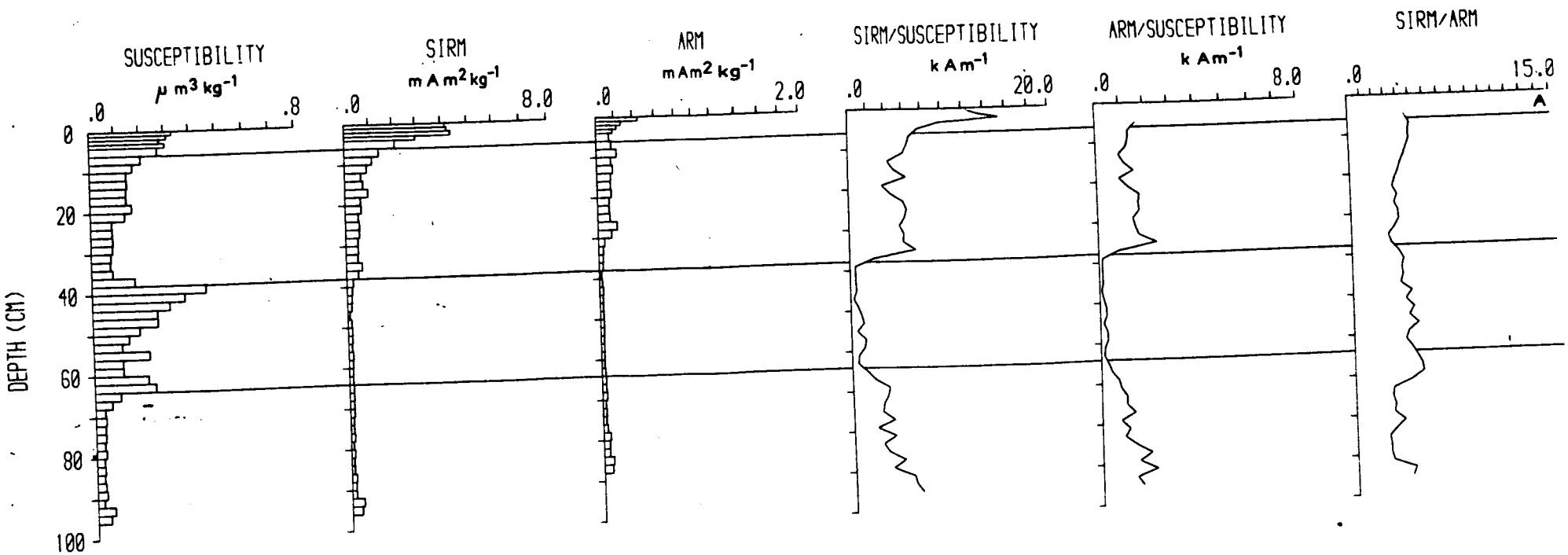

Figure 4.13 Single-sample magnetic measurements for core 40/200

susceptibility peaks at the extremities of cores).

Peak B (120/-100 68-78 cm (base); 40/-20 67-77 cm; 50/90L 70-100 cm; 40/200 38-64 cm).

This horizon exhibits maxima in χ, but relatively low SIRM and ARM and therefore low SIRM/χ and ARM/χ. The values of the two latter parameters are significantly lower than in any of the other sections of the cores. In core 50/90L, peak B has been subdivided into two horizons, B1 and B2; only horizon B2 exhibits values of SIRM/χ as low as those of peak B in the other three cores.

Peaks A and B appear to represent the only common features in the set of cores. In cores 120/-100 and 40/200 the sediments inbetween peaks A and B exhibit low and relatively uniform values of χ, SIRM and ARM and little variation in the three ratios; in core 40/-20 they exhibit a series of minor peaks in SIRM, but more uniform ARM and χ, together with maxima in SIRM/χ and ARM/χ immediately above peak B. In core 50/90L two distinct features (numbered 1-2 in Figure 4.12) are apparent, in order of increasing depth: (1) a minor peak in χ, SIRM and S_{40} (this is considered to correlate with k peak 1, described in section 4.3.2 (above)) (ca. 22-32 cm); (2) a peak in χ and SIRM, and a maximum in SIRM/χ (ca. 54-70 cm).

The sediments below peak B in cores 50/90L and 40/200 exhibit low χ and SIRM; in 50/90L, which contains the longer-sequence, SIRM/χ is also low and uniform, while S_{40} rises from a minimum immediately below peak B and then declines with depth; in core 40/200, SIRM/χ and ARM/χ rise slightly through this section.

Comparison of the lithostratigraphy and magnetic stratigraphy of core 50/90L (Figure 4.12) reveals a clear association between peak B and the variously-coloured laminated clayey sediments between ca. 75 and 109 cm. In this core, peaks A, 1 and 2 are not reflected in visible lithostratigraphic changes. The occurrence of laminated clayey layers at many of the boring sites in the central and southern sectors (section

4.2, above) at depths compatible with those for the occurrence of magnetic peak B implies that this relationship is consistent.

4.4.3 Measurements of specific susceptibility and SIRM on additional cores

The results described above demonstrate the ability of measurements of χ, SIRM and ARM to characterise the whole core k peaks: in all cases the largest sub-surface susceptibility peak (B) may be distinguished by its relatively low values of SIRM (ARM)/χ. Because the variation in SIRM/ARM in Figures 4.10-4.11 and 4.13 is relatively slight, and because SIRMs are more rapidly and easily grown in samples than are ARMs (Chapter 3, section 3.4.4) emphasis was placed on the use of a combination of χ and SIRM measurements for confirming the widespread occurrence of a horizon of relatively high χ but negligible remanence. Figure 4.14 attempts to illustrate this. It shows plots of χ and SIRM for 12 cores from the lake basin, including those previously illustrated in Figures 4.10-4.13. Features A, 1, 2 and B are indicated on the diagram. The following conclusions are drawn from the results:

The plots substantiate the whole core k correlation scheme illustrated in Figure 4.11: in every core the largest sub-surface χ peak does not exhibit a comparable increase in SIRM. However, this horizon exhibits a variable development: in core 60/60L, which has the most extended sequence of deposition, it is diffuse; and in core 60/-20 there are two discrete χ peaks with low SIRM/χ, although the fact that each is immediately preceded stratigraphically by a minor peak in SIRM may indicate slumping of sediment and consequent repetition of the sequence, particularly since this site is located in an area of relatively steep bathymetric gradient.

Although the cores illustrated in Figure 4.14 constitute only ca. 15 percent of the set of main grid cores, they clearly indicate the tendency for the vertical thickness and magnetic concentration of

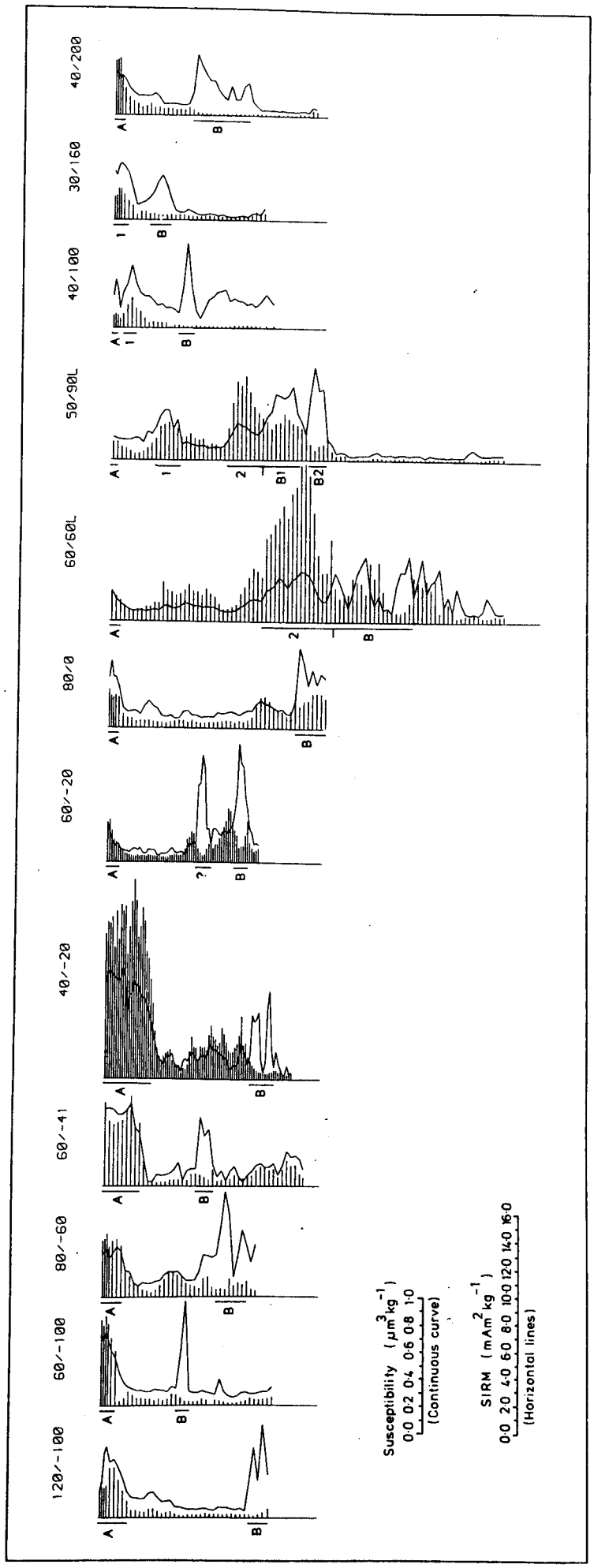

Figure 4.14 Single-sample magnetic measurements for 12 main grid cores

peak A to be greater in the northern sector than in the central and southern sectors. However, considerable fine-scale variation is also evident: for example, in core 40/-20 the thickness of this horizon is four times greater than in core 60/-20, 20 m away and from a similar water depth.

In view of the occurrence of peak B close to the sediment surface in cores 20/100, 20/120 and 20/140 (see Figure 4.8), indicating the cessation of sediment accumulation at these sites, the uppermost peak in magnetic concentration in core 30/160 is correlated with peak 1 (cf. cores 50/90L and 40/100 in Figure 4.14) rather than with peak A. Although there is no lithostratigraphic record at site 40/200 of the black-coloured sediments associated with peak A (see Chapter 5, section 5.2; Figure 5.1) and although peak 1 is strongly represented near the sediment surface in cores 60/140 and 50/160 (see Figure 4.8), the uppermost peak in magnetic concentration in core 40/200 is assigned preferentially to peak A because of its relatively high values of SIRM/χ. However, in the absence of single-sample magnetic measurements from additional cores from the southern sector the precise extent of peak A sediments within this area of the lake basin remains uncertain.

Similarly, although peak 2 is clearly visible in cores 60/60L and 50/90L, without additional single-sample measurements it is difficult to identify it, and also to extend the subdivision of peak B (cf. peaks B1 and B2 in core 50/90L), within the 2 m-long central sector cores for which whole core k records only are available. In view of the smoothing effect of whole core measurements it is possible that several of the major k peaks in Figure 4.7 represent more than one peak.

To conclude, the single-sample magnetic measurements confirm the identification of two horizons: (i) of high susceptibility and high remanence (peak A) and (ii) high susceptibility but negligible remanence (peak B) over the majority of the area of the lake basin. Although it

is possible to identify additional magnetic features (peaks 1 and 2) in some cores, their areal extent is too limited to use them to estimate volumes of accumulated sediment.

4.5 Lithostratigraphy of the southern margin

4.5.1 Introduction

This section describes the results of a series of shallow Russian corer borings carried out in the southern margin of the present lake basin. The borings were performed for two reasons. Firstly, because of the absence of k peaks in the southernmost minicores (cores 20/220, 30/220 and 10/240; see Figure 4.8) and because of the correspondence between magnetic peak B and visually apparent changes in sediment lithology (see Figure 4.12) it was hoped that the correlation of this feature could be extended into the area of the lake basin south of the /200 line by lithostratigraphically-based core correlations. Secondly, since it is possible to estimate the age of the lake mud - reedswamp peat - bog peat transition beneath the Goddionduon bog by ^{14}C-dating (Chapter 5, section 5.3.4) it was hoped that the establishment of the stratigraphic relationship between the laminated clayey sediments and the seral succession beneath the bog would aid the construction of a chronology of sediment accumulation for the lake basin. During the course of the borings, additional material was sampled for ^{14}C-dating. (The results and significance of all the ^{14}C-datings are described and considered in Chapter 5, section 5.2).

4.5.2 Results

Figure 4.15 shows plots of the lithostratigraphy of the boring sites, together with their location. Blank areas in the uppermost part of some of the sediment columns represent unsampled intervals.

Three types of sediment were discernable at almost all of the sites investigated, in order of occurrence with increasing depth: (i) a dark

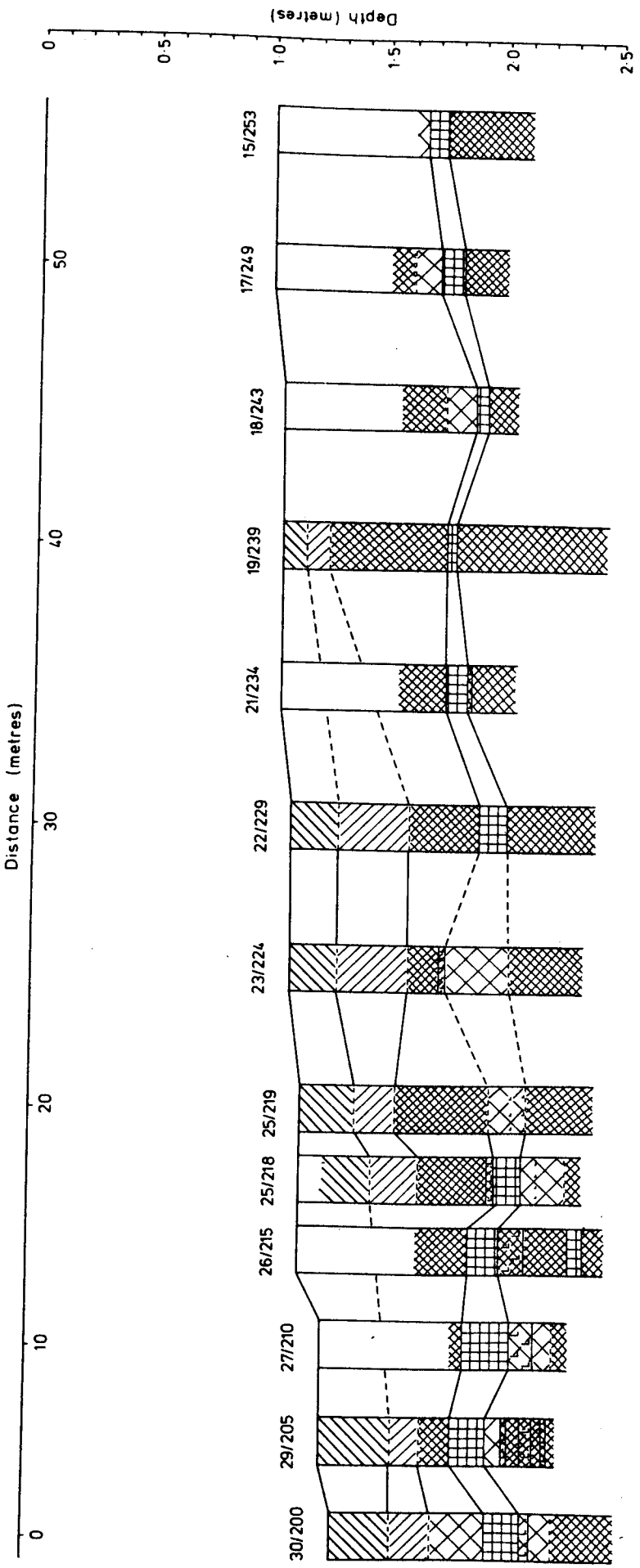

Figure 4.15 Shallow water boring transect

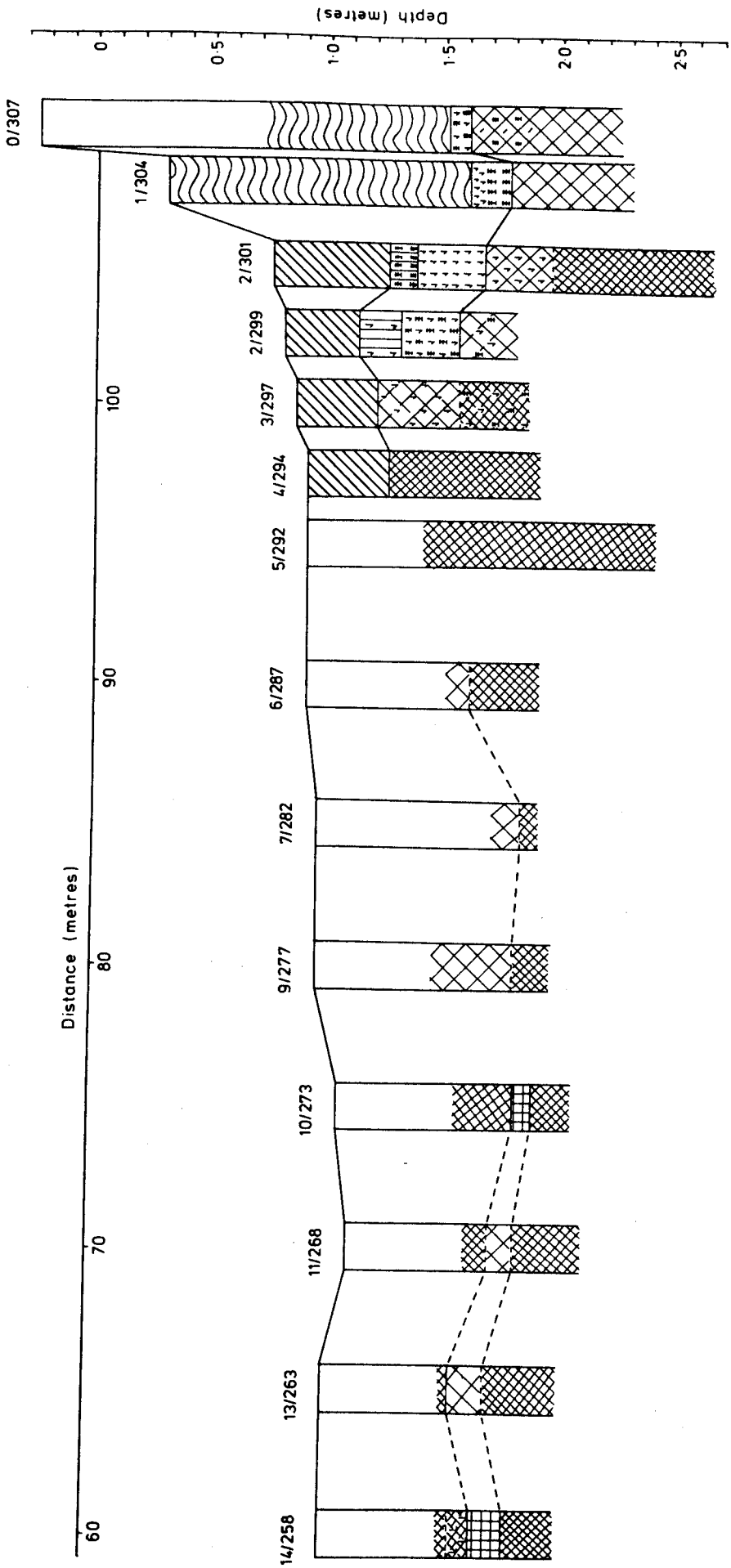

Figure 4.15 continued

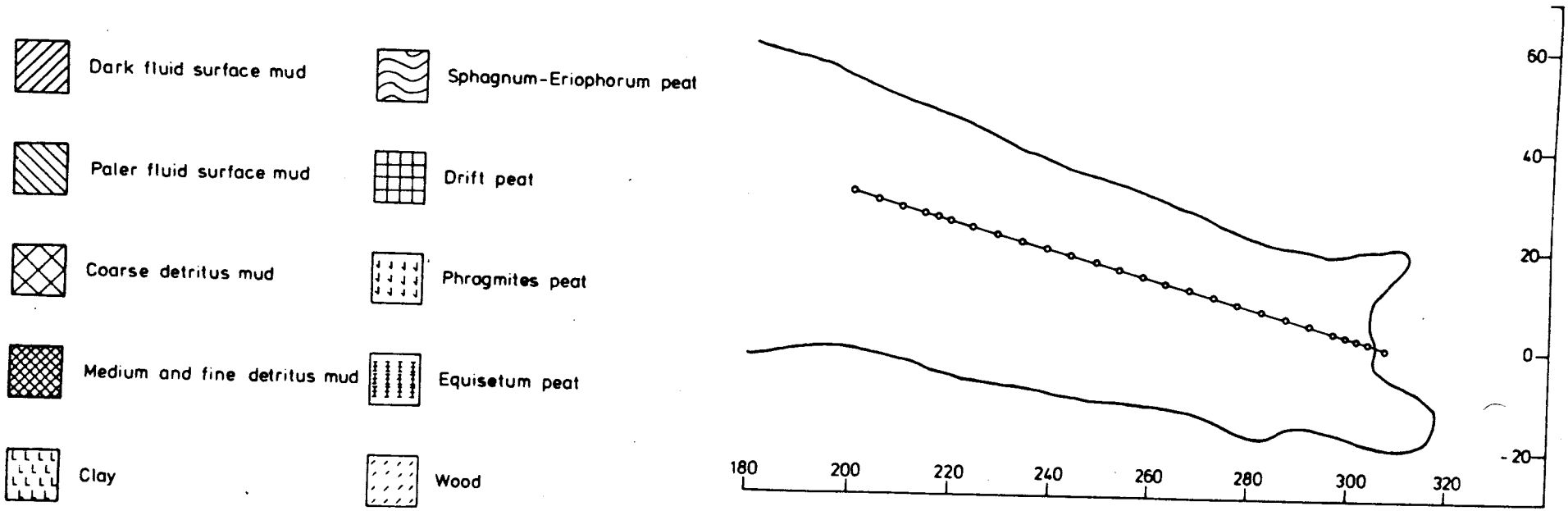

Figure 4.15 continued

brown, very fluid surface mud with abundant coarse plant detritus; (ii) a paler, more coherent coarse detritus mud (this deposit was absent at the sites immediately adjacent to the bog); and (iii) a series of medium and fine detritus muds. At many of the sites the medium and fine detritus muds were interrupted by one or more of three additional types of deposit, generally of limited vertical extent: (i) a dark brown drift peat; (ii) a slightly clayey detrital mud with grey, cream or green laminations (magnetic peak B sediments); and (iii) a brown coarse detritus mud. The distinction between the drift peat and the coarse detritus mud deposits was not always obvious and they are clearly intergradational.

The laminated clay muds are only consistently present at the sites at the northern end of the transect: at sites 30/200, 29/205, 27/210 and 26/215 they occur as discrete bands within (or immediately below) the brown coarse detritus mud, which at these sites grades upwards into the drift peat deposit; at site 26/218 they also occur immediately above the latter. At all of these sites the laminated clay muds occur at depths exceeding those sampled by the three minicores cited in section 2.5.1.

At sites 25/219 and 23/224 the drift peat is absent and the clay muds are represented only by thin (ca. 1 cm thick) bands within the coarse detritus mud. Of the remaining sites, only 21/234 and 14/258 exhibit the clay muds. At site 22/229, the drift peat reappears and is present from here up to site 14/258, whereupon between the latter site and site 6/287 it tends to grade into the brown coarse detritus mud. At sites 6/287 and 5/292 the only visible lithostratigraphic change was that from the fluid surface mud to a medium-fine detritus mud.

The remaining borings, adjacent to the bog, record the open water - reedswamp - peat bog succession. At sites 2/299-0/307, the depth of the contact between the open water detritus muds and the reedswamp peat varies from ca. 1.5-1.8 m below the present lake level.

The following points emerge from the above: if the assumption of the correspondence between magnetic peak B and the laminated clay muds is valid for this area of the lake basin then it is possible to extend the correlation of this feature to within at least ca. 50 m of the southern margin of the present lake basin. Although it is not possible to establish the precise stratigraphic relationship of the laminated clay muds to the seral succession beneath the peat bog, the results of the borings provide information of potential significance for the reconstruction of the environmental history of the lake basin.

The occurrence of the drift peat/coarse detritus mud deposits (within which, at some sites at least, the laminated clay muds are interstratified) provides clear evidence of fluctuations in lake level. A reduction in water depth increases the substrate available for macrophyte colonisation, resulting in an outward displacement of reedswamp. Areas which previously were situated sufficiently far from reedswamp so as to receive fine detritus deposition may now be brought within range of coarse detritus deposition. A subsequent rise in water-level may result in a forcing back of the reedswamp and therefore a return to fine detritus deposition. Such a sequence of events would explain the fine/medium detritus mud - drift peat/coarse detritus mud - fine/medium detritus mud alternation observed at several of the sites on the boring transect.

Radiocarbon dating of samples from boring site 27/210 suggest that the fluctuations in water-level responsible for these lithostratigraphic changes post-date those assumed to be responsible for the initiation of peat formation on the bog (see Chapter 5, section 5.3.3).

CHAPTER 5 SEDIMENT CHRONOLOGY

5.1 Introduction

The core correlation scheme described in Chapter 4 provides a basis for the estimation of volumes of total sediment accumulation within the Goddionduon lake basin. However, transformation of these to estimates of rates of sediment influx requires a chronology of sedimentation. Four techniques were potentially available for the direct dating of the Goddionduon lake sediments: assay of the three radio-isotopes ^{137}Cs, ^{210}Pb and ^{14}C, and palaeomagnetism.

Lead-210 dating is becoming an increasingly popular technique for dating recent (of the last ca. 100-150 yr) lake sediments (e.g. Pennington et al., 1976; Battarbee and Digerfeldt, 1976; Battarbee, 1978a; Robbins et al., 1978). However, obtaining reliable sediment age estimates from the variation of unsupported ^{210}Pb concentration down sediment cores is increasingly being shown to require the assumption of a constant rate of supply of unsupported ^{210}Pb to the sediment surface (e.g. Appleby and Oldfield, 1978; Oldfield et al., 1978c). The alteration of the size of the Goddionduon watershed consequent upon the construction (during the Victorian period) and eventual blocking (during the 1960s) of a channel connecting the lake basin with the stream draining Llyn Bychan (see Chapter 2, section 2.4) suggested the likelihood that there will have been significant changes in the flux rate of unsupported ^{210}Pb to the sediment surface. For this reason ^{210}Pb was precluded as a dating technique.

Comparison of palaeomagnetic declination and inclination variations with geomagnetic secular variation master curves calibrated by archaeomagnetic and ^{14}C dating (e.g. Turner and Thompson, 1979; Turner and Thompson, 1981) has also been used for sediment dating (e.g.

Pennington, 1973). However, measurements of the direction and intensity of the horizontal component of the Natural Remanent Magnetisation (NRM) of 18 whole cores, together with detailed single-sample NRM measurements of three cores, indicated that the Goddionduon lake sediments do not carry a reliable secular variation record (Towler, unpublished).

For these reasons attempts to construct a chronology of sediment accumulation were focussed upon ^{137}Cs and ^{14}C dating.

5.2 ^{137}Cs dating

5.2.1 Introduction

Several workers have demonstrated the use of atmospheric fall-out of ^{137}Cs to date lake sediments of a few decades in age (e.g. Pennington et al., 1973; Ritchie et al., 1973; Battarbee and Digerfeldt, 1976) The procedure relies upon comparison of ^{137}Cs concentrations in sediment cores with recorded variations in atmospheric levels since 1954. Caesium-137 profiles in cores may exhibit two significant peaks: reflecting the onset of nuclear bomb testing in 1954 and the date of maximum ^{137}Cs fall-out in 1963 (Cambray et al., 1972). Comparison of ^{137}Cs profiles with horizons of known age (for example, dated by varve counts and by reference to clay inwash layers of known age (Digerfeldt et al., 1975)) have established the reliability of the technique.

The occurrence of elongated 'tails' in some published ^{137}Cs profiles, thereby making difficult the precise identification of the 1954 horizon of first significant occurrence, has led to the suggestion that the distribution of the radio-nuclide in sediments may be affected by downward diffusion or bioturbation (Pennington et al., op cit.). However, a cause could also be the downcarriage, during coring and/or sample extrusion, of sediment in immediate contact with the core tube wall. With this in mind, core 50/-43 was extruded and sliced into 2 cm intervals as described in Chapter 3 (section 3.3) with the exception that the

outer ca. 3-4 mm of each sediment slice were removed using an empty film container as a 'pastry cutter'. Caesium-137 assay was performed at the Atomic Energy Research Establishment, Harwell.

5.2.2 Results

Figure 5.1 shows the ^{137}Cs distribution together with down-core χ, SIRM, SIRM/χ and the lithostratigraphy for core 50/-43. The likely minimum pollen analytically-derived ages of two horizons are indicated (see below).

From the base of the core to a depth of 18 cm, magnetic concentration is low and uniform; it then rises gradually to a depth of 10 cm, and then increases abruptly to the top of the core. SIRM/χ also exhibits a distinct increase over the interval 18-0 cm. The base of magnetic peak A is defined at the base of the steep rise in magnetic concentration at 10 cm. A lithostratigraphic change from brown mud (below) to black mud (above) occurs in the 8-10 cm sample, illustrating the association between magnetic peak A and black-coloured sediments (see Chapter 4, section 4.3.1).

The first detectable occurrence of ^{137}Cs is in the 6-8 cm sample; maximum concentration of the radio-isotope occurs at the top of the profile.

During the relatively well-documented period of Forestry Commission management of the Goddionduon watershed there have been only three significant environmental disturbances: drainage-ditching (1921), the forest fire (1951) and road construction (1960-61) (see Chapter 2, section 2.3). Assuming that the first detectable occurrence of ^{137}Cs at 6-8 cm corresponds to 1954, then the occurrence of the base of peak A 2 cm below tends to implicate the 1951 forest fire as the cause of the steep rise in magnetic concentration. This accords with evidence for the production of large volumes of secondary ferrimagnetic minerals during forest fires and their subsequent persistence in soils and

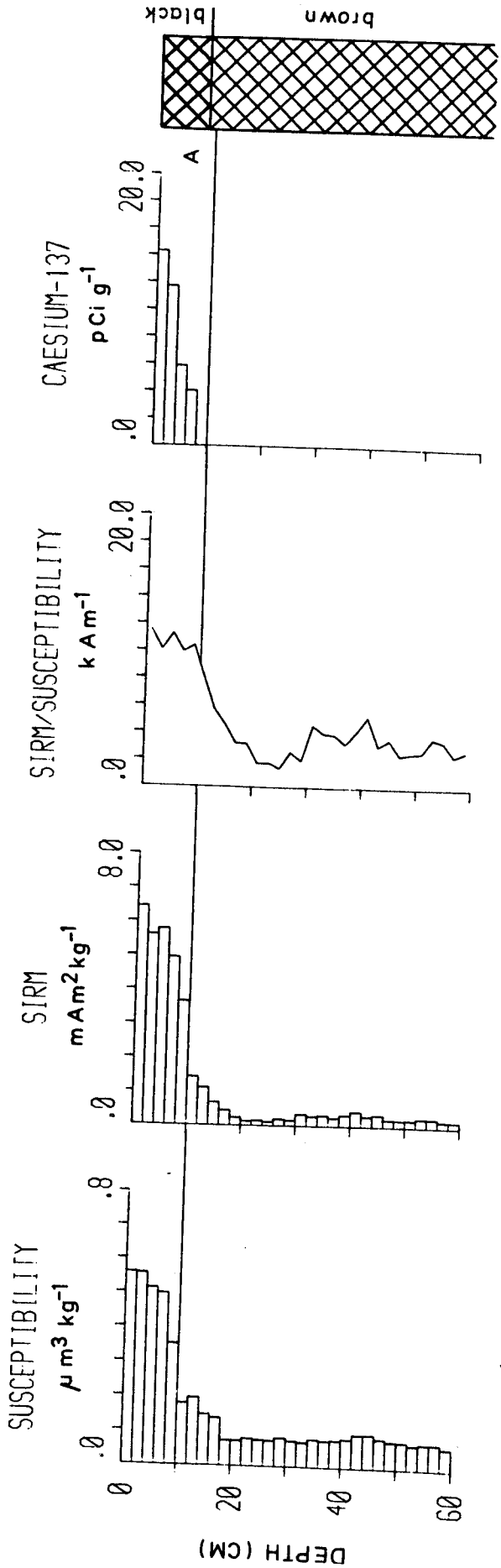

Figure 5.1 Caesium-137 profile and single-sample magnetic measurements for core 50/-43

sediments (Rummery, 1981). Therefore the base of peak A is assigned the date of 1951. (The possible effects of recent watershed disturbances on the magnetic properties of the uppermost sediments are discussed in relation to all available evidence in Chapter 9, section 9.1). The absence of a decline in ^{137}Cs concentration at the top of the profile does not accord with the known pattern of declining ^{137}Cs deposition after 1963, and suggests that there has been negligible sediment accumulation at this site during the last ca. 10-15 years.

The results of pollen analyses (performed subsequent to ^{137}Cs assay) are of interest. Reference to Table 4.2 (Chapter 4, section 4.3) shows that samples 58-60 cm and 20-22 cm pre-date ca. 7 000 bp and ca. 2 000 bp respectively, suggesting an extremely slow sediment accumulation rate over this interval and possibly also a major stratigraphic unconformity. The contrast between the accumulation time of the ca. 60-20 cm interval (at least 5000 years) and that of the 10-0 cm interval (a maximum of 26 years) clearly demonstrates the spasmodic nature of sedimentation at this coring site.

5.3 ^{14}C dating

5.3.1 Introduction

Carbon-14 dating is now a well-established technique for dating late Quaternary sediments and peats. Nevertheless, in recent years several uncertainties have arisen regarding the application of the technique, particularly in the case of materials which have accumulated in aquatic or semi-aquatic environments: such materials often yield dates which are substantially too old (Olsson, 1974). One particular problem appears to relate to the incorporation into lake sediments of old (^{14}C depleted) carbon from peat and moorland soils; such influxes often appear to be accelerated by human activity within lake watersheds. These effects are often readily apparent: at several lake sites, ^{14}C dating has produced inverted age-depth relationships (e.g. O'Sullivan

et al., 1973; Pennington et al., 1976; Battarbee and Digerfeldt, 1976; Edwards and Rowntree, 1980). However, the recent construction of a well-dated British geomagnetic secular variation master curve (Turner and Thompson, 1981), together with the increasing number of palaeomagnetic studies being carried out on lake sediments as an adjunct to ^{14}C dating, has indicated that even where an apparently conformable set of ^{14}C dates has been obtained, these may still be significantly too old (Thompson and Wain-Hobson, 1979; Turner, 1979).

Because of the widespread occurrence of peaty soils in the Goddionduon watershed, it is likely that the ^{14}C dates from the lake basin (described below) are to some degree affected by 'old' carbon from terrestrial sources. In addition, in view of the lithostratigraphic evidence for water-level changes (see Chapter 4, section 4.5) it is possible that reworking of marginal sediments may constitute a further possible source of 'old' carbon. Both possibilities indicate that considerable caution is required in the interpretation of the results.

5.3.2 ^{14}C dates from cores 60/-41 and 40/200

In order to attempt to date magnetic peak B, four samples from cores 60/-41 and 40/200 were submitted to the NERC Radiocarbon Laboratory, East Kilbride, for ^{14}C assay. The dates and sample depths are given in Table 5.1.

CORE	DEPTH (cm)	AGE (^{14}C years bp)	NUMBER
60/-41	36-42	870±130	SRR-1469
60/-41	54-60	2510±130	SRR-1470
40/200	28-34	400±110	SRR-1467
40/200	70-76	1860±100	SRR-1468

Table 5.1 ^{14}C dates from cores 60/-41 and 40/200

At the time of sample submission it was considered that susceptibility peaks in lake sediments necessarily reflected periods of watershed disturbance and increased allochthonous influx (cf. Thompson et al., 1975 and see Chapter 7, section 7.2). Therefore, with the intention of attempting to minimise 'old carbon error', for each core two samples were obtained immediately above and below magnetic peak B, rather than from the susceptibility peak itself. The magnetic stratigraphy for cores 40/200 and 60/-41 is shown in Figures 4.13-4.14 (Chapter 4, section 4.4).

Graphs of age versus depth constructed from the ^{14}C dates are shown in Figure 5.2 (a and b). For each point, the vertical error limit relates to the thickness of the sediment slice from which the date was obtained, and the horizontal error limit to $\pm$ 1 σ analytical confidence. The right-hand side of each graph shows the depth of the base of magnetic peak A (= AD 1951) and the depth of magnetic peak B (taken as the sample with the highest χ).

In order to supplement the chronology available from direct dating of the Goddionduon sediments, an attempt was made to transfer dates from the calibrated geomagnetic secular variation record from Llyn Geirionydd (Turner, 1979), situated ca. 5 km northeast of Goddionduon, to the Goddionduon sediments via pollen correlations (see Chapter 8, section 8.3, and Appendix I). Figure 5.2 (a) shows a date obtained from a tentative pollen correlation between core 60/-40 (obtained 1 m away from core 60/-41 and with an almost identical magnetic stratigraphy) and Llyn Geirionydd core GEIR2, for which palaeomagnetic dates and pollen analyses are available (see Appendix I). The size of the error box for this datum in Figure 5.2 (a) shows the likely error involved in (i) obtaining the age of the pollen feature in the GEIR2 pollen diagram from the GEIR2 age-depth curve and (ii) correlation of the pollen feature between cores 60/-40 and GEIR2.

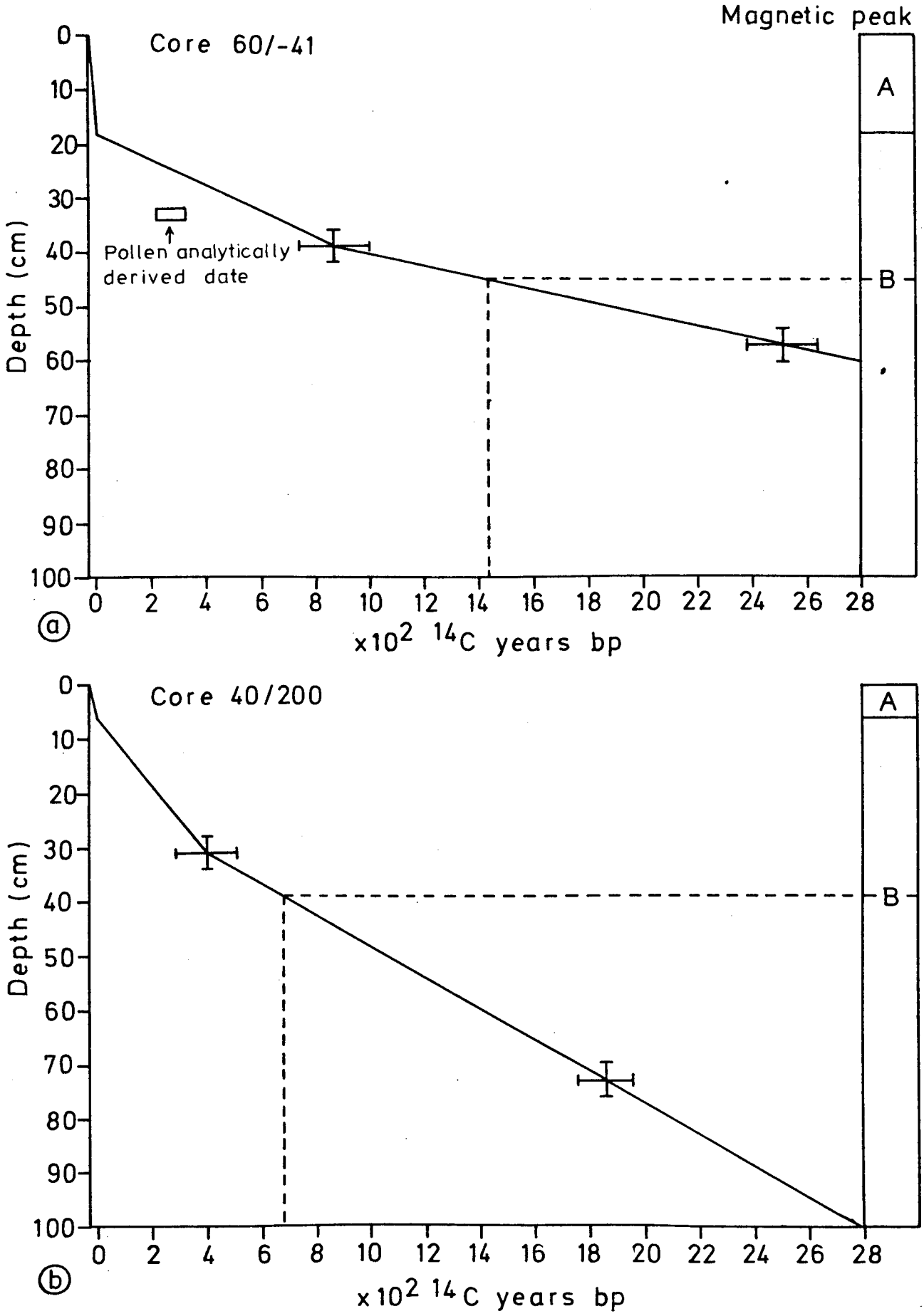

Figure 5.2 Age-depth curves for cores 60/-41 and 40/200

Linear interpolation between the ^{14}C dates gives ages of ca. 1430 bp (^{14}C years before present) and ca. 670 bp for magnetic peak B (point of highest χ) in cores 60/-41 and 40/200, respectively. Before accepting the clear discrepancy as evidence for the non-synchroneity of the magnetic stratigraphy of the two cores, the possibility of 'old carbon error' needs to be considered. This is strongly indicated in the case of the dates from core 60/-41, since extrapolation of the age-depth relationship indicated by them implies that the age of the base of the core is greater than 6000 bp, a date which is precluded by pollen-analytical data from adjacent core 60/-40 (see Chapter 8, section 8.5). Comparison of the pollen date (320-220 BP (calendar years before present) for the interval 33-35 cm) with the uppermost ^{14}C date also implies that the latter is too old.

5.3.3 ^{14}C dates from site 27/210

Because of the consistently close juxtaposition at several of the southern lake margin boring sites (see Chapter 4, section 4.5) of laminated clayey sediments (associated with magnetic peak B) with peaty and coarse detrital layers (which constitute material suitable for ^{14}C dating), two samples were collected from site 27/210 for dating. The stratigraphy of the original boring at this site is as follows:

0-55 cm	Unsampled
55-62 cm	Brown medium detritus mud
62-80 cm	Peaty (coarse reedswamp detritus) with occasional pieces of rotted wood
80-90 cm	Faintly banded, slightly clayey mud (= magnetic peak B sediments)
90-98 cm	Brown coarse detritus mud
98-105 cm	Brown medium detritus mud

A Russian corer was used to collect two samples (each consisting of a number of aggregated samples) corresponding approximately to sediment depths 60-80 cm and 90-100 cm. Prior to submitting the samples to the NERC Radiocarbon Laboratory, East Kilbride, an attempt was made to reduce the likelihood of contamination of the samples by allochthonous

'old' carbon. As it seemed likely that this would be present in fine particulate form, the less than 250 micron fraction of both samples was removed by wet sieving with distilled water. The ^{14}C ages of the two samples are shown in Table 5.2.

DEPTH (cm)	AGE (^{14}C years bp)	NUMBER
ca. 60-80	880±60	SRR-1717
ca. 95-100	775±150	SRR-1718

Table 5.2. ^{14}C dates from site 27/210

The greater volume of material submitted for SRR-1717 is reflected in the considerably lower analytical standard error. The fact that the ^{14}C ages are inverted may suggest either (i) that the sediment accumulation rate between 60 and 100 cm was rapid and that the inversion may be accounted for by the relatively large analytical standard error for SRR-1718; or (ii) that the samples are contaminated. Because of the preparation procedure adopted, contamination would probably be more likely to be by 'young' rather than 'old' carbon. Because of the nature of the corer used, the possibility of down-carriage of surface material during sampling cannot be completely excluded; however, examination of the material during sample preparation revealed no evidence of down-carried material and on this basis the preferred interpretation is that the dates are valid.

A summary of all the dates available from the lake basin is shown in Figure 5.4.

5.3.4 ^{14}C dates from the peat bog

Because of the uncertainties associated with the ^{14}C dates from the lake basin, and because problems of 'apparent age' seem relatively

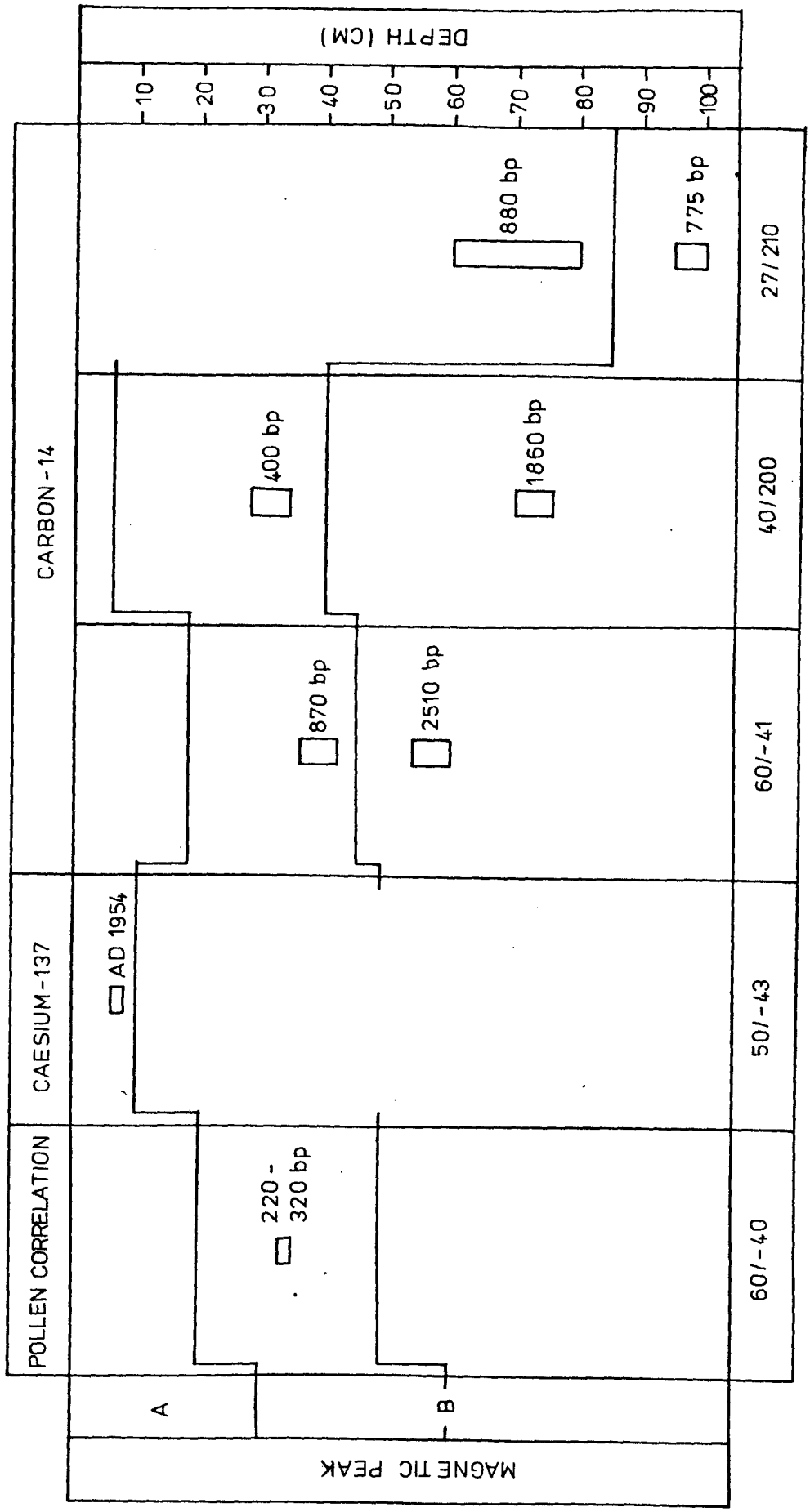

Figure 5.3 Summary of dates available for the Goddiondun lake sediments

less significant in the case of organic deposits which have accumulated in terrestrial contexts, an attempt was made to obtain an 'unambiguous' ^{14}C chronology from the small bog overlying marginal lake sediments at the southern end of the present lake basin. It was hoped that such a chronology could be transferred to the lake basin via pollen-analytical correlations.

Material for ^{14}C dating and pollen analyses was obtained from the bog at site 0/310 by driving in a 1.5 m long, 19.5 cm internal diameter PVC pipe, using a sledge hammer. After insertion, the pipe was removed by excavating a trench at one side. The peat core obtained by this means was 123 cm long. The peat stratigraphy at the site was as follows:

0-7 cm	Fresh, unhumified Sphagnum-Eriophorum peat
7-170 cm	Sphagnum-Eriophorum peat
170-183 cm	Predominantly Phragmites peat
183-192 cm	Equisetum peat
192-200 cm	Brown coarse detritus mud, sharp upper contact

After transport to the laboratory, the core was sliced into 2 cm intervals using a stainless steel knife. Six samples were submitted to the Palaeoecology Laboratory, Queen's University, Belfast, for ^{14}C assay. The dates are shown in Table 5.3 below.

DEPTH (cm)	AGE (^{14}C years bp)	NUMBER
10-12	Modern	UB-2288
32-34	205 ± 40	UB-2287
54-56	575 ± 30	UB-2286
75-77	770 ± 40	UB-2285
97-99	935 ± 35	UB-2284
119-121	1130 ± 55	UB-2283

Table 5.3. ^{14}C dates from core 0/310

Pollen analytical data from this core (see Chapter 8, section 8.4) indicate the occurrence of a sustained period of flooding during the accumulation of the upper ca. 22 cm of the deposit; however, the pollen record from the remainder of the core suggests accumulation above the lake level and therefore it is unlikely that the dates have been significantly affected by allochthonous 'old' carbon from the lake basin.

Figure 5.4 shows an age-depth curve for core 0/310, constructed from the ^{14}C dates in Table 5.3. The age of UB-2287 has been increased by 100 years due to the likelihood of its having accumulated during a period of significant atmospheric enrichment of ^{14}C (G.W. Pearson, personal communication); the remaining dates are uncalibrated. The accumulation rate through the profile varies from 0.133 cm yr^{-1} (76-98 cm) to 0.080 cm yr^{-1} (7-33 cm) ($\bar{X}$ = 0.108 cm yr^{-1}). Backward extrapolation of the age-depth relationship indicated by the two lowermost dates suggests ages of 1350 bp and 1650 bp for the Sphagnum-Eriophorum peat and Equisetum peat/detritus mud contacts respectively, although the latter date must be regarded as tentative because of the uncertainty in assuming the same accumulation rate in the reedswamp peat as in the bog peat.

The intention was to transfer the ^{14}C chronology from the peat bog to the lake basin via pollen-analytical correlations between cores 0/310 and 60/-40. However, despite detailed pollen analyses having been performed on both cores it proved impossible to achieve this. The problems involved are discussed in Chapter 8 (section 8.3).

Although the value of the peat-based chronology is therefore substantially reduced it is possible to use it to obtain information of potential significance for estimation of the age of magnetic peak B. The pollen diagram from core 0/310 exhibits evidence compatible with a reduction in lake level, corresponding to the interval ca. 640-835 bp on the age-depth curve shown in Figure 5.4. This accords with the ^{14}C dates obtained from the peaty/coarse detrital layers from boring site

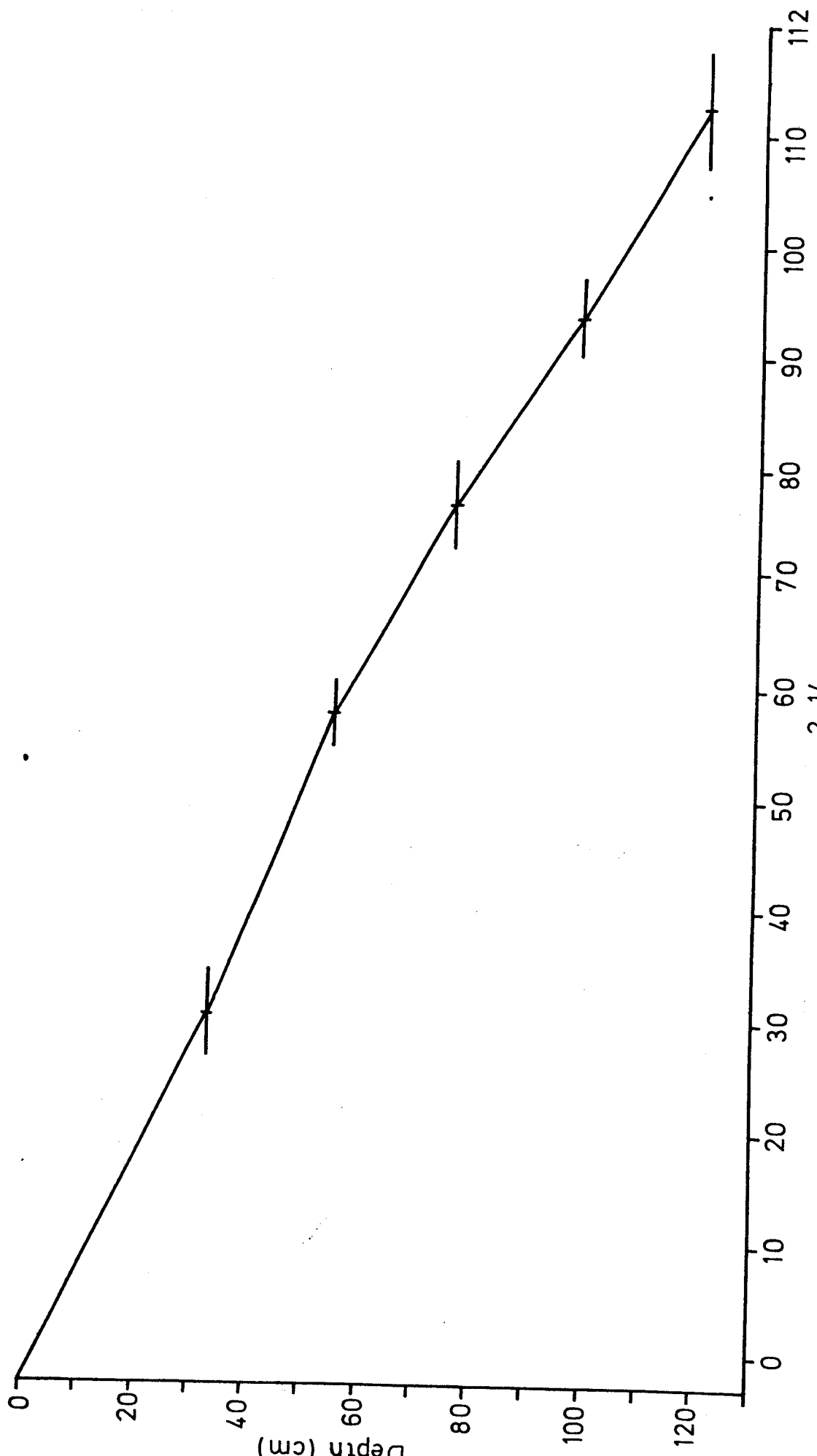

Figure 5.4 Age-depth curve for core 0/310

27/210 (Table 5.2), which as suggested in Chapter 4 (section 4.5) are also considered to reflect lowered lake levels.

Table 5.4 summaries the range of ages obtained for magnetic peak B.

CORE/SITE	AGE (^{14}C years bp)	DERIVATION
60/-41	1430	^{14}C dating of lake sediments
40/200	670	^{14}C dating of lake sediments
27/210	775-880	^{14}C dating of peaty/coarse detrital layers interstratified with laminated clayey sediments
0/310	640-835	^{14}C dating of palynological evidence for lowered lake levels

Table 5.4. Summary of the dates available for magnetic peak B or associated features

5.4 Discussion

Assuming that ^{137}Cs dating provides an acceptable age estimate for the base of magnetic peak A, then the remaining uncertainty regarding the provision of a chronology of sediment accumulation is focussed upon the varying ages obtained for magnetic peak B. It does not seem possible to completely resolve the problem on the basis of the data available. Some of the difficulties may indirectly stem from the effects of the changes in lake levels (apparent in the lithostratigraphic record) which appear to have taken place more or less concurrently with the deposition of magnetic peak B sediments. Lowered lake levels may have resulted in the reworking of marginal material and in terms of attempting to date the sediments this may have had two significant effects: affecting the ^{14}C dates by the redeposition of 'old' carbon, and affecting the pollen record by the redeposition of 'old' pollen,

thereby preventing the establishment of pollen correlations between the lake basin and the ^{14}C-dated peat profile. Both kinds of effect were considered to have been brought about by a lake-level lowering at Växäsjön, Sweden (Battarbee and Digerfeldt, 1976; Digerfeldt, 1977a). Influxes of organic matter from the terrestrial part of the watershed may also have contributed to the problem of apparent age of the lake sediments and affected the pollen biostratigraphy.

In view of the absence of peaty/coarse detrital mud and laminated clayey layers (associated with magnetic peak B) beneath the peat bog, the date of 1650 bp obtained for the lake mud/reedswamp peat contact at site 0/310 constitutes a maximum possible upper boundary for the age of magnetic peak B. For reasons given above, of the estimates shown in Table 5.4, the date of 1430 bp from core 60/-41 seems likely to be too old. The remaining dates, from core 40/200 and site 27/210, span the range 670-880 bp. Since this is supported by the pollen-analytically derived age-range for lowered lake levels (core 0/310) peak B is tentatively assigned the age of ca. 800 bp.

CHAPTER 6. CONTOUR MAPPING OF SEDIMENT THICKNESSES AND THE ESTIMATION OF TOTAL SEDIMENT VOLUMES AND RATES OF INFLUX.

6.1 Introduction

This chapter attempts (i) to use the core correlations described in Chapter 4 to construct contour maps of the thicknesses of three contiguous layers of sediment within the Goddionduon lake basin, and to use the maps to estimate the total volume of each layer; and (ii) to use the sediment chronology established in Chapter 5 to estimate the rate of influx of each layer.

6.2 Methods

The first of the three contour maps illustrated and described below portrays the depth of sediment from (or near) the contact between the Loch Lomond Stadial clays and the early Flandrian clay muds (abbreviated to LLSC/EFCM) and magnetic peak B; this is named sediment layer 1.

The LLSC/EFCM contact is assumed to constitute a synchronous horizon throughout the lake basin and is assigned the age of 10 400 bp (see Chapter 4, section 4.2, Table 4.1). The second contour map portrays the depth of sediment between magnetic peak B and the base of magnetic peak A (sediment layer 2); and the third, the thickness of magnetic peak A (sediment layer). The nature and limitations of the data used to construct the maps are briefly considered below.

The majority of the data for the depth of the LLSC/EFCM contact were obtained from the results of the Russian corer borings (Chapter 4, section 4.2). In 20 out of 26 borings in the present lake basin and on the peat bog at the southern end of the watershed, it was possible to penetrate to the LLSC/EFCM contact; for the remainder of the borings, no attempt has been made to estimate the depth of the contact and the maximum penetrated sediment depths are used as data. For 18 out of 19 sites

on the peat bog only the depth of sediment to impenetrable basement is available: this is likely to result in an overestimate (possibly within the range of 10-20 percent) of the volume of Post-glacial sediment beneath the bog. However, this volume is estimated to represent only ca. 10 percent of the total Post-glacial accumulation within the lake basin. Since the results of ^{14}C-dating (Chapter 5, section 5.3) and Russian coring (Chapter 4, section 4.5) suggest that the lake mud - peat contact beneath the bog pre-dates the deposition of magnetic peak B, all of the sediment beneath the bog is included within sediment layer 1.

In the northern sector of the lake basin, where Ruasian borings were not carried out, the depth of the LLSC/EFCM contact was estimated from the occurrence of Late-glacial clay in the minicores (Chapter 4, section 4.3). In addition, the depths of sediment in cores which did not contain clay were also used as data wherever pollen analyses or location in or close to the trench indicated the probability of an early Flandrian age (see Chapter 4, sections 4.3-4.4). Numerous field records of the occurrence of impenetrable substrate (= 0 sediment depth), either rock or clay, were also used as data for all three maps.

The depths of magnetic peak B were obtained from the whole core k and single-sample χ records (Chapter 4, sections 4.3-4.4). Over the majority of the area of the lake this simply involved obtaining the depth of the largest sub-surface susceptibility peak. However, the central sector presents some difficulty, since in several cores there is either more than one major sub-surface susceptibility peak (eg. cores 80/0L, 60/80L) or no pronounced susceptibility maximum (eg. cores 80/60L, 60/60L) (see Chapter 4, sections 4.3-4.4; Figures 4.7 and 4.14). In these cases the mid-point of the section of increased sub-surface magnetic concentration was used as data.

At 17 sites, 4 of which are in the southern margin where magnetic peak B is not recorded in the whole core k records, boring records of the

mid-point of the laminated clayey sediments associated with this feature are used as data.

The greatest degree of uncertainty is probably associated with the estimation of the depth of magnetic peak A, since it is difficult to define this precisely from the whole core k records. In addition, difficulties remain in determining the areal extent of this feature in the southern sector of the lake basin without recourse to many more single-sample magnetic measurements (see Chapter 4, section 4.4.2). Therefore, the contour map for sediment layer 3 and the volume calculated from it probably provide a minimum estimate of its occurrence in the lake basin (see section 5.4, below). In four cases, the susceptibility records of magnetic peak A were supplemented by lithostratigraphic records of black-coloured sediments (see Chapter 4, section 4.3.1 and Appendix D).

The contouring was implemented using the GPCP package (CALCOMP, 1971) on the University of Newcastle IBM 370 computer, using a digitised outline of the lake basin, the data points for which were also included as data (= 0 sediment depth) in the three sets of sediment depths. The sediment volume for each data set was calculated as the volume of the solid represented by the contoured area, a standard facility of the GPCP package. This approach contrasts with that of other workers (eg. Davis, 1976; Dearing et al., in press), who have tended to extrapolate the mean depth of a correlated horizon either over the whole, or over part of, the lake basin under study. It seems likely that, assuming the accuracy of a given core-correlation scheme, the approach adopted here is likely to provide more accurate estimates of sediment volume. The SYMVU package (Muxworthy, 1977) was used to produce a simulated three-dimensional view of each sediment layer. In order to simplify and summarise the patterns presented by the contour maps, trend surface analyses were carried out on the same data sets used for contouring. Maps of the locations of the data points used for all the analyses, together with the data values, are given in Appendix E.

6.3 Description of the contour maps

Figures 6.1-6.3 show isopach maps for sediment layers 1-3, respectively. The variation in the extent of the contoured area (for example, there is a relatively large uncontoured area in Figure 6.1) reflects the different contour intervals used: 50 cm; 10 cm and 2.5 cm for Figures 6.1-6.3, respectively.

Sediment layer 1: sedimentation from ca. 10 400 to 800 bp (Figure 6.1). The relative paucity of sediment accumulation in the northern sector of the lake basin over the time interval represented by the map is sriking. Comparison of Figure 6.1 with the present bathymetry (Chapter 2, section 2.4; Figure 2.4) demonstrates that the greatest thicknesses of sediment are located in what are currently the shallowest parts of the lake basin, in the central and southern sectors. Therefore, this pattern does not solely reflect the morphometry of the original basin.

Two main foci of sediment accumulation are evident: located north and south of the ridge which lies approximately along the /120 line (Chapter 4, section 4.2). Computation of sediment volumes over discrete areas of the contour map indicated that ca. 54 percent of the total sediment body occurs north of the /120 line, and ca. 15 percent south of the /310 line, beneath the peat bog.

The steep contour gradients in the southern sector illustrate well the steep-sided, trough-like morphometry of this area of the basin.

Sediment layer 2: sedimentation from ca. 800 bp to AD 1951 Figure 6.2). Because of the absence of data points for the southernmost part of the lake basin, the contours for this area have been suppressed.

Reference to the present basin bathymetry (Figure 2.4, op. cit.) indicates an absence of sediment accumulation in the 'trench' during this interval. Two other areas are devoid of sediment: (i) much of the shallow western littoral area, corresponding in part to the area of the

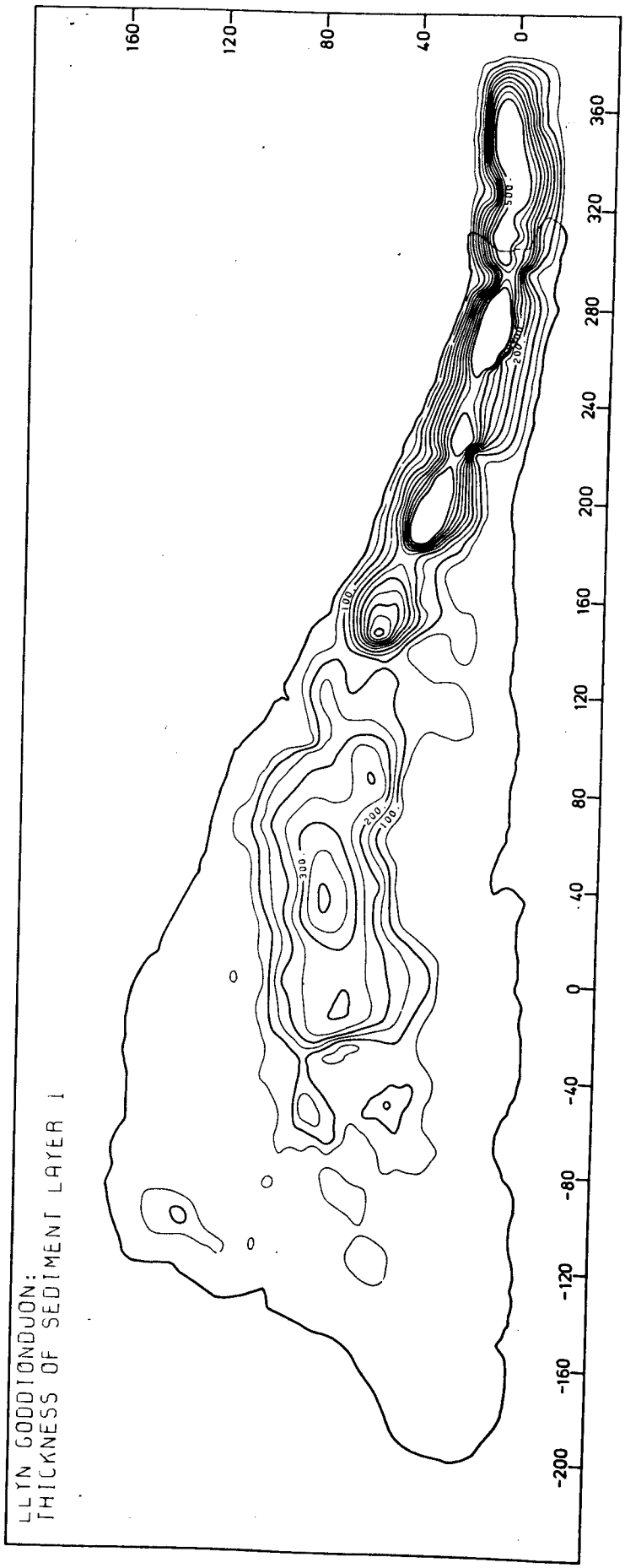

Figure 6.1 Contour map of the thickness of sediment layer 1. (All contours in cm).

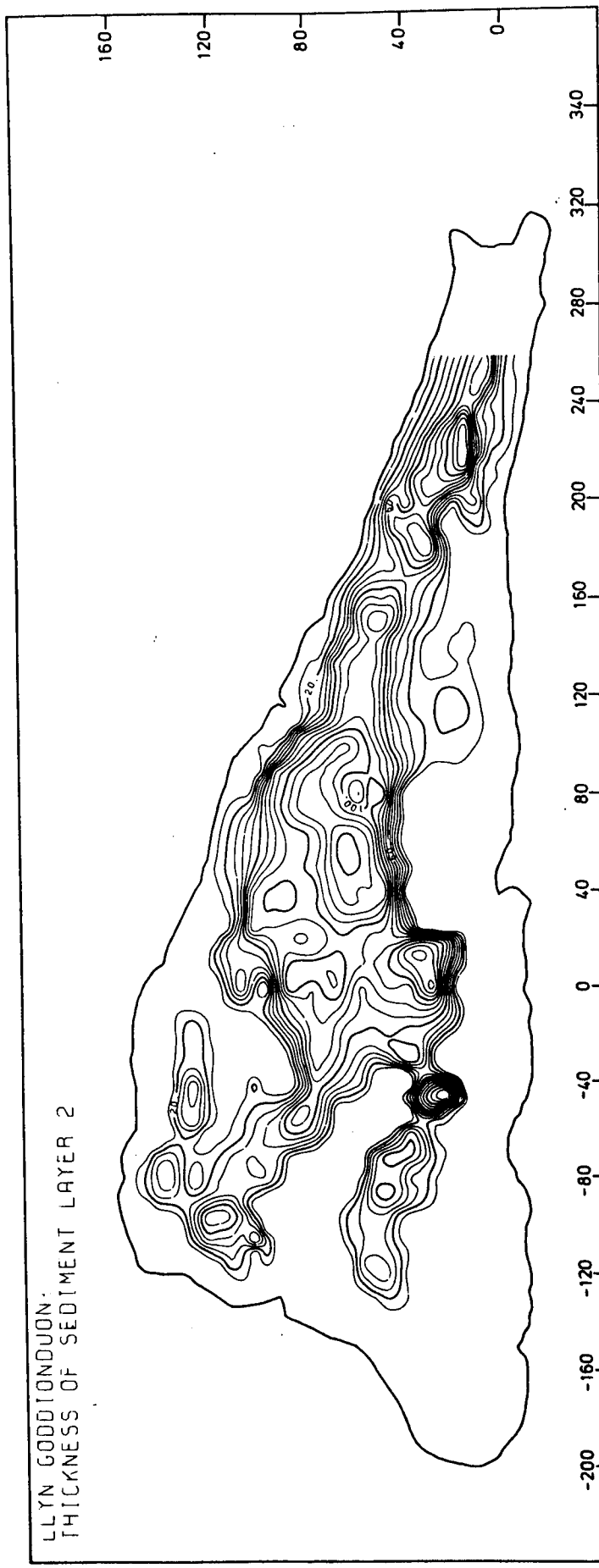

Figure 6.2 Contour map of the thickness of sediment layer 2

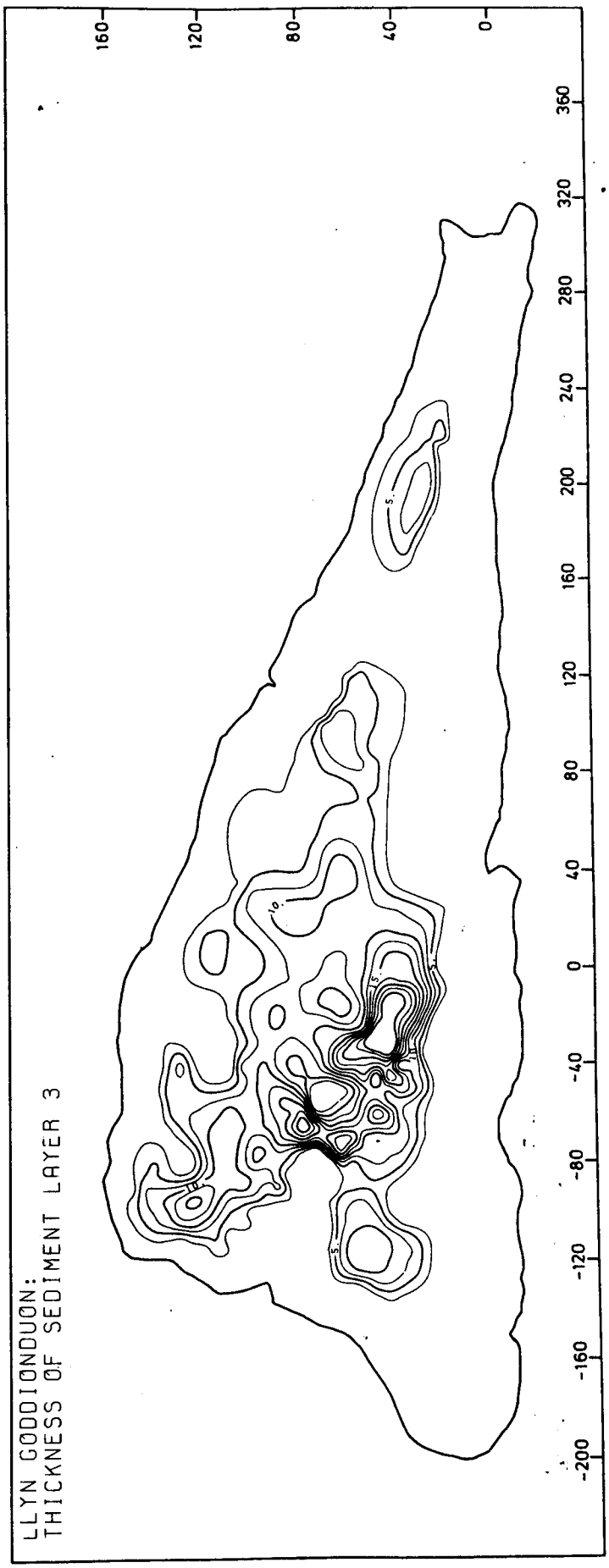

Figure 6.3 Contour map of the thickness of sediment layer 3

lake basin occupied by emergent macrophytes (Chapter 2, section 2.6; Figure 2.6). (ii) The small area in the northeastern part of the basin; in this case, the absence of sediment is not immediately related to the (present) bathymetry, since areas of comparable depth to the north, south and east have accumulated sediment.

Computation of the proportion of the sediment body lying north of the /120 line produced a value of 78 percent, indicating a northward shift in the focus of sediment accumulation during the time interval represented by the deposition of sediment layers 1 and 2. Maximum sediment thickness (greater than 120 cm) occurs in the central sector, between the /0 and /100 lines.

Sediment layer 3: sedimentation from AD 1951 to 1977 (Figure 6.3).

The disposition of the base-line contour (i.e. 2.5 cm) is comparable with that for sediment layer 2, in that several features delimited in Figure 6.2 are repeated: for example, the area devoid of sediment in the northeastern part of the basin; and the 'finger' of sediment accumulation extending into the northwestern part of the basin. Nevertheless, the overall pattern of sediment accumulation differs markedly from that depicted in either Figure 6.1 or 6.2, since the bulk of the sediment volume lies in the northern sector, with the focus of accumulation located in the central and southwestern parts of the 'trench'.

Figure 6.4 shows SYMVU plots of the three sediment layers.

6.4 Trend surface analysis

First, 2nd, 3rd and 4th order least squares polynomial trend surfaces were fitted to the data sets for sediment layers 1, 2 and 3. All of the surfaces were significant at the 0.01 level, as were the percentage increases in explanation obtained by the fitting of surfaces of successively higher order (Davis, 1973; Mather, 1976); however, only the results from the 4th order surfaces are presented here.

Reference to Table 6.1 shows that the trend surfaces fitted to the data for sediment layers 2 and 3 account for over 50 percent of the

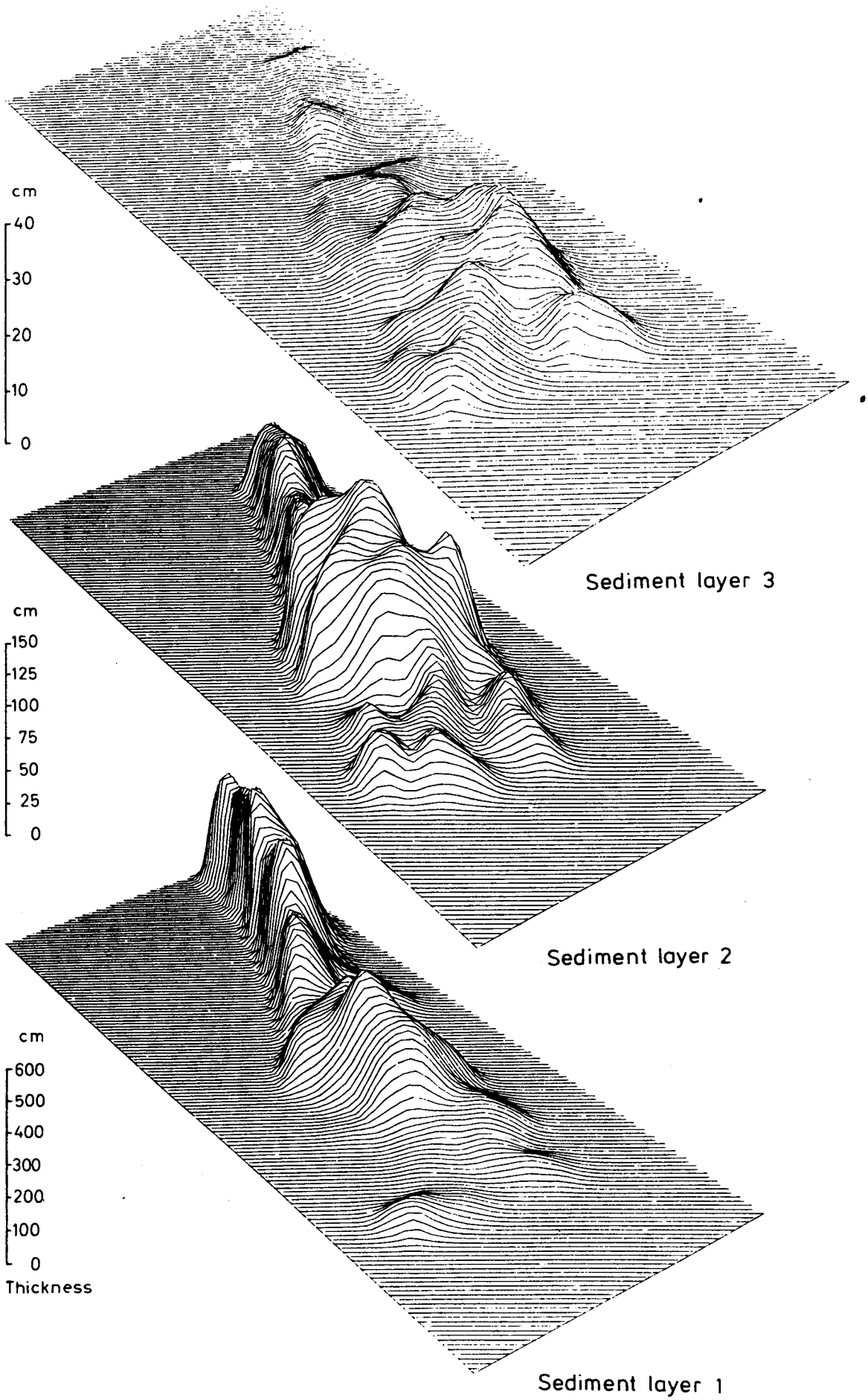

Figure 6.4 SYMVU plots of the thicknesses of sediment layers 1, 2 and 3

Sediment Layer	Number of Data Points	Source of Variation	Sums of Squares (SS)	Degrees of Freedom (DF)	Mean Square (MS=SS/DF)	Calculated F (MS Polynomial/ MS Deviation)	Tabulated F	% Explanation
3	416	POLYNOMIAL	4 111.88	14	293.71	39.16	2.04	57.76
		DEVIATION	3 006.59	401	7.50			
2	452	POLYNOMIAL	169 901.35	14	12 135.81	33.12	2.04	51.48
		DEVIATION	160 145.66	437	366.47			
1	452	POLYNOMIAL	1 510 781.14	14	107 912.93	14.48	2.04	31.69
		DEVIATION	3 256 687.40	437	7 452.37			

Method after Davis (1973)

Table 6.1. Statistical output for 4th order trend surfaces

total variation; however, the surface fitted to the data for layer 1 accounts for a significantly lower percentage (ca. 30 percent).

Figures 6.5-6.7 show maps of the three trend surfaces. They do not add significantly to the observations made of the contour maps (section 6.3, above); nevertheless, they provide a striking visual impression of the change in the spatial pattern of accumulation shown by sediment layer 3.

6.5 Estimates of total sediment volume and dry mass

The contour maps (Figures 6.1-6.3) enable estimates to be made of the volumes of the three sediment layers (see section 6.2, above). Expression of this data more meaningfully in terms of total dry mass and dry masses of the organic and mineral fractions requires estimates of the dry weight/wet volume ratio and percentage organic matter content of the sediment.

Table 6.2 shows mean values of dry weight/wet volume for core 60/60L

Interval (cm)	Number of Samples	Dry weight/wet volume ($g\ cm^{-3}$)
0-6	3	0.1063
6-184.5	89	0.1684

Table 6.2. Mean values of dry weight/wet volume ratio for core 60/60L

and Table 6.3 shows mean values of percentage weight loss on ignition for core 60/-20. Since these parameters often vary

Interval (cm)	Number of Samples	% weight loss on ignition
0-6	6	30.52
6-70.5	65	21.34

Table 6.3. Mean values of percentage weight loss on ignition for core 60/-20

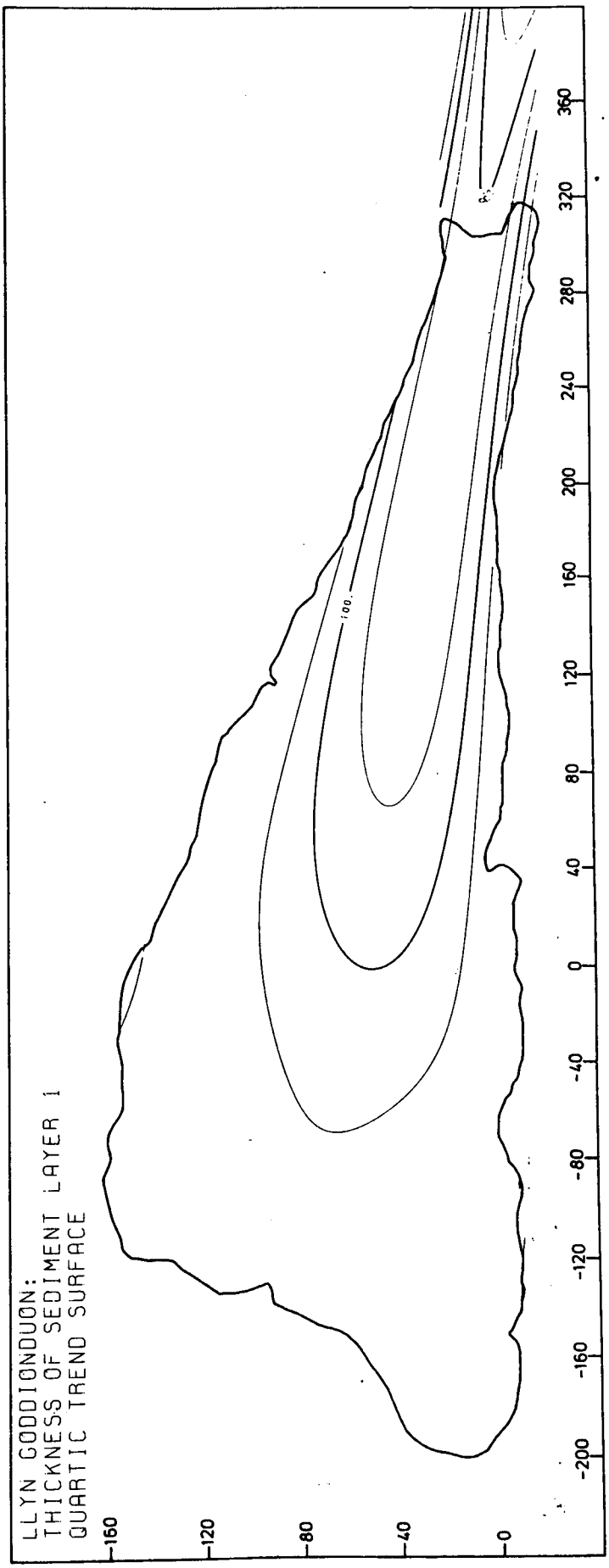

Figure 6.5 Quartic trend surface for the thickness of sediment layer 1

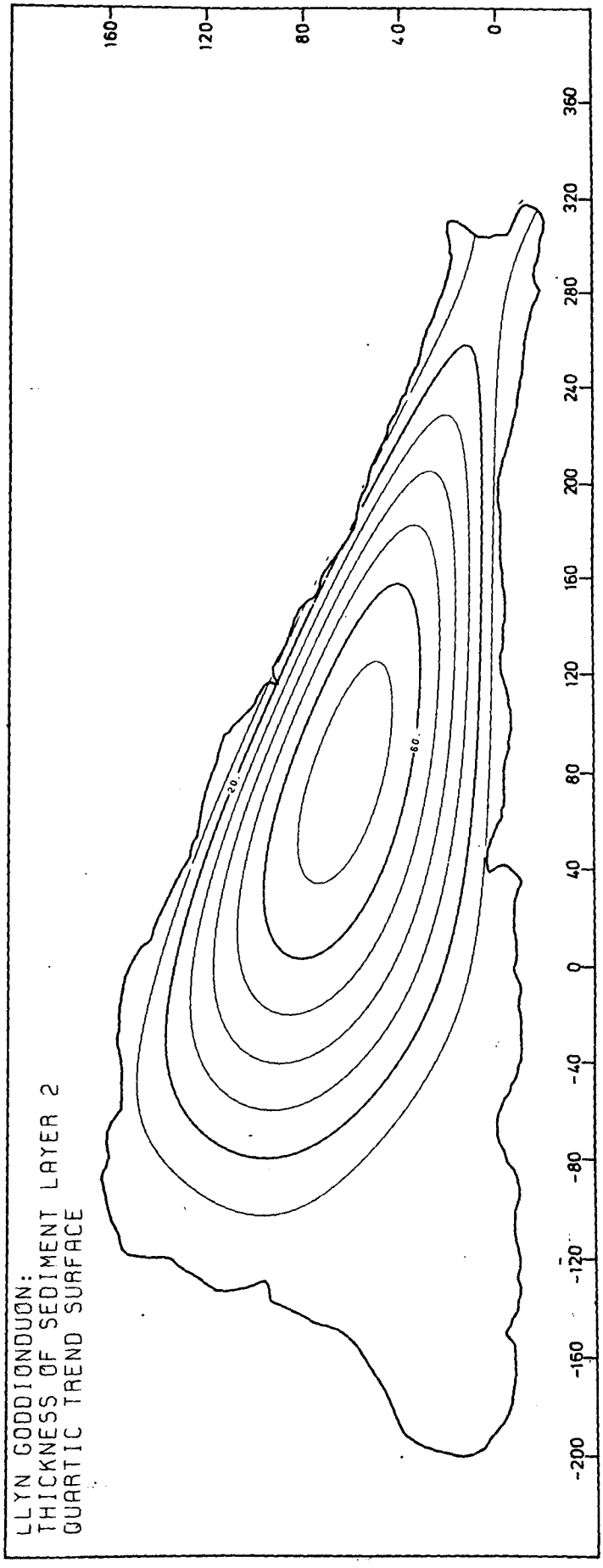

Figure 6.6 Quartic trend surface for the thickness of sediment layer 2

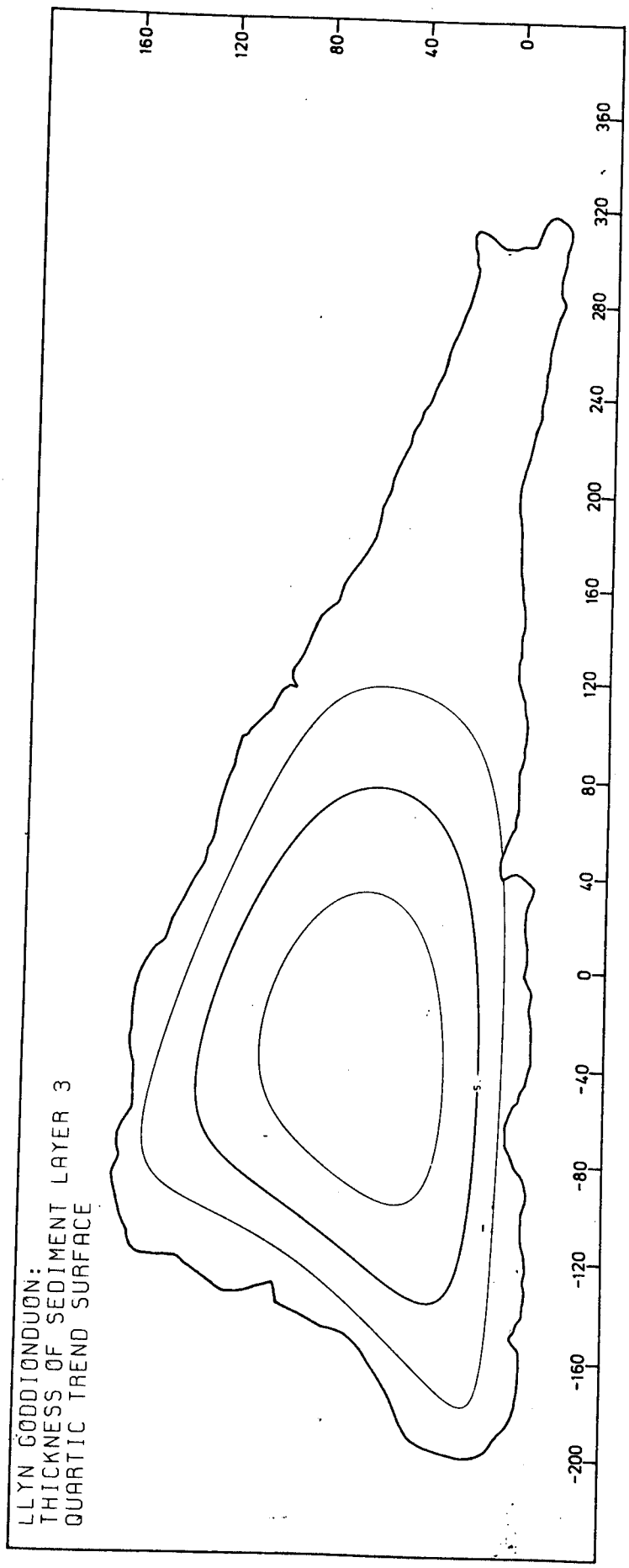

Figure 6.7 Quartic trend surface for the thickness of sediment layer 3

significantly down lake sediment cores, estimates were obtained from discrete sections of cores 60/60L and 60/-20. The interval 0-6 cm in both cores (corresponding to magnetic peak A) was used to obtain estimates for sediment layer 3, and the remainder of the cores for estimates for sediment layers 1 and 2. (The data for sediment wet density, percentage water content and percentage weight loss on ignition required for these estimates are shown graphically in Appendix B).

Table 6.4 shows estimates of the wet volume, total dry mass, dry

Sediment layer	Calculated volume (m^3)	Total dry mass ($X10^3$ kg)	Mass of organic matter ($X10^3$ kg)	Mass of ash ($X10^3$ kg)
3	1 612-1 990	171-212	52-65	119-147
2	14 909	2 511	536	1 975
1	51 528	8 677	1 852	6 825

Table 6.4. Estimates of wet volume, total dry mass of the organic fraction and mass of ash for sediment layers 1, 2 and 3

mass of the organic fraction and the mass of ash for each sediment layer. There are two estimates for layer 1. The smaller estimate was obtained by calculating the volume of the solid represented by the contour map in Figure 6.3, as described in section 6.2. Because of the uncertainty regarding the representation of magnetic peak A in the southern sector of the lake basin (see Chapter 4, section 4.4.3), an additional estimate was made of the volume of sediment layer 3. This was obtained by calculating the volume of layer 3 which occurs north of the /-10 line (where magnetic peak A is clearly represented in the whole core k records) in the same manner as for sediment layers 2 and 3, and then extrapolating the mean depth of the base of magnetic peak A (calculated from the whole core and single sample magnetic

records for sites south of the /-10 line) over the remainder of the area of the lake basin bounded by the 1 m isobath, and using this to obtain a separate volume calculation for this area of the basin. The 1 m isobath was selected because the K records of cores from water depths shallower than this indicate the absence of recent sediment accumulation (see Chapter 4, section 4.3.2). The two estimates were summed and the result is included in Table 6.4.

Two points concerning the origin and composition of the sediment are relevant for the interpretation of the data shown in Table 6.4. Firstly, in view of the current extremely low biological productivity of Llyn Goddionduon (see Chapter 2, section 2.7) it is a reasonable assumption that for the most recent period of lake history only a small proportion of the sedimentary organic matter originates from within the lake basin itself. However, this need not have been so in the past, since several studies (e.g. Pennington et al., 1972; Walker, 1977; Digerfeldt,1977b) demonstrate that currently oligotrophic lakes have exhibited a transient phase of eutrophy at some stage during their (usually early) history. Although techniques are available which permit the differentiation of organic compounds from terrestrial and limnetic sources (e.g. electron spin resonance: see Tutin, 1969; Pennington and Lishman, 1971) they were beyond the scope of the present study. The small number of diatom analyses that has been performed (see Appendix F) suggest a low trophic state during the period of deposition of sediment layer 2. However, no analyses are available for sediment layer 1 and therefore it remains uncertain what proportion of the calculated mass of organic matter for this layer is likely to be of autocthonous origin.

Secondly, since no determinations of either the numbers of diatoms per unit volume of sediment, or the concentration of alkali-soluble silica (which approximates diatom silica), an unknown

proportion of the estimated masses of ash consists of biogenically-precipitated silica. Digerfeldt (op. cit.) gives values of alkali-soluble silica ranging from 1.2-58 ($\overline{X}$ = 36) (percentages of the sum of true minerogenic material plus alkali-soluble silica) for Post-glacial sediments from an oligotrophic lake in the South Swedish Uplands. Kjensmo (1978) gives values of alkali-soluble silica ranging from 1-22 (percentages of total sediment) for Post-glacial sediments from a small meromictic lake in southeast Norway. Transference of these values to the Goddionduon sediments depends upon a number of unverifiable assumptions; however, the cited data indicate that a significant proportion of the calculated masses of ash shown in Table 6.4 may be of autocthonous origin.

Finally, since lake sediments are subject to diagenetic change usually involving some decomposition and reduction in organic matter content during the process of transformation to chemically stable sediment, it is likely that the loss-on-ignition data used for sediment layers 1 and 2 are underestimates of their organic matter content at the time of deposition.

6.6 Estimates of rates of total sediment influx and yield

Table 6.5 shows the results from Table 6.4 transformed to estimates of rates of total sediment influx and yield per unit area of the terrestrial part of the Goddionduon watershed, using the accumulation times of sediment layers 1, 2 and 3 established in Chapter 5. In addition to the fact that the estimate of the duration of the accumulation time of layer 2 is tentative, this procedure introduces a further source of uncertainty since it assumes negligible and constant sediment loss via the outflow. However, despite the numerous sources of error and uncertainty entailed in the production of the data shown in Table 6.5, the magnitude of the differences in the estimated rates of influx and yield for the three sediment layers seems

Sediment layer	Period	Duration (yr)	Total sediment influx ($Kg\ yr^{-1}$)	Organic matter influx ($Kg\ yr^{-1}$)	Ash influx ($Kg\ yr^{-1}$)	Total sediment yield ($Kg\ ha^{-1}\ yr^{-1}$)	Organic matter yield ($Kg\ ha^{-1}\ yr^{-1}$)	Ash yield ($Kg\ ha^{-1}\ yr^{-1}$)
3	AD 1951-1977	26	6 577-8 154	2 000-2 500	4 577-5 654	263-326	80-100	183-226
2	ca. 800 bp-AD 1951	ca. 800	3 139	670	2 469	126	27	99
1	ca. 10 400-800 bp	ca. 9 600	904	193	711	36	8	28

Table 6.5 Estimates of the rates of influx and yield per unit area of the terrestrial part of the Goddionduon watershed of total sediment, organic matter and ash.

likely to reflect genuine variations in the rate of sediment export from the terrestrial part of the watershed.

CHAPTER 7. MAGNETIC MINERALOGY OF THE LAKE SEDIMENTS, AND INVESTIGATION OF POTENTIAL LAKE SEDIMENT SOURCES

7.1 Introduction

This chapter attempts (i) to identify the magnetic mineralogies responsible for the down-core changes in susceptibility and SIRM which provide the basis for the core correlation scheme described in Chapter 4; and (ii) to use magnetic measurements to identify possible lake sediment source materials within the watershed. It was hoped that these efforts would aid both the reconstruction of the environmental history of the lake watershed and the interpretation of the changes in the estimated rates of sediment influx. Additionally, it was hoped that a contribution could be made to the increasing number of studies which attempt to interpret the down-profile variations in the susceptibility and other mineral magnetic properties of lake sediments in terms of changing sediment sources and erosional processes (see references in section 7.2, below). To provide a context for the latter intention, section 7.2 gives a summary of current interpretations of changes in magnetic concentration down lake sediment cores.

7.2 Interpretations of stratigraphic changes in the magnetic concentration of lake sediments

Thompson et al. (1975) ascribed increases in the susceptibility of sediments in cores from Lough Neagh, Northern Ireland, to increases in the concentration of detrital titanomagnetite. The peaks in susceptibility were found to correlate closely with pollen-analytical evidence for periods of forest clearance and cultivation which were assumed to have increased the rate of minerogenic influx to the lake basin. Subsequently, similar relationships have been noted at several lake sites between increases in magnetic concentration within sediment cores and pollen analytical and chemical evidence for increased rates of minerogenic influx during both the Late-Devensian and Flandrian periods (e.g. Oldfield et al.,1978b; Dickson et al., 1978).

Dearing (1979) developed a descriptive model, based on empirical evidence, which attempts to predict changes in sediment susceptibility in lake watersheds underlain by a variety of geological substrates. He envisaged two extremes: (i) Lake watersheds in which substrate susceptibility is dominated by primary ferrimagnetic minerals. On the basis of observations by Ade-Hall (1964) that the modal size of titanomagnetite grains in basalt lava flows corresponded to the fine sand-coarse silt size range, together with measured variations in the susceptibility of particle-size fractions of basalt-derived soils and sediments which tended to support this view, Dearing (op. cit.) suggested that erosional processes (principally stream channel side erosion) which preferentially supplied particulates of this size range to lakes would effect increases in sediment susceptibility. On this basis, changes in lake sediment susceptibility would reflect changes in sediment particle-size distribution. (ii) Lake watersheds with substrates intrinsically poor in primary ferrimagnetic minerals, but with concentrations in the top-soil of fine-grained ($\ll 1$ μm) secondary ferrimagnetic minerals formed from weakly magnetic forms of iron by burning or 'fermentation' (Le Borgne, 1955; 1960; Mullins, 1977). In this case, increases in sediment susceptibility would be effected by erosional processes (such as rain splash and surface wash) which preferentially supplied the finer fractions of topsoil to the lake basin. Subsequently, Dearing and Flower (in preparation) have noted a correspondence between increases in the susceptibility of trapped seston samples from Lough Neagh (which would correspond to case (i), above) and the magnitude of monthly rainfall totals, which they interpret in terms of increased fluvial activity leading to increases in the influx rate of the relatively coarser particulates which dominate the sediment susceptibility. Therefore, they envisage the association between peaks in susceptibility and the pollen-analytical evidence for forest clearance and cultivation in the Flandrian

sedimentary record from Lough Neagh as operating via the effect of such activities in increasing the rate of surface runoff and stream discharge and consequently the erosive capacity of inflowing streams

In sediments from Loch Lomond, Scotland, in which again the mineral magnetic record appears to be dominated by detrital·magnetite, Thompson and Morton (1979) noted that the highest susceptibility occurred in the medium-fine silt (ca. 31-4 μm) particle-size range and explained increases in sediment susceptibility in terms of increases in the rate of influx of such particles effected by the action of rain splash and overland flow. Again, therefore, changes in sediment susceptibility are seen as resulting from changes in the sediment particle-size distribution.

In view of the significant estimated rates of atmospheric deposition of magnetic spherules, derived from industrial combustion processes, obtained from the study of the uppermost horizons of ombrotrophic peat bogs (Oldfield et al., 1978a; Oldfield et al., 1981b) it is possible that in lake watersheds with substrates devoid of both primary and secondary ferrimagnetic minerals, the susceptibility of the recent sediments may be significantly enhanced by this flux. Increases in the magnetic concentration in the uppermost sediments of Bar Mere (Cheshire) have been provisionally ascribed to this source (J. Smith, personal communication).

Finally, dramatic increases in the magnetic concentration of lake sediments have been interpreted as resulting from the production at high temperatures during major forest fires of large volumes of secondary ferrimagnetic minerals, followed by their rapid incorporation in the lake sediments as a consequence of the associated accelerated soil erosion (Rummery et al., 1979 b Rummery, 1981).

It may be seen from the above that increases in the magnetic concentration of lake sediments are almost always interpreted in terms

of the increased influx of particulate detrital, and in some cases atmospheric, ferrimagnetic material.

7.3 Magnetic mineralogy of the Goddionduon lake sediments

7.3.1 Susceptibility versus SIRM diagrams

Figures 7.1-7.2 show double logarithmic plots of χ versus SIRM for 1023 bulk sediment samples from the Goddionduon lake basin. For a given distribution of points, this form of presentation illustrates trends in magnetic concentration (diagonally, from left to right) and in magnetic mineralogy/magnetic grain size/magnetic grain shape (diagonally from right to left). Figure 7.1 shows samples from magnetic peaks A and B (see Chapter 4, section 4.4.2), while Figure 7.2 shows the remaining samples. Figure 7.1 includes the areas of the distributions shown in Figure 7.2; there is considerable overlap between the three distributions. Table 7.1 shows statistical parameters for each distribution. Viewing the data set as a whole, although both χ and SIRM vary through approximately two orders of magnitude, the majority of values are considerably lower than comparable data from lakes receiving drainage from substrates containing substantial volumes of primary ferrimagnetic minerals (e.g. Stober, 1978; Thompson and Morton, 1979).

Figure 7.1 illustrates well the essential difference between magnetic peaks A and B: although they have comparable susceptibilities, the SIRM values of peak B are up to one order of magnitude lower. The very low values of SIRM/χ (less than 1 kAm^{-1}) of some of the samples from peak B are the most notable feature of Figure 7.1. They are significantly lower than the experimental values obtained by Parry (1965; 1980) and Dunlop (1972) for multi-domain and stable single-domain sized magnetite powders (see Table 1.2; Chapter 1, section 1.8). For comparison, Table 7.2 shows the maximum and minimum values of SIRM/χ for bulk Post-glacial sediment samples from a variety of European lakes, together with the corresponding χ and SIRM values. For some of the

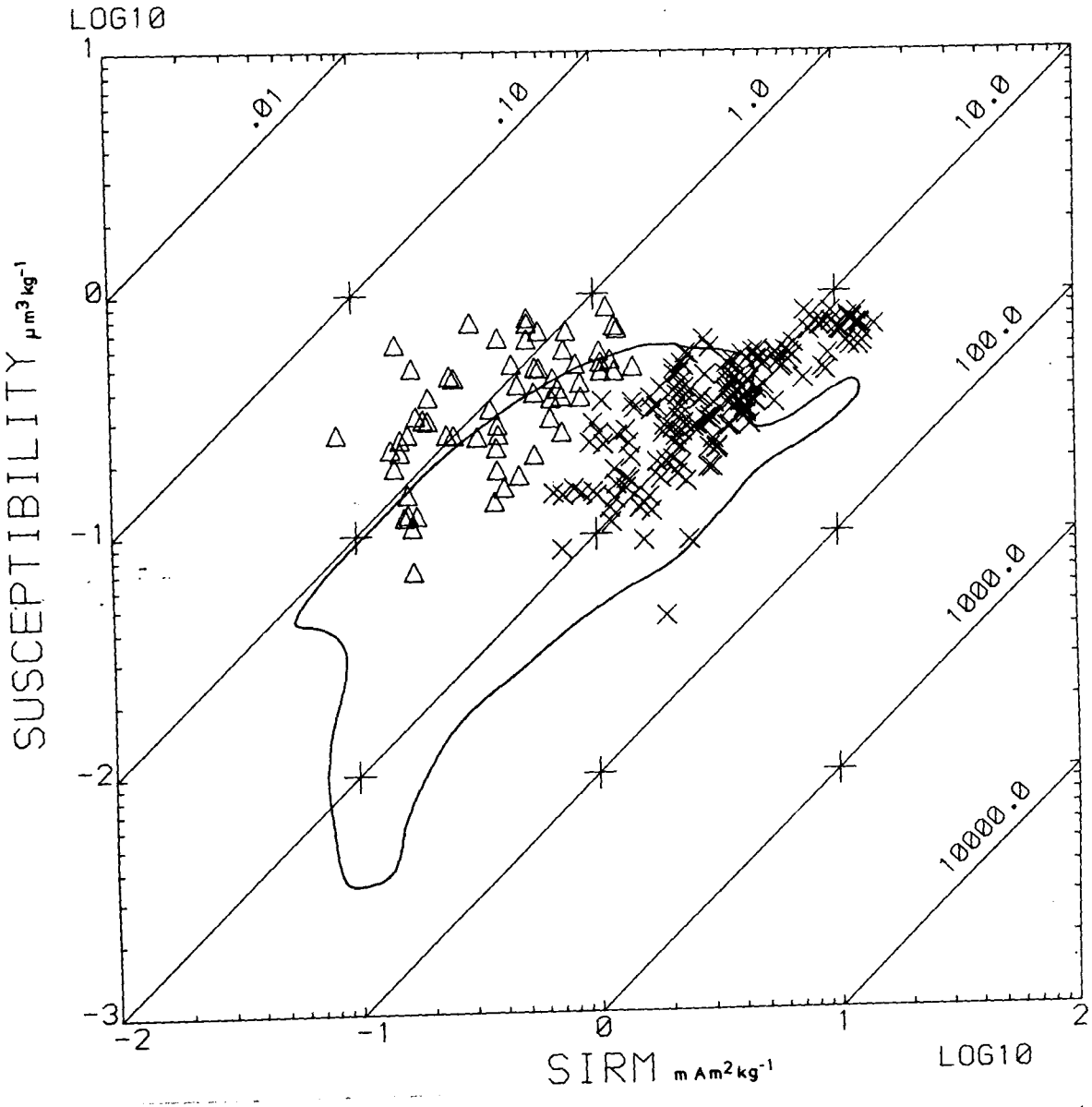

Figure 7.1 χ plotted against SIRM for samples from magnetic peaks A (crosses) and B (triangles).

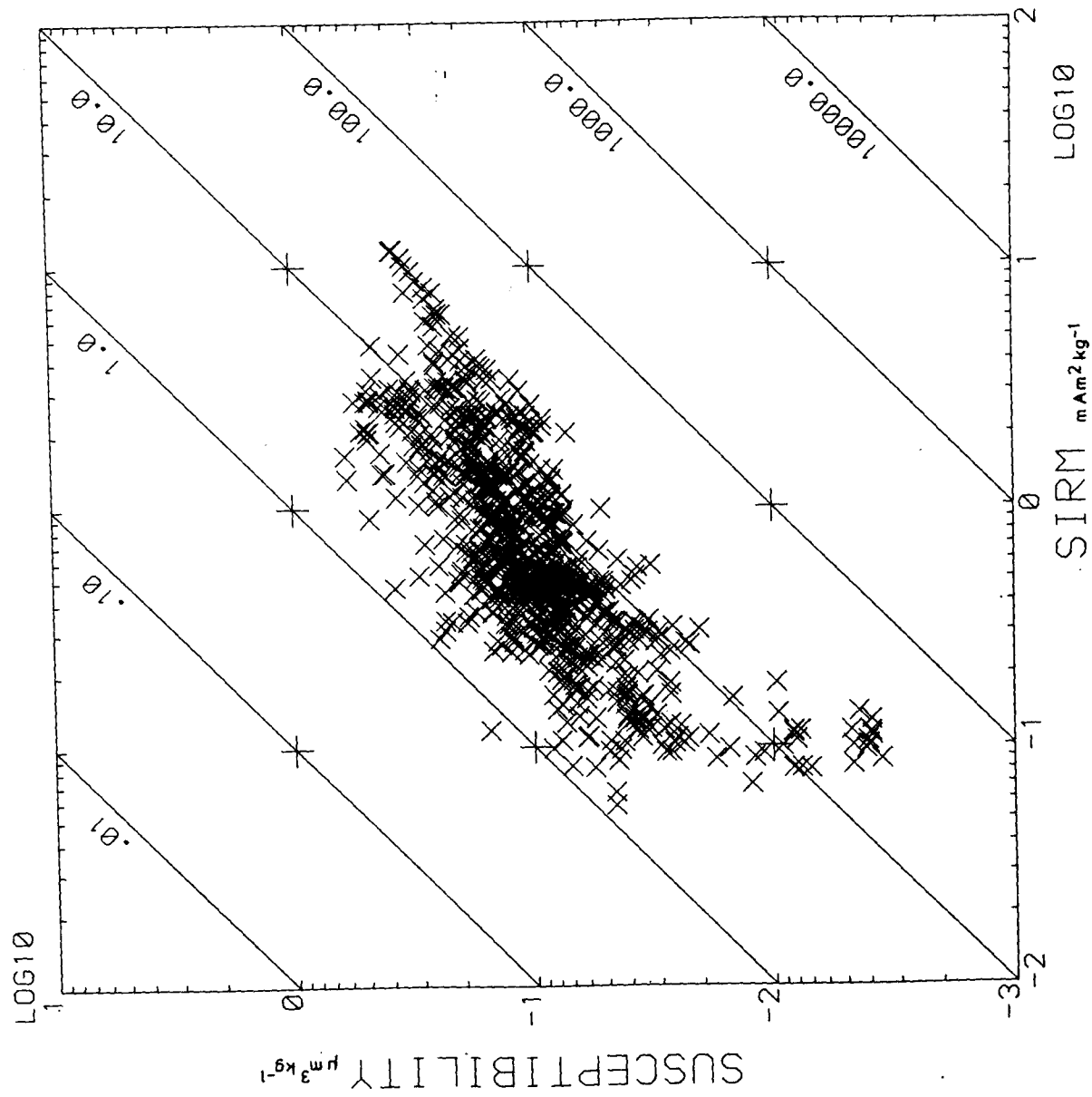

Figure 7.2 χ plotted against SIRM for samples other than those from magnetic peaks A and B

Distribution	N	Susceptibility ($\mu m^3\ kg^{-1}$)			SIRM (mAm^2kg^{-1})			SIRM/susceptibility (kAm^{-1})		
		Range	Mean	Standard Deviation	Range	Mean	Standard Deviation	Range	Mean	Standard Deviation
Magnetic Peak A	161	0.045-0.835	0.391	0.189	0.668-14.7	4.26	3.31	3.01 -21.1	10.5	5.02
Magnetic Peak B	63	0.071-0.886	0.399	0.200	0.084- 1.45	0.515	0.345	0.239- 2.92	1.38	0.72
Other Samples	799	0.004-0.603	0.132	0.096	0.057-11.7	1.12	1.40	0.766-30.6	8.14	5.98

Table 7.1. The range, mean and standard deviation of the χ, SIRM and SIRM/χ values for the three distributions of samples shown in Figures 7.1-7.2

Site	Source	Minimum SIRM/χ			Maximum SIRM/χ		
		χ ($\mu m^3 kg^{-1}$)	SIRM ($mAm^2 kg^{-1}$)	SIRM/χ (kAm^{-1})	χ ($\mu m^3 kg^{-1}$)	SIRM ($mAm^2 kg^{-1}$)	SIRM/χ (kAm^{-1})
Lake Paajarvi, Finland	1	0.28	1.84	6.5	0.20	3.80	19.0
Lake Ormajarvi, Finland	1	0.20	1.49	7.5	0.19	3.61	19.0
Lake Vuokonjarvi, Finland	1	0.19	0.66	3.5	0.68	15.41	22.7
Lake Pielinen, Finland	1	1.70	12.9	7.6	0.30	9.36	31.2
Lake Kiteenjarvi, Finland	1	0.35	1.0	4.9	0.39	10.5	26.9
Loch Lomond, Scotland	2	0.60	4.50	7.5	1.00	11.7	11.7
Llyn Geirionydd, Wales	3	-	-	11	-	-	40
Lake Windermere, England	3	-	-	11	-	-	37
Lough Neagh, Ulster	4	-	-	21	-	-	25
Newton Mere, England	5	0.036	0.197	5.5	0.035	0.382	10.9
Lac d' Annecy, France	6	0.126	0.40	3.2	0.119	2.0	16.8
Llyn Goddionduon, Wales	-	0.627	0.150	0.239	0.380	11.6	30.6

Sources: 1. Stober (1978). 2. Thompson and Morton (1979). 3. Turner (1979). 4. Thompson et al. (1975). 5. J. Smith (personal communication). 6. Dearing (1979)

Table 7.2. Minimum and maximum values of SIRM/χ, together with the corresponding χ and SIRM values, from twelve European lakes

sites, only wet volume-based data are available and in these cases only SIRM/χ is quoted. For the majority of sites the respective authors ascribe the magnetic properties of the sediments to the presence of primary ferrimagnetic minerals derived from soils, drift and bedrock. Lac d' Annecy is an exception in that here pedogenic magnetite is likely to make a significant contribution. With the exception of the minimum value from Llyn Goddionduon all of the SIRM/χ values fall within the range of values given by Dunlop (op. cit.) and Parry (op. cit.). The five Finnish sites exhibit consistently low values; in all cases, drift derived from acid igneous rocks constitutes the main sediment source (Stober, 1978).

Within the context of the range of SIRM/χ values shown in Table 7.2, the Goddionduon peak B sediments appear, therefore, to be relatively unusual. The characteristics - relatively high χ but negligible remanence - of these sediments could be explained by either (i) the presence of a high concentration of paramagnetic material, or (ii) by the presence of ultra-fine ($\ll 1$ μm) magnetite, which because of the effect of thermal agitation causing repeated reorientation of the magnetic moments of individual grains is unable to carry a stable remanence at room temperature. The susceptibility of such an assemblage of (superparamagnetic) grains may be very much greater than that of an assemblage of the same volume of ferrimagnetic grains (Stacey and Banerjee, 1974). On this basis it would be expected that the χ of these samples would be dominated by (i) or (ii) and their IRM characteristics (section 7.3.2, below) would reflect additional ferrimagnetic and canted antiferromagnetic forms of iron present in relatively low 'background' concentrations. Conceivably, very coarse grained multi-domain ferrimagnetic material, in which thermally activated domain wall movements may result in low magnetic retentivity, could also account for values of SIRM/χ of less than 1 kAm^{-1}; however, this would result in considerably lower coercivity of

SIRM values for these sediments than is the case (see below).

The majority of the SIRM/χ values for magnetic peak A and for the remainder of the samples are compatible with those for magnetite. The highest SIRM/χ values (ca. 15-40 kAm^{-1}) occur in Figure 7.2. They are contributed almost entirely by magnetic peak 2, apparently recorded only in the central sector of the lake basin (cores 60/60L and 50/90L; see Chapter 4, sections 4.4.2-4.4.3). These values are compatible with those for fine-grained multi-domain or stable single-domain magnetite.

7.3.2 Coercivity of SIRM measurements

Figures 7.3-7.6 show a selection of normalised coercivity of SIRM ($(B_0)_{CR}$) curves for samples from cores 120/-100, 40/-20, 50/90L and 40/200. Plots of χ, SIRM, ARM and various remanence ratios for these cores are shown in Figures 4.10-4.13 (Chapter 4, section 4.4.2). The $(B_0)_{CR}$ curves are plotted on two scales: from 0-100 mT (on the right) and from 0-1000 mT (on the left). The upper left part of each graph shows the core code, the depth of the top of the sample in centimetres and the sample symbol. The samples are grouped according to their location in relation to the system of magnetic peaks described in Chapter 4 (section 4.4.2). The values of χ, SIRM, SIRM/χ, $(B_0)_{CR}$ and S_{100} for the samples are shown in Table 7.3.

The overall degree of variation shown by the curves is relatively slight. In terms of their concave shape and relatively low $(B_0)_{CR}$ values (less than 50 mT in over 80% of the samples), most of the curves indicate that the SIRM of these samples is carried predominantly by medium-fine grained ferrimagnetic material. However, in almost all cases the incomplete back saturation at 200 mT (shown by the failure of the curves to intersect the base of the graphs at this field) suggests a significant canted antiferromagnetic content.

The spectra from magnetic peak A have $(B_0)_{CR}$ values from 34 to 46

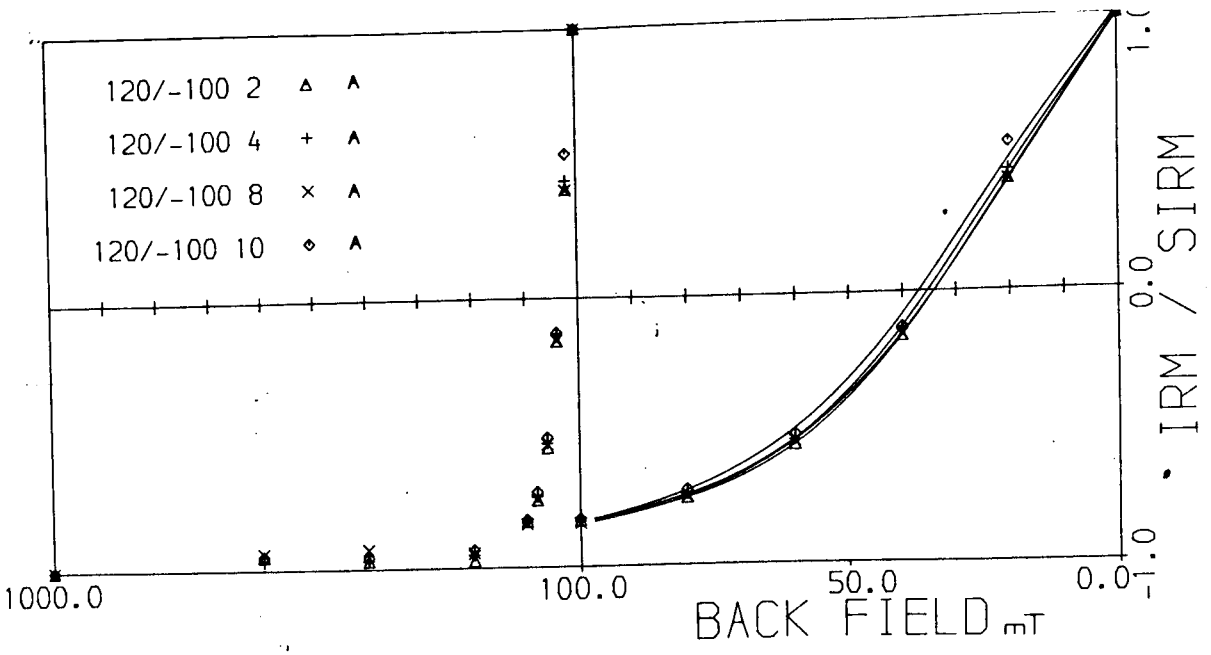
120/-100 2 A
120/-100 4 A
120/-100 8 A
120/-100 10 A
1000.0
100.0
50.0
0.0
1.0
0.0
-1.0
IRM / SIRM
BACK FIELD mT

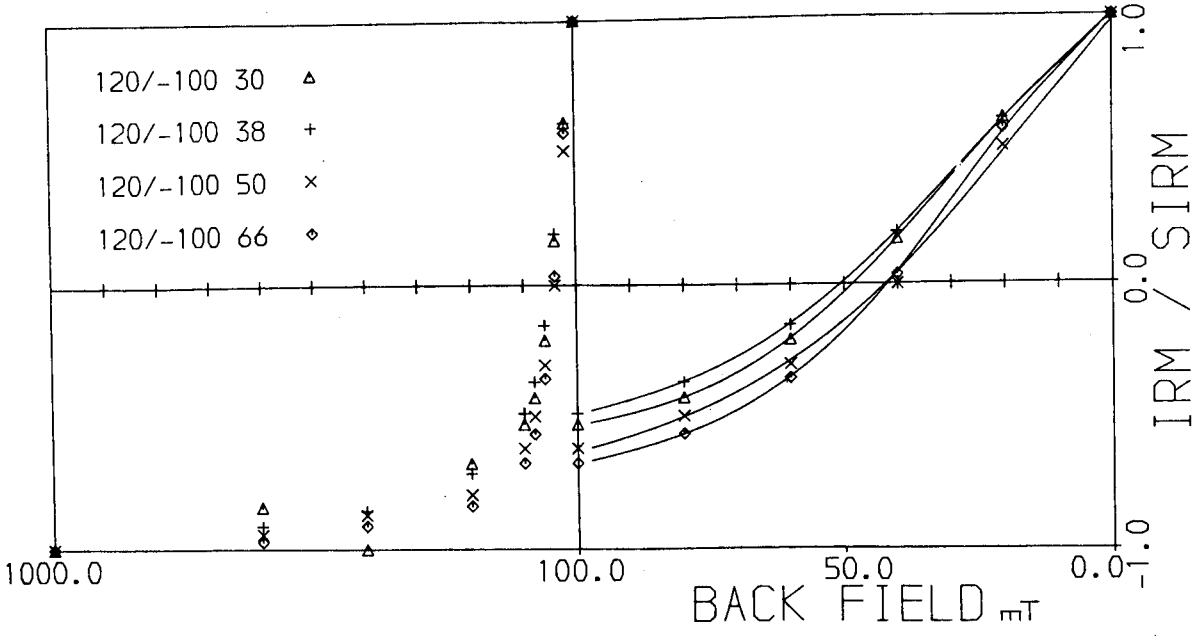
120/-100 30
120/-100 38
120/-100 50
120/-100 66
1000.0
100.0
50.0
0.0
1.0
0.0
-1.0
IRM / SIRM
BACK FIELD mT

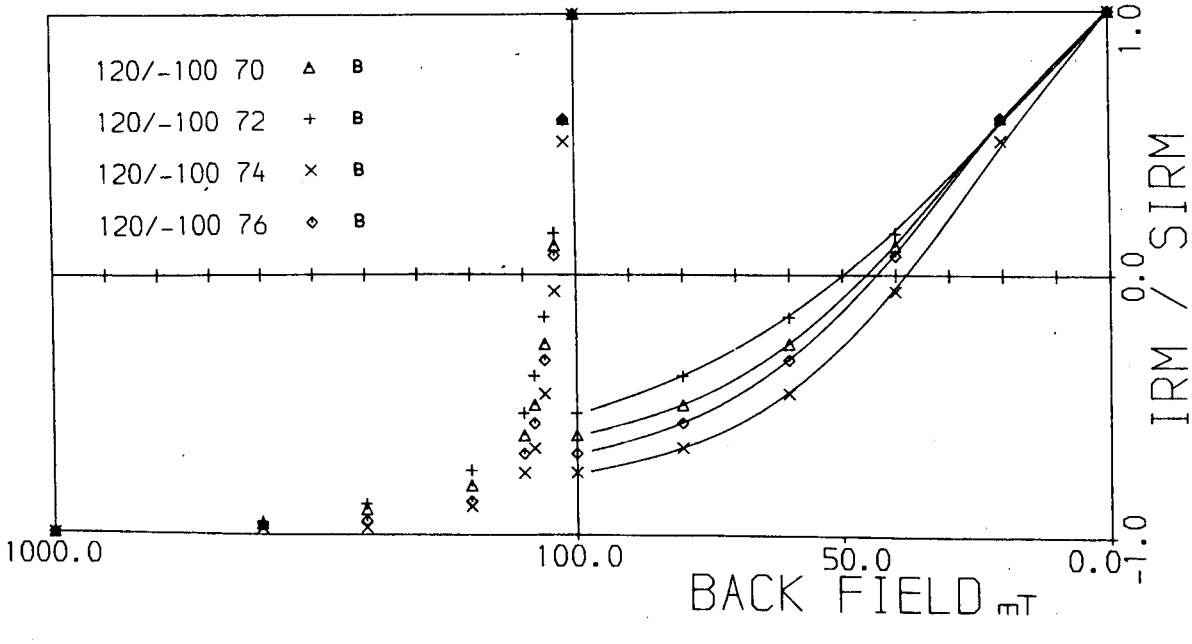
120/-100 70 B
120/-100 72 B
120/-100 74 B
120/-100 76 B
1000.0
100.0
50.0
0.0
1.0
0.0
-1.0
IRM / SIRM
BACK FIELD mT

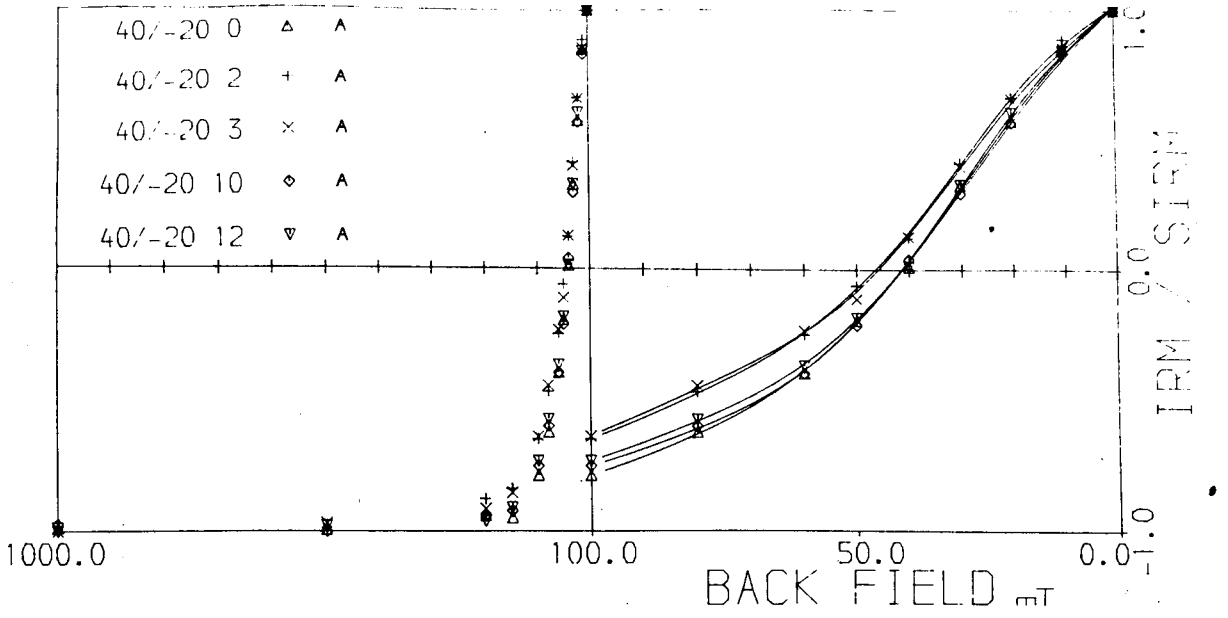

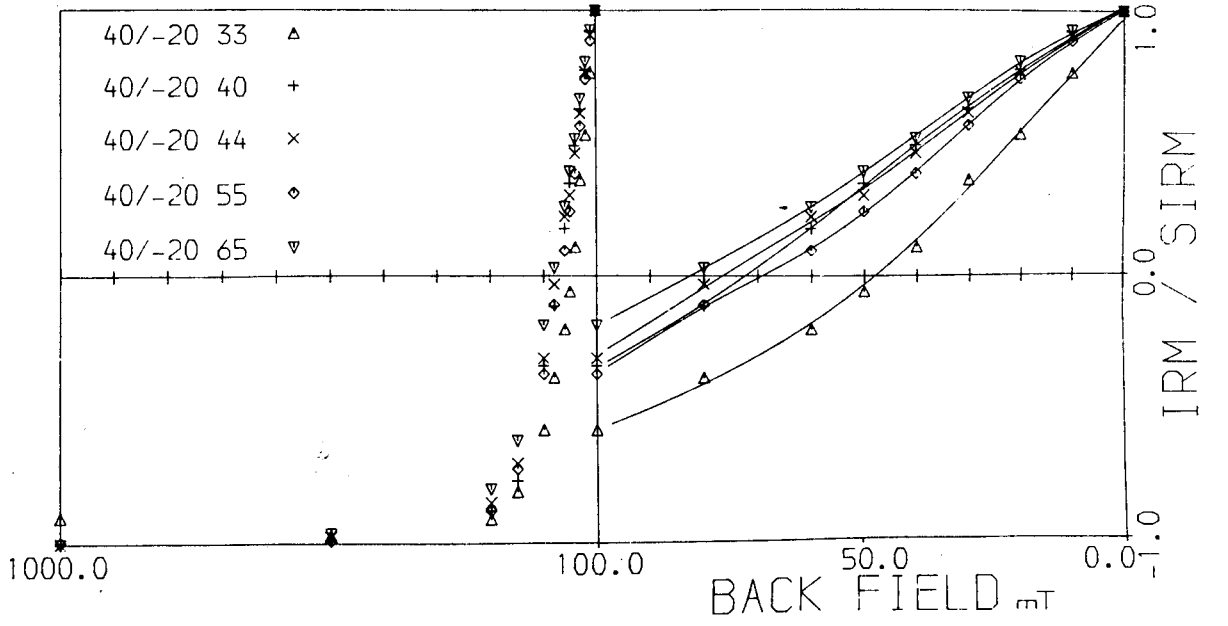

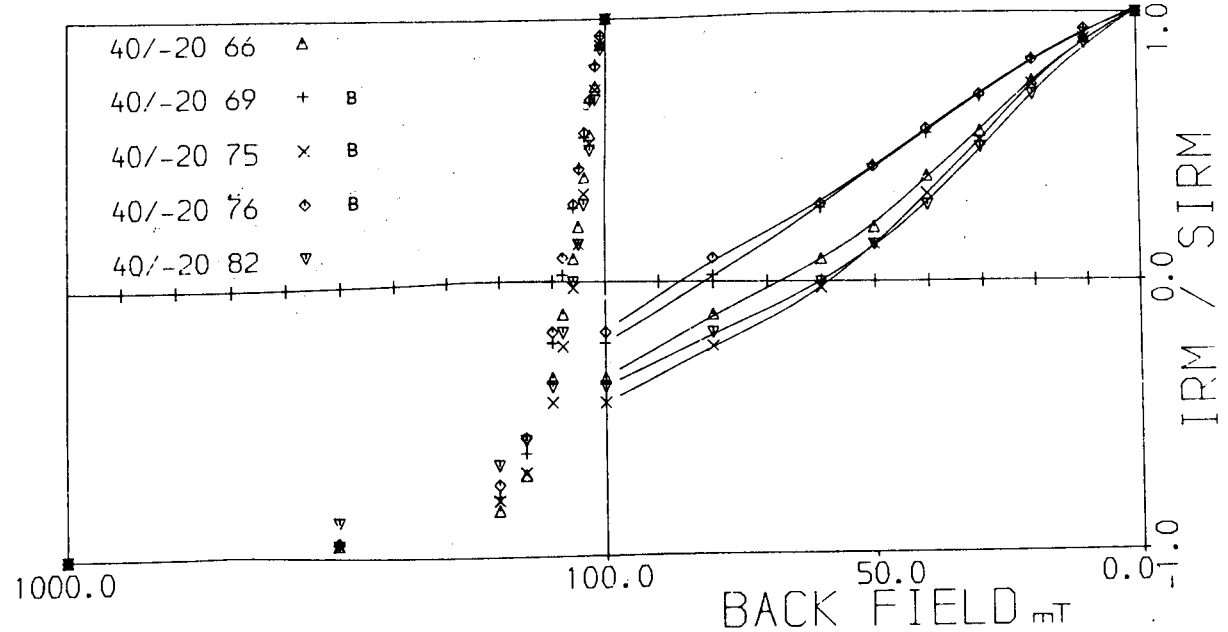

Figure 7.4 Coercivity of SIRM curves for samples from core 40/-20

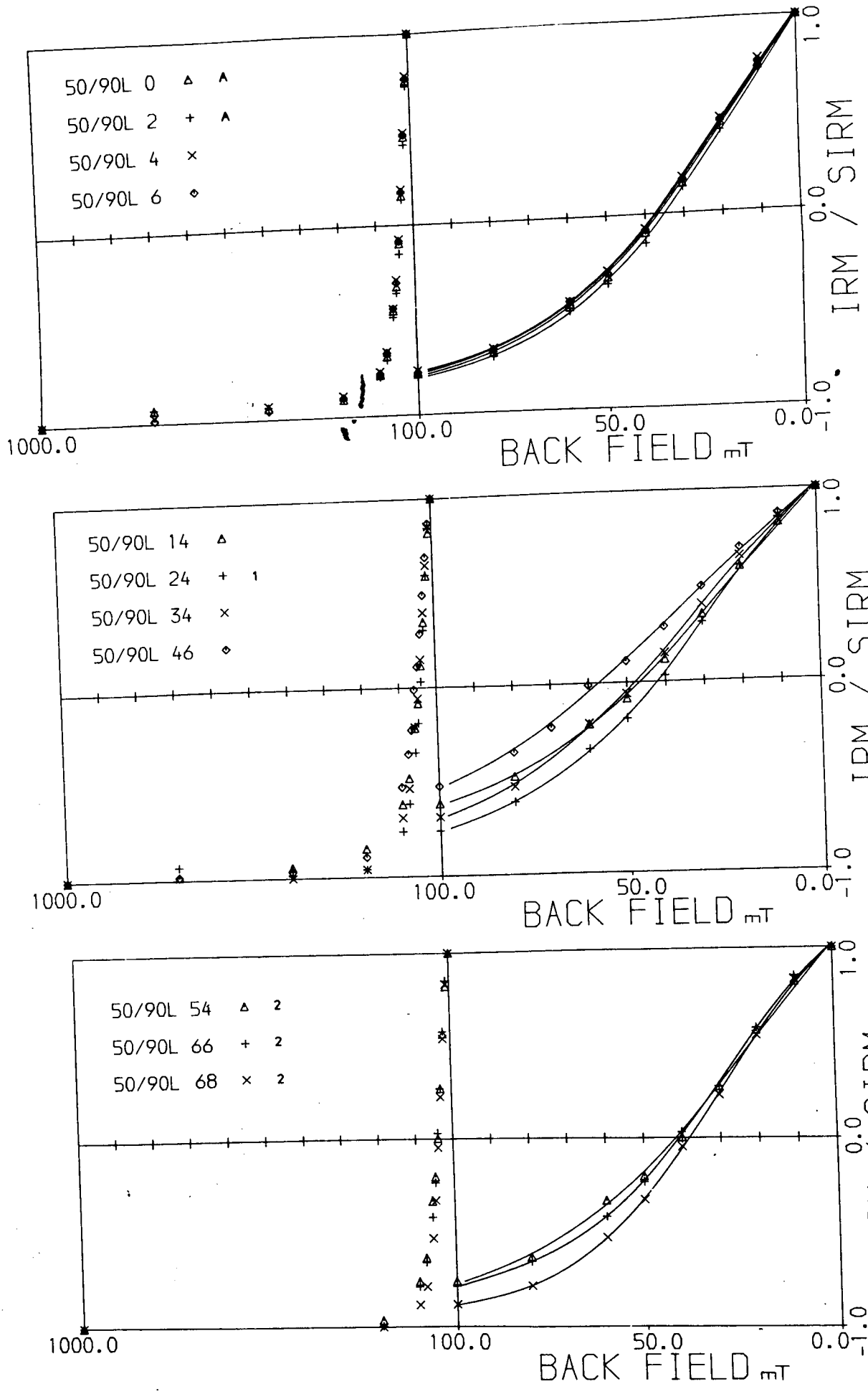

Figure 7.5 Coercivity of SIRM curves for samples from core 50/90L

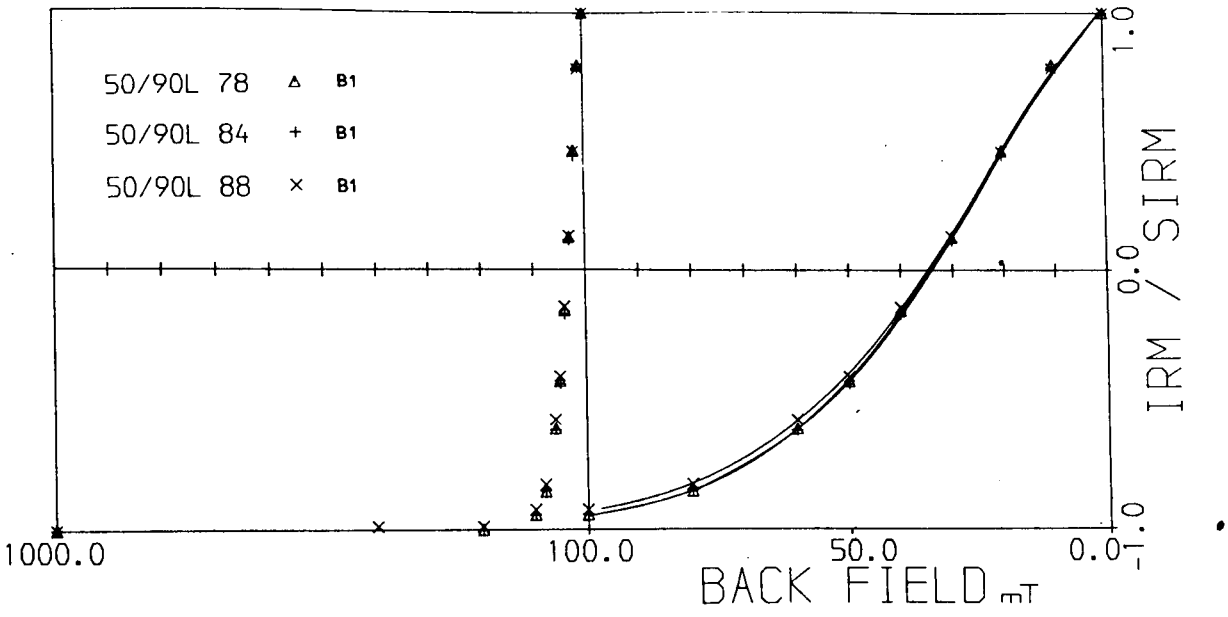

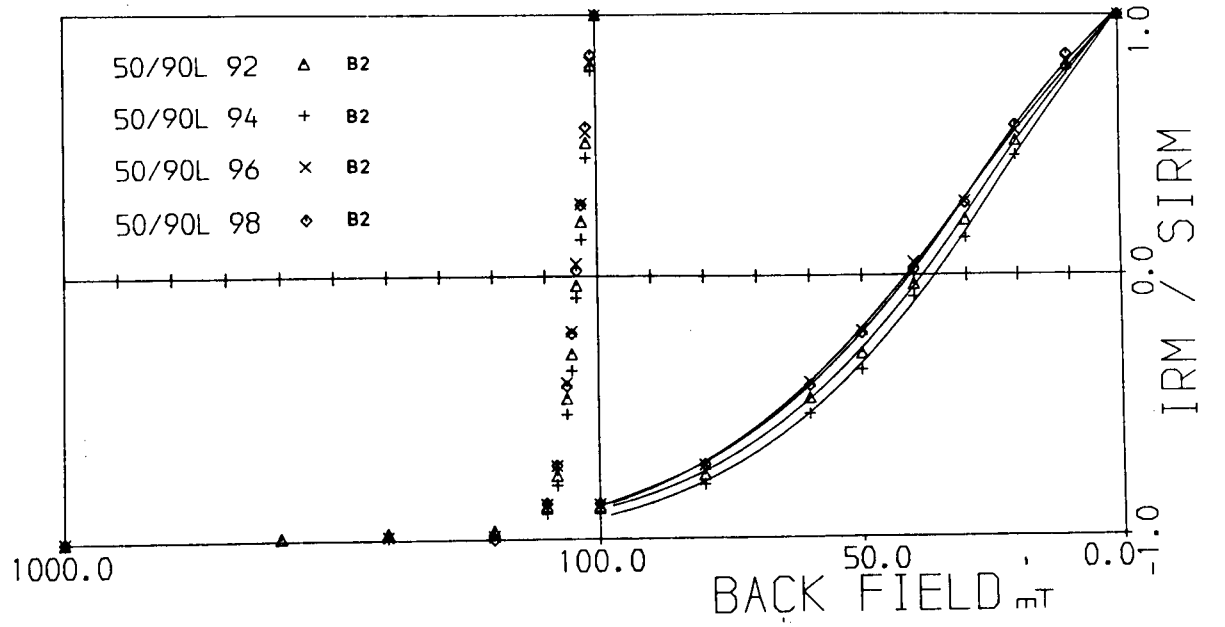

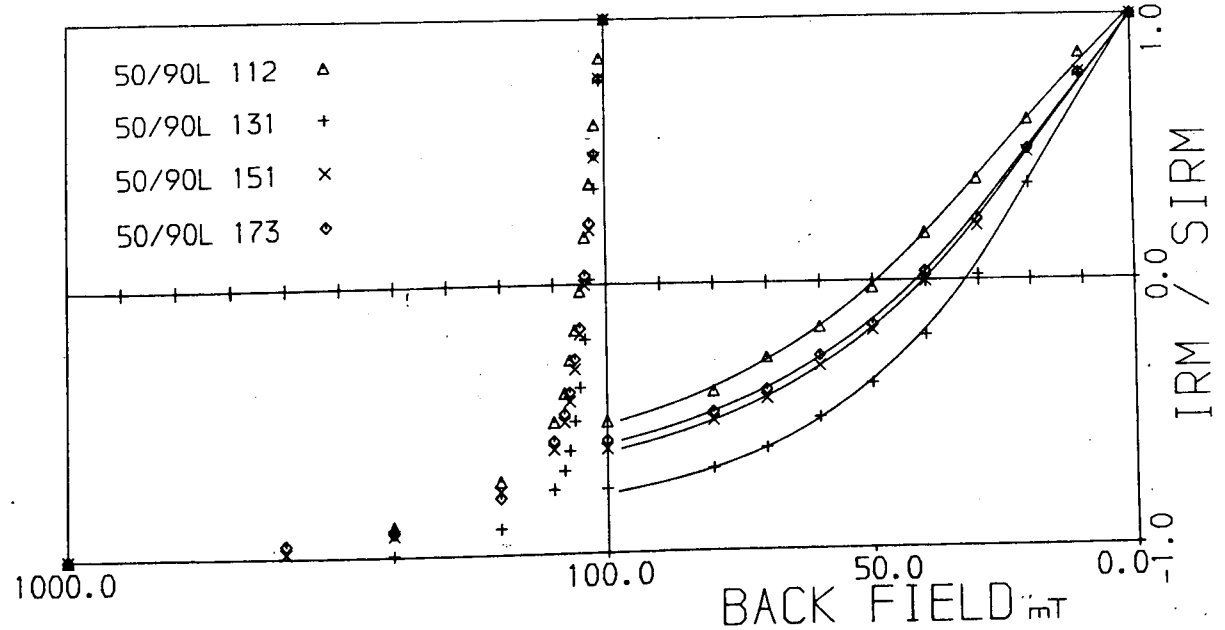

Figure 7.5 continued

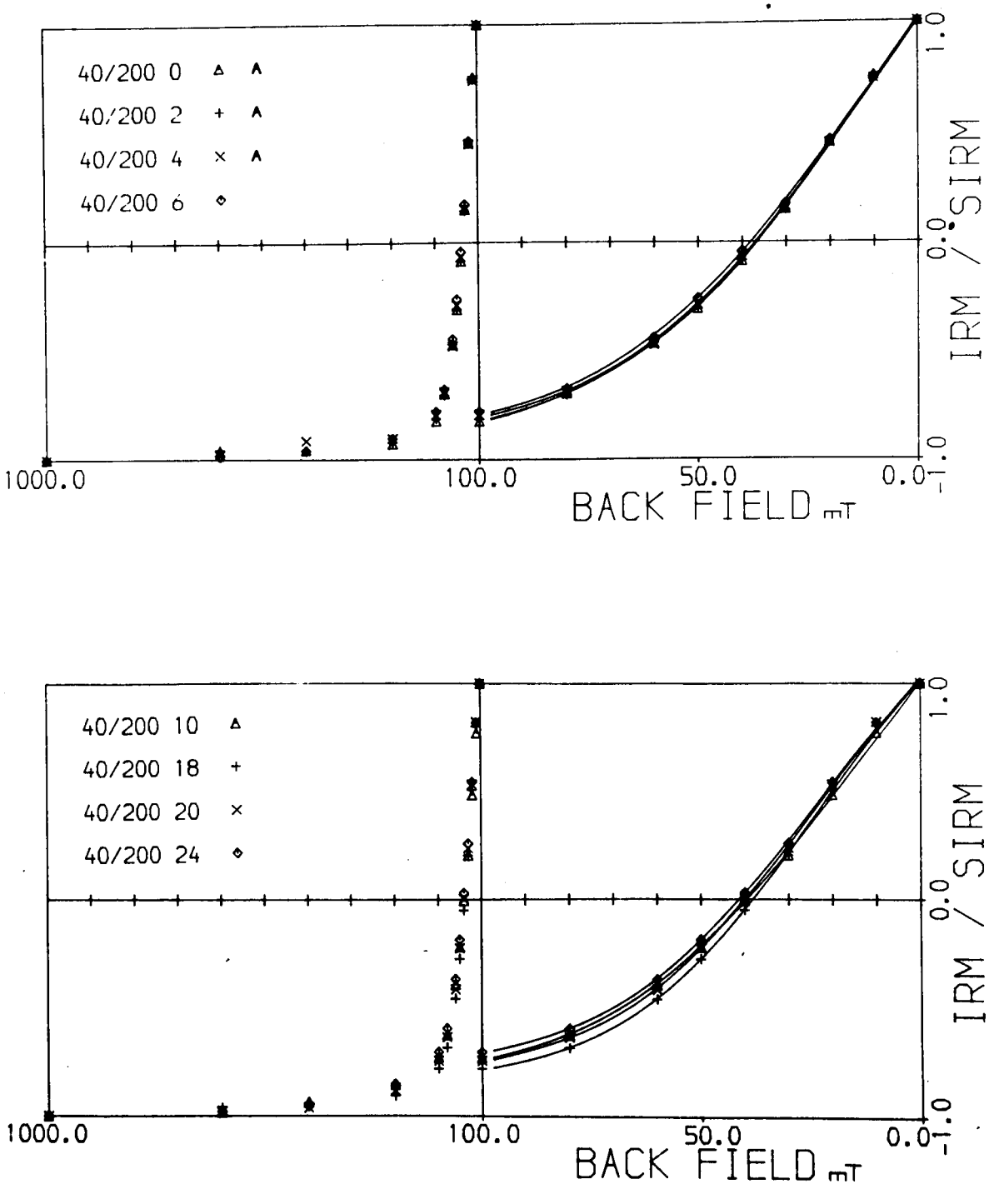

Figure 7.6 Coercivity of SIRM curves for samples from core 40/200

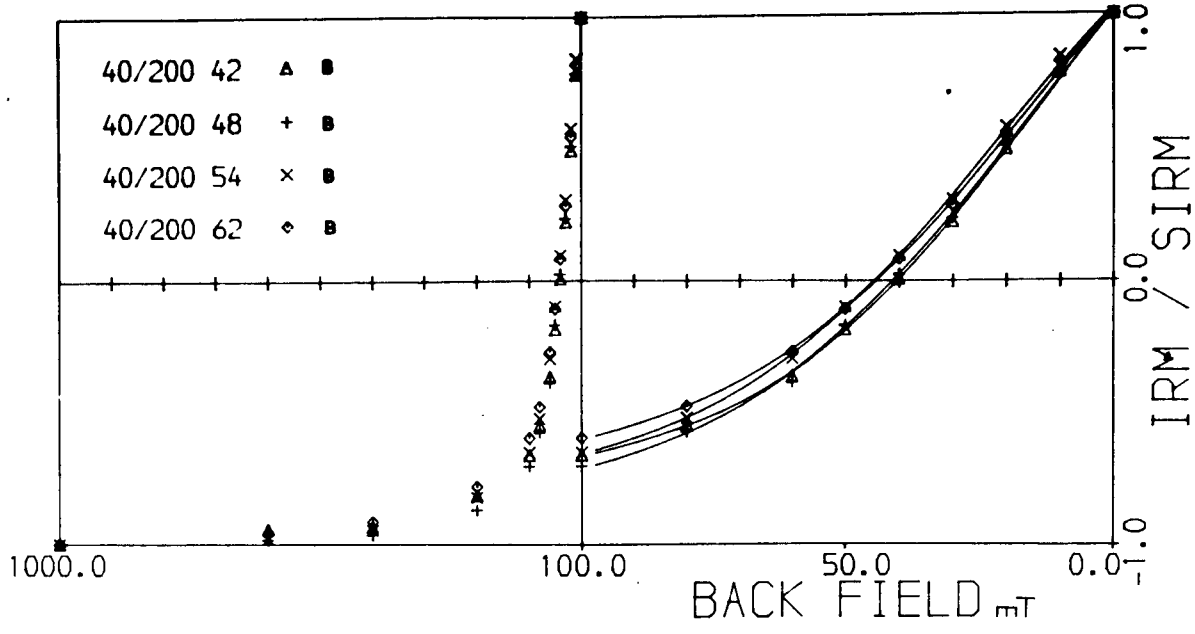

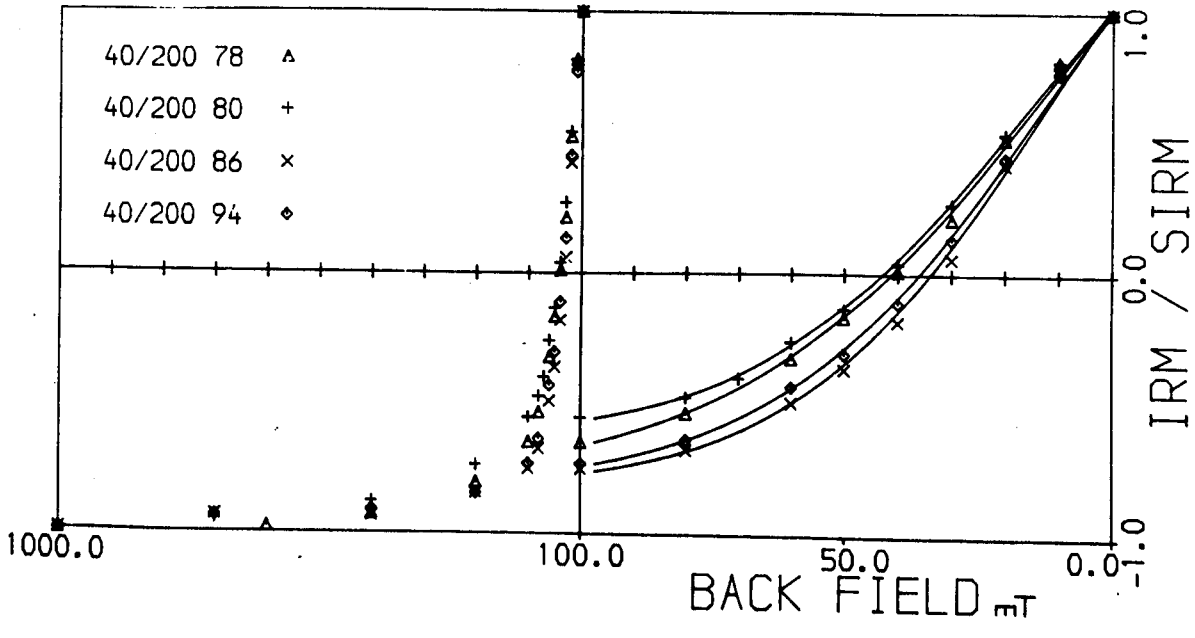

Figure 7.6 continued

Core	Depth (cm)	Magnetic peak	χ ($\mu m^3 kg^{-1}$)	SIRM ($mAm^2 kg^{-1}$)	SIRM/χ (kAm^{-1})	$(B_0)_{CR}$ (mT)	S_{100} (%)
	2-4	A	0.459	2.16	4.69	34	92
	4-6	A	0.397	3.56	8.97	35	92
	8-10	A	0.358	2.73	7.62	34	92
	10-12	A	0.281	1.96	6.97	37	92
	30-32	-	0.119	0.429	3.60	48	77
120/-100	38-40	-	0.068	0.180	2.65	51	75
	50-52	-	0.055	0.251	4.56	42	81
	66-68	-	0.047	0.271	5.71	42	84
	70-72	B	0.499	0.176	0.352	46	81
	72-74	B	0.263	0.244	0.926	50	77
	74-76	B	0.661	0.397	0.600	38	88
	76-79	B	0.307	0.653	2.13	44	85
	0-1	A	0.693	10.6	15.3	42	90
	2-3	A	0.789	11.4	14.4	46	83
	3-4	A	0.769	11.9	15.4	46	83
	10-11	A	0.470	9.11	19.4	42	88
	12-13	A	0.617	13.0	21.1	41	87
	33-34	-	0.085	1.08	12.7	48	80
	40-41	-	0.204	3.13	15.3	72	68
40/-20	44-45	-	0.171	2.43	14.2	76	66
	55-56	-	0.147	3.39	23.0	69	69
	65-66	-	0.162	2.72	16.8	83	60
	66-67	-	0.108	1.71	15.8	68	68
	69-70	B	0.428	0.873	2.04	81	62
	75-76	B	0.514	0.453	0.881	59	72
	76-77	B	0.653	0.524	0.802	86	60
	82-83	-	0.033	0.337	10.2	60	69
	0-2	A	0.170	1.36	7.97	37	90
	2-4	A	0.155	1.35	8.69	35	90
	4-6	-	0.150	0.981	6.53	38	89
	6-8	-	0.148	0.878	5.92	37	89
	14-16	-	0.131	0.653	5.00	47	81
	24-26	1	0.374	2.66	7.10	42	88
50/90L	34-36	-	0.134	1.75	13.1	48	85
	46-48	-	0.091	1.24	13.6	58	76
	54-56	2	0.155	2.38	15.4	42	80
	66-68	2	0.197	4.02	20.3	41	89
	68-70	2	0.186	3.54	19.1	38	94
	78-80	B1	0.479	2.79	5.84	34	97
	84-86	B1	0.551	2.74	4.98	34	97
	88-90	B1	0.284	2.37	8.35	35	97

Table 7.3 Susceptibility, SIRM, SIRM/χ, $(B_0)_{CR}$ and S values for the samples shown in Figures 7.3-7.6

Con/....

	Depth (cm)	Magnetic peak	χ ($\mu m^3 kg^{-1}$)	SIRM ($mAm^2 kg^{-1}$)	SIRM/χ (kAm^{-1})	$(B_0)_{CR}$ (mT)	S_{100} (%)
50/90L	92-94	B2	0.478	1.21	2.54	38	94
	94-96	B2	0.704	0.766	1.09	36	96
	96-98	B2	0.522	1.06	2.04	.42	94
	98-100	B2	0.535	1.17	2.19	41	94
	112-114	-	0.025	0.109	4.33	49	76
	131-133	-	0.031	0.206	6.73	33	89
	151-153	-	0.027	0.095	3.56	41	81
	173-175	-	0.041	0.175	4.22	42	80
40/200	0-2	A	0.313	4.24	13.6	37	91
	2-4	A	0.306	3.02	9.90	37	91
	4-6	A	0.274	2.12	7.73	37	90
	6-8	-	0.209	1.42	6.78	38	89
	10-12	-	0.150	0.915	6.11	40	87
	18-20	-	0.170	0.633	3.73	38	89
	20-22	-	0.141	0.658	4.67	40	88
	24-26	-	0.089	0.569	6.41	42	86
	42-44	B	0.315	0.182	0.578	41	83
	48-50	B	0.191	0.146	0.764	41	85
	54-56	B	0.229	0.142	0.619	45	83
	62-64	B	0.251	0.156	0.620	45	80
	78-80	-	0.042	0.105	2.49	42	83
	80-82	-	0.033	0.148	4.49	43	78
	86-88	-	0.037	0.201	5.48	34	88
	94-96	-	0.055	0.401	7.35	36	87

Table 7.3 continued

mT and S_{100} values from 83-92%. Those from peak A in core 40/-20 (0-12 in Figure 7.4), together with the spectra from magnetic peaks 2 and B1 in core 50/90L (54-72 and 78-88 in Figure 7.5) exhibit sigmoidal curves, indicative of fine-grained (but not viscous) ferrimagnetic material; consistent with this assumption, reference to Table 7.3 shows that these samples also have high values of SIRM/χ. The almost complete back saturation at 100 mT (with S_{100} values of 96-97%) of the samples from magnetic peak 2 indicates a negligible canted antiferromagnetic content.

The range of $(B_0)_{CR}$ values for magnetic peak B is considerable: from 36-86 mT (S_{100} values from 60-96%), with the 'hardest' spectra occurring in core 40/-20; therefore, $(B_0)_{CR}$ and S values are of little value for characterising these sediments.

7.3.3 Magnetization hysteresis loop measurements

Although the coercivity of SIRM spectra permit a broad differentiation of groups of samples on the basis of ferrimagnetic versus antiferromagnetic contrasts, since they are only able to characterise the magnetically retentive fraction of a magnetic mineral assemblage they shed little light on the mineralogy responsible for the magnetic properties of peak B. Because the low values of SIRM/χ of these sediments could be ascribed to either paramagnetic or superparamagnetic material (section 7.3.1, above) an attempt was made to carry out magnetization hysteresis loop measurements which enable the estimation of saturation magnetization (M_S) and coercive force $(B_0)_C$ (see Chapter 1, section 1.6). Considerable use has been made of the parameters M_{RS} (SIRM)/M_S and $(B_0)_{CR}/(B_0)_C$ for inferring the size characteristics and domain state of magnetite grains, particularly for basalts (e.g. Wasilewski, 1973; Radhakrishnamurty and Deutsch, 1974), although it has been emphasised that considerable problems are involved in interpreting these parameters obtained from samples containing complex assemblages of magnetic grains (Mullins, 1974), such as in soils and sediments.

Paramagnetic substances exhibit a linear increase in magnetization upto M_S with increasing applied field, with an absence of hysteresis (see Figure 1.1, Chapter 1, section 1.6). In contrast, although from theory an assemblage of superparamagnetic grains should exhibit zero, or negligible, $(B_0)_C$ and M_{RS}, in practice finite values of these parameters are observed (cited in Radhakrishnamurty and Deutsch, op. cit.). Therefore, it was hoped that simple reference to the shape of the hysteresis loop for magnetic peak B sediments would determine which of the two alternatives was correct.

Figure 7.7 shows the hysteresis loops for two samples from core 40/200, from peak B (40-42 cm) and from peak A (4-6 cm). The linear variation of magnetization with applied field (i.e. absence of hysteresis) shown by the sample from peak B corresponds exactly to that which would be expected of a paramagnetic substance. (This conclusion is supported by the results of Mössbauer effect spectroscopy measurements: see Appendix G). In contrast, the sample from magnetic peak A clearly exhibits hysteresis. The shape of this loop reflects contributions from a number of magnetic components and for this reason no attempt was made to estimate M_{RS}/M_S. The absence of shallowing gradient of the path of M versus B_0 at the extremities of the loop could be interpreted as indicating a substantial antiferromagnetic component, while the shape of the central portion reflects a ferrimagnetic contribution. The gain setting on the magnetometer was adjusted to enable estimation of $(B_0)_C$ (=4.7 mT), while separate measurement of $(B_0)_{CR}$ (37 mT) gave a value of 7.9 for $(B_0)_{CR}/(B_0)_C$. No definitive conclusions may be drawn from these results; however, it is possible that the relatively low $(B_0)_C$ and relatively high $(B_0)_{CR}/(B_0)_C$ reflect paramagnetic and/or superparamagnetic contributions, either of which would be expected to considerably reduce $(B_0)_C$.

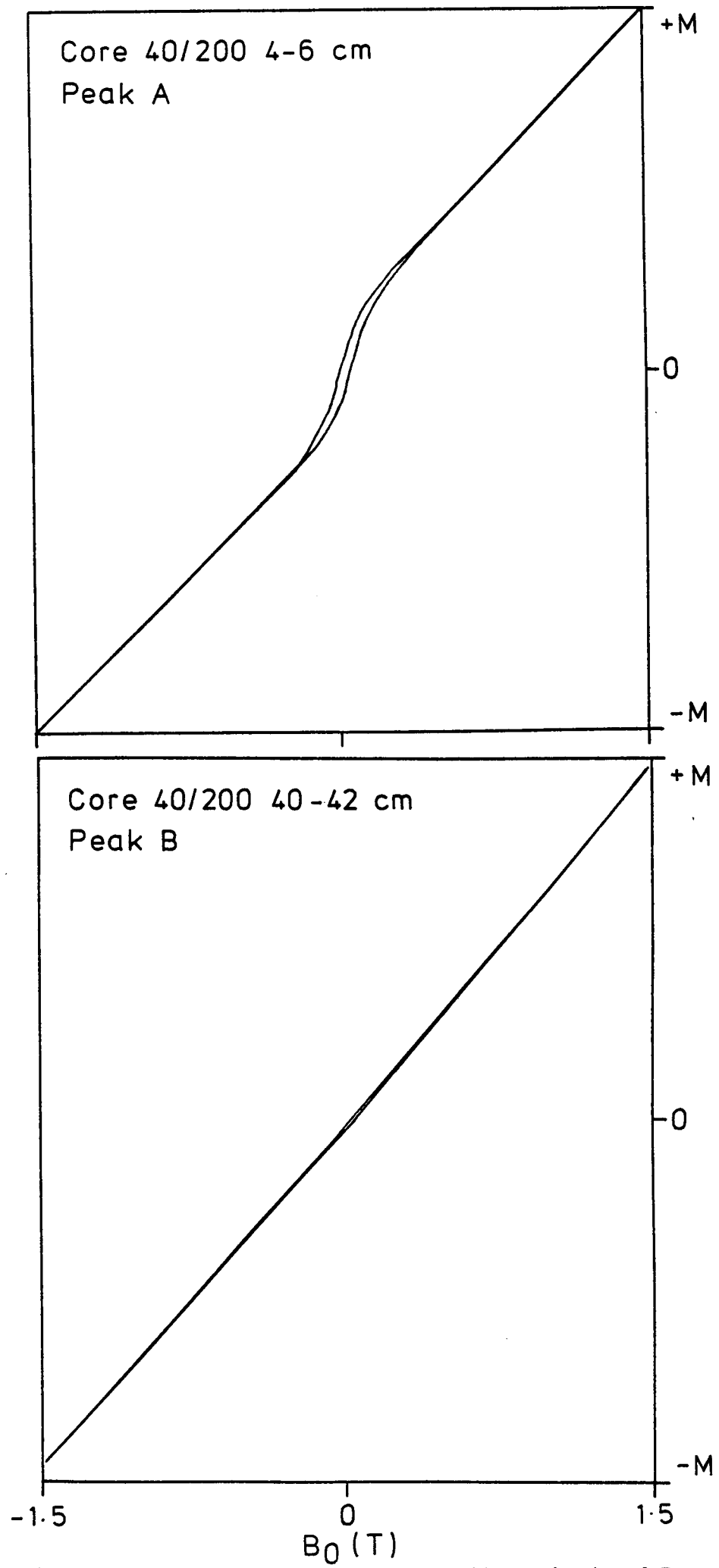

Figure 7.7 Hysteresis loops for samples from magnetic peaks A and B

7.4 Chemical analyses of the lake sediments

7.4.1 Introduction

Since the identification of magnetic peak B sediments as concentrations of paramagnetic material does not fall within the ambit of the interpretations of changes in magnetic concentration in lake sediments described in section 7.2 (above), chemical analyses were carried out in order to attempt to further characterise these sediments.

Preliminary analyses using X-ray fluorescence (XRF) were carried out on the interval 58-79 cm, spanning magnetic peak B, in core 120/-100. The relative concentrations of the following elements were determined: Fe, Mn, Al, S, Sn, K, Ca, Zn, Ba, I, Ni, Cu, Pb and Ti. Of these, only variations in Fe and Mn exhibited a significant relationship with the magnetic stratigraphy. Accordingly, quantitative determinations of the concentrations of these elements, together with Al, were carried out for the following intervals: 0-79 cm (base) of core 120/-100; 0-32 cm of core 30/160 (both analysed by XRF) and 0-18 cm of core 60/20 (analysed by atomic absorption spectrophotometry). These intervals spanned magnetic peak A (cores 120/-100 and 60/20), magnetic peak 1 (core 30/160) and magnetic peak B (cores 120/-100 and 30/160). Details of the analytical methods are given in Chapter 3 (section 3.6) The results shown below may be considered to represent total concentrations of each of the three elements.

7.4.2 Results

The variations of χ, SIRM, SIRM/χ, Fe, Mn, Al, Fe/Al, Mn/Al and χ/Fe + Mn for the analysed intervals are shown in Figure 7.8. Magnetic peaks A, 1 and B are delimited by horizontal lines. The downprofile variation of additional magnetic parameters (ARM, ARM/χ and SIRM/ARM) for core 120/-100 is shown in Figure 4.10 (Chapter 4, section 4.4.2). The interval 0-ca. 8 cm of the section from core 60/20 exhibits the typical characteristics of magnetic peak A: viz. increased X and

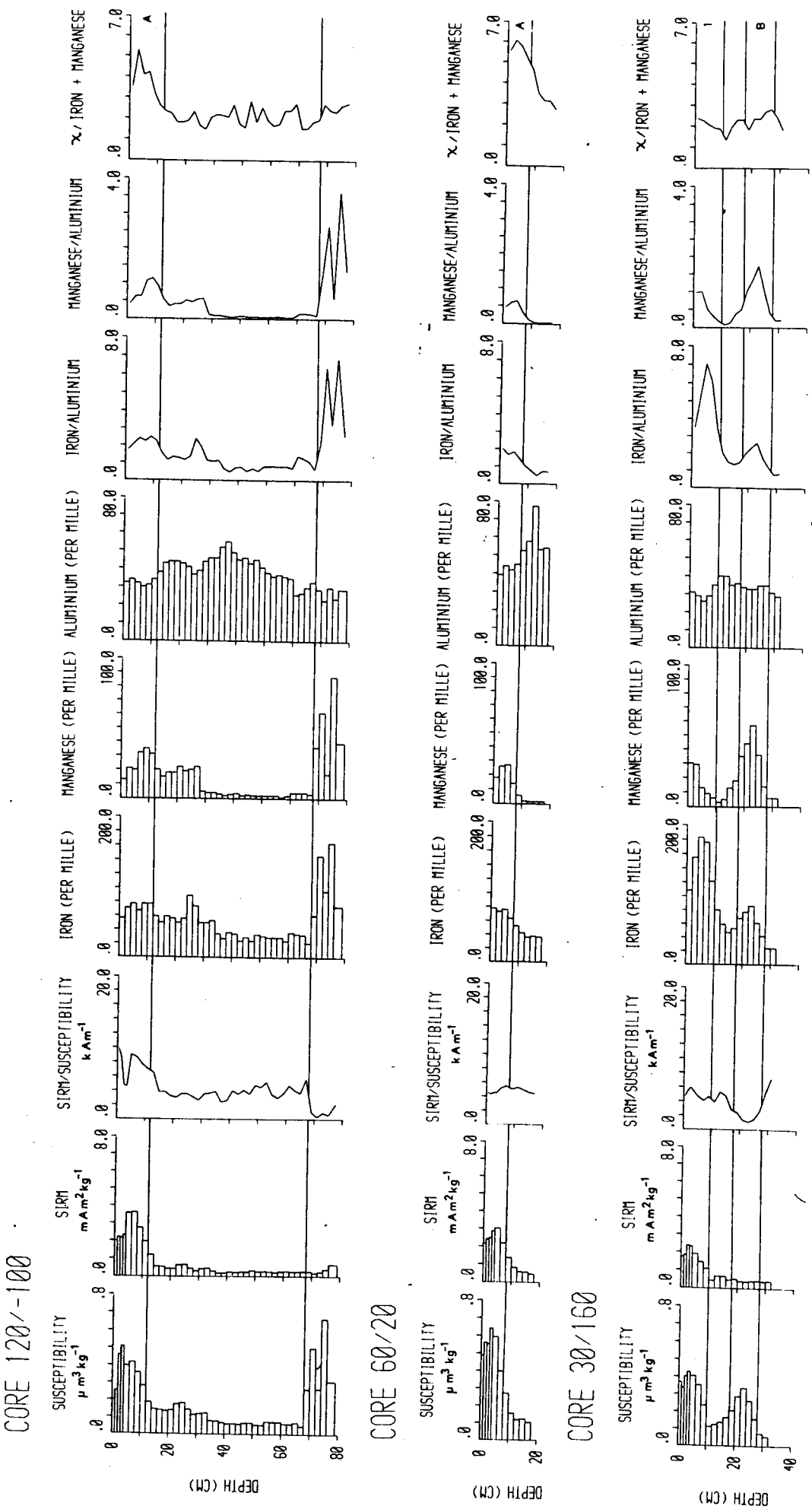

Figure 7.8 Magnetic measurements and chemical analyses of cores 120/-100, 60/20 and 30/160

SIRM. For reasons given in Chapter 4 (section 4.4.3) the uppermost peak in magnetic concentration in core 30/160 is correlated with magnetic peak 1; in this core, it exhibits a significant peak in χ, a moderate peak in SIRM and consequently relatively low SIRM/χ.

For all three profiles, the range of Fe concentration is 21-183 per mille, the maximum occurring within magnetic peak 1 in core 30/160. (The maximum Fe concentrations are high: a sedimentary rock is classed as an ore deposit if it contains 150 per mille or more Fe (Wedepohl, 1970)). The range of Mn concentration is 1-87 per mille, the maximum occurring within magnetic peak B in core 120/-100; the amplitude of variation of Mn concentration is, therefore, markedly higher than that of Fe. In comparison with Fe and Mn, the variation of Al concentration is relatively small (24-77 per mille). In all three profiles, the correspondence between the Fe and Mn curves and the χ curve is striking, particularly over the intervals corresponding to magnetic peaks 1 and B. In each profile, peaks in Fe and Mn concentration correspond to maxima in Fe/Al and Mn/Al. The highest values of χ/Fe + Mn occur in magnetic peak A in cores 120/-100 and 60/20.

7.4.3 Implications of the results of the chemical analyses for the interpretation of the magnetic stratigraphy

The covariation, in the Goddionduon lake sediments, of χ and Fe and Mn concentration is at variance with comparable published data. For example, there is a relatively poor correspondence between variations in total Fe and χ in a 3 m core from Lough Neagh, Northern Ireland (Thompson et al., 1975); similarly, determinations of Fe and Mn concentration in particle-sized fractioned samples from Loch Lomond, Scotland, exhibit no correspondence with χ (Thompson and Morton, 1979). At both sites the dominant contributor to χ is considered to be detrital magnetite, and, as noted by Thompson et al. (op. cit.) this is not normally the major contributor to the total iron content of lake sediments.

Since the χ of paramagnetic substances is determined by the magnetic moments and concentrations of the constituent paramagnetic ions it is possible to use the results of the chemical analyses, together with the known magnetic moments of the ferrous, ferric and manganic ions, to calculate the χ of the observed concentrations of Fe and Mn. Assuming an Fe^{3+}: Fe^{2+} ratio of 7:3 (see Appendix G), and using the formula given by Vernon (1961), the calculated χ values of samples from magnetic peak B in cores 30/160 and 120/-100 were found to correspond approximately (averaging within ca. 20 percent) to the measured χ values. Therefore, it is reasonable to conclude that the observed relatively high concentrations of Fe and Mn (presumably present as paramagnetic oxides or hydroxides) corresponding to magnetic peaks 1 and B make a substantial or dominating contribution to the χ.

The ratio of measured χ/Fe + Mn should illustrate the varying contribution of paramagnetic material to the χ. The significantly lower values of χ/Fe + Mn (Figure 7.8) for magnetic peaks 1 and B than for magnetic peak A indicate a correspondingly greater paramagnetic contribution to χ. This result is clearly in accordance with the contrasts in SIRM, SIRM/χ and hysteresis characteristics (section 7.3, above) between magnetic peaks A and B, since these indicate the presence of ferrimagnetic material (with a much greater χ per unit mass of metal oxide than paramagnetic material) in the former, but not in the latter.

Finally, the high concentrations of Fe associated with magnetic peak B accord with the observed lithostratigraphy of these sediments (see Chapter 4, section 4.2 and Figure 4.12, section 4.4.2), since yellow, brown and orange colouration is usually taken to reflect the presence of ferric oxides in both soils and sediments (Carroll, 1958; Fitzpatrick, 1971).

7.4.4 Comparison of the results of the chemical analyses with published data

Table 7.4 compares the maximum values of Fe and Mn concentration recorded in the analysed Goddionduon profiles with the maximum values from lake sediments, surficial oxidate crusts from lakes and a podsolized soil. As far as is known, no published geochemical data exist for the Upper Crafnant Volcanic Formation and Llanrhychwyn Slates, which underlie the Goddionduon watershed; therefore, Fe and Mn concentrations for comparable lithologies in the Snowdon area are included, together with the lithospheric averages for these elements. The maximum concentrations of Fe, and particularly Mn, in the Goddionduon sediments are substantially higher than the values for both the lithospheric average and the pumice tuffs, rhyolitic ash and slates. Although the maximum Fe concentrations for Goddionduon are comparable with those for several of the other lake sites, the maximum Mn concentrations are exceeded only by those for the oxidate crusts and iron pan.

The occurrence within lake basins of concentrations of Fe and Mn substantially in excess of the lithospheric average has usually been interpreted in two principal ways. Either the source of the Fe and Mn has been considered to lie within the sediment body itself, and that concentration of these elements results from post-depositional solubilization under appropriate conditions of pH and Eh, followed by migration and precipitation within discrete horizons, or more usually, the Fe and Mn are considered to have been derived from external sources and transported into the basin in solution, frequently as part of organic complexes, or in fine particulate form. Within the basin, precipitation may be effected by contact with oxygenating lake water, or more rarely by the oxygenating activity of iron (and manganese) bacteria. The lake sites in Table 7.4 provide illustrations of both of these cases, and since the suggested interpretations are of potential significance for the interpretation of the Goddionduon results they are briefly described below.

Site	Deposit	Fe (per mille)	Mn (per mille)	Source
Lithospheric average	-	47	1	Gorham and Swaine, 1965
Llyn Goddionduon, Wales	Magnetic peak B (Core 120/-100)	164	87	-
	Magnetic peak 1 (Core 30/160)	183	57	
Windermere and Esthwaite, England	Surficial oxidate crusts	72-386	14-132	Gorham and Swaine, 1965
Windermere, South Basin, England	Post-glacial sediments	70	13	Mackereth, 1966
Lake Superior, North America	Post-glacial sediments	210	9.9	Mothersill and Shegelski, 1972
Lake Immeln, Sweden	Early Post-glacial sediments	145-265	0.39-0.64	Digerfeldt, 1973
Lake Hakojärvi, Finland	Post-glacial sediments	130	7.4	Huttunen et al., 1978
Loch Sionascaig, Scotland	Post-glacial sediments	150	15	Pennington et al., 1972.
Cors Geuallt, Wales	Late-glacial sediments	65	2.6	Crabtree, 1965
Lake Vilbergt-jern, Norway	Late-glacial sediments	220	7.4	Kjensmo, 1978
Newfoundland	Iron (podsolized soil	250	150	McKeague et al., 1968
Snowdonia, Wales	Pumice tuff	91	1.1	Ball et al., 1969
	Rhyolitic ash	60	1.7	
	Llandeilo slate	64	1.0	

Table 7.4 Concentrations of Fe and Mn in a variety of geological deposits. (See text for explanation).

The high Fe concentrations for the Late-glacial and early Post-glacial sediments from Lakes Flarken and Vilbergtjern are considered to result from the solution of Fe by acid drainage waters and its subsequnt passage through the substrate, entry into and precipitation within the lake basins. In both cases, the situation of the basins within areas of highly permeable sandy till is thought to have facilitated the entry of the Fe-charged ground-water, and later decreases in Fe concentration within the sediments appear to result from the sealing of the basins by the deposition of organic sediment and consequent exclusion of sub-surface drainage. The relatively high concentrations of Mn in Windermere and of Fe and Mn in Loch Sionascaig are interpreted as having arisen through the development of reducing conditions as a result of biological activity in the soils (in the former case) and waterlogging associated with blanket peat formation (in the latter), followed by mobilisation of Fe and Mn and transport to and precipitation within oxidizing lake basins. At both sites, high sedimentary concentrations of these elements have been maintained throughout the middle and late Flandrian.

Sediments of parts of the Lake Superior basin provide an example of the migration and precipitation of Fe and Mn within the sediment body itself. In this case, it is suggested that relative enrichment of the uppermost few centimetres of sediment results from the mobilisation of Fe and Mn under anaerobic conditions in the lowermost sediments, followed by their transport in inter-stitial water upwards through vertical fractures and eventual precipitation in zones of higher Eh. However, since Fe is precipitated at a lower Eh than is Mn (Mortimer, 1941) there is complete segregation between Fe-enriched and Mn-enriched layers, the latter always overlying the former.

The possible relevance of the mechanisms described above for the interpretation of the origin of the Fe and Mn-enriched layers in Llyn

Goddionduon is discussed in relation to all available evidence in Chapter 9 (section 9.1).

7.4.5 Summary of the results of the single-sample magnetic measurements and chemical analyses

The χ and SIRM values of the majority of the Goddionduon lake sediment samples show that the overall magnetic concentration is relatively low. However, in many of the cores sections of increased magnetic concentration with distinctive magnetic and chemical characteristics are identifiable:

Magnetic peak A

The relatively high SIRM/χ and S_{100} values, and relatively low $(B_0)_{CR}$ values, together with the magnetization hysteresis characteristics of these sediments, indicate the predominance of ferrimagnetic material. However, the rise in the Fe and Mn curves for this interval in cores 120/-100 and 60/20 implies an additional paramagnetic contribution.

Magnetic peak 1

The occurrence of a minor peak in SIRM, but relatively low SIRM/χ values, together with the relatively high concentrations of Fe and Mn for this feature in core 30/160, suggest both ferrimagnetic and paramagnetic contributions.

Magnetic peak 2

This feature is only recorded in the central sector of the lake basin. High SIRM/χ values and sigmoidal $(B_0)_{CR}$ curves are indicative of fine-grained multi-domain and/or single-domain ferrimagnetic material. No chemical analyses are available for this interval.

Magnetic peak B

The very low values of SIRM/χ and the absence of hysteresis identify these sediments as concentrations of paramagnetic material. The concentrations of Fe and Mn for this interval in cores 120/-100 and 30/160

are sufficiently high to account entirely for the measured χ values. (Within the interval of increased χ assigned to magnetic peak B in core 50/90L, the occurrence of a significant peak in SIRM (peak B1: see Figure 4.12; Chapter 4, section 4.4.2) with $(B_o)_{CR}$ curve characteristics indicative of ferrimagnetic material, suggests that in addition to the large paramagnetic contribution from iron and manganese oxides the χ of sections of the extended laminated clayey sequences in the central part of the lake basin (Figure 4.1; Chapter 4, section 4.2) may also be contributed by ferrimagnetic material).

7.5 Magnetic measurements of potential lake sediment source materials

7.5.1 Introduction

For the majority of its history, Llyn Goddionduon has received no stream channel drainage; therefore, topsoil material has presumably constituted the predominant sediment source during the Post-glacial period. However, during the present century Forestry Commission drainage-ditching and road construction (Chapter 2, sections 2.3-2.4) would be expected to have supplied subsoil material to the lake basin. Consequently, magnetic measurements were performed on topsoil and subsoil samples and on bedload material from the drainage ditches to compare their magnetic properties with those of the lake sediments. The results are given in sections 7.5.2-7.5.3. Because of possible intermittent contributions to the late Flandrian lake sediments from reworked marginal Late-glacial sediments, magnetic measurements were also performed on Late-glacial samples obtained from beneath the peat bog. The results are given in section 7.5.4.

7.5.2 Magnetic measurements of bulk soil samples

Figure 7.9 shows the variation of χ, SIRM, SIRM/χ, S_{40} and S_{100} down six soil profiles from the Goddionduon watershed. The location of each profile is shown in Figure 2.1 (Chapter 2, section 2.1). Horizon nomenclature follows Hodgson (1974). The χ and SIRM measurements are not expressed on an ashed basis (i.e. as χ or magnetic moment per unit mass of the mineral fraction), so that magnetic concentration is affected by down-profile variations in organic matter content; however, it is unlikely that such variations would significantly affect the trends depicted in Figure 7.9.

The profiles may be divided into two groups on the basis of their horizonation and magnetic characteristics. The first group (profiles GS1, GS2, GS6 and GS12) consists of peaty podzolic soils with well

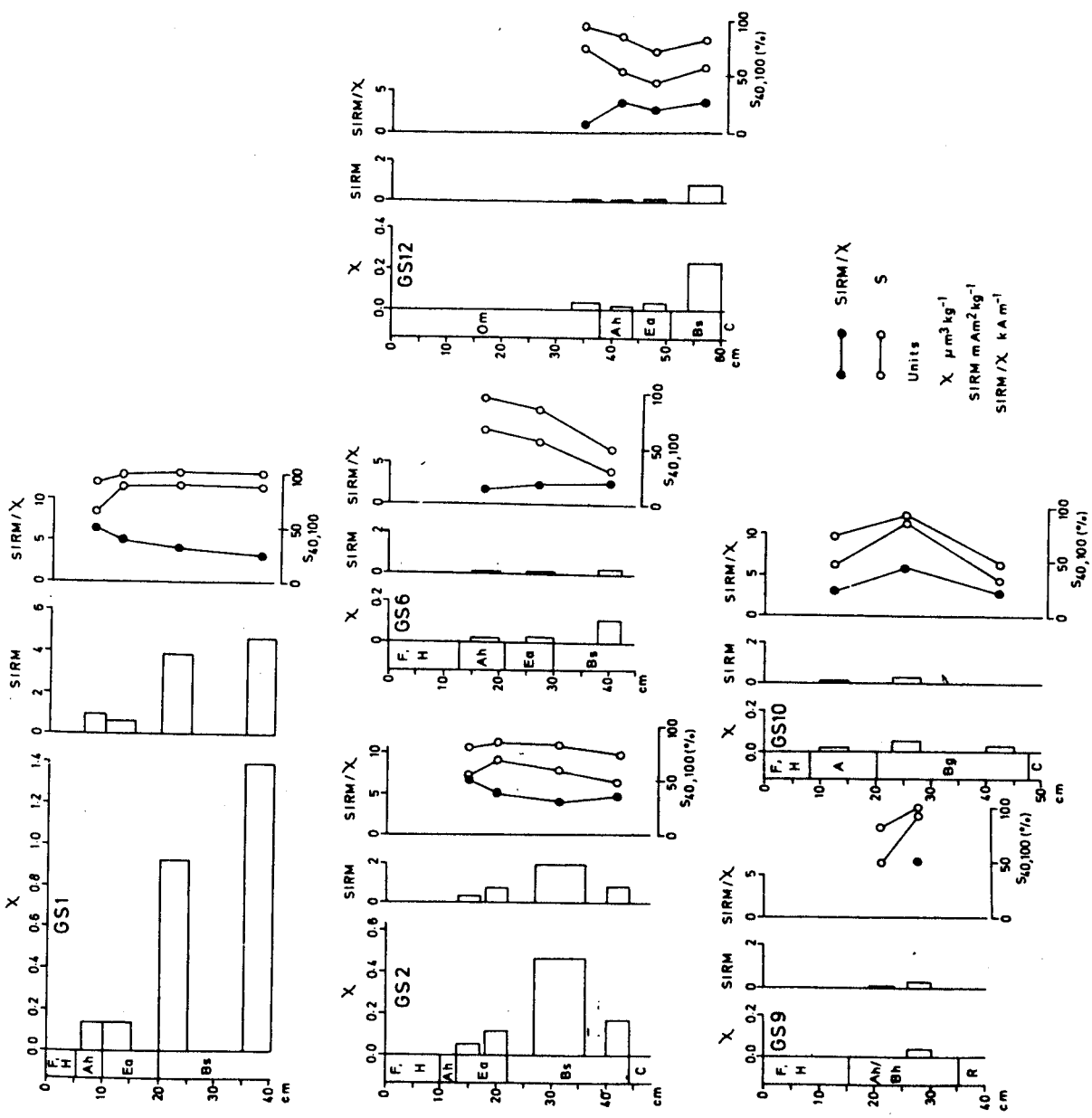

Figure 7.9 Magnetic stratigraphy of Goddiondun soil profiles

developed Ea and Bs horizons. All of the profiles exhibit highest magnetic concentration in the Bs horizon, with relatively low magnetic concentration in the Om/Ah and Ea horizons. In profiles GS1 and GS2 there is a tendency for SIRM/χ values to decline slightly with depth; however, this is not shown in GS6 and GS12. In GS1, which has markedly higher χ and SIRM values than any of the other profiles, all of the samples have S_{40} values of ca. 60-90% and S_{100} values of ca. 80-100%, indicating a high ferrimagnetic : antiferromagnetic ratio. S values in profiles GS2, GS6 and GS12 and consistently lower.

The second group of profiles (GS9 and GS10) exhibit substantially lower magnetic concentration than those in the first group. In terms of its shallowness and horizonation, GS9 (a shallow phase peaty podzolic soil) is characteristic of many of the profiles on the relatively steeply-sloping eastern side of the watershed. Magnetic concentration in the two samples from the mineral horizon is low; the uppermost horizon did not possess a measureable χ. GS10 (a peaty gleyed soil) is representative of soils in the relatively flatter northern and western areas of the watershed, although these tend to have thicker Om horizons. Magnetic concentration is low in both the A and Bg horizons; there is a slight maximum in magnetic concentration, SIRM/χ and S in the sample from the upper part of the Bg horizon.

Figure 7.10 summarises trends in magnetic concentration and SIRM/χ for 37 bulk soil samples from 15 profiles from the Goddionduon watershed, including those from the profiles illustrated in Figure 7.9. The envelopes for the three distrubutions of lake sediment samples (section 7.3.1) are included. The samples have been divided into two groups: topsoil and subsoil samples, distinguished by different symbols. Topsoil samples include those from Om, Ah and Ea horizons; subsoil samples include those from Bs and Bg horizons. The diagram underlines the tendency shown in Figure 7.9 for the highest values of χ

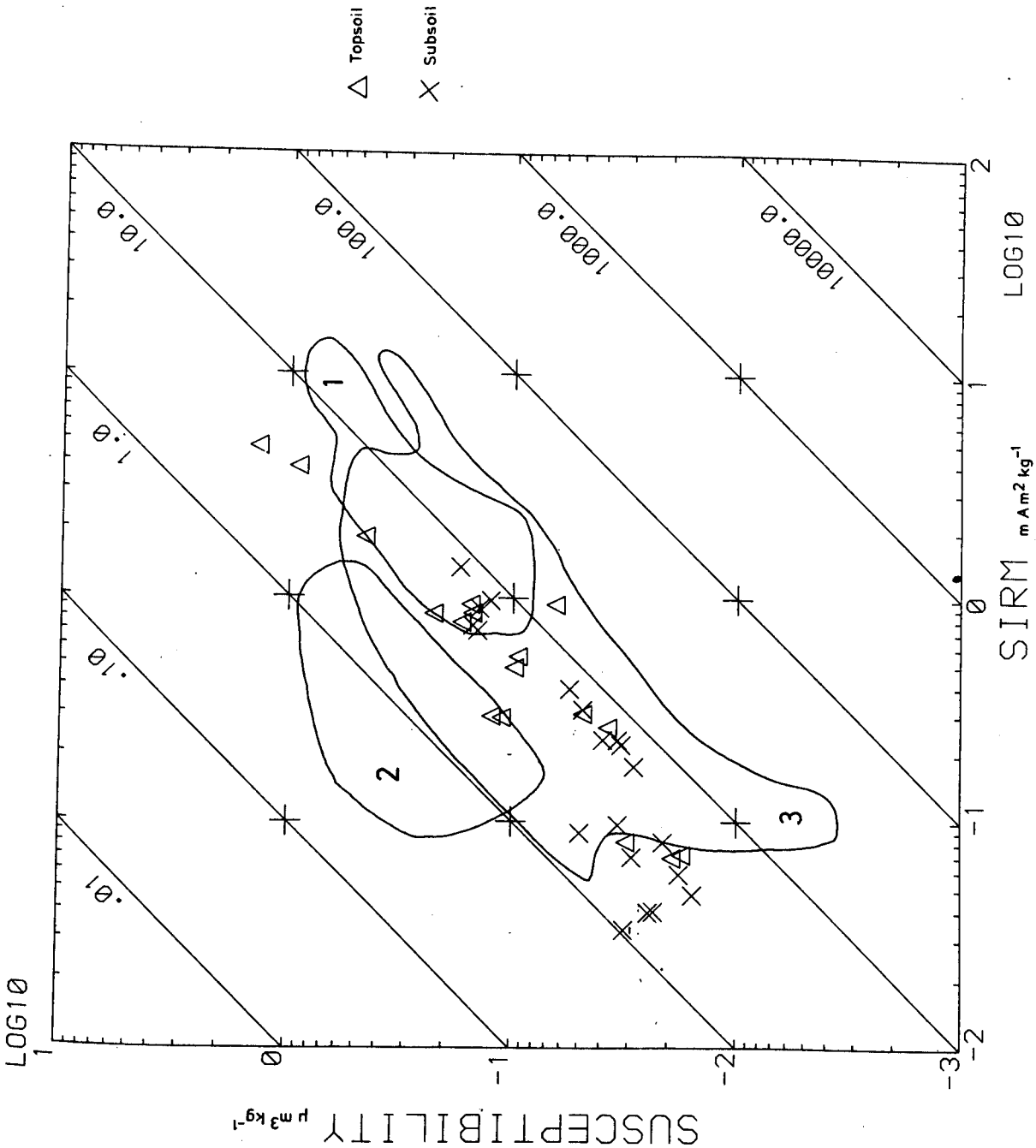

Figure 7.10 χ plotted against SIRM for bulk soil samples

and SIRM to occur in the subsoil. The majority of samples falls around the lower end of envelope 3; however, the small number of samples prevents firm conclusions. None of the samples has a value of SIRM/χ either as high or as low as those from the peaks in magnetic concentration in the lake sediments. The χ values of samples with values of SIRM/χ approaching 1 k Am^{-1} (i.e. comparable with those of magnetic peak B) are low (less than ca. 0.5 $\mu m^3 Kg^{-1}$). The two samples with highest χ and SIRM, lying outside any of the three lake sediment envelopes, are from the Bs horizon of profile GS1. The SIRM/χ values of these samples approach those of magnetic peak A.

7.5.3 Magnetic measurements of fractioned soil and stream bedload samples

Because of the possibility that the poor correspondence between the magnetic properties of the bulk soil samples and those of the peaks in magnetic concentration in the lake sediments could be explained by differences in particle size distribution (the lake sediments consisting predominantly of silt and clay-sized particles with the bulk soil samples containing a significantly larger coarser component) (see section 7.2) a limited amount of fractionation of soil and stream bedload samples was performed and magnetic measurements made on the discrete fractions. The locations of the sample sites are shown in Figure 2.1. Sample MDC1 was taken from the base of a Forestry Commission drainage channel, GD1 from the small delta at the distal end of the same channel, GS17A from the Bs horizon of a peaty podzolic soil and GS18 from the Ag horizon of a peaty gleyed soil.

Figure 7.11 shows the variation of χ, SIRM, SIRM/χ and S with particle size for these samples, while Figure 7.12 shows χ plotted against SIRM for the same samples with the envelopes for the three distributions of lake sediment samples included. Values of χ and SIRM in

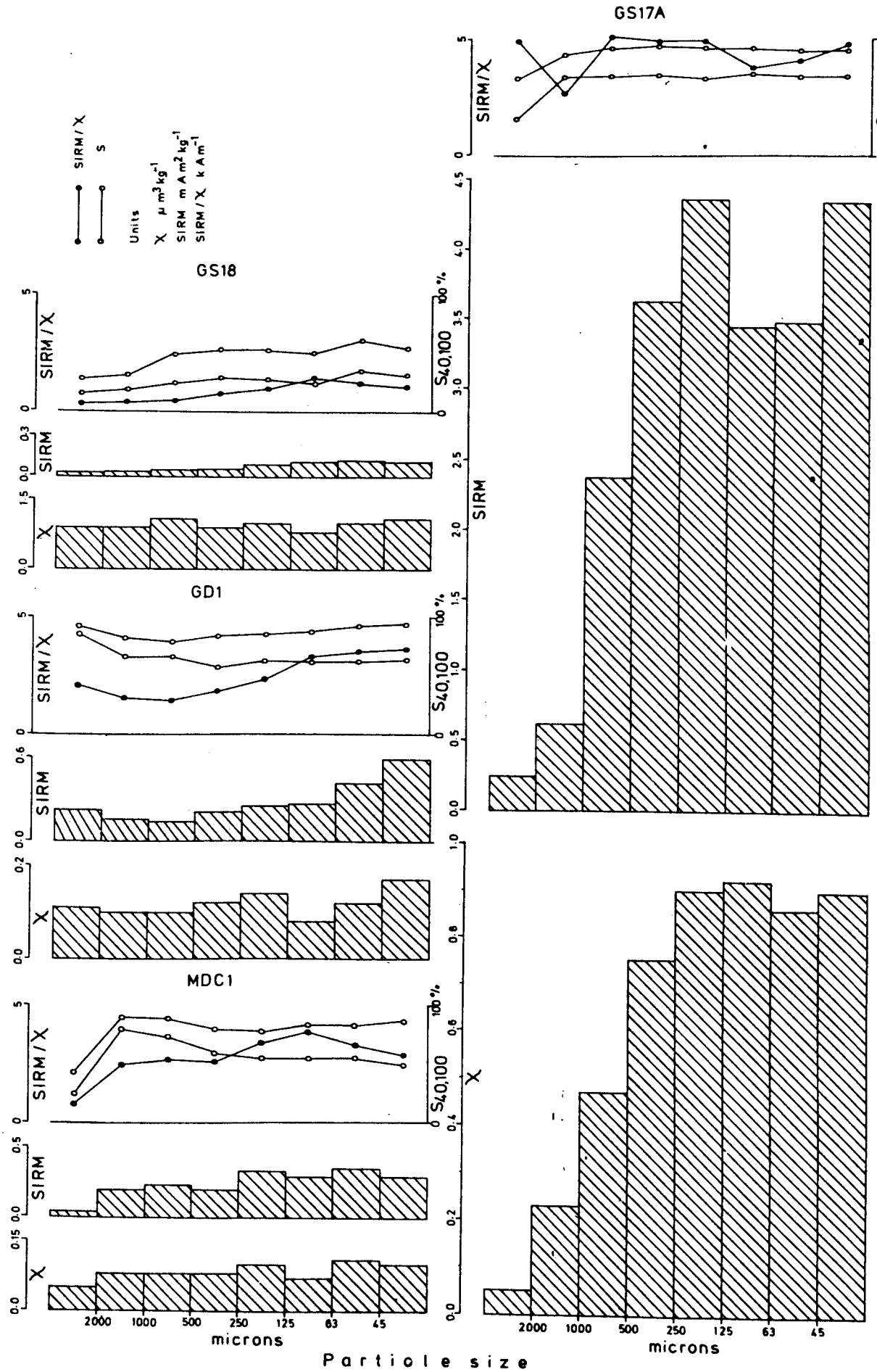

Figure 7.11 Magnetic measurements of fractioned soil and stream bedload samples

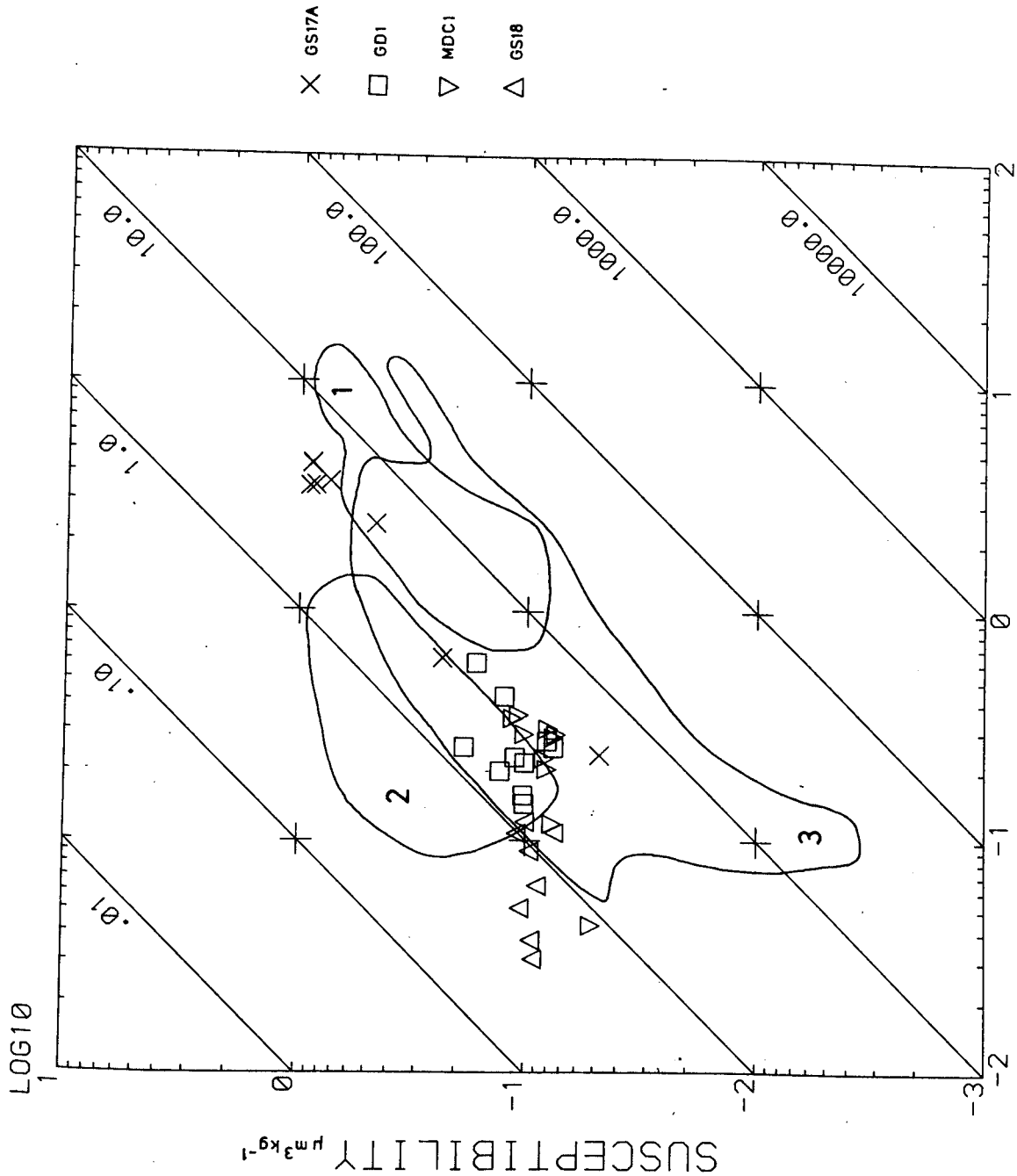

Figure 7.12 χ plotted against SIRM for fractioned soil and stream bedload samples

samples MDC1 and GD1 are low in all fractions and there are no trends in SIRM/χ or in S. Reference to Figure 7.12 shows that the samples are located within the overlap between envelopes 2 and 3. Examination of the coarser fractions indicated a predominant lithology of slates.

Values of χ and SIRM in the fractions from sample GS18 are low. χ is more or less invariant with particle size; however, there is a tendency for SIRM, and therefore SIRM/χ, to increase gradually with decreasing particle size. Reference to Figure 7.12 shows that some of the values of SIRM/χ of these samples are comparable with the lowest of those from magnetic peak B; however, the χ values are substantially lower. Examination of the coarser fractions indicated a predominant lithology of tuffs and slates.

In accordance with the values of χ and SIRM in bulk samples from the Bs horizons of the podsolized soils (section 7.5.2) magnetic concentration in the less than 1000 μm fractions in sample GS17A is markedly higher than in any of the other fractioned samples. There are no significant trends in SIRM/χ with particle size. The SIRM/χ values are comparable with those of the bulk samples from the Bs horizon of profile GS1 (Figure 7.9). Examination of the less than 1000 μm fractions revealed the presence of large numbers of weakly cemented, yellowish brown aggregates composed of silt-clay sized material which clearly had not been adequately dispersed by the techniques used (Chapter 3, section 3.4.2). Aggregates were not observed in any of the other fractioned samples. Examination of the coarser fractions revealed the presence of slates and tuffs, frequently with brown iron oxide smears, in addition to the aggregates. Since χ and SIRM are low in samples GS18, MDC1 and GD1, the coarser fractions of which consist predominantly of slates and/or tuffs, it is likely that the relatively high magnetic concentration of the samples from GS17A is contributed by the aggregates.

The occurrence of a significant concentration of remanence-carrying, magnetically soft ferrimagnetic material in the Bs horizons is of interest, since Mullins (1974) states with regard to these horizons that "both our investigation and that of Scollar (1965) show that iron is reprecipitated in a non-magnetic (i.e. paramagnetic) form". The precipitation of paramagnetic material would be expected to result in an increase in χ but the material would be unable to carry a remanence. Vadyunina and Babanin (1972) cite the occurrence of relatively high χ values in the Bs horizons of podsolic soils but do not offer a convincing explanation.

7.5.4 Susceptibility and SIRM measurements of Late-glacial sediments

Because of the stratigraphic association in the southern margin of the lake basin between the laminated clayey sediments associated with magnetic peak B and the peaty/coarse detritus mud layers which are presumed to reflect reductions in lake level (Chapter 4, section 4.5), a possible source of these sediments could be the reworking, during periods of lowered lake level, of marginal Late-glacial sediment. Two factors appeared to support this possibility. Firstly, Late-glacial clay layers in many of the 'trench' cores and marginal cores exhibit high volume susceptibility (Chapter 4, section 4.3). Secondly, Crabtree (1965) notes the occurrence of relatively high concentrations (greater than 70 per mille) of total Fe in Late-glacial clays from an infilled lake basin ca. 5 km west of Llyn Goddionduon; Mackereth (1966) also refers to the concentration (by mechanical separation of fine particulate material) of Fe and Mn in Late-glacial lake sediments. Therefore, measurements of χ and SIRM were made on samples from the Late-glacial section beneath the Goddionduon peat bog. The samples were obtained as part of a separate project (Ince, 1980).

Figure 7.13 shows χ plotted against SIRM for 158 Late Devensian and early Flandrian samples. The lithologies include silt-sand, clay

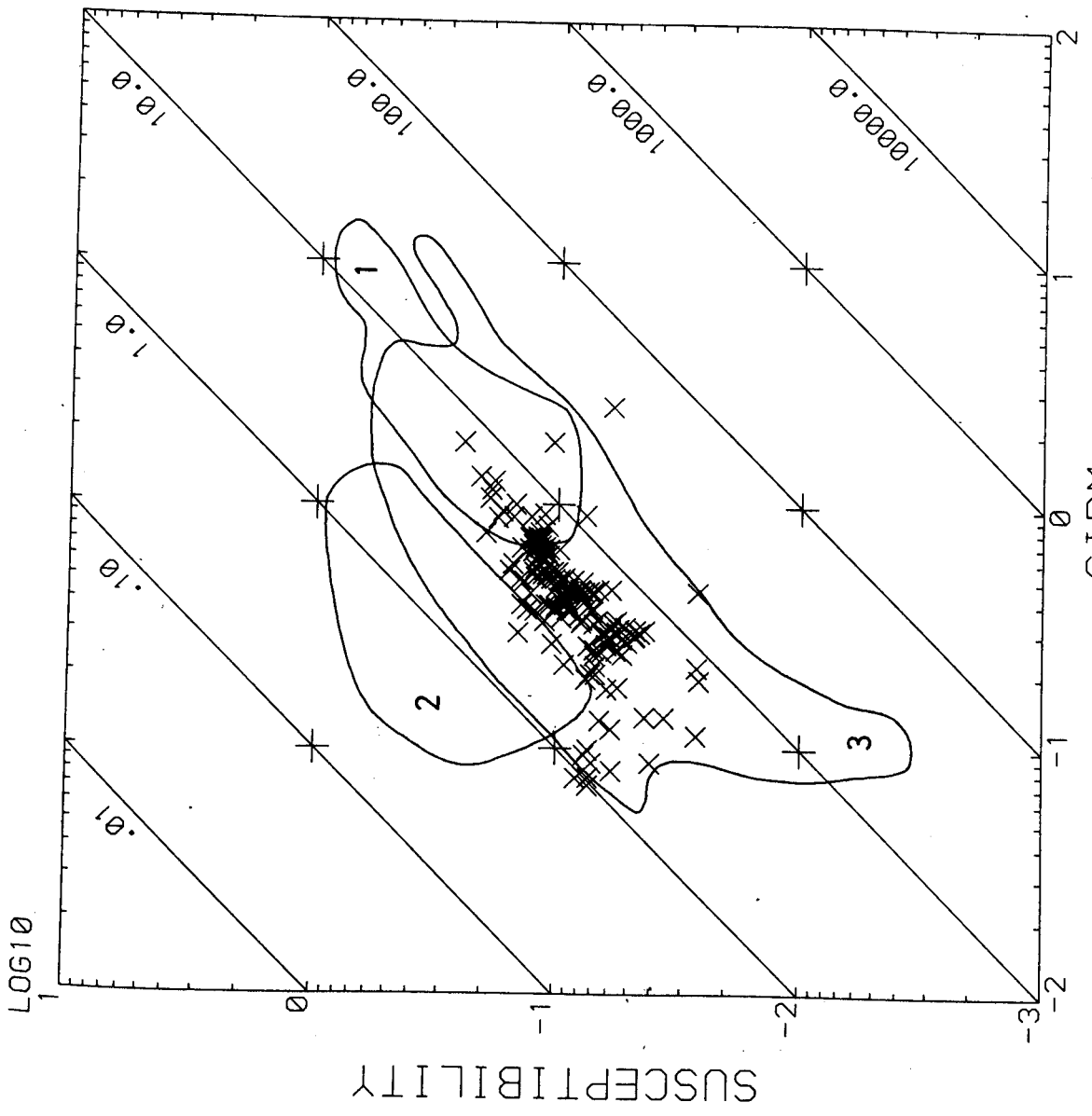

Figure 7.13 χ plotted against SIRM for Late-glacial samples

and clay-mud. Envelopes for the three distributions of late Flandrian samples shown in Figures 7.1-7.2 are included. Almost all of the samples fall within envelope 3. This indicates that the high k of the Late-glacial samples is a function of their high wet density: when expressed on a dry-weight specific basis their magnetic concentration is comparable with that of the late Flandrian detritus muds. Some of the samples have SIRM/χ values comparable with those of magnetic peak B; however, their χ values are substantially lower. Therefore, Late-glacial sediments are precluded as source materials for magnetic peak B.

7.5.5 Significance of the results of the magnetic measurements of potential lake sediment sources

Two main points emerge from the above: (i) There is no evidence at the present time of significant magnetic enhancement (sensu Le Borgne, 1955; 1960; Tite and Mullins, 1971; see section 7.2) in the topsoils of any of the profiles examined, including those in the vicinity of the area affected by the 1951 forest fire (Chapter 2, section 2.3). Efforts to locate topsoil concentrations of ferrimagnetic material within this area using a metal detector (cf. Longworth et al., 1979) have also been unsuccessful. Such features may have been removed by erosion, or alternatively their absence may support the suggestions of several workers (e.g. Vadyunina and Babanin, 1972; Mullins, 1974) that gleying and/or the decomposition products generated in the production of acidic humus may either inhibit the pedogenic formation of ferrimagnetic minerals or effect their actual chemical breakdown.

(ii) Magnetic concentrations comparable with those of the χ peaks in the lake sediments only occur in the subsoil, in the Bs horizons of podsols. However, the values of SIRM/χ of bulk samples from these horizons are higher than those of magnetic peak B but lower than those

of peaks 2 and A. Expression of the magnetic properties of the soil and stream bedload samples on a particle size-specific basis does not significantly improve their correspondence with those of the lake sediment peaks. Values of SIRM/χ comparable with those of the lowest from magnetic peak B occur in the coarse fractions of sample GS18 and in some of the Late-glacial samples; however, the χ values are substantially lower. They presumably reflect the presence of paramagnetic ions in relatively unweathered parent material.

CHAPTER 8 POLLEN ANALYSES

8.1 Introduction

Pollen analyses were carried out for two reasons: (i) to attempt to transfer the radiocarbon chronology for peat core 0/310 (see Chapter 5, section 5.3.4) and the palaeomagnetic chronology for Llyn Geirionydd (Turner, 1979), ca. 1.5 Km northeast of Llyn Goddionduon (see Chapter 5, section 5.3.2, and Appendix I) to the Goddionduon lake sediments; (ii) in the absence of documentary evidence relating to land-use change within the Goddionduon watershed for the period prior to Forestry Commission acquisition, to attempt to reconstruct the vegetation history of the surrounding area. This is used in Chapter 9 (section 9.3) to interpret the changes in the estimated rates of sediment influx. Methods of preparation of pollen samples, pollen identification and counting are described in Chapter 3 (section 3.7).

8.2 Choice of pollen sum

Since it was intended to attempt to transfer the radiocarbon chronology for core 0/310 (from the peat bog) to core 60/-40 (from the lake basin) via the cross-matching of common variations in their pollen biostratigraphies, considerable attention needed to be given to the choice of pollen sum used for calculating the frequencies of the pollen types in view of the likelihood that the respective pollen records from the cores reflect contributions from different pollen source areas. Table 8.1 shows an attempt to define the likely sources of the pollen present in the lake basin and in the peat bog, and in each case to indicate the possible relative magnitude of the pollen contribution. The terms local, extra-local and regional follow Janssen (1966). The table is based on studies of pollen dispersal and of the origin of pollen within lake sediments (e.g. Janssen, op. cit.; Berglund, 1973;

Lake		Bog	
Source	Relative magnitude of contribution	Source	Relative magnitude of contribution
Local pollen from plants growing adjacent to and within the lake	Moderate	Local pollen from plants growing directly on the sampling site, or situated a few m to a few tens of m away.	Large
Extra-local pollen from within and beyond the watershed	Large	Extra-local pollen from beyond the watershed	Moderate
Regional pollen from beyond the watershed	Moderate	Regional pollen from beyond the watershed	Moderate
Local, extra-local and regional pollen preserved within organic soil horizons and transported to the lake basin by soil erosion	?	Local, extra-local and regional pollen derived from the lake basin during periods of high lake level	?
Local, extra-local and regional pollen from reworked marginal sediments	?		

Table 8.1. Potential sources of pollen grains, and the possible relative magnitude of their contribution, within the Goddionduon lake basin and peat bog.

Peck, 1973; Bonny, 1976; Pennington, 1979). It ignores the complications introduced by the effects of watershed transport mechanisms (e.g. Peck, op. cit.) and limnological sorting processes (e.g. Davis and Brubaker, 1973) on the ultimate composition of the pollen spectra obtained from lake sediment cores. In the pollen diagrams shown below, a pollen sum has been used which attempts to exclude the local component in Table 8.1, since the pollen spectra from the bog are likely to be greatly influenced by the large and erratic deposition of pollen from plants growing directly on the sampling site. Local pollen contributors were defined as those taxa which are either growing on or adjacent to the bog at the present day, or which are likely to have done so in the past. They include the following numerically important contributors to the pollen spectra from cores 0/310 and 60/-40: Calluna vulgaris, Myrica gale, Cyperaceae, Narthecium ossifragum and Gramineae. The decision on whether or not to exclude Gramineae was problematical, since grass pollen is likely to constitute a significant proportion of both the regional and extra-local (e.g. from dry land pasture) and local (e.g. from Phragmites reedswamp) pollen components. However, the decision to exclude it was supported by the results of numerical analyses (see Appendix H).

8.3 The pollen diagrams

Figure 8.1 shows the pollen diagram for core 0/310. Only selected taxa are shown. Part (a) includes those taxa assumed predominantly to constitute the regional and extra-local pollen components. The pollen sum ranges from 208 to 1 245, with a mean of 485. Part (b) includes those taxa assumed predominantly to constitute the local pollen component. The pollen sum ranges from 718 to 2 679 with a mean of 1 306. The pollen types have been grouped into categories according to the type of habitat from which they are likely to be derived. Table 8.2 shows the key to the habitat codes. Some overlap is inevitable

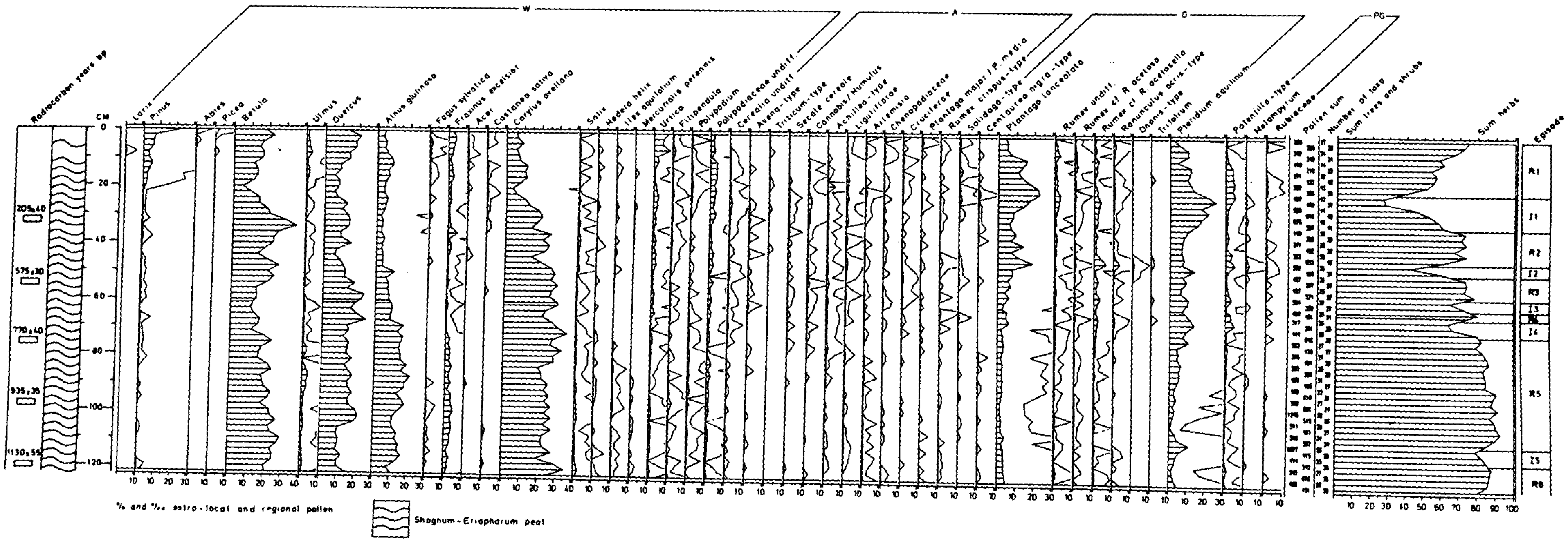

LLYN GODDIONDUON BOG CORE O/310.

Figure 8.1 Pollen diagram from core O/310 (part a)

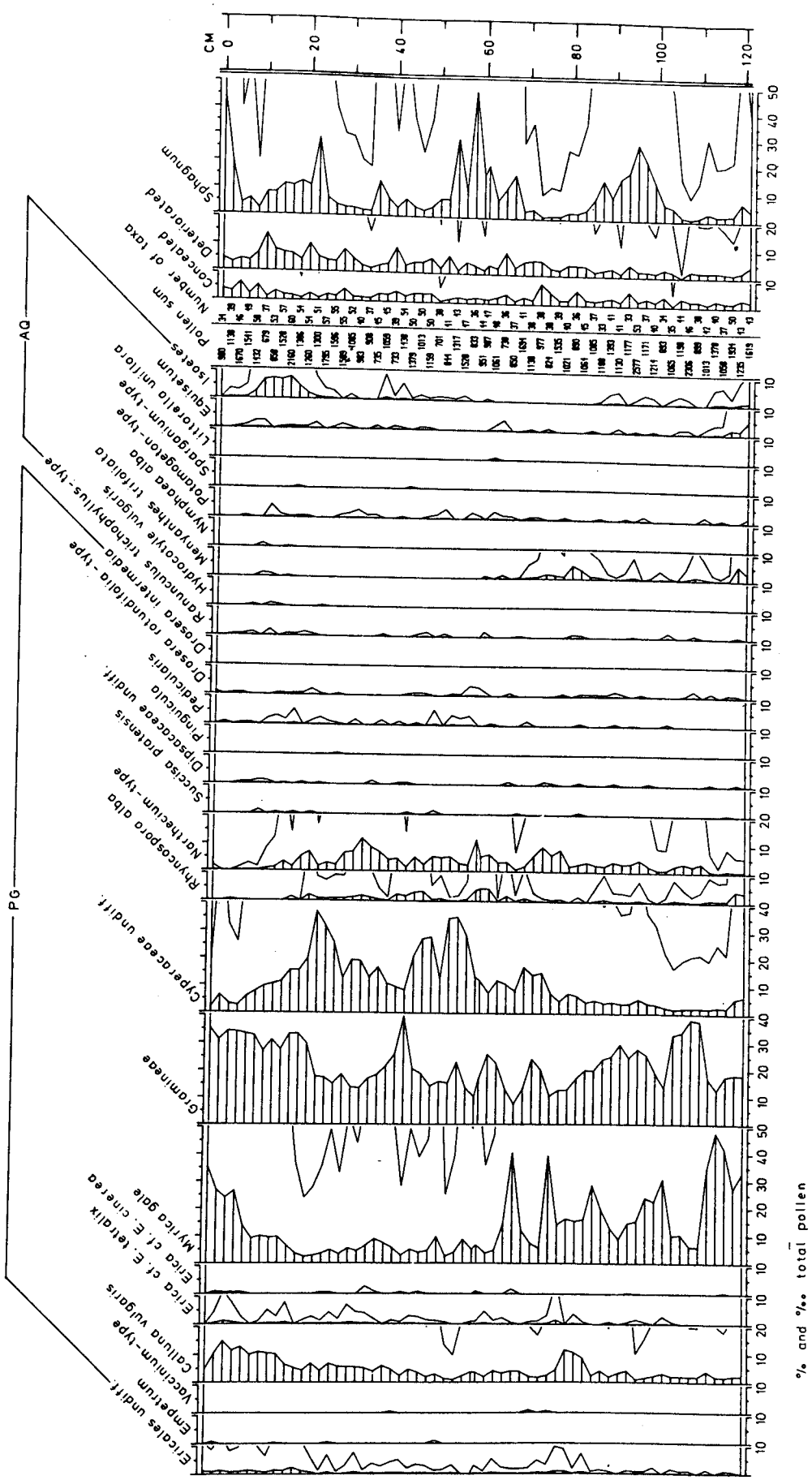

Figure 8.1 continued (part b)

Code	Habitat
W	Woodland and open woodland
A	Arable land
G	Grassland, including land maintained for pastoralism
PG	Poor grassland, moorland, bog
AQ	Aquatic

Table 8.2. Key to the habitat codes shown in Figures 8.1-8.2.

since several of the taxa are indicative of more than one habitat.

The summary pollen diagram (shown in part (a)) (constructed from the frequencies of regional and extra-local pollen types) has been used to divide the pollen stratigraphy into a series of vegetation interference (I) and regeneration (R) episodes, which are presumed to reflect periods of increased and reduced human activity, respectively. I episodes are defined by reductions in the ratio tree plus shrub: herb pollen (TS:H), and R episodes by the recovery of this ratio. The characteristics of individual episodes are described and interpreted in section 8.5 (below). The ratio TS:H varies between 0.27 and 0.90.

Figure 8.2 shows the pollen diagram together with the single-sample volume susceptibility record for core 60/-40. The diagram is constructed in the same manner as that for core 0/310. The pollen sum for part (a) ranges from 246 to 553 with a mean of 386; and that for part (b) ranges from 728 to1 252 with a mean of 979 . Isoetes is excluded from the pollen sum of part (b) because of its very large, and variable, frequencies.

The most striking feature about Figure 8.2 is the general uniformity of the pollen curves in part (a). Reference to the summary diagram shows that despite the efforts to employ a pollen sum that would facilitate the correlation of pollen biostratigraphical changes between

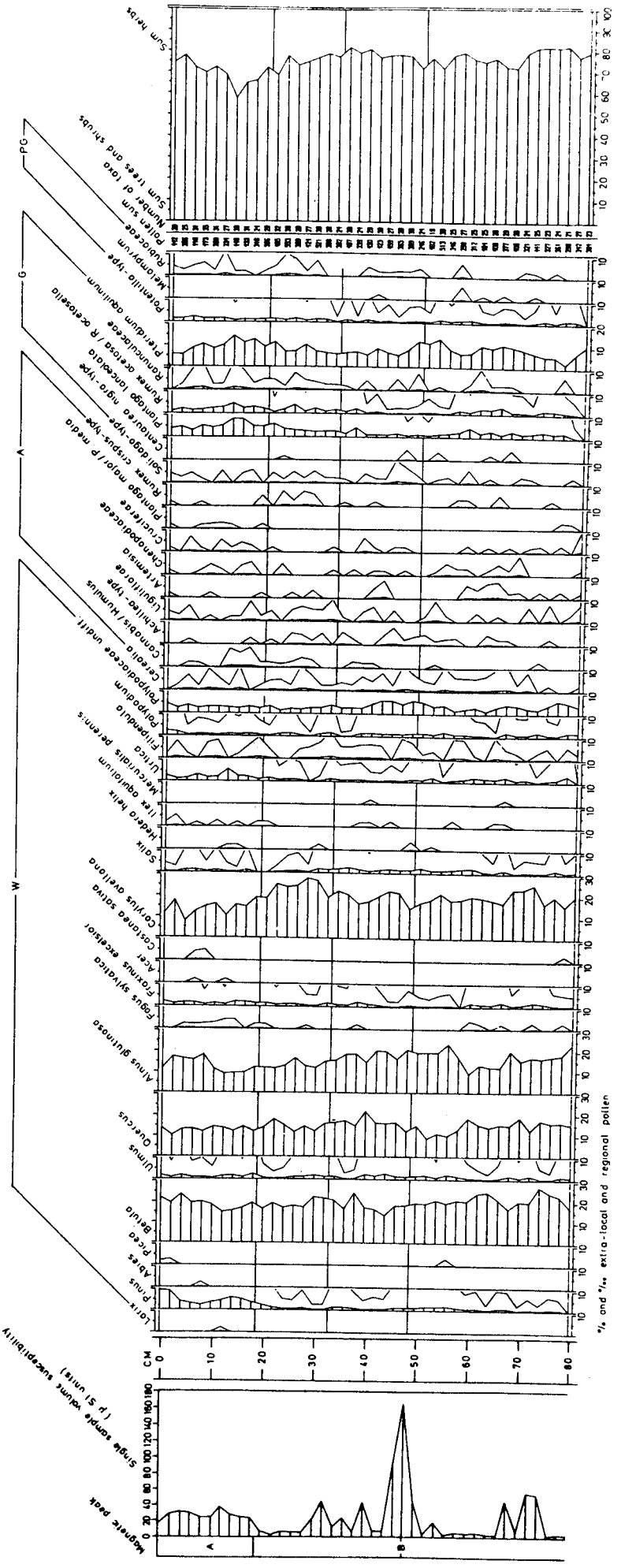

Figure 8.2 Pollen diagram from core 60/-40 (part a)

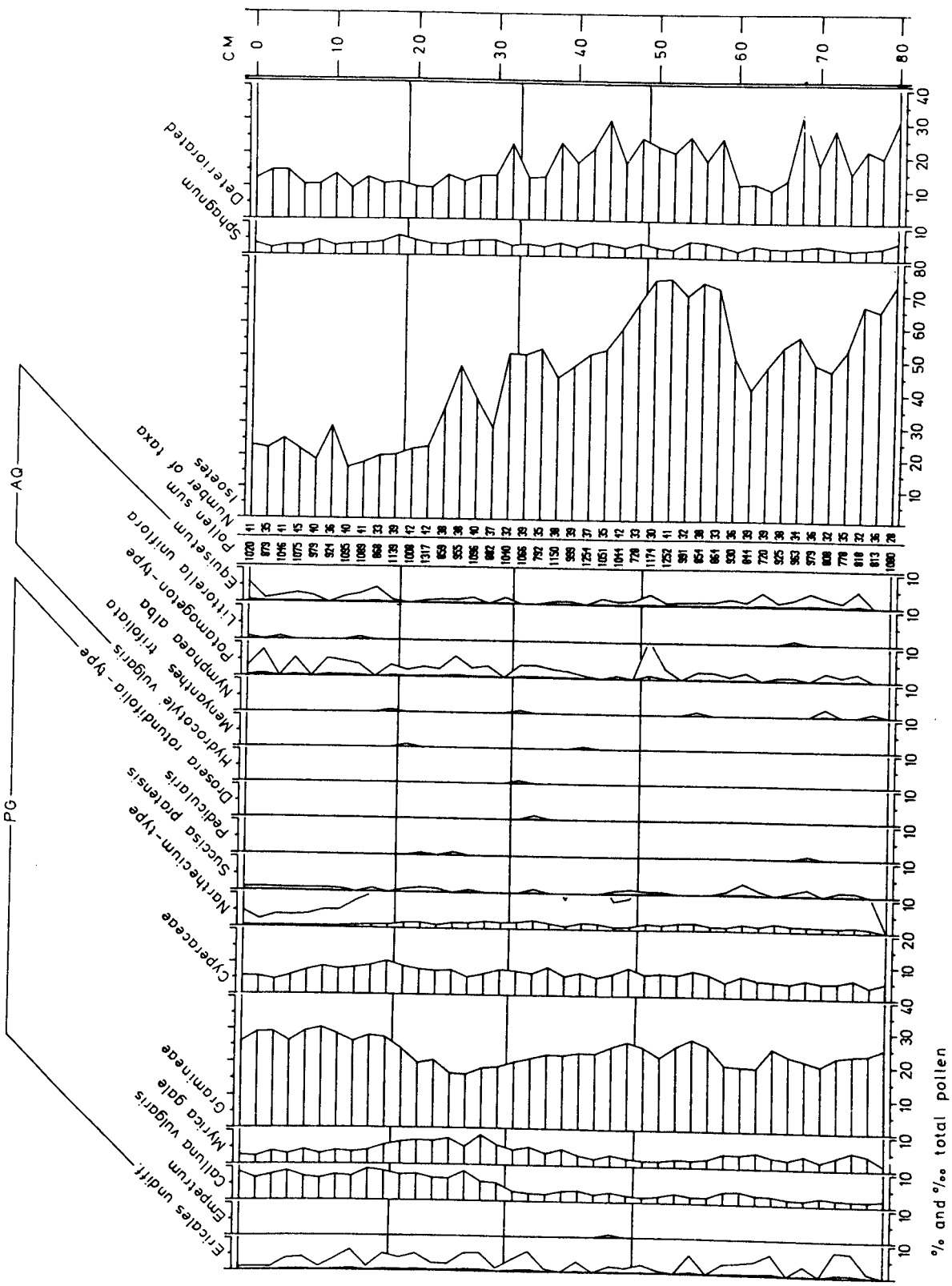

Figure 8.2 continued (part b)

the two cores, none of the large fluctuations in the ratio TS:H evident in core 0/310 is present in core 60/-40. TS:H varies only between 0.56 and 0.81 in Figure 8.2. Because of the absence of any points of correlation between the two diagrams (possible reasons for which are considered below) it is impossible to fulfil the intention of transferring the peat-based ^{14}C chronology from the peat bog to the lake basin. The basis of the horizontal division of the pollen diagram for core 60/-40 is as follows:

49 cm. This level corresponds to magnetic peak B (point of highest k). It broadly coincides with an interval of maximum Isoetes representation; however, there are no significant changes in any of the other taxa at this level. The level is assigned the age-range 670-880 bp (AD 1070-1280).

34 cm. This level corresponds to the beginning of a sustained rise in the frequencies of Calluna vulgaris and Myrica gale, and coincides with the beginning of a sustained reduction in Isoetes frequencies. The increase in Calluna is tentatively correlated with a rise in Ericales frequencies in a pollen diagram from the palaeomagnetically-dated core GEIR2 from Llyn Geirionydd (see Appendix I). This latter feature falls within the age range 320-220 BP (AD 1630-1730) on the GEIR2 age-depth relationship (Appendix I).

20 cm. This level corresponds to the base of magnetic peak A (sediment layer 3) and is assigned the date of AD 1951 (see Chapter 5, section 5.2). The interval 0-20 cm exhibits substantially increased Pinus frequencies, together with the slight representation of the exotic conifers Picea, Larix and Abies. Plantago lanceolata and Gramineae frequencies are rather higher than in the rest of the diagram.

The reasons for the less highly resolved pollen record from the lake basin in comparison with the peat bog are unknown. However, two factors may be significant: (i) Birks (1972) notes the poor stratigraphic

resolution of the post-5000 bp period in a pollen diagram from Loch Dungeon, Galloway, in comparison with a pollen diagram from an adjacent raised bog, and attributes this to the influx of pollen preserved within eroding peat and soil (cf. Table 8.1), thereby incorporating pollen of a variety of ages into the lake sediments. A large increase in the frequency of Calluna vulgaris, the pollen tetrads of which may occur abundantly in peaty soils, in a pollen diagram from Devoke Water, Cumbria, has been ascribed to this mechanism (Tutin, 1969). At this site, the increase in Calluna is accompanied by a decline in the representation of the aquatic macrophyte Isoetes lacustris, a plant which appears to be adversely affected by the influx of acid organic matter (Birks op. cit.). Both of these features, the Calluna rise and Isoetes decline, occur more or less synchronously in core 60/-40. Together with the probability of anomalously old ^{14}C dates in adjacent core 60/-41 (Chapter 5, section 5.3.2) and the trend of increasing organic matter influx to the lake basin (Chapter 6, section 6.6), much of which must be of allochthonous origin, they point to the likelihood of the incorporation of soil and peat-derived pollen into the lake sediments.

(ii) The evidence in the lithostratigraphic record from the southern margin (Chapter 4, section 4.5) for a period of lowered lake level suggests the possibility of the redeposition of pollen from reworked marginal sediments. This effect, attributed to a lake level lowering, has been noted in the recent sedimentary record of Lake Växäsjön, Sweden (Digerfeldt, 1977a), in this case producing anomalously high tree pollen frequencies.

8.4 Chronological significance of biostratigraphic evidence for a lowered lake level in core 0/310

Although it is impossible to directly transfer the ^{14}C dates from the peat bog to the lake basin, part (b) of the pollen diagram for core 0/310 (Figure 8.1) is of potential significance for the establishment of a chronology of sediment accumulation for the lake basin. Most of

the changes probably reflect local vegetation successions on the peat bog and in the adjacent margin of the lake basin. Detailed consideration of these is beyond the concern of the present study. Of principal interest is the possible evidence for changes in lake level suggested by the variations in the occurrence of Isoetes microspores. At the present time, Isoetes lacustris is largely confined to water depths greater than ca. 1.5 m (Chapter 2, section 2.6). Two contrasting periods of relative Isoetes representation are evident: a period of maximum representation over the interval ca. 22-8 cm (AD 1785-1960) and a period of complete absence of this species from the microfossil record over the interval ca. 85-62 cm (ca. AD 1115-1310). Since Isoetes microspores are of exclusively limnetic origin, their significant representation (upto ca. 7% at 16-18 cm) constitutes strong evidence for a period of relatively high lake level and consequent flooding of the bog surface (cf. Table 8.1). Conversely, although constituting only negative evidence, the complete absence of Isoetes (considered significant in view of the large pollen counts employed) between ca. AD 1115-1310 is compatible with a relatively low lake level during this period. The duration of the interval accords with the ^{14}C dates obtained from the drift peat/coarse detritus mud layers in the southern margin of the lake basin (see Chapter 5, section 5.3.3) which are also considered to reflect a lowered lake level. Since these layers are stratigraphically associated with the laminated clayey sediments characteristic of magnetic peak B, the age of the interval of minimal Isoetes representation supports the date used for the calculation of the rate of influx of sediment layer 2.

8.5 Inferred land-use change within the Llyn Goddionduon area

This section attempts to interpret the pollen biostratigraphical changes in Figures 8.1-8.2 in terms of changing vegetation and hence changing land-use in the Llyn Goddionduon area. Reference is made to

documented regional environmental history and to pollen analytical data from other sites in Wales in order to aid the interpretation. The conclusions are used in Chapter 9 (section 9.2) to provide a context for the evaluation of the changes in the estimated rates of sediment influx.

There are two intransigent problems, the subject of much recent investigation by palynologists (e.g. Birks and West, 1973), involved in attempting to use the pollen data for this purpose. Firstly, pollen spectra cannot be interpreted directly in terms of the vegetation within the effective pollen source area (i.e. the area contributing the bulk of the pollen deposited at a given site; Tauber, 1965) because there are large variations in pollen productivity and in the efficiency of pollen dispersal between species; and as a result some taxa are greatly over-represented in the pollen record and many are not represented at all. Secondly, except in certain situations it is difficult or impossible to relate an observed pollen stratigraphic change to a particular area: for example, in theory the same pollen stratigraphical change could be effected by either a major change in vegetation composition a long distance from the site or by a small change in vegetation composition close to the site (cf. Oldfield, 1970). This is a particularly serious problem since the effective pollen source area may itself be altered considerably by a change in vegetation structure, such as is brought about by forest clearance.

Some of the interpretational problems involved in pollen-analytical reconstruction may be illustrated by comparing the uppermost pollen spectrum from core 0/310 with the present vegetation composition within and surrounding the Goddionduon watershed. The Forestry Commission plantations contain extensive stands of *Picea* and *Larix*; however, these taxa are scarcely represented in the pollen spectrum, which is dominated by *Pinus*, *Betula* and *Quercus*. Both *Picea* and *Larix* are known to be inadequately represented in pollen diagrams, either through low pollen

productivity and/or poor pollen dispersal (Davis, 1963; Anderssen, 1970).

Prior to a consideration of vegetation changes decipherable from the pollen records, a brief summary is given below of the history of human activity in Snowdonia during the period preceding that covered by the pollen diagrams.

The palynological evidence of Crabtree (1965) and Walker (1977) indicates that at the time of the incursion of Neolithic farmer colonists into northwestern Europe (at around 5500-5000 bp) Snowdonia was occupied by mixed deciduous forest which probably extended to at least 600 m O.D. Neolithic impact on the vegetation of the area was limited since their settlements were confined to the coastal lowlands (Grimes, 1965). Both the later Neolithic megalith builders and the Beaker peoples were also sparsely settled in the area.

During the subsequent Bronze Age (ca. 4000-2500 bp) human occupation of Snowdonia increased considerably. Temporary forest clearances were carried out for livestock grazing (Crabtree op. cit.). A Bronze Age clearance episode (the peak of which is dated to ca. 2820 BP) within the Glyn area is evident in the pollen record from Llyn Geirionydd (Appendix I).

The onset of the Iron Age (ca. 2500 BP) with the invasion of Wales by Celtic-speaking tribes and their rapid spread during the centuries before the Roman conquest, resulted in considerable deforestation and lowering of the tree-line, evidenced by detailed pollen-analytical studies from Mid Wales (Turner, 1964; Moore and Chater, 1969). It is likely that the activities of these sedentary farmers accelerated the natural trends of podsolization, soil waterlogging and peat formation, and the spread of Ericaceous plants which had become more pronounced after the beginning of the relatively cool and wet Sub-Atlantic period (ca. 2500 bp) (Godwin, 1975).

The Roman invasion and subjugation of Wales between AD 43 and 78

generated a substantially increased demand for grain and resulted in an acceleration of deforestation reflected in the pollen data cited above. However, the weakening and eventual ending of Roman control in AD 400, with the resulting decline in the demand for agricultural produce led to a slowing down of economic life and also to considerable inter-tribal warfare which continued throughout much of the Dark Ages. Forest regeneration during this period is evidenced by the reference of Giraldus Cambrensis, who toured Wales in AD 1188, to the widespread occurrence of "bristling forest" (Emery, 1969).

Because of the lack of stratigraphic resolution in the pollen diagram from core 60/-40, much of the following interpretation is based on the diagram from core 0/310. The vegetation interference and regeneration episodes (section 8.3) are used to provide the basis for the diagram description. The durations of the episodes are obtained from the age-depth curve for this core (Figure 5.4; Chapter 5, section 5.3.4).

Episode R5 (107-69 cm; AD 940-1245).

The sum of tree and shrub pollen (the latter mostly Corylus avellana) averages over 85% throughout. The woodland herb taxa Polypodium and Mercurialis perennis are significantly represented.

This episode spans the middle part of the mediaeval period. As noted above, for a substantial length of time following the Roman withdrawal, there was a slackening of agricultural activity within Wales and consequent woodland regeneration. On the basis of the pollen data this interpretation appears to be applicable to the Glyn area.

Extrapolation of the age data available for core 60/-40 (see section 8.3) indicates that the base of this core is likely to date from at least AD 450. Therefore, the significant representation of Calluna and Sphagnum throughout core 60/-40 suggests the likelihood that moorland development and peat formation within at least part of the

Goddionduon watershed had been initiated by this time.

Episodes I4 (69-63 cm; AD 1245-1300) and I3 (60-56 cm; AD 1325-1365). Episode I4 is characterised principally by a major reduction in the frequency of Alnus glutinosa; however, significant reductions also occur in Betula and Quercus. Ulmus and Fraxinus excelsior frequencies are considerably reduced just below the R5-I4 boundary. There are substantial increases in Pteridium aquilinum and Potentilla-type and more modest increases in Plantago lanceolata and Rumex cf. R. acetosella. Episode I3 exhibits similar characteristics; however, the principal tree pollen type affected is Quercus. The limited representation of category A pollen types (Table 8.2) suggests that both episodes were predominantly of pastoral character.

There is historical evidence of clearance and pasture extension during the period spanning episodes I4 and I3. The Cistercian abbey of Aberconway was founded in AD 1168 and owned over 12 000 ha in and around Snowdonia (Emery, 1969). The Cistercians carried out extensive assarting movements, or the systematic clearance of woodland and scrub, principally for sheep grazing, and the increased representation of pasture indicators in pollen diagrams from Mid Wales during this period has been directly attributed to the founding of the Strata Florida estate (Turner, op. cit.; Moore and Chater, op. cit.). The marked reduction in Alnus in episode I4 may suggest that clearance was concentrated in lowland and/or valley bottom habitats during this period.

Episode R3 (54-48 cm; AD 1365-1460).

Betula is the only tree and shrub pollen type to exhibit an increase during this period, suggesting some recolonisation of formerly cleared areas by birch woodland. The frequencies of most of the herbaceous pollen types are correspondingly reduced.

This episode may be tentatively correlated with three events - the Black Death in AD 1349, Owain Glyndwr's revolt in AD 1400-1410 and the

PAGE
MISSING
IN
ORIGINAL

Wars of the Roses in AD 1455-1485 - which in combination led to the economic devastation and to considerable depopulation of the Snowdonia area (Scott, 1949).

Episode I2 (48-44 cm; AD 1460-1510).

Reference to the summary diagram for core 0/310 shows that this period exhibits a major reduction in the ratio TS:H. Betula is the taxon particularly affected. Significant peaks occur in the category G pollen types: Plantago lanceolata, Pteridium aquilinum, Rumex cf. R. acetosella, Ranunculus acris-type and Ononis-type. Again, therefore, these changes appear to be principally associated with pastoralism.

The establishment of the Tudor dynasty in AD 1485 brought relative stability to Snowdonia and with it the rapid growth of cattle raising, initially for dairying but later in the 16th and 17th centuries for the store cattle trade. This resulted in further forest clearance and the extensive enclosure of land in the lowlands for hay and grazing. The upland grasslands were also intensively used for summer grazing (Scott, op. cit.).

R2 (44-32 cm; AD 1510-1675)

This episode is characterised by the increased representation of Quercus, Fraxinus and Corylus, and particularly by Betula which increases to 35% towards the end of the period. Category G pollen types are reduced. In line with the interpretation of R3, the pollen data indicate the recolonisation of formerly cleared areas by birch, ash, oak and hazel.

Direct evidence of the status of Snowdonian woodland in AD 1530 is available from the journals of John Leland, kept during a tour of Wales. These indicate that the Llanberis - Capel Curig - Betws-y-Coed area was relatively well-wooded at this time[1].

---

[1] "Al Cregeeryi (Snowdon) is forest. The best wood of Cairnarvonshire is by Glinne Kledder (Glyn Lledr), by Glin Llughy (Llugwy), and by Capel Kiryk (Curig), and at Llanperis. Meately good wood aboute Conwey Abbay and Penmachno and about Coiteparke (near Bethesda)".(Toulmin-Smith, 1906).

Episode I1 (32-20 cm; AD 1675-1775).

Minima in the representation of Betula, Quercus and Corylus occur during this period. The minimum value of the ratio TS:H (0.27) for the entire profile occurs at the end of the episode. Plantago lanceolata (upto 22%), Pteridium aquilinum (upto 25%), Potentilla-type, Rumex spp, Cerealia and Cannabis/Humulus exhibit their highest representation. On the basis of a tentative correlation with a palaeomagnetically-dated pollen diagram from Llyn Geirionydd (Appendix I), the age range for the increase in Calluna vulgaris at ca. 34 cm in core 60/-40 largely falls within this period.

On the basis of both pollen analytical and historical evidence this was a period of major and sustained impact on Snowdonian woodland. As well as the demands for agricultural land and for wood for charcoal burning, ship-building began to generate a major demand for timber, and from AD 1754-1760 oak to the value of £50 000 was sold from the Gwydyr estate (near Llanrwst) for this purpose (Emery, 1969). At the end of the period, the absence of woodland in the area was noted by Thomas Pennant who toured Wales in the 1760's and 1770's[1].

In addition to an acceleration in woodland clearance, the period also saw a significant change in livestock patterns. From the middle 18th century the sheep population of Snowdonia began to increase and soon became the dominant livestock on the upland farms (Ratcliffe, 1959). It is likely that moor burning was increasingly used as a management technique to promote grassland extension during this period. Crabtree (1965) attribites minerogenic horizons in the uppermost sections of

---

[1] "The venerable oaks, spoken of by Leland, are no more. Avarice, or dissipation, and its constant follower, poverty, have despoiled much of our principality of its leafy beauties ... I fear IS cloathed with trees, must be supplied by the traveller with WAS". (Rhys, 1883).

valley peat deposits near Capel Curig to the probable increased soil erosion resulting from this practice.

The relatively high frequencies of Cerealia and Cannabis/Humulus (probably hemp) (also apparent in the pollen diagram from Llyn Geirionydd) are not paralleled in the available historical records by references to increased arable activity during this period, although Aikin (1797) refers to cultivation in the Conway valley. There are references (Scott, op. cit.) to intensive cereal cultivation at altitudes of at least 280 m during a subsequent period of inflated grain prices engendered by the Napoleonic wars (1793-1815); however, this is not apparent in the pollen stratigraphy and on the basis of the ^{14}C time scale from core 0/310.

Since the pollen tetrads of Calluna vulgaris are poorly dispersed in air and are predominantly water-transported to lake sites (Peck, 1973), it is unlikely that the Calluna rise in core 60/-40 ascribed to this period reflects a change in the regional pollen rain. Either a significant extension of Calluna within the vegetation of the Goddionduon watershed or the influx of derived Calluna tetrads in eroding peat or soil may be envisaged (cf. Table 8.1). Since the pattern of land-use within Snowdonia has tended to promote the extension of acidic grassland rather than Callunetum (Ratcliffe, op. cit.) the latter alternative may be more likely. Either moor burning and/or an increase in grazing pressure may initiate or accelerate soil and peat erosion (e.g. Imeson, 1971), and both are compatible with the historical evidence for the nature of land-use change during this period.

Episode R1 (20-0 cm; AD 1775-1978)

This period is characterised by steadily increasing tree pollen representation, principally Pinus, Betula, Quercus, Fraxinus and Fagus. In the 0-2 cm sample the proportion of tree pollen (nearly 40% of which is Pinus) is comparable with that of episode R5. Several of the G category

pollen types (*Plantago lanceolata*, *Potentilla*-type and *Pteridium aquilinum*) are strongly represented during the first half of this period but are substantially reduced thereafter.

The pollen analytical data for the beginning of the period indicate a continuation of intensive pastoral land-use. The gradual rise in the tree pollen frequencies reflects afforestation by private landowners. Aikin (op. cit.) refers to the latter activity on the Gwydyr estate at the end of the 18th century. During the last 60 years private afforestation has been supplemented on an enormous scale by the Forestry Commission, clearly illustrated in the uppermost sample by the high *Pinus* frequency and the presence of pollen of the exotic conifers *Picea* and *Larix*. The history of land-use specifically within the Goddionduon watershed for this most recent period is well-documented (Chapter 2, section 2.3).

CHAPTER 9. DISCUSSION

9.1 The mineral magnetic record

This section discusses the mineral magnetic record from the Goddionduon lake watershed with the intention of attempting (i) to use the conclusions to aid the interpretations of the sediment yield data (section 9.2), and (ii) to contribute to continuing efforts to interpret changes in the mineral magnetic properties of lake sediments (see Chapter 7, section 7.2).

Relatively few magnetic measurements have been made on the Goddionduon lake sediments below magnetic peak B (i.e. sediments deposited prior to around 800 bp). Measurements of Late-glacial and early Flandrian sediments and of sediments immediately below peak B (for example over the interval 183-100 cm in core 50/90L) indicate that magnetic concentration is relatively low and uniform, and comparable with that of contemporary stream bedload, podzolic topsoil and gleyed soil. In contrast, the sediments deposited subsequent to around 800 bp exhibit major fluctuations in their mineral magnetic characteristics, both spatially within the lake basin, and temporally.

In view of the interpretations of fluctuations in magnetic concentration in lake sediments described in Chapter 7 (section 7.2), the paramagnetic Fe and Mn layers (magnetic peaks 1 and B) are of considerable interest. Magnetic peak B covers almost the whole of the lake basin, while magnetic peak 1 is confined to parts of the central and southern sectors. The evidence given in Chapter 7 (sections 7.4-7.5) shows firstly, that concentrations of paramagnetic material comparable with those of the lake sediments do not occur within the range of potential lake sediment source materials that has been sampled, and secondly, that concentrations of Fe and Mn in other lake sediment

deposits comparable with those in the Goddionduon paramagnetic peaks have been interpreted in terms either of their solubilization within the sediment body itself, followed by migration and precipitation within horizons of favourable pH and Eh, or more commonly by solubilization within the watershed soils and substrate, followed by transportation to and precipitation within the lake basin.

Since Fe and Mn are precipitated at different values of Eh and pH, their mobilisation, movement, and subsequent precipitation within the sediment body itself produces segregated Fe-enriched and Mn-enriched layers (Chapter 7, section 7.4.4.). This is not so in the present case. Also, it is difficult to understand why such a process should have operated discontinuously in time, and the diatom evidence (Appendix F) gives no indication of a qualitative change in the lake waters at the time of the deposition of peak B. Therefore, a source of Fe and Mn external to the basin appears more likely.

As indicated in Chapter 7 (section 7.4.4) several lakes have received large influxes of Fe and Mn under two main kinds of circumstance: (i) as a result of the mobilisation of Fe and Mn within the watershed soils through the onset of reducing conditions as a result of blanket peat development and consequent waterlogging; in this case high sedimentary concentrations of these elements have been maintained throughout the late Flandrian. (ii) For a relatively short period during the early Post-glacial due to the entry of Fe-charged sub-surface drainage; subsequent deposition of organic sediment has sealed the basin from this influence. Although peat development in the Goddionduon watershed is likely to have increased the influx of Fe and Mn in solution (as in (i)) this would not be expected to operate intermittently; in addition, the exclusion of sub-surface drainage by the deposition of organic sediment (as in (ii)) could hardly explain the abruptness of the paramagnetic peaks, since

firstly, there is more than one peak and secondly, the peaks occur in the late Flandrian, long after such a sealing would have begun.

Conceivably, a hydrological change affecting the rate of groundwater seepage into the lake basin could be invoked as a possible explanation for the paramagnetic layers. This implies that groundwater within the watershed contains a substantial concentration of Fe and Mn in solution and therefore that it is oxygen deficient and/or acidic, (Mortimer, 1941). High concentrations of Fe in both groundwater and surface water may be brought about by acidification through the production of sulphuric acid by pyrite oxidation (cited in Kjensmo, 1978); and in so far as pyrite is locally common in the area (Howells et al, 1978) this may be a possibility. However, the relatively low permeability of the Goddionduon substrate together with the reported blocking effect of organic sediment might be expected to result in low rates of groundwater seepage. Nevertheless, significant hydrological changes in the form of lake level fluctuations are evident in the sediment and peat stratigraphies. The microfossil evidence and ^{14}C dates from core 0/310 suggest a relatively high lake level during the period ca. AD 1785-1960 (Chapter 8, section 8.4) and lithostratigraphic evidence (peaty/coarse detrital layers in the southern margin) suggest a relatively low lake level more or less concurrent with the deposition of magnetic peak B (Chapter 4, section 4.5). Interestingly, Bengtsson and Persson (1978) attribute a rise in the concentration of Fe and Mn in a sediment core from lake Södra Bergundasjön, Sweden, to a lake level lowering but do not suggest a causal mechanism.

In the context of Llyn Goddionduon a change in lake level would be likely to reflect either a climatic change (a change in humidity) or human interference with the outflow. The ^{14}C dates from the peaty/coarse detrital layers at site 27/210 in the southern margin fall

within the mediaeval warm period (ca. AD 1150-1300) during which there are likely to have been periods of summer drought (Lamb, 1965). However, to the writer's knowledge there are no published references to lowered lake levels at other British lake sites during this period; and in addition, if the association between lake level fluctuations and increases in the solutional influx of Fe and Mn were accepted, then the absence of paramagnetic layers in a 2 m-long core from nearby Llyn Bychan (writer's unpublished data) would argue against a climatic cause.

The recent period of raised lake level is likely to be due to outflow regulation (R. Hughes, personal communication).

Despite the circumstantial evidence linking magnetic peak B with a lowered lake level, in the absence of hydrogeological and further geochemical data (e.g. chemical analyses of the groundwater) for the watershed, together with the sparsity of published literature on interrelationships between lakes and groundwater (emphasised for example by Born et al., 1979) the suggested association remains entirely speculative.

Although the mode of origin of the paramagnetic layers is uncertain they demonstrate that in lake watersheds with substrates with low concentrations of ferrimagnetic material (such as the Goddionduon watershed) paramagnetic material may make a significant contribution to the lake sediment susceptibility record. In view of the assumed solutional mode of entry of the paramagnetic Fe and Mn this is of considerable significance for attempts to interpret susceptibility changes in lake sediments in terms of erosional processes (Chapter 7, section 7.2).

The remaining major peaks in magnetic concentration in the late Flandrian lake sediments are dominated by ferrimagnetic material. Magnetic peak 2 is only recorded within the area of relatively rapid

sediment accumulation in the central part of the lake basin. On the basis of single-sample magnetic measurements of cores 60/60L and 50/90L its magnetic properties are indicative of fine-grained multi-domain or stable single-domain ferrimagnetic material. It extends to over 20 cm in core 60/60L. Unlike the paramagnetic layers there are no associated changes in sediment lithostratigraphy.

The magnetic properties of peak A are also indicative of ferrimagnetic material, although there may also be significant paramagnetic and superparamagnetic components. In many of the cores, this feature could be identified lithostratigraphically as black-coloured sediment. Both the vertical thickness and magnetic concentration of peak A are highest in the northern sector of the lake basin, although there are substantial variations in these attributes over short distances.

In the case of the magnetic properties of peak 2 there are no obvious analogues within the range of potential lake sediment sources (Chapter 7, section 7.5). Soil from the Bs horizons of podzols is the only potential source with a comparable magnetic concentration; however, the values of SIRM/χ of this material are significantly lower than those of peak 2. There is no way of establishing the age of this feature, nor of relating it to the available pollen stratigraphy. Interpretation is therefore difficult.

These problems are not so apparent in the case of magnetic peak A. In core 50/-43 the base of peak A is 2 cm above the 1954 horizon of first detectable occurrence of the radioisotope ^{137}Cs (Chapter 5, section 5.2). Since part of the Goddionduon watershed was affected by a major forest fire in 1951 (Chapter 2, section 2.3) the origin of the relatively high magnetic concentration of this horizon was suggested to be the production of secondary ferrimagnetic minerals at high temperatures during the forest fire and their subsequent incorporation in the lakes sediments through soil erosion.

The importance of heating in the production of high concentrations of secondary ferrimagnetic minerals is now relatively well documented: Le Borgne (1960) and Rummery (1981) illustrate their production and subsequent persistence in soils and sediments; Longworth et al. (1979) describe the mineralogy of secondary magnetic oxides produced by uncontrolled burning in the field; and Mullins (1974) and Oldfield et al. (1981a) demonstrate the effects of various laboratory-controlled heating temperatures and atmospheres and rates of heating and cooling on the mineralogy and grain size of secondary magnetic minerals produced in initially weakly magnetic materials (see Chapter 1, section 1.9).

Magnetic concentrations in excess of those of magnetic peak A have been recorded in the tops of lake sediment cores and in soil profiles sampled in the Llyn Bychan watershed, adjacent to Goddionduon, and are attributed to the major Glyn forest fire of 1976 (Rummery, 1981). Deep water cores obtained from the Bychan lake basin four months after the fire exhibited highly magnetic, black-coloured surficial sediment; the black colouration is attributed to the presence of finely disseminated highly oxidised peat (T. Rummery, personal communication).

Since on the basis of the ^{137}Cs dating, the base of peak A postdates the mid-19th century marked rise in the flux density of magnetic spherules derived from industrial combustion processes (Chapter 7, section 7.2) then the only other potential alternative source of peak A is podsolic subsoil. Since it has been demonstrated that road construction substantially increases the rate of sediment yield in watersheds (e.g. Beschta, 1978) it would be expected that road building within the northern part of the Goddionduon watershed during 1960-61 would have had this effect. Most of the road network (see Figure 2.3, Chapter 2, section 2.3) is situated away from the lake edge and within an area of mature, dense coniferous forest and this

is likely to have reduced the quantity of sediment supplied to the lake basin from this source (cf. Bormann and Likens, 1979). However, one section of road extends to the northwestern edge of the basin and a substantial section of podzolic subsoil is exposed along its western edge. Therefore, it might be expected that this would facilitate the erosion, transport to, and deposition of Bs horizon material within the lake basin. In addition, the location of the bulk of magnetic peak A sediment within the northern sector of the lake basin could be considered compatible with a source within the northern part of the watershed.

However, despite this, five factors militate against the conclusion that Bs horizon material is a significant component of magnetic peak A sediment: (i) In core 50/-43 the occurrence of the 1954 ^{137}Cs horizon above the base of peak A is incompatible with the 1960-61 date of road construction. (ii) The ^{137}Cs analyses imply negligible sediment accumulation at site 50/-43 after the mid-1960's; this is more compatible with an erosion episode pre-dating rather than post-dating ca. 1960. (iii) Although relatively few magnetic measurements have been performed on soil samples, samples from Bs horizons have lower SIRM/χ values than those of peak A. (iv) In terms of its black colouration, peak A sediment is lithostratigraphically similar to surficial sediment from LlynBychan; the latter is directly attributable to the 1976 Glyn forest fire. (v) Less significantly, hydrodynamic factors have clearly exerted an important influence upon the spatial pattern of sediment accumulation in the past (section 9.3) and the location of sediment source areas may bear little relationship to patterns of final accumulation.

Although, therefore, the evidence favours the 1951 forest fire as the predominant source of magnetic peak A sediment, in view of the demonstrated variability of the Goddionduon sedimentary record

(Chapter 4) an additional ^{137}Cs profile would be desirable to confirm the conclusions derived from the analyses of core 50/-43.

9.2 Sediment yield and land-use within the Goddionduon watershed

9.2.1 Limitations of the data

In addition to uncertainties derived from analytical errors - in the core correlations, sediment volume calculations and sediment datings, and from uncertainties relating to the origin of the various sedimentary components, the magnitude of sediment loss down the outflow and sediment diagenesis (Chapter 6, section 6.5) - further inherent limitations of the estimates of sediment influx and yield need to be borne in mind.

The three sediment yield estimates represent values for periods of substantially different duration: approximately 9 600 yr, 800 yr and 26 yr for sediment layers 1, 2 and 3 respectively. Clearly, the estimates for layers 1 and 2 are long term averages and the periods of watershed history which they represent are likely to have experienced significant variations in rates of sediment yield. Therefore, they constitute records of rather low resolution. (In the present study this is a function of the relatively small number of correlatable basin-wide features in the susceptibility and lithostratigraphic records: in some other studies with similar aims and employing similar techniques to the present work a more highly resolved susceptibility stratigraphy has enabled the construction of a much more detailed record of changing sediment yield, for example in the watershed of the former Llyn Peris, Gwynedd (Dearing et al., in press)). This lack of resolution makes it difficult to relate the sediment yield estimates to specific ecological conditions or events within the watershed. In sharp contrast to sediment layers 1 and 2, layer 3 may be almost entirely the product of a single 'catastrophic' event within a relatively small fraction of the terrestrial part of the watershed.

Depending upon the aims of a particular study it is possible to envisage the desirability of obtaining estimates of sediment yield

which average out the effects of random variations in sediment yield (for example, produced by individual major storms) but which indicate the magnitude of sediment yield under individual types of land-use regime.

9.2.2 Discussion

Sediment layer 1

The lower boundary of sediment layer 1 is defined lithostratigraphically by the Loch Lomond Stadial clay/early Flandrian clay mud contact which is dated to ca. 10 400 bp. This contact is the product of the climatic amelioration which followed the arctic conditions with periglacial erosion of mineral soils which prevailed during the Loch Lomond stadial. The upper boundary is defined by magnetic peak B which is dated to ca. 800 bp. Only lithostratigraphical data are available for the whole of this period. Over most of the lake basin, relatively homogeneous clay muds and detrital muds were deposited. Single-sample magnetic data for the interval 183-100 cm in core 50/90L span an unknown length of time during the deposition of the uppermost part of sediment layer 1. Magnetic concentration over this interval is low and uniform.

Around 8 700 tonnes of sediment (1 900 tonnes of organic matter and 6 800 tonnes of ash) were deposited within the lake basin during the ca. 9 600 years of this period, representing an annual rate of sediment yield of 36 kg ha^{-1} (8 kg of organic matter and 28 kg of ash). An unknown, but possibly small, proportion of the sediment is likely to consist of organic matter and silica which are of limnetic origin.

The period during which sediment layer 1 was deposited was one of significant climatic and environmental change, and this is likely to have resulted in substantial changes in rates of sediment yield. On the basis of estimated rates of sediment accumulation in similar contexts at other sites (e.g. Likens and Davis, 1975), there is likely

to have been a trend of declining sediment yield consequent upon the stabilisation of bare, unstable watershed substrate by forest establishment and the addition of humus. Conversely, sediment yield is likely to have increased towards the end of the period, since pollen analytical data from core 60/-40 indicate the presence of moorland within the watershed from at least ca. AD 450, thereby implying that some degree of deforestation had taken place by this time. Nevertheless, for the majority of the period the Goddionduon watershed is likely to have been occupied by relatively undisturbed mixed deciduous forest.

Undisturbed woodland ecosystems are highly conservative of both particulate material and solutes (Likens et al., 1977; Bormann and Likens, 1979) and reference to Table 9.1 shows that the value for total sediment yield for layer 1 from Goddionduon is comparable both with estimates for present day woodland ecosystems (Hubbard Brook watershed 6, at Silsoe and in West Virginia and Kentucky) and also for the pre-settlement yield in the Frains lake watershed, obtained by sediment core correlations.

The data for Hubbard Brook indicate that for this watershed the solute yield is substantially higher than the sediment yield. There is no way of estimating the ratio of sediment : solute yield in the Goddionduon watershed; some of the solute influx to the lake basin is likely to have been precipitated biogenically; however, much is likely to have been lost down the outflow. Sediment : solute ratios for a variety of rivers given by Gregory and Walling (1973) indicate that sediment load tends to exceed solute load.

Site	Context	Method	Source
Llyn Goddionduon	Sediment layer 3 Sediment layer 2 Sediment layer 1		
Hubbard Brook Watershed 6 New Hants	Undisturbed northern hardwood forest	CM[1] of total sediment yield. 8 yr $\bar{X}$.	Likens et al., 1977
Hubbard Brook Watershed 2. New Hants.	Deforested-vegetation left in-situ	CM of total sediment yield. 5 yr $\bar{X}$.	Bormann et al., 1974
North Esk reservoir, Midlothian	Grazed upland moorland	Reservoir survey	Ledger et al., 1974
Hopes reservoir, Midlothian	Grazed upland moorland	Reservoir survey	Ledger et al., 1974
Hodge Beck, Yorkshire	Grazed and burnt-over moorland	CM suspended sediment	Imeson, 1974
Grains Gill, Cumbria	Upland moorland - active gully erosion	CM Box traps	Harvey, 1974
Silsoe, Bedfordshire	Bare ground Grassland ley Woodland	CM Traps, splash cups, volumetric channel determinations	Morgan, 1977
Frains lake, Michigan	1830-1970 Roads, arable. ? -1830 Oak forest.	Lake sediment core correlation	Davis, 1976.
Llyn Peris, Gwynedd	19th-20th centuries. Slate mining	Lake sediment core correlation	Dearing et al., in press

Notes: 1. CM = continuous monitoring. 2. Source = cited in Bormann et al., 1974.

Table 9.1. Measured rates of soil erosion /Cont.

Site	W'shed area (ha)	Total sed. kg/ha/yr	Org. sed. kg/ha/yr	Inorg. sed. kg/ha/yr	Solutes kg/ha/yr
Llyn Goddionduon	24.8	263-326 126 36	80-100 27 8	183-226 99 28	-
Hubbard Brook Watershed 6 New Hants	15.6	33.28	11.13	22.15	147.2
Hubbard Brook Watershed 2 New Hants	13.2	155.63	36.28	122.95	580.6
North Esk reservoir, Midlothian	700	260	-	-	-
Hopes reservoir, Midlothian	500	250	-	-	-
Hodge Beck, Yorkshire	1900	4803	-	-	-
Grains Gill, Cumbria	?	$400X10^3$	-	-	-
Silsoe, Bedfordshire	-	$2.5\text{-}18X10^3$ 2400 20	-	-	-
Frains Lake, Michigan	18.4	907 96	7 6	900 90	-
Llyn Peris, Gwynedd	?	-	-	$3.7\text{-}43X10^3$	-

Site	Context	Method	Source
Maesnant Watershed, Plynlimon	Grazed moorland	Survey of 1 yr's channel accumulation	Lewin, et al., 1974
Needle Branch Watershed, Oregon	Forested Logging, road construction	CM suspended sediment	Beschta, 1978
Coalburn w'shed, Carlisle	Grazed moorland Drainage ditching	CM suspended sediment	Robinson & Blyth, 1982
Baltimore	Construction site	-	2
Montana	Forest clearance, arable, pastoral ag.	-	2
West Virginia	Secondary forest, mountains	-	2
Kentucky	Forest	-	2
Sierra Ancha, Arizona	Burnt pine forest, steep slopes	-	cited Dyrness, 1967

Site	W'shed area (ha)	Total sed. kg/ha/yr	Org. sed. kg/ha/yr	Inorg. sed. kg/ha/yr	Solutes kg/ha/yr
Maesnant Watershed, Plynlimon	54	37	-	-	-
Needle Branch Watershed, Oregon	75	530 1460	-	-	-
Coalburn W'shed, Carlisle	150	30 120	-	-	-
Baltimore	?	$490X10^3$	-	-	-
Montana	?	$36X10^3$	-	-	-
West Virginia	39	32	-	-	-
Kentucky	220	53	-	-	-
Sierra Ancha, Arizona	-	$80-400X10^3$	-	-	-

Sediment layer 2

The lower boundary of sediment layer 2 is defined by magnetic peak B, dated to ca. 800 bp. The upper boundary is the base of magnetic peak A, dated to AD 1951. Major variations in sediment stratigraphy occur within this layer, viz: the paramagnetic iron and manganese layers, magnetic peaks 1 and B, the latter associated in the southern margin of the lake basin with lithostratigraphic evidence of lake level fluctuations. In the central sector of the basin, which experienced the highest rates of sediment accumulation during this period, there is a layer of ferrimagnetic material (magnetic peak 2), interpreted as fine-grained multi-domain and/or stable single domain magnetite. Possible causes of some of these features are discussed in section 9.1 (above).

Around 2 500 tonnes of sediment (500 tonnes of organic matter and 2 000 tonnes of ash) were accumulated within the lake basin during this period, representing an annual rate of sediment yield of 126 kg ha^{-1} (99 kg of ash and 27 kg of organic matter), a value ca. 3.5 times greater than the average for the preceding 9 600 years of Flandrian time. Although as has been suggested (Chapter 6, section 6.5) it is uncertain what proportion of sediment layer 1 is of allochthonous origin, in view of the current very low level of biological productivity of Llyn Goddionduon, together with the results of the diatom analyses (Appendix F) which indicate that this condition is likely to have prevailed at least throughout the period post-dating the deposition of magnetic peak B, it is probable that the data genuinely reflect a large increase in the rate of sediment yield.

Because of the nature of the available pre-20th century land-use history (Chapter 8, section 8.5) interpretation of the increase has to be made with reference to environmental change on a regional scale. As has been suggested, in view of the pollen analytical

evidence from core 60/-40, conversion of the Goddionduon watershed from forest to moorland and blanket bog must have begun prior to 800 bp. Unfortunately the rate and timing of this conversion cannot be inferred from the data available; however, it would have been of major significance in influencing the rates of sediment yield from the watershed. Initial removal of forest vegetation greatly accelerates the erosion of particulate material by increasing the likelihood of surface runoff and by increasing soil erodibility (sensu Cooke and Doornkamp, 1973), although sediment yields are likely to decline subsequently with the eventual stabilisation of the land surface (cf. Davis, 1976; Pennington et al., 1976).

The pollen data from core 0/310 (Chapter 8, section 8.3) indicate the occurrence of a series of episodes of increasingly intensive (largely pastoral) land-use during the period of deposition of sediment layer 2. These are tentatively correlated with aspects of the regional environmental history: clearances by the Cistercians for sheep grazing from the end of the 12th Century (episodes I4 and I3); clearances associated with the expansion of the cattle industry at the end of the 15th Century (episode I2) and the major clearance from the late 17th to the late 18th centuries which was associated with the rapid growth of the regional sheep population (episode I1). During the latter episode the pollen data indicate an almost completely deforested landscape and the representation of pastoral indicators is very high. The degree to which these phases are representative of the nature and intensity of land-use specifically within the Goddionduon watershed is uncertain; however, there is possible evidence of an increase in soil and peat erosion in core 60/-40 concurrent with episode I1, and which is ascribed to burning and/or overgrazing.

It is widely known that Forestry Commission ground preparation may increase the rate of sediment yield in watersheds (e.g. Newson,

1980; Robinson and Blyth, 1982). No attempt has been made to determine by field survey the present volume of the drainage ditches which were dug in the 1920's (Chapter 2, section 2.4); however, the total ditch length is estimated to be around 600 m, and assuming an average ditch depth and width of 0.5 x 0.5 m, a soil dry weight/wet volume ratio of 1.3 g cm^{-3}, and assuming that all of the ditch material has reached the lake basin then the contribution to sediment layer 2 amounts to around 200 tonnes, or 8%.

The available evidence suggests that the data for layer 2 may be considered to represent the sediment yield from moorland subjected to grazing pressure of varying intensity and possibly also to periodic burning. Comparison with data for deforested watersheds which have not been subjected to major soil disturbance - e.g. Hubbard Brook watershed 2, the North Esk and Hopes reservoir sites, the Hodge Beck, Maesnant and Coalburn watersheds - indicates a rough agreement. However, specific circumstances within individual watersheds prevent meaningful comparisons: for example, the North Esk and Hopes reservoir sites are subject to widespread active gully erosion, but local sediment deposition results in a relatively low ratio of sediment yield to total sediment production (Ledger et al., 1974). Similarly, the very high sediment yield for the Hodge Beck watershed is attributable to the occurrence of large areas of bare ground (Imeson, 1974).

Sediment layer 3

In section 9.1 (above) it is argued that evidence favours the 1951 Goddionduon forest fire as the predominant source of the ferrimagnetic material which represents magnetic peak A. With this assumption, and allowing for the uncertainty in the estimation of the volume of sediment layer 3, then around 171-212 tonnes of sediment

(52-65 tonnes of organic matter and 119-147 tonnes of ash) were accumulated within the lake basin during 1951-1977, representing an annual rate of sediment yield of 263-326 kg ha^{-1} (80-100 kg of organic matter and 183-226 kg of ash). In terms of total sediment yield (ash plus organic matter) these values are around 2 to 2.5 times greater than that for sediment layer 2 and around 7 to 9 times greater than that for sediment layer 1.

Assuming that layer 3 is predominantly the product of soil erosion effected by the 1951 forest fire (although some contribution from road construction in 1960-61 seems likely) then it is misleading to express the data as average annual sediment yield per unit area of the total terrestrial part of the watershed for the period 1951-1977, since firstly the fire affected only a relatively small fraction of the watershed (estimated at around 1 ha on the basis of the size of the reafforested area) and secondly the ^{137}Cs results for core 50/-43 indicate negligible sediment accumulation (at least at this coring site) since the mid-1960's.

The effects of major forest fires in terms of the destruction of soil organic matter and soil structure, increasing surface runoff and consequently accelerating the rate of soil erosion is well known (e.g. Ahlgren and Ahlgren, 1960; Dyrness, 1967; Wright, 1976). In the adjacent LlynBychan watershed the major forest fire of 1976 resulted in accelerated sheet and rill erosion, and consequently to the rapid transfer of soil (identified by the presence of large concentrations of secondary ferrimagnetic materials) to the lake basin (Rummery, 1981). In the case of the Goddionduon fire, the estimated total mass of sediment layer 3 (171-212 tonnes) seems large in relation to the possible size of the burnt area. However, slopes within this area are steep (upto 20-30°) and Dyrness (op. cit.) cites erosion losses of 80-400 tonnes ha^{-1} during a one-year period following a fire in a pine forest on steep slopes in Arizona (see Table 9.1).

The evidence from core 50/-43 implying a low rate of sediment yield for the most recent period of lake history is compatible with the known reafforestation of the burnt area during 1960-61 and eventual reattainment of a protective crown cover. The high percentage of the watershed area currently occupied by Forestry Commission plantations might be expected to result in rates of sediment yield comparable with those which obtained during the deposition of sediment layer 1.

Although the sediment yield data for layer 3 are markedly higher than those for layers 1 and 2, reference to Table 9.1 shows that the rates of soil loss are low compared with those for other watersheds which have been subjected to major disturbances involving disruption of the soil surface, such as logging and road construction at Needle Branch and construction in Baltimore. As is suggested, this is a function of the areal and temporal standardisation of the data for layer 3 and localised erosion rates during relatively short periods may have been much higher.

9.3 The pattern of sediment accumulation

9.3.1 Introduction

An increasing number of studies using lake sediments to reconstruct the ecological history of lake watersheds has attempted to aid palaeoecological interpretation by expressing sedimentary parameters such as total sediment, microfossils, chemical elements or organic matter in terms of rates of annual accumulation (e.g. Digerfeldt, 1972; Battarbee, 1978a). Frequently such attempts are based on analyses of one or a small number of sediment cores, usually obtained from the deepest part of a lake basin, and the extent to which the records are representative of the sedimentary record contained within the whole of the basin has tended to be assumed rather than tested.

Studies which for example attempt to reconstruct the history of changing rates of watershed sediment yield from the record of changes in the rate of sediment accumulation at a single coring site (e.g. Edwards and Rowntree, 1980) require the assumption of a constant relationship over time between the rate of sediment influx to the whole lake basin and the accumulation rate at that site (cf. Davis et al., 1973). If this relationship changes, then the record of sediment accumulation is likely to provide a misleading record of changes in the rate of sediment yield. Awareness of sedimentary processes which may affect this relationship are therefore of great importance.

There is a substantial literature documenting the importance of the process of 'sediment focussing' in small lakes with relatively extensive littoral areas and more limited areas of deep water (e.g. Davis, 1973; Davis and Brubaker, 1973; Likens and Davis, 1975; Davis, 1976; Manny et al., 1978; Huttunen et al., 1978). Sediment focussing may arise through the resuspension (by turbulence induced

by wind stress) of sediment in shallow water followed by its redistribution and redeposition throughout the lake basin. Deep water areas (relatively less affected by turbulence) may not exhibit the same degree of sediment resuspension and consequently can exhibit rates of accumulation several times greater than those in the littoral areas of the same basin. Likens and Davis (op. cit.) note that in lakes subject to sediment focussing, changes in basin morphometry effected by the process of sediment infilling will produce changes in the accumulation rate at individual sites within the lake basin which are unrelated to changes in the rate of sediment influx to the whole basin. Lehman (1975) gives a series of mathematical formulae which attempt to predict the effect of the sediment focussing mechanism in order to transform changes in sediment accumulation rates recorded in a single core from the deepest part of a series of lake basins of idealised morphometry to estimates of rates of sediment influx to the whole basin.

9.3.2 Discussion

In the context of the work cited above, the patterns of sediment accumulation within the Goddionduon lake basin revealed by the results of the core correlations (Chapter 4) and sediment isopach contour mapping (Chapter 6) are of considerable interest and relevance. The relevant findings of these Chapters are: (i) the assymetrical pattern of basin infilling indicated by the northward movement of the focus of sediment accumulation over the period of time represented by the deposition of sediment layers 1, 2 and 3; (ii) the negligible Flandrian sediment accumulation in the trench; (iii) the variability of rates of sediment accumulation over short distances (20 m or less) indicated by pronounced differences in the vertical extent of magnetic features between adjacent cores.

Precise reasons for the observed patterns are unknown. Interpretation is hindered by the fact that most studies of lake hydrodynamics and of sedimentary processes within lakes are overwhelmingly concerned with very large lakes (see reviews in Csanady, 1978; Sly 1978 and Rea et al., 1981; see also Graf and Mortimer, 1979), in which fetch and water depth are sufficiently great so as to generate features such as circulation cells and internal seiches which do not occur in small lakes (Hutchinson, 1957).

Presumably the observed patterns of sediment accumulation in Goddionduon are the result of a complex integration of the effects of morphometry and wind stress, the latter affected by the topography of the watershed and the surrounding area (cf. Hansen, 1979). The assymetrical pattern of infilling may be the result of persistently greater turbulence in the northern part of the lake basin (and the consequent inhibition of sediment accumulation) through exposure to a prevailing wind direction (west to south-west in the area). On this basis the northward movement over time of the focus of sediment accumulation would reflect the progressive shallowing of the southernmost areas of the basin and a resulting reduction in rates of accumulation in these areas through increasing sediment resuspension. However, the configuration of sediment layer 3 does not entirely accord with this schema, since the occurrence of the greatest thickness of magnetic peak A sediment within and around the southwestern end of the trench represents a very abrupt northward shift of the focus of sediment accumulation. That this abrupt shift is not merely an artifact of the large difference in the accumulation times of sediment layers 2 and 3 (ca. 800 versus 26 years) is suggested by the fact that in many of the trench cores, peak A sediment appears to unconformably overlie much older sediment, indicating that accumulation in the trench area is a very recent phenomenon. The reasons for this are

unknown. One, or a combination of the following factors may be possible: the fact that layer 3 is likely to have originated as a rapid influx of sediment from a relatively small source area; a change in the pattern of wind stress as a result of recent afforestation (cf. Hansen, op. cit.); the possibility that layer 3 does not constitute permanently settled sediment.

The paucity of Flandrian sediment accumulation in the trench is at variance with the mechanism of sediment focussing described above. Again, the reasons for this are unknown but may in some way reflect prevailing patterns of water turbulence and current directions. The results demonstrate that the occurrence of sediment focussing in lakes, perhaps especially in relatively highly wind-stressed lakes, cannot be assumed and cast doubt on the widespread applicability of attempts to predict its effects based solely on the presumed influence of lake basin morphometry (cf. Lehman, op. cit.). The presence only of Late-glacial and early Flandrian sediment over the majority of the area of the trench may be a function of the relatively high minerogenic content (and therefore high density) of these sediments, the accumulation of more organic (less dense) sediments being prevented by turbulence and/or current action.

Pronounced variations in sediment accumulation rates over short disctances have been observed in several lakes. In the case of Lough Neagh, Northern Ireland, variations in sediment accumulation rates within and between more or less adjacent 1 m-long cores have been attributed to post-depositional movement of sediment rather than to primary sediment deposition into preferred areas (Battarbee, 1978b). In Blelham tarn, a small lake in the English Lake District, similar variations in 1 m cores have been attributed more specifically to post-depositional flowing of sediment downslope (Pennington et al., 1976); in this case the coring sites were located within the 8 m

depth contour and were considered to be sufficiently deep so as to obviate the likelihood of sediment resuspension by turbulence. The shallowness of the Goddiconduon lake basin impiles that sediment resuspension cannot be excluded as a possible cause of the variability of sediment accumulation rates over short distances observed in the 1-2 m-long sediment cores.

CHAPTER 10 SUMMARY AND CONCLUSIONS

10.1 Summary of the results

i) Magnetic measurements and lithostratigraphical description have been used to establish the depths below the sediment surface of a series of horizons within a set of cores sampled from a closely-meshed grid network covering the whole of a small lake basin. The horizons and their characteristics are as follows:

a) The Loch Lomond stadial clay/early Flandrian clay-mud contact, corresponding to the beginning of the Post-glacial period.

b) Magnetic peak B. Detailed magnetic measurements have identified this feature as a high concentration of paramagnetic meaterial. Chemical analyses indicate the presence of concentrations of Fe and Mn sufficiently high to account entirely for the measured susceptibility of this horizon. Peak B is characterised lithostratigraphically by variously-coloured broad laminations of increased fine minerogenic content. In the southern margin of the lake basin it is flanked by peaty and coarse detrital horizons, indicative of lake level fluctuations.

c) Magnetic peak A. Detailed magnetic measurements indicate the presence of ferrimagnetic material. The feature is characterised lithostratigraphically by a black colouration.

Magnetic measurements have enabled the definition of two additional horizons within limited areas of the lake basin:

a) Magnetic peak 2. Detailed magnetic measurements indicate the presence of fine-grained multidomain and/or single domain ferrimagnetic material.

b) Magnetic peak 1. Chemical analyses suggest that this consists predominantly of paramagnetic material.

Inter-core comparison of the thickness of magnetic peaks, and

the depths below the mud surface at which they occur, indicate the occurrence of marked variations in sediment accumulation rates over short distances (tens of metres). Detailed core sampling in the deepest area of the basin shows that there has been virtually no Post-glacial sediment accumulation there.

ii) Radiometric dating has been used to estimate the ages of the correlated horizons.

a) A ^{14}C date of 10 400 bp is available for the Loch Lomond stadial clay/early Flandrian clay-mud contact beneath the Goddionduon peat bog (Ince, 1980).

b) An age of ca. 800 bp for magnetic peak B was obtained by comparison of ^{14}C dates from various sources: from the peaty/coarse detrital layers associated with peak B in the southern margin of the lake basin; from the Goddionduon peat bog by the dating of a pollen biostratigraphical horizon assumed to reflect a lowered lake level; and from direct dating of the sediments in the main lake basin. In the latter case, problems were encountered in that some of the ^{14}C dates obtained appear to be affected by old carbon error, possibly as a result of influxes of soil organic matter or through the reworking of marginal sediment.

c) ^{137}Cs dating of magnetic peak A suggests that it post-dates 1954. The feature is ascribed to an influx of secondary ferrimagnetic minerals formed during a forest fire in 1951.

iii) Contour maps were obtained of the thicknesses of the three sediment layers defined by the correlated horizons. The maps clearly depict: the paucity of sediment accumulation in the 'trench'; a progressive northward movement of the focus of sediment accumulation during the Post-glacial period; and an abrupt northward shift in the focus of accumulation represented by the uppermost sediment layer (layer 3).

iv) The contour maps are used to estimate the volumes of sediment represented by the three sediment layers. Estimates of sediment wet density, percentage water content and percentage organic matter content are used to transform the sediment volumes to estimates of the dry masses of the mineral and organic fractions. These data are then converted to estimates of annual rates of total sediment influx and sediment yield per unit area of the terrestrial part of the watershed using the chronology outlined in (ii).

v) Magnetic measurements of potential lake sediment sources (topsoil, subsoil, ditch bedload and Late-glacial lake sediments) indicate that concentrations of paramagnetic material comparable with those in the late Flandrian lake sediments do not occur within these materials. Therefore, it is suggested that the paramagnetic layers result from influxes of Fe and Mn in solution, possible during periods of lowered lake level. Potential sediment source material with magnetic properties comparable with those of magnetic peaks 2 and A only occur in the Bs horizons of podzolic soil; however, the values of SIRM/susceptibility of the latter are considerably lower. Expression of the magnetic properties of the source materials on a particle size-specific basis does not significantly improve their correspondence with those of the magnetic peaks in the lake sediments. This reinforces the suggested association between magnetic peak A and the 1951 forest fire.

vi) Pollen analytical studies indicate that woodland clearance and conversion of the Goddionduon watershed to moorland must have begun some time during the latter part of the deposition of sediment layer 1. However, comparison of the sediment yield data for layer 1 with those for undisturbed woodland ecosystems obtained by continuous monitoring indicates some accordance. The pollen data suggest that the watershed was occupied by moorland and blanket bog during the deposition

of layer 2; there is palynological evidence for an increase in the rate of soil erosion between ca. AD 1600 and 1700. The estimated rate of sediment yield for layer 2 is roughly comparable with estimates of current rates from watersheds under similar forms of land-use. The estimated rate for layer 3 is substantially lower than those recorded for watersheds and plots which have been subjected to major soil disturbance. This may result from the likelihood that layer 3 represents a relatively short period of accelerated soil erosion within a relatively small fraction of the watershed.

10.2 Significance of the results for studies of total sediment influx and yield

The study has demonstrated the potential of the use of lake basins in conjunction with the rapid methods of core correlation provided by magnetic measurements for the quantification of past and present rates of sediment flux within a lake watershed. Sampling and the establishment of the basis for a whole core susceptibility-based correlation scheme within a suite of cores around one order of magnitude larger than any that has been previously employed in comparable studies using conventional techniques was performed in two weeks. Subsequently, single-sample magnetic measurements of a relatively small number of cores were able to confirm the whole core susceptibility correlation scheme. Also, the variations in the magnetic properties of the late Flandrian lake sediments have been shown to be significantly more reflective of ecological change within the watershed than most of the other sedimentary parameters analysed, such as the pollen stratigraphy. However, the study has illustrated several problems, for example involving the sediment datings, the relatively small number of correlatable features in the magnetic record and the rather complicated pattern of sediment accumulation, which aid the definition of a list of criteria for the selection of the type of

lake watershed in which this kind of study is likely to be most successful:

i) The lake basin should have a regular morphometry with a hemiellipsoidal cross-section and be sufficiently deep and/or sheltered to reduce wind stress. These criteria could be expected to minimise the resuspension and reworking of marginal sediment, sediment focussing effects and uneven sediment distribution. The more regular the sediment distribution, the fewer the number of cores required to accurately estimate total sediment volumes.

ii) The lake basin should have no extensive deltaic deposits.

iii) The lake basin should not be prone to lake level fluctuations; these are likely to cause sediment reworking and consequent problems in sediment dating and interpretation of the biostratigraphical records.

iv) In order to minimise 'old carbon error', if radiocarbon dating is employed there should be no accumulations of organic matter within the watershed.

v) In order to aid the interpretation of estimated rates of sediment yield the lake watershed should have a documented land-use history.

vi) There should be no marginal hydroseral development, which is likely to trap sediment.

vii) Regular winter freezing would facilitate accurate core location.

viii) The lake sediments should be dominated by allochthonous influxes, unless quantification of aspects of lake biological productivity is a specific aim of the study. Therefore, marl lakes and highly productive lakes should be avoided.

ix) Frequent fluctuations in magnetic concentration within the sediment column enable more highly resolved whole core susceptibility records, and therefore potentially more detailed estimates of changing

sediment influx, to be obtained. Lakes which exhibit this tend to have watersheds with substrates containing relatively high concentrations of primary ferrimagnetic minerals, a well-developed relief and inflowing streams: for example, Lochs Frisa and Lomond, Scotland (Dearing, 1979; Thompson and Morton, 1979) and Lough Neagh, Northern Ireland (Thompson et al., 1975). In such lakes, increases in the magnetic concentration of the sediments appear to be effected by influxes of the relatively coarser particle sizes within which the bulk of the ferrimagnetic grains tend to occur (Chapter 7, section 7.2), and the combination of relatively steep slopes and streams provides the relatively high energy conditions required to deposit layers of coarser particles within the lake basin. Relative decreases and increases in sediment particle size (and therefore magnetic concentration) are brought about by variations in the level of stream activity (see Dearing, 1979 and Dearing et al., in press). However, the entry of large streams is likely to result in major deltaic deposition and therefore uneven sediment distribution.

Finally, lakes receiving relatively large influxes of ferrimagnetic minerals are also likely to be more suitable for palaeomagnetic dating (see Oldfield, 1981),

Very few lake basins are likely to satisfy all or even most of the criteria listed above; however, that the approach may be applied successfully even in less-than-ideal lake basins is demonstrated by the results of the present study.

10.3 Significance of the results for influx studies employing small numbers of cores

Besides demonstrating that the mechanism of sediment focussing in lakes (Lehman, 1975) cannot automatically be assumed, the patterns of sediment accumulation in Goddionduon show that no single coring site could be used to obtain an accurate record of changing material

flux. Since relatively few detailed studies of the pattern of sediment accumulation within lakes have been performed, it is uncertain to what extent the results obtained from Goddionduon may be representative of other lake basins. However, in terms of size and topographic situation the Goddionduon lake watershed is not untypical of those commonly employed for palaeoecological studies; and it is suggested that the conclusions derived from influx studies which employ one or a small number of cores and in which the lake basin sediment stratigraphy has not been fully investigated, should be treated with caution. The now quite widely-demonstrated value of mineral magnetic measurements for core correlation obviates some of the problems involved in employing larger numbers of cores for influx studies.

10.4 Significance of the results for the interpretation of the mineral magnetic properties of lake sediments

Most interpretations of the causes of changes in the magnetic concentration of lake sediments assume variations in the accumulation rate of strongly magnetic minerals derived from soils and substrates or from the atmosphere to be responsible (Chapter 7, section 7.2). In this context, the significant contribution of paramagnetic Fe and Mn to the Goddionduon sediment susceptibility record is of some interest, particularly since the high concentrations of these elements are assumed to result from their entry in solution. However, significant paramagnetic contributions to lake sediment susceptibility are only likely to occur in lake watersheds with substrates poor in ferrimagnetic minerals.

APPENDIX A DRAINPIPE CORER

Figure A.1 shows the corer used to obtain the 2 m-long cores obtained from the central sector of the Goddionduon lake basin during July, 1979 (see Chapter 3, section 3.2). The 2.5 m-long drainpipe is used to drive the core tube over the fixed piston into the sediment. The design of the piston is based on Rowley and Dahl (1956).

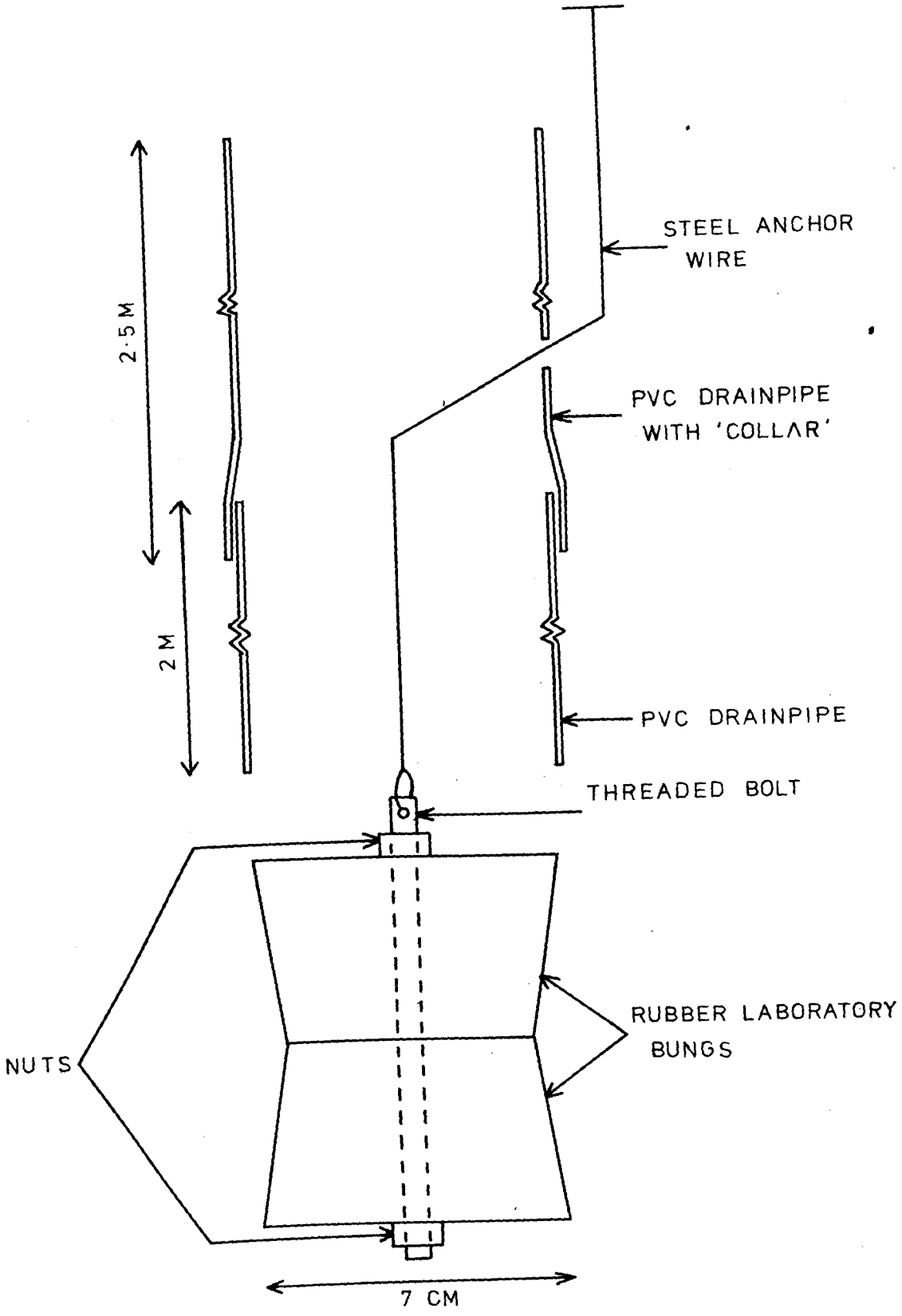

Figure A.1 Drainpipe corer

APPENDIX B MEASUREMENTS OF WET DENSITY, PERCENTAGE WATER CONTENT AND PERCENTAGE WEIGHT LOSS ON IGNITION

Figures B.1-B.2 show plots of χ, wet density, percentage water content and percentage weight loss on ignition for cores 60/-20 and 60/60L. These data are used in Chapter 6 (section 6.5) to estimate the dry masses of total sediment, inorganic sediment and organic sediment for sediment layers 1, 2 and 3.

GODD. CORE 60/-20

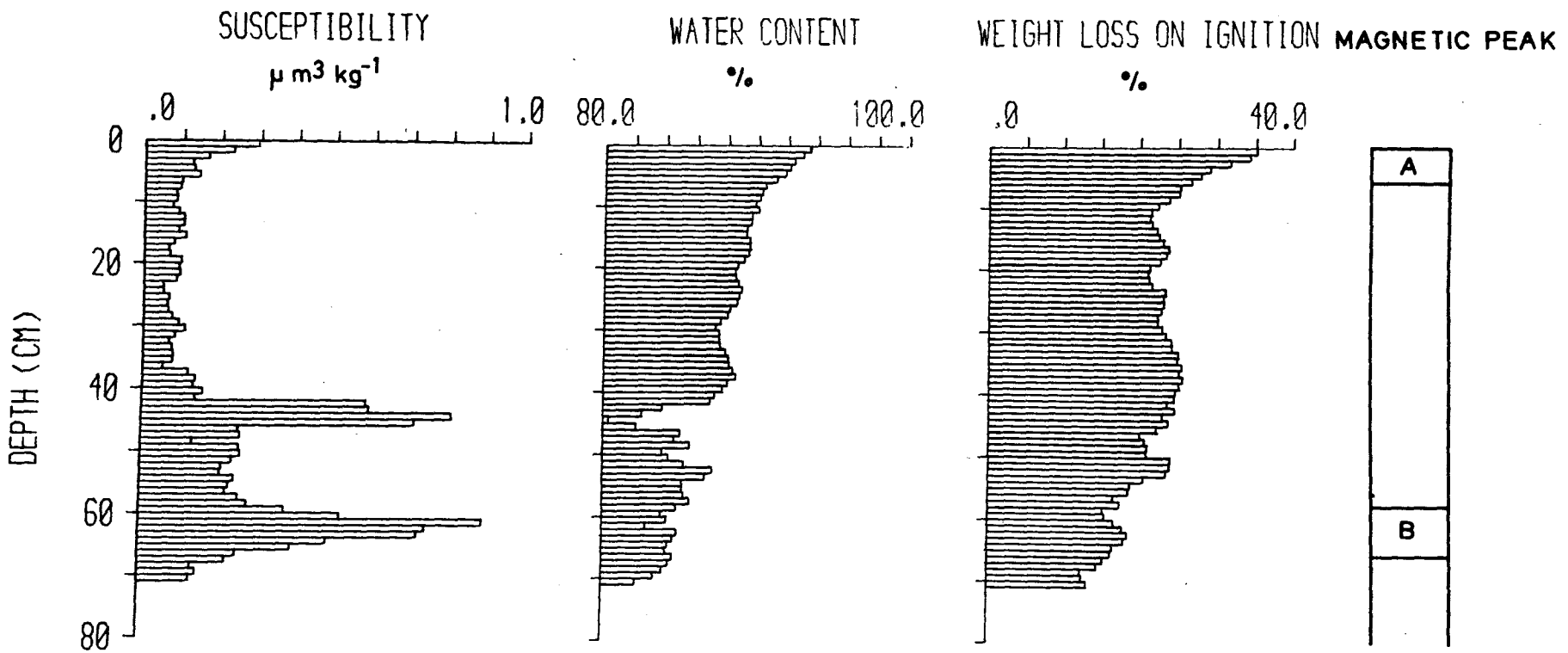

Figure B.1 Percentage water content and percentage weight loss on ignition for core 60/-20

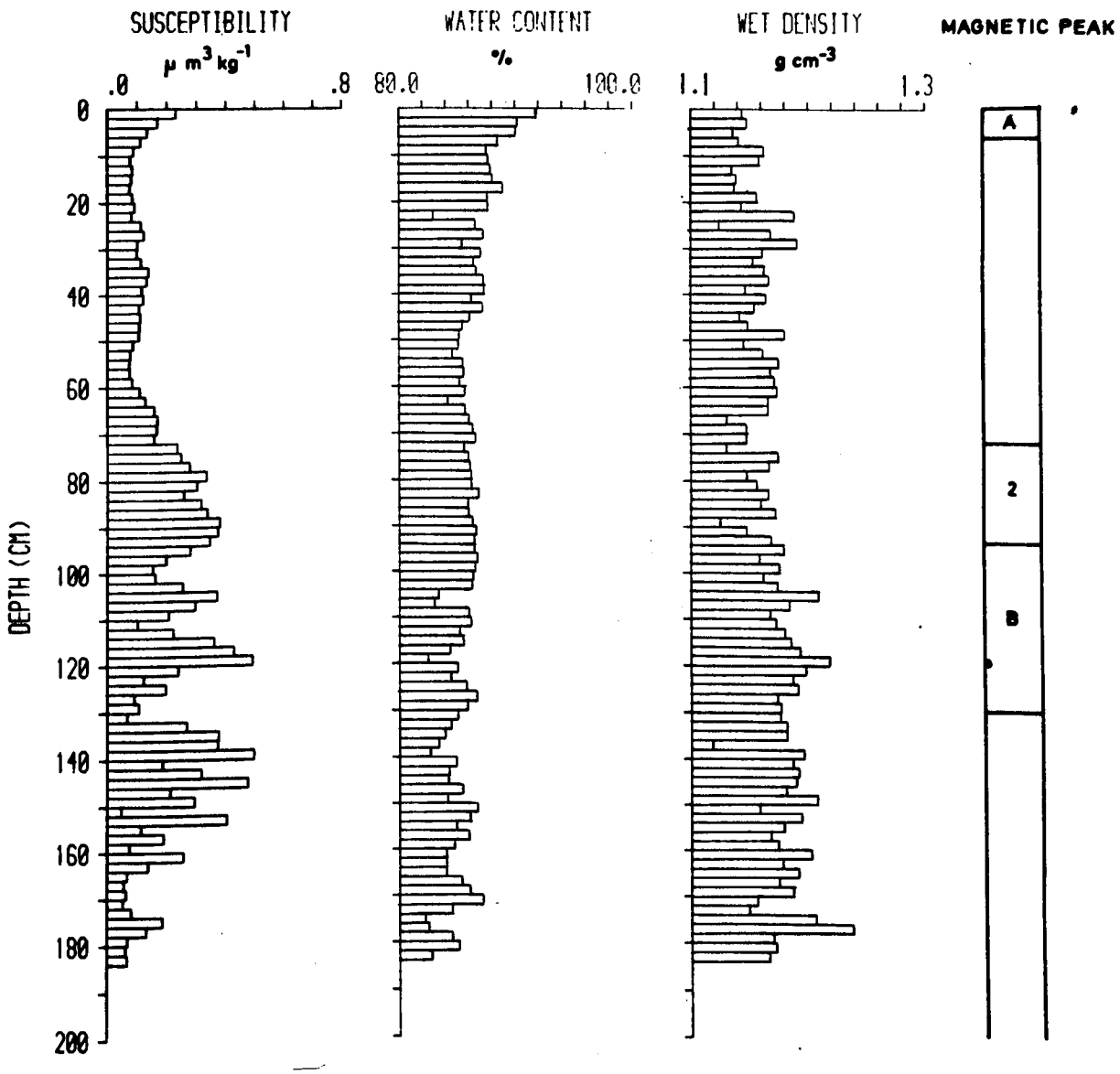

Figure B.2 Wet density and percentage water content for core 60/60L

APPENDIX C POLLEN DATA

Table C.1 shows the results of the pollen analyses described in Chapter 4 (section 4.3). With the exception of that from core 86/-79, all of the counts were performed on unprepared samples.

Taxon	Core/sample	140/-100 52-54 cm	140/-100 65-70 cm	60/-80 58 cm	60/-80 94.5 cm	86/-79 30-31 cm	55/-55 116-117 cm	48/-48 116-END	50/-43 20-22 cm	50/-43 58-60 cm	41/-41 92-94 cm	34/-34 116-118 cm
Picea						0.10						
Pinus sylvestris		21.99	1.60			0.70	21.19	51.61	4.46	32.56	2.17	2.50
Betula		12.06	42.40		1.96	50.15	21.19	9.68	9.55	23.26	14.13	2.50
Tilia									0.64			
Fraxinus				1.03							2.17	
Quercus		11.35		5.15	5.88		8.47	10.75	24.84	22.48	14.13	10.00
Ulmus		3.55			1.96		4.24	3.23	7.01	1.55	1.09	
Alnus		15.60		5.15	11.76				13.38	0.78	9.78	5.00
Carpinus											1.09	
Ilex				1.03								
Juniperus			5.60				1.30					
Salix			4.00	1.03		0.90			0.64			
Corylus avellana		20.57		7.22	3.92			9.68				5.00
Myrica gale		0.71	0.80	9.28	9.80							
Corylus/Myrica				1.03					24.20	1.55	19.57	
Betula/Corylus/ Myrica		0.71		1.03	5.88		29.66	15.05	4.46	10.85	9.78	15.00
Calluna vulgaris			1.60	12.37	3.92		0.85			0.78	3.26	
Empetrum			0.80			0.30						
Ericales undiff.			2.40	10.31	7.84	0.40			1.27	0.78	1.09	2.50
Gramineae		2.13	12.00	15.46	3.92				4.46	0.78	7.61	22.50
Cyperaceae				9.28	3.92					0.78	6.52	10.00
Artemisia											1.09	
Rumex acetosa						0.70						2.50
Rumex acetosella				1.03								
Rumex crispus-type						0.30						

Table C.1 Pollen data

Taxon \ Core/Sample	140/-100 52-54 cm	140/-100 65-70 cm	60/-80 58 cm	60/-80 94.5 cm	86/-79 30-31 cm	55/-55 116-117 cm	48/-48 116-END	50/-43 20-22 cm	50/-43 58-60 cm	41/-41 92-94 cm	34/-34 116-118 cm
Rosaceae undiff.			1.03		0.10			0.64	0.78		2.50
Potentilla-type			1.03								
Filipendula		1.60			1.20						
Succisa pratensis				3.92				0.64			2.50
Urtica					0.60				0.78		
Cruciferae			1.03	1.96							
Plantago lanceolata			1.03								
Ranunculus acris-type					0.10						
Ranunculaceae undiff.			1.03								
Thalictrum					0.20						
Osmunda regalis					0.10	0.85					
Polypodium	1.42			1.96				1.27			2.50
Pteridium								1.91			7.50
Thelypteris dryopteris	0.71										
Thelypteris phegopteris					0.20						
Dryopteris filix-mas-type		9.60	2.06					0.64	0.78		
Ophioglossum					0.10						
Polypodiaceae undiff.		15.20	1.03	5.88		0.85			1.55	1.09	7.50
Lycopodium			1.02								
Hydrcotyle vulgaris									0.78		
Typha latifolia-type		0.79			0.10						
Sparganium-type											
Littorella uniflora						0.10					
Isoetes	7.24	1.57	38.99	17.74				5.42	14.00		
Equisetum											4.76
Deteriorated	9.22	2.40	11.34	25.49	2.50						
Pollen sum	141	125	97	51	999	118	93	157	129	92	40
Sphagnum				5.56	0.10			1.26		5.15	14.89

Table C.1 continued

APPENDIX D SEDIMENT COLOURS

Table D.1 shows the recorded colours of 22 unextruded minicores.

Core/Sample

50/-120		48 - 61	Mottled yellow-brown mud
0 - 10	Black mud	61 - 64	Light-grey mud
10 - 46	Brown mud	64 - 76	Brown mud
46 - 57	Mottled blue-grey mud	60/- 40	
57 - 61	Light-brown mud	0 - 29	Black mud
61 - 72	Brown mud	29 - 56	Brown mud
72 - 83	Light-brown mud	56 - 72	Light-brown mud
83 -122	Brown mud	72 - 96	Brown mud
60/-120		34/- 34	
0 - 14	Dark grey mud	0 - 12	Black mud
60/-100		12 - 88	Brown mud
0 - 12	Black mud	88 -123	Grey-brown mud
100/- 90		40/ 0	
0 - 9	Black mud	0 - 10	Black mud
9 - 12	Brown mud	10 - 60	Brown mud
12 - 51	Grey clay	60 - 66	Mottled yellow-brown mud
51 - 76	Blue clay	66 -121	Mottled red-brown mud
40/- 80		60/ 0	
0 - 2	Light-brown mud	0 - 1	Black mud
2 - 26	Mottled red mud	1 - 41	Brown mud
26 - 30	Red-brown mud	41 - 80	Light-brown mud
30 - 40	Brown mud	80 -105	Brown mud
40 - 90	Grey brown	80/ 0	
69/- 69		0 - 2	Black mud
0 - 4	Black mud	2 - 36	Brown mud
4 - 59	Brown mud	36 - 79	Light-brown mud
59 -114	Grey brown	79 -101	Brown mud
65/- 65		100/ 0	
0 - 10	Black mud	0 - 4	Black mud
10 - 70	Brown mud	4 - 10	Brown mud
70 - 90	Grey-brown mud	10 - 13	Black mud
90 -111	Light-grey mud	13 - 24	Blue clay
70/- 60		120/ 0	
0 - 16	Black mud	0 - 2	Black mud
16 - 60	Brown mud	2 - 24	Brown mud
60 -107	Light-brown mud	24 - 38	Light-grey clay
55/- 55		38 - 43	Red-grey clay

Core/Sample	
0 - 12	Black mud
12 - 60	Brown mud
60 -114	Grey-brown mud
60/- 41	
0 - 26	Black mud
26 - 48	Brown mud
16 - 25	Mottled red mud
25 - 34	Brown mud
34 - 41	Light-brown mud
41 - 70	Brown mud
70 - 77	Dark-brown mud
80/ 100	
0 - 20	Brown mud
20 - 56	Mottled yellow-grey -brown mud
56 - 88	Dark-brown mud
20/ 120	
0 - 10	Brown mud
10 - 25	Mottled yellow-brown mud
25 - 55	Mottled purple-yellow -brown mud
55 - 80	Mottled purple-grey mud
40/ 200	
0 - 39	Brown mud
39 - 56	Mottled red-brown mud
56 - 89	Mottled red-grey-brown mud
89 -105	Brown mud
43 - 57	Grey clay
80/ 60	
0 - 3	Black mud
100/ 60	
0 - 4	Black mud
4 - 16	Brown mud

Table D.1 Recorded colours of 22 unextruded minicores.

APPENDIX E. CONTOURING DATA

Table E.1 shows the data used for the construction of Figures 6.1-6.7. Figures E.1-E.3 show the locations of the data points for each sediment layer.

Core/Site	Depth (cm)	Core/Site	Depth (cm)
Base of sediment layer 3			
40/-120	8	37/-44	11
50/-120	11	44/-44	22
60/-120	11	51/-44	16
115/-115	5	50/-43	10
104/-104	5	50/-42	16
60/-100	8	41/-41	8
110/-100	5	60/-41	18
120/-100	12	80/-40	5
140/-100	8	105/-40	8
97/-97	5	130/-40	8
93/-93	3	37/-37	14
90/-90	8	44/-37	24
100/-90	9	34/-34	5
93/-86	8	30/-30	5
82/-82	8	70/-30	11
50/-80	8	40/-20	24
60/-80	5	60/-20	6
100/-80	5	100/-20	8
110/-80	11	40/0	16
140/-80	5	60/0	8
86/-79	5	80/0	8
65/-72	19	100/0	4
72/-72	5	120/0	5
79/-72	14	40/20	8
50/-70	8	60/20	8
69/-69	5	80/20	11
65/-65	11	50/40	5
72/-65	3	60/40	11
62/-62	8	80/40	5
40/-60	8	50/60	5
50/-60	19	60/60	6
70/-60	16	80/60	3
80/-60	10	100/60	4
90/-60	14	50/80	6
100/-60	8	60/80	8
110/-60	11	80/80	3
120/-60	8	50/90L	4
58/-58	8	40/100	3
65/-58	5	40/200	6
55/-55	11		
44/-51	11	Thickness of sediment layer 2	
51/-51	11	40/-120	0
58/-51	5	50/-120	43
48/-48	11	115/-115	27
47/-47	14	111/-111	30
50/-45	8	100/-108	25
53/-45	14	104/-104	60

Table E.1 Data used for the construction of Figures 6.1-6.7.

Core/Site	Depth (cm)	Core/Site	Depth (cm)
60/-100	31	50/-42	0
110/-100	44	41/-41	0
120/-100	63	60/-41	27
140/-100	0	100/-40	0
97/-97	0	105/-40	22
93/-93	0	130/-40	57
90/-90	0	37/-30	68
100/-90	0	70/-30	67
86/-86	0	40/-20	52
93/-86	0	60/-20	57
82/-82	0	100/-20	0
40/-80	30	130/-20	30
50/-80	57	90/-10	68
70/-80	0	30/0	131
100/-80	38	40/0	86
110/-80	35	50/0	89
120/-80	30	60/0	69
140/-80	46	70/0	110
86/-79	0	80/0	91
65/-72	0	90/0	106
72/-72	0	100/0	0
79/-72	0	110/0	58
50/-70	60	120/0	0
100/-70	33	60/20	93
69/-69	0	80/20	82
58/-65	0	50/40	128
65/-65	0	60/40	129
72/-65	0	70/40	126
62/-62	0	80/40	91
30/-60	10	90/40	107
40/-60	51	60/60L	136
50/-60	0	80/60L	100
80/-60	47	100/60	64
100/-60	41	50/80	11
110/-60	19	60/80	79
58/-58	0	70/80	115
65/-58	0	90/80	103
55/-55	0	50/90L	89
44/-51	0	20/100	16
51/-51	0	40/100	35
58/-51	0	80/100	86
48/-48	0	20/120	22
47/-47	0	40/120	22
53/-45	0	60/120	86
37/-44	75	80/120	22
44/-44	0	20/140	14
51/-44	0	40/140	35
50/-43	0	60/140	76

Table E.1 continued 1/

Core/Site	Depth (cm)	Core/Site	Depth (cm)
30/160	23	50/-60	89
35/160	33	80/-60	15
50/160	68	100/-60	32
60/160	74	110/-60	8
20/180	6	58/-58	65
40/180	62	65/-58	87
10/200	43	55/-55	103
20/200	16	44/-51	88
40/200	40	58/-51	83
45/200	69	48/-48	106
29/205	87	50/-42	78
26/215	91	41/-41	98
14/258	60	100/-40	47
		130/-40	0
Thickness of sediment layer 1		30/0	128
		50/0	219
40/-120	38	70/0	286
50/-120	68	90/0	206
115/-115	54	100/0	9
111/-111	50	110/0	54
100/-108	54	120/0	19
104/-104	24	50/40	197
60/-100	49	70/40	386
110/-100	14	90/40	187
140/-100	77	50/80	279
97/-97	44	70/80	217
93/-93	8	90/80	176
90/-90	6	20/120	58
100/-90	3	40/120	87
93/-86	60	60/120	104
82/-82	3	80/120	105
40/-80	46	20/140	64
70/-80	67	35/160	121
100/-80	0	45/160	374
110/-80	26	60/160	262
86/-79	30	20/180	90
65/-72	22	15/200	178
72/-72	25	25/200	511
79/-72	48	35/200	560
30/-70	83	45/200	183
50/-70	21	10/240	333
100/-70	15	25/240	352
69/-69	109	-5/280	251
58/-65	66	10/280	570
65/-65	84	-10/315	225
62/-62	41	-10/325	350
30/-60	50	-10/335	400
40/-60	32	-10/345	300

Table E.1 continued 2/

Core/Site	Depth (cm)
-10/355	160
-10/365	150
-10/375	125
0/305	425
0/315	475
0/325	580
0/335	500
0/345	552
0/355	545
0/365	425
0/375	250
5/310	590
10/305	450
10/315	400
10/325	175

Observations of impenetrable substrate

8/-120	30/140
20/-120	10/180
119/-118	60/180
108/-108	5/200
20/-100	
40/-100	
80/-100	
100/-100	
86/-86	
20/-80	
130/-80	
80/-78	
76/-76	
20/-60	
110/-40	
115/-40	
120/-40	
140/-40	
27/-26	
120/-20	
140/-20	
20/0	
140/0	
100/20	
40/40	
40/60	
20/80	
40/80	

Table E.1 continued 3/

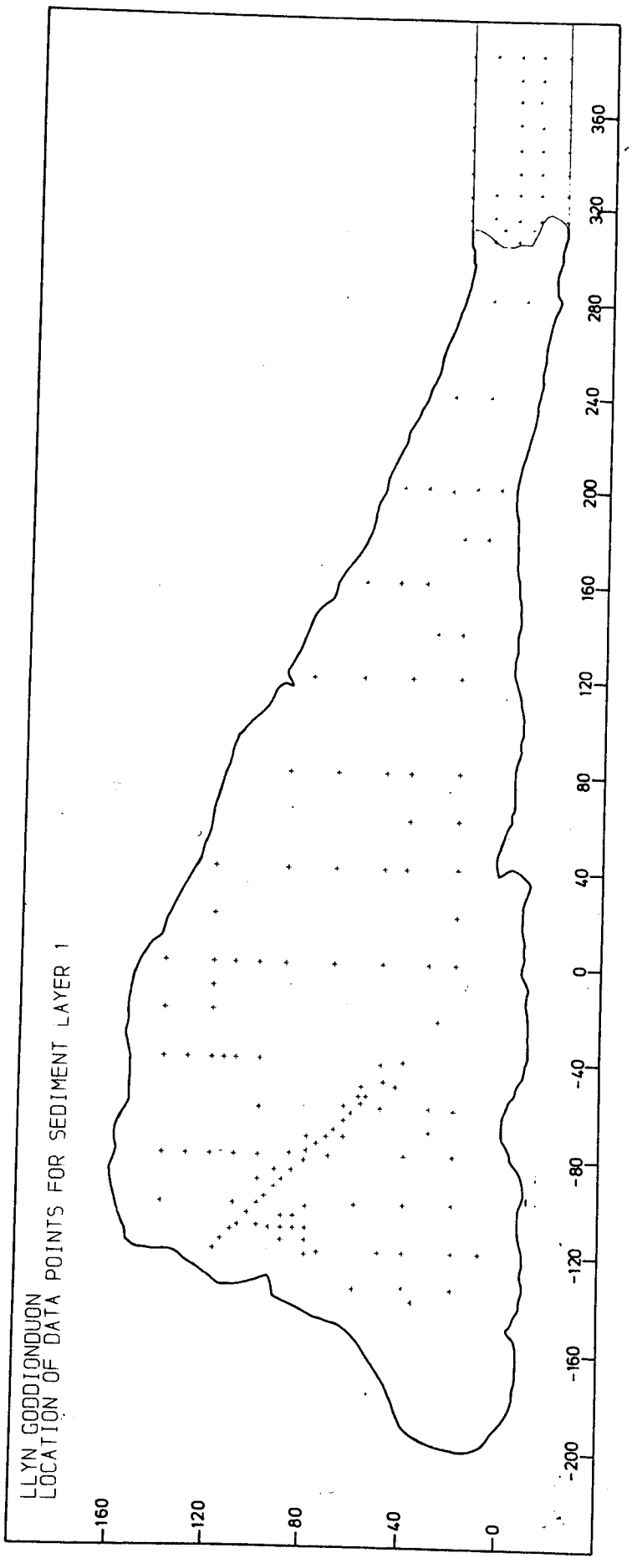

Figure E.1 Location of contouring data points for sediment layer 1

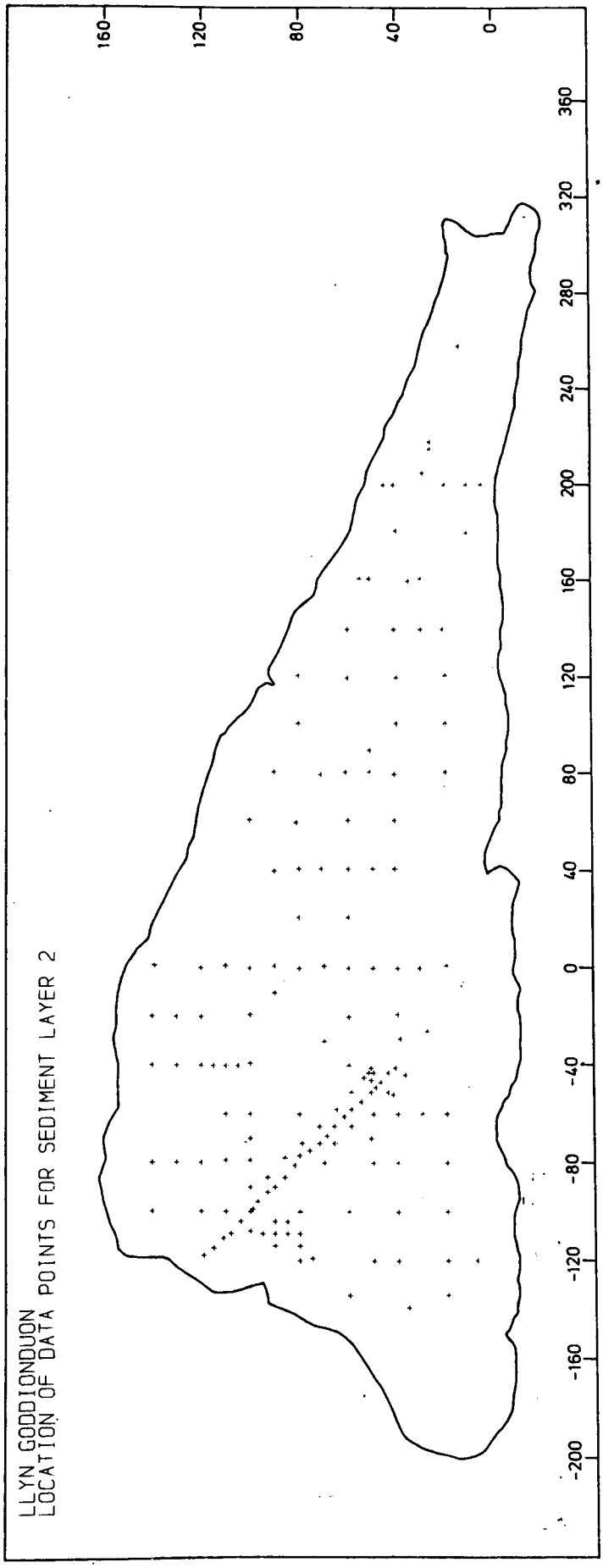

Figure E.2 Location of contouring data points for sediment layer 2

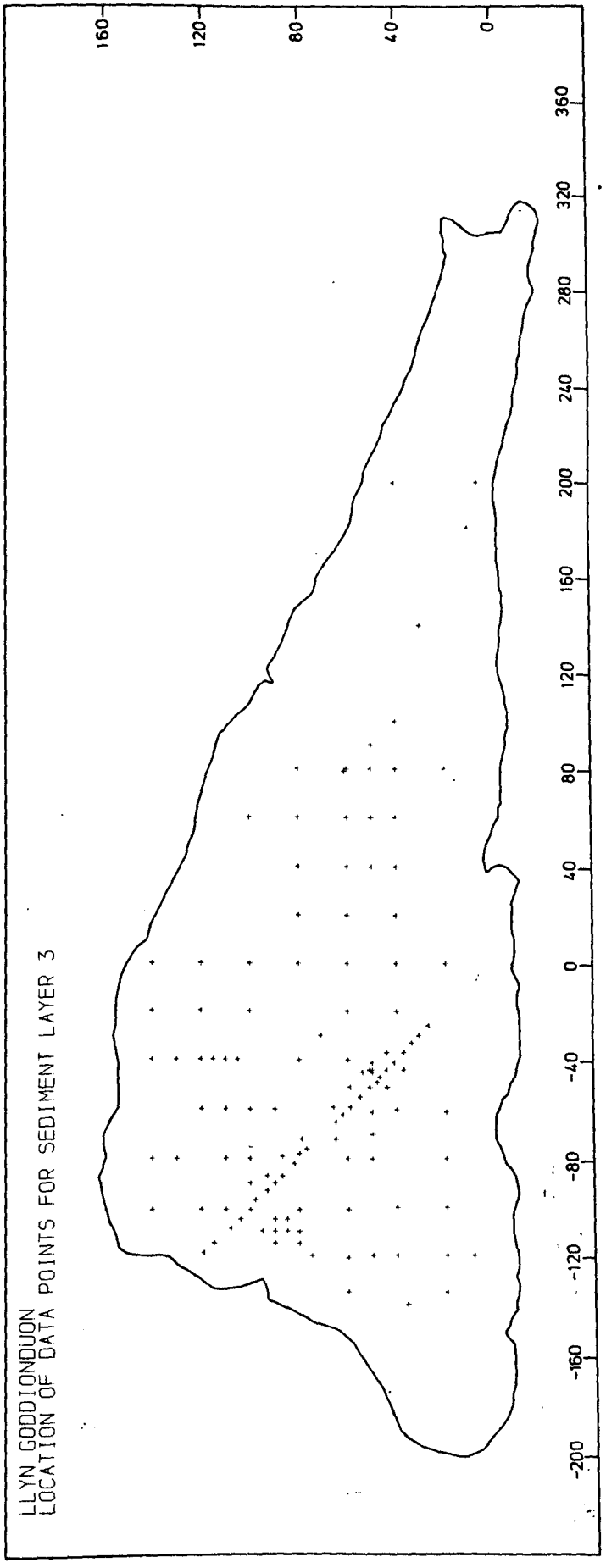

Figure E.3 Location of contouring data points for sediment layer 3

APPENDIX F. DIATOM ANALYSES

Diatom analyses were carried out on three samples from core 40/-20: 4-5 cm (from magnetic peak A), 34-35 cm and 76-77 cm (the latter from magnetic peak B). Since the composition of fossil diatom spectra is diagnostic of lake trophic state and water pH (Digerfeldt, 1972) it was hoped that the analyses would indicate whether or not the deposition of magnetic peak B sediments had been accompanied by any change in limnological conditions. For each sample, between two and three hundred diatoms were counted, and additionally the slides were surveyed for taxa which had not been included in the counts. The results are shown in Table F.1.

The following interpretation is based on R. Nelms (personal communication). Four taxa are present in proportions greater than 10% in any sample: Fragilaria elliptica, F. virescens, F. virescens var oblongella and Achnanthes minutissima. These are all littoral species and are more or less indifferent to water pH and nutrient status. Eleven further taxa were found at frequencies greater than 3% in any sample, and of these Melosira italica, Fragilaria brevistriata, Anomoeoneis vitrea and Cymbella lunata are indifferent to water type; Fragilaria brevistriata var inflata may prefer alkaline water; Eunotia pectinalis var minor, E. veneris, Frustulia rhomboides, F. rhomboides var saxonica and Anomoeoneis serians var brachysira are commonest in acidic waters; and Eunotia monodon is restricted to acidic waters. Of the remaining 58 taxa, which occur at frequencies of less than 3% in all samples, 47 taxa are indifferent to water quality; Amphora ovalis var pediculus, Gomphonema angustatum and G. intricatum tend to prefer alkaline waters; Eunotia robusta, E. praerupta, E. flexuosa, Anomoeoneis serians, Pinnularia microstauron and Stenopterobia intermedia prefer acidic waters; and Eunotia exigua and E. monodon var constricta are restricted to acidic waters. Of all

the taxa recorded, only Cyclotella comta (maximum frequency 2% in sample 76-77 cm) is considered to be planktonic.

The abundance of periphytic forms, and paucity of planktonic forms, suggests that the lake waters have been clear and shallow. Although there are considerable differences in the relative proportions of the taxa between the three samples, there is no suggestion of a change in pH or a noticeable change in trophic level of the lake water. The lake has remained acidic and rather oligotrophic over the period covered by the samples.

Species (%)	Sample depth (cm)		
	4-5	34-35	76-77
Melosira italica	3.0	0.5	2.5
Cyclotella kutzingiana		0.5	2.0
Cyclotella comta			2.0
Cyclotella meneghiniana	0.5		0.5
Fragilaria construens		+	+
Fragilaria pinnata		0.5	
Fragilaria elliptica	14.0	31.5	14.0
Fragilaria virescens	18.0	29.0	4.0
Fragilaria virescens var oblongella	37.5	9.0	1.0
Fragilaria brevistriata	0.5	1.5	5.0
Fragilaria brevistriata var inflata	0.5	3.5	1.0
Peronia erinacea			0.5
Eunotia robusta (E. serra)	0.5		0.5
Eunotia praerupta	+		
Eunotia exigua	1.0	1.5	
Eunotia pectinalis var minor	0.5	1.0	5.0
Eunotia veneris	+	1.0	5.0
Eunotia monodon	0.5	0.5	3.5
Eunotia monodon var constricta			+
Eunotia flexuosa	0.5		
Achnanthes minutissima	4.0	7.0	10.5
Frustulia rhomboides	3.0	0.5	0.5
Frustulia rhomboides var saxonica			8.0
Caloneis limosa	+	0.5	+
Neidium bisulcatum			+
Neidium iridis	+	+	
Diploneis smithii	+	0.5	
Stauroneis phoenioenteron	1.0	+	1.0
Stauroneis anceps	+		
Anomoeoneis follis			+
Anomoeoneis serians		+	0.5
Anomoeoneis serians var brachysira	2.5	0.5	7.0
Anomoeoneis vitrea			4.0
Navicula mediocris	1.5	0.5	0.5
Navicula americana		+	+
Navicula pupula		1.0	
Navicula pupula var rectangularis			0.5
Navicula pusio		0.5	+
Navicula crucicula			0.5
Navicula arvensis	0.5		
Navicula sublitissima	0.5		2.0
Navicula cryptocephala	0.5	1.0	1.0
Navicula radiosa		+	1.0
Navicula radiosa var parva	0.5		
Navicula angusta	1.5	0.5	
Navicula pseudoscutiformis		0.5	
Pinnularia interrupta	+		1.0
Pinnularia microstauron	+	1.0	0.5
Pinnularia divergens		0.5	
Pinnularia episcopalis			0.5

Table F.1. The percentage frequencies of diatom taxa in samples from core 40/-20 ('+' denotes seen on scanning the slide)

Con/...

Species (%)	Sample depth (cm)		
	4-5	34-35	76-77
Pinnularia alpina			0.5
Pinnularia gibba	+		
Pinnularia stomatophorum			0.5
Pinnularia maior	+	+	0.5
Pinnularia dactylus	0.5	+	+
Amphora ovalis var pediculus	+		
Cymbella ehrenbergii	+	+	+
Cymbella lunata	4.0	2.5	5.0
Cymbella minuta var pseudogracilis			+
Cymbella cf.helvetica			1.5
Gomphonema acuminatum var coronata	+	+	+
Gomphonema subtile			0.5
Gomphonema angustatum	0.5	0.5	2.0
Gomphonema intricatum		0.5	0.5
Epithenia sorex			0.5
Rhopalopodia gibba		+	
Rhopalopodia gibberula			+
Nitzschia angustatum var acuta	1.5	1.5	1.0
Nitzschia fonticola	1.5	1.5	1.0
Stenopterobia intermedia			0.5
Surirella robusta	+		0.5
Tabellaria fenestrata	0.5		1.0
Tabellaria floculosa	0.5	0.5	+

Table F.1 continued

APPENDIX G MÖSSBAUER EFFECT SPECTROSCOPY

Mössbauer spectroscopy relies on the use of highly monochromatic gamma rays to measure the perturbations of the nuclear energy levels by the surrounding electrons, the hyperfine interactions, which give rise to an absorption spectrum characteristic of a given compound; the effect is specific to certain radio-isotopes, of which the most useful is ^{57}Fe (Longworth et al., 1979). The hyperfine interactions are of three kinds: (i) the chemical (or isomer shift) determines the centroid of the spectrum and indicates the iron oxidation state; (ii) the quadrupole interaction leads to a splitting of the spectrum into a doublet (in the absence of magnetic effects) which is affected by the iron oxidation state and the nature and arrangement of the neighbouring atoms; (iii) the magnetic hyperfine interaction arises if there is a magnetic field at the ^{57}Fe nucleus, and leads to a six-line spectrum (Oldfield et al., 1981a). In a magnetically-ordered material (e.g. a ferrimagnet) a six-line spectrum will normally occur at room temperature. However in superparamagnetic material, thermal fluctuations will destroy the magnetic interaction, in which case the spectrum becomes a doublet. As the temperature is reduced, the thermally-excited spontaneous reversals of magnetization begin to slow down and six-line splitting becomes evident in the Mössbauer spectrum. Fuller information relating to the measurement and the interpretation of Mössbauer spectra from soil and sediment samples is given for example by Coey (1974), Longworth and Tite (1977), Longworth et al. (op. cit.) and Oldfield et al. (op. cit.).

In view of the characteristic temperature-dependent nature of the Mössbauer spectra of superparamagnetic material, measurements were performed on sample 96-98 cm (core 50/90L) from magnetic peak B (which was suspected of containing either paramagnetic or superparamagnetic material). The measurement techniques are identical

to those described in Oldfield et al. (op. cit.).

Figure G.1 shows Mossbauer spectra obtained at three different temperatures: 77K, 4.2K and 1.3K. Two main points follow from the results: (i) the 77K spectrum shows two quadrupole doublets, one corresponding to Fe^{3+} and the other to Fe^{2+}; an Fe^{3+}: Fe^{2+} ratio of 7:3 may be deduced (D.P.E. Dickson, personal communication). (ii) Six-line magnetic splitting is apparent in the spectra for 4.2K and 1.3K; however, if superparamagnetic material were a dominant contributor to the spectra then six-line splitting would be expected to have set in at 77K. Consequently, the observed behaviour is indicative of paramagnetic, rather than superparamagnetic material (F. Oldfield, personal communication). Similar behaviour, with six-line splitting only apparent in spectra obtained at 4.2K, has been observed in Post-glacial lake sediment from Conniston water, Cumbria (Coey, op. cit.), in this case being attributed to the presence of paramagnetic amorphous ferric gel.

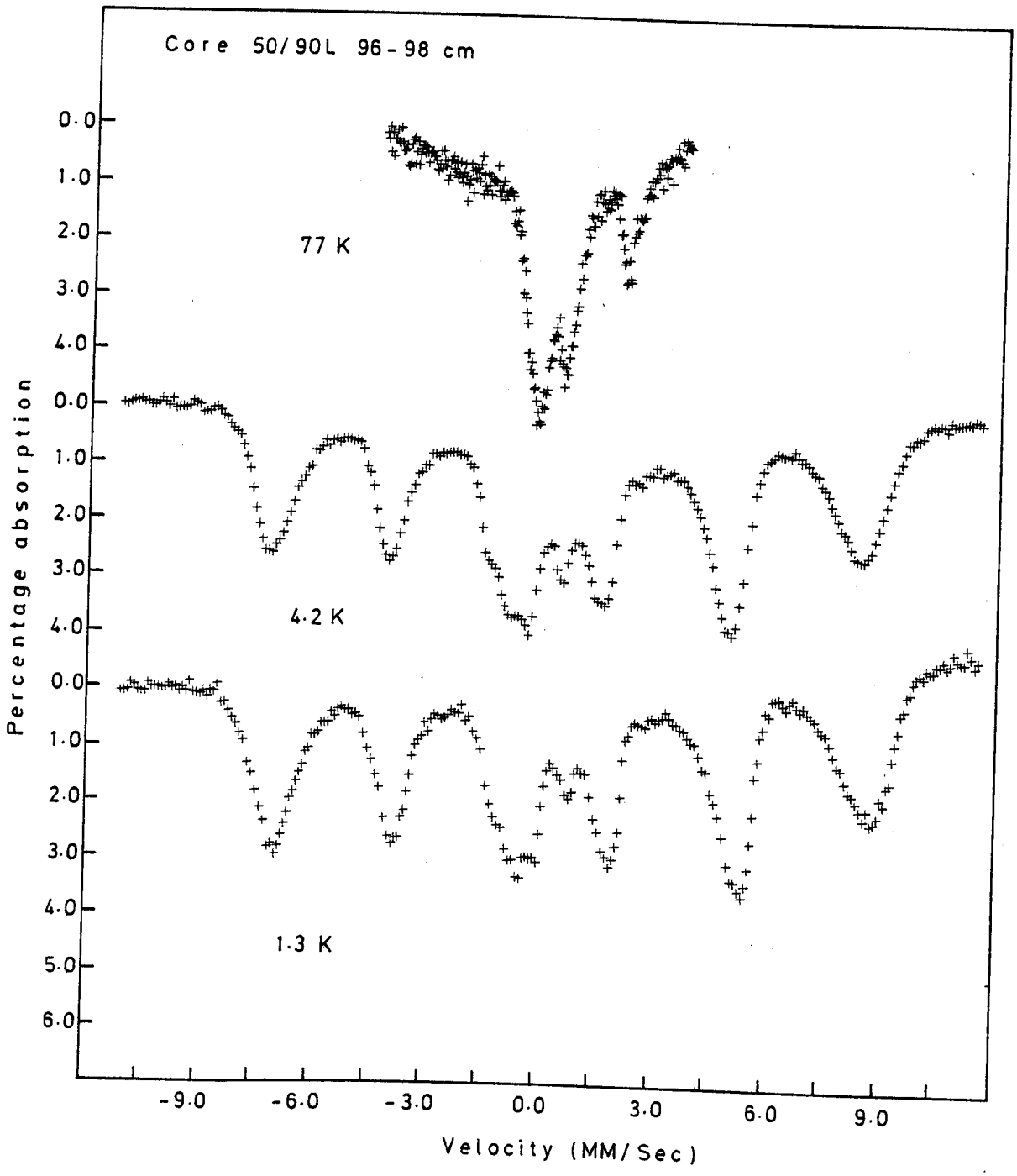

Figure G.1 Mössbauer spectra for magnetic peak B

APPENDIX H PRINCIPAL COMPONENTS ANALYSIS OF THE POLLEN DATA

In order to summarise the patterns shown by the variations of some of the major pollen and spore types shown in Figures 8.1-8.2 (Chapter 8) principal components analysis was performed on the data. This technique is being increasingly used to summarise variations in pollen biostratigraphical data (e.g. Birks, 1974; Birks and Berglund, 1979; Birks and Madsen, 1979; Pennington and Sackin, 1975) and has also been applied to chemical stratigraphical data from lake sediment cores (Pennington and Sackin, op. cit.). PCA aims to display the structure of a large number of interrelated variables in terms of a smaller, and therefore more comprehensible, set of new uncorrelated variables (principle components). Providing there are prominent patters ('structure') in the data, the first few components will account for most of the variance in the data, while the remainder, accounting for a relatively small proportion of the total variance, may be discarded (Birks et al., 1975). Mathematical and computational details of the technique are given in Davis (1973) and Mather (1976).

For the pollen biostratigraphical data from cores 60/-40 and 0/310, PCA was performed on a matrix of correlation coefficients obtained for selected pollen and spore types using a standard statistical package. The percentages used for calculation of the correlation coefficients were based on the pollen sum of the selected taxa. Tables H.1-H.2 summarise the results. They show the variable loadings on the first four principal components (these loadings are the correlation coefficients between the original pollen types and the principal components), together with the eigenvalue for each principal component (indicating the variance of that component) and the percentage of the total variance accounted for by each principal component. In

	1	2	3	4
Betula	0.549	0.407	0.121	0.473
Pinus	-0.262	-0.661	0.457	-0.224
Ulmus	0.524	-0.276	-0.181	0.000
Quercus	0.523	0.494	0.171	-0.362
Alnus	0.792	0.116	-0.226	-0.262
Fraxinus	0.588	-0.305	0.015	0.370
Corylus	0.647	0.614	-0.058	-0.113
Salix	0.507	0.088	-0.003	0.557
Gramineae	-0.451	-0.830	-0.004	0.046
Cerealia	-0.511	0.636	0.320	0.013
Compositae	-0.677	0.235	0.008	0.203
Cannabis	-0.557	0.528	0.302	0.061
Filipendula	0.051	-0.059	0.027	0.474
Plantago lanceolata	-0.815	0.087	-0.232	0.313
Potentilla-type	-0.605	0.041	-0.577	-0.120
Ranunculus acris-type	-0.563	-0.144	-0.508	0.020
Rumex	-0.774	0.281	-0.206	-0.006
Urtica	-0.436	-0.430	0.608	0.034
Pteridium	-0.680	0.532	0.169	-0.043
Variance (eigenvalue)	6.40	3.49	1.62	1.32
Percent of total variance	33.7	18.4	8.5	7.0
Cumulative percent of total variance	33.7	52.0	60.6	67.5

Table H.1. Results of principal components analysis for core 0/310

	1	2	3	4
Betula	0.374	-0.650	0.408	-0.269
Pinus	-0.683	0.303	0.207	-0.235
Quercus	0.434	-0.646	0.072	0.055
Ulmus	0.153	0.383	-0.336	0.080
Alnus	0.804	0.209	0.118	0.011
Fraxinus	-0.369	-0.443	0.191	-0.157
Corylus	0.500	-0.522	-0.463	-0.166
Salix	0.472	-0.059	0.059	0.378
Calluna	-0.796	-0.042	-0.374	-0.241
Gramineae	0.020	0.821	0.456	0.131
Cerealia	0.175	-0.301	-0.110	0.305
Cyperaceae	-0.115	0.514	-0.458	0.155
Compositae	0.242	-0.096	-0.586	0.123
Potentilla-type	-0.426	0.037	-0.009	-0.486
Rumex	-0.546	-0.594	-0.016	-0.136
Filipendula	0.217	0.057	-0.104	-0.279
Plantago lanceolata	-0.858	-0.071	-0.025	0.001
Ranunculus	-0.540	-0.154	0.009	0.380
Urtica	-0.555	-0.183	0.495	0.375
Cannabis	-0.667	-0.107	-0.387	0.223
Pteridium	-0.246	-0.315	-0.002	0.714
Variance (eigenvalue)	5.18	3.16	1.91	1.71
Percent of total variance	24.7	15.1	9.1	8.2
Cumulative percent of total variance	24.7	39.7	48.8	57.0

Table H.2. Results of principal components analysis for core 60/-40

core 0/310 (Table H.1) the first two components account for 52% of the total variance, while in core 60/-40 (Table H.2) the first two components account for a significantly lower percentage (ca. 40%). This supports the observations made in Chapter 8 (section 8.3) regarding the poor resolution of the pollen biostratigraphical data from core 60/-40 in comparsion with those from core 0/310.

Figures H.1-H.2 show plots of the loadings of the pollen types on the first two principal components. Figure H.1 is of main interest. In Figure H.1, component 1 expresses a basic forest versus non-forest dichotomy: the woodland pollen types (e.g. Quercus, Betula, Fraxinus, Alnus) have moderate to high positive loadings on this component, while the dry land pasture and arable pollen and spore types (e.g. Plantago lanceolata, Pteridium, Cannabis) have moderate to high negative loadings. Fraxinus and Ulmus, with high positive loadings on component 1 and moderate-negative loadings on component 2, are reduced relatively early on in Figure 8.1 (part a) but increase substantially towards the top of the diagram. Corylus, Betula and Quercus, with high positive loadings on both components, exhibit high frequencies throughout the lower and middle part of the pollen diagram but are strongly reduced thereafter. Taxa with moderate to high negative loadings on component 1 (e.g. Pinus, Gramineae) exhibit their highest frequencies in the uppermost part of the pollen diagram. Gramineae with high negative loadings on both components, is plotted well away from the dry land pasture and arable indicators, suggesting that this taxon is contributed by 'local' pollen types (see Table 8.1) and supports its exclusion from the pollen sum in Figure 8.1 (part a).

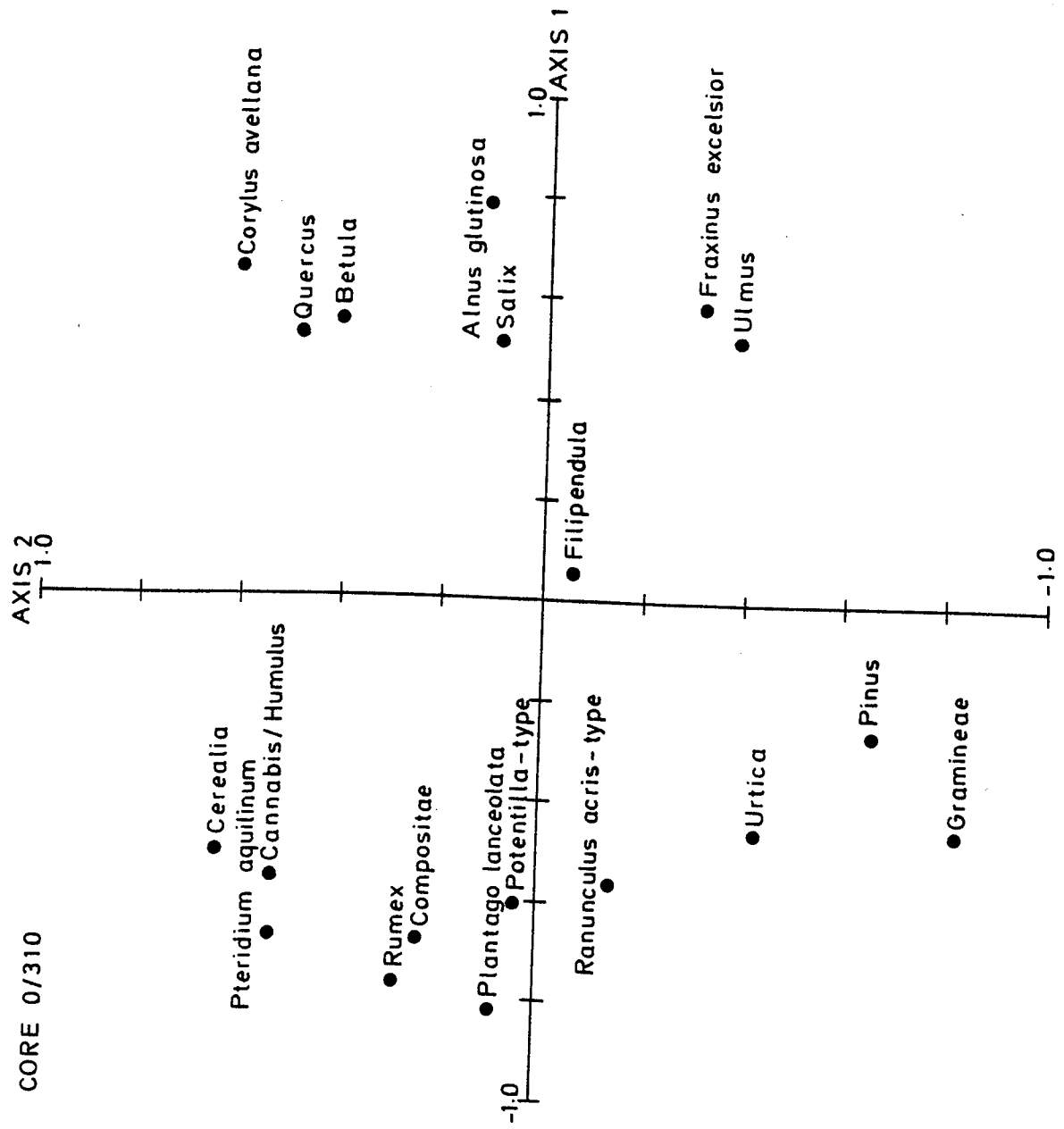

Figure H.1 Principal components analysis of core 0/310: plot of the variable loadings on the first two principal components

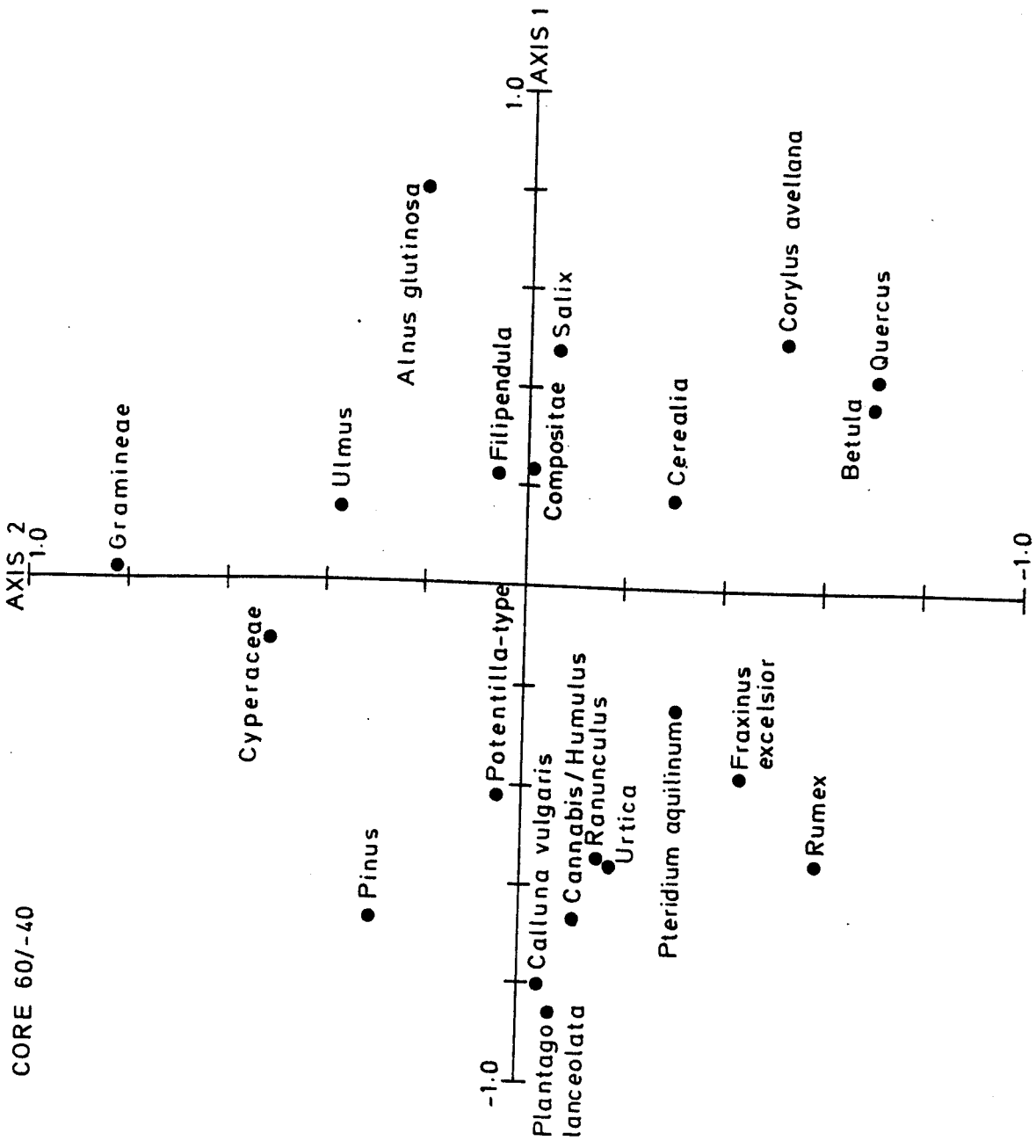

Figure H.2 Principal components analysis of core 60/-40: plot of the variable loadings on the first two principal components

APPENDIX I. POLLEN DIAGRAM AND PALAEOMAGNETIC DATES FROM LLYN GEIRIONYDD

Figure I.1 shows a pollen diagram from Llyn Geirionydd (Grid Ref. SH762607), ca. 1.5 Km northeast of Llyn Goddionduon. The diagram is divided horizontally at the point of a marked increase in the frequency of Ericales. This horizon is tentatively correlated with a rise in the frequency of Calluna vulgaris at 34 cm depth in Goddionduon core 60/-40 (see Chapter 8, section 8.3). According to the palaeomagnetically-based age-depth curve shown in Figure I.2 (see Turner, 1979) the rise in Ericales is assigned the date of 320-220 BP.

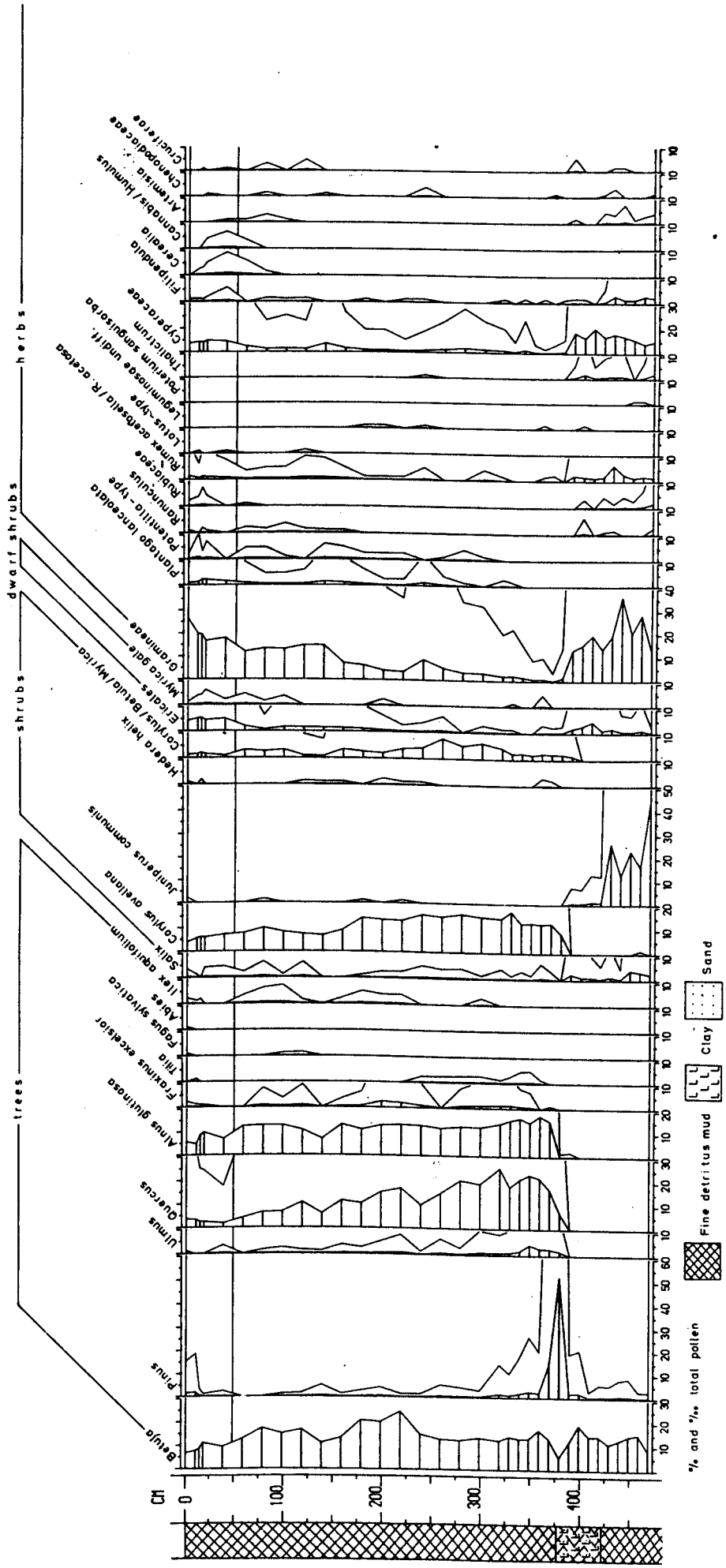

Figure I.1 Pollen diagram from Llyn Geirionydd core 2

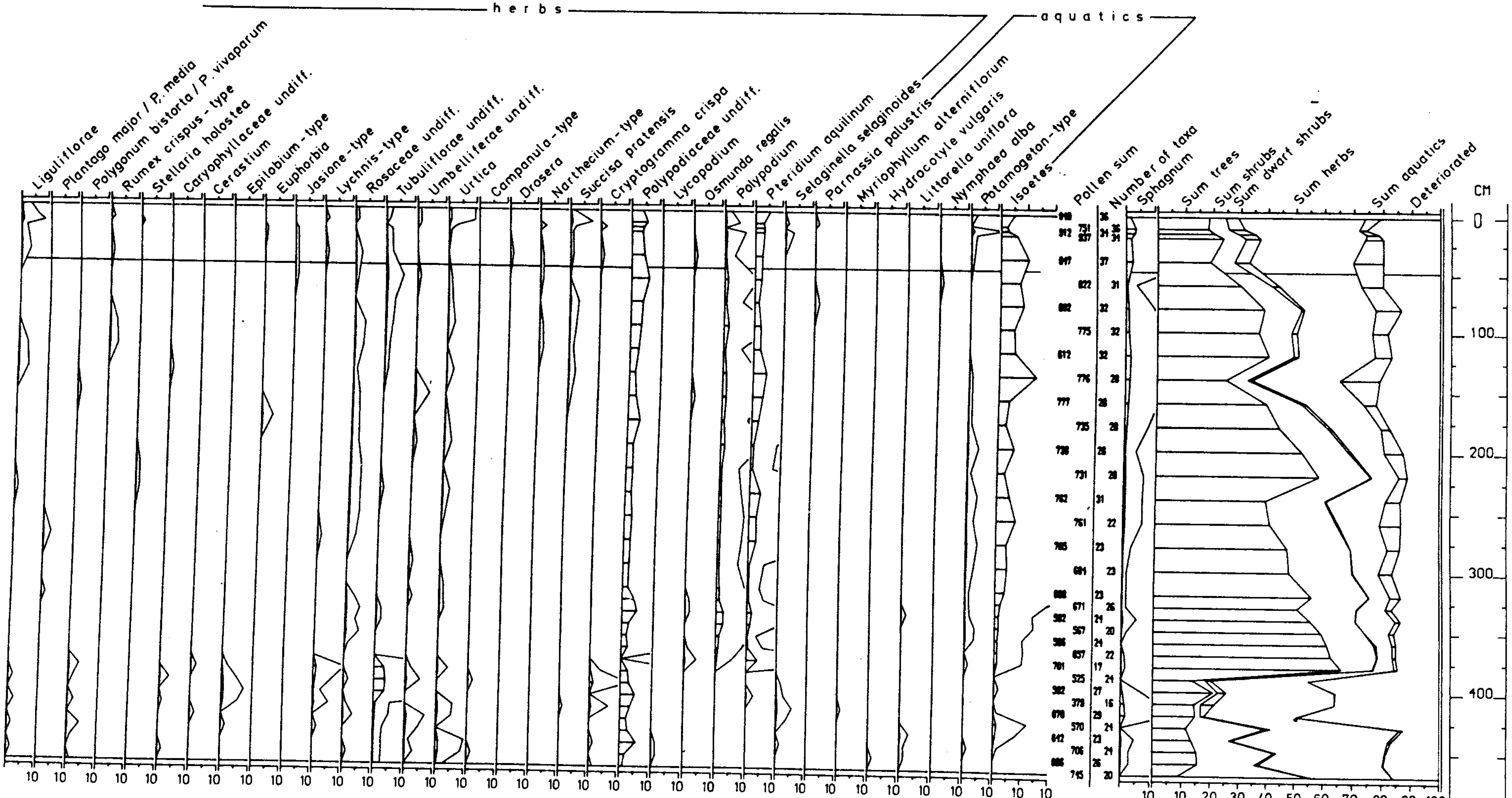

Figure I.1 continued

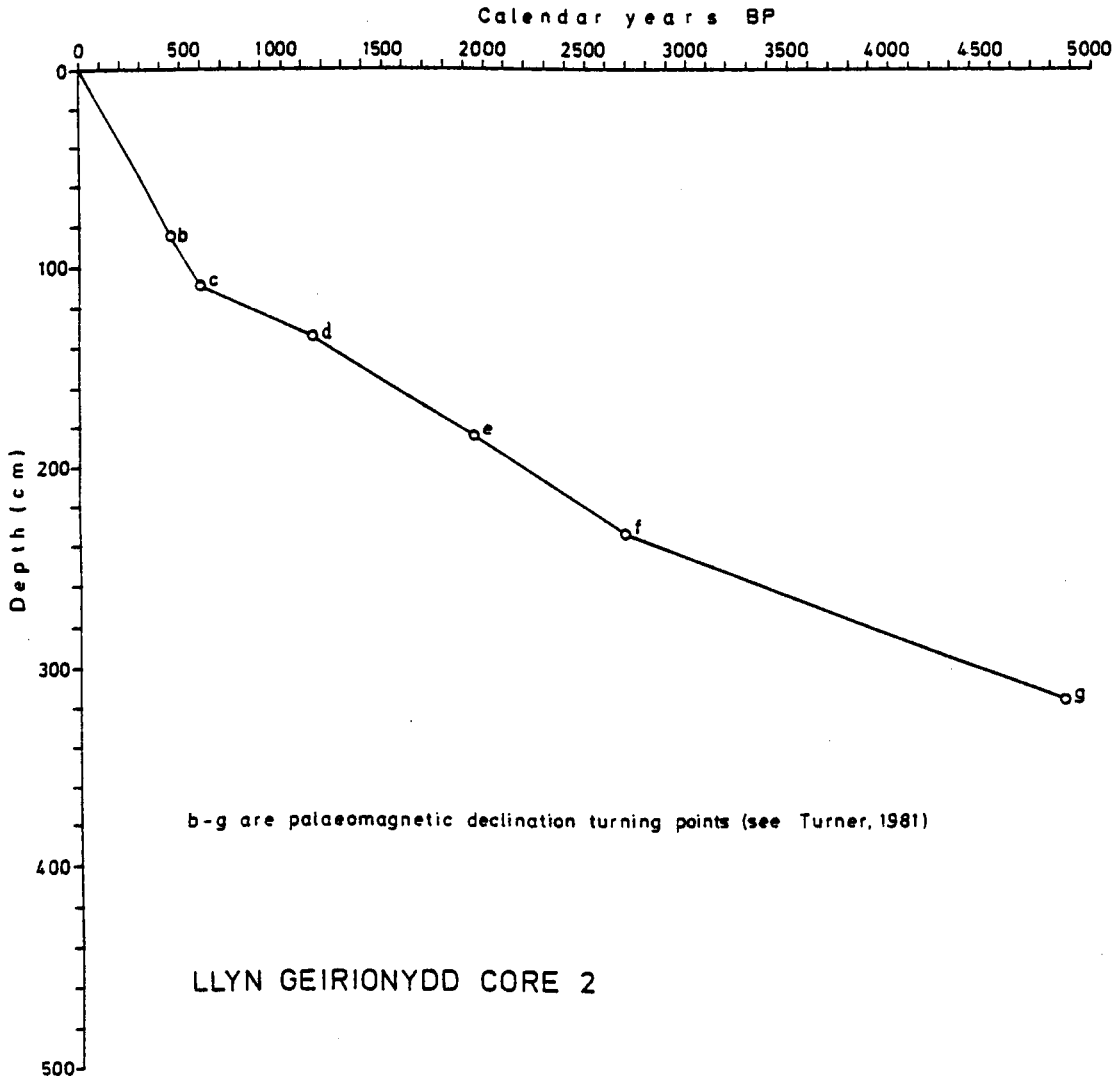

Figure I.2 Age-depth curve for Llyn Geirionydd core 2

REFERENCES

Ade-Hall, J.M. (1964). Electron probe microanalyser analyses of basaltic titanomagnetites and their significance to rock magnetism. Geophys. J., 8, 301-311.

Ahlgren, I.F. and Ahlgren, C.E. (1960). Ecological effects of forest fires. Bot. Rev., 26, 483-533.

Aikin, A. (1797). Journal of a Tour through Wales. London.

Andersen, S.T. (1970). The relative pollen productivity and pollen representation of North European trees, and correction factors for tree pollen spectra. Danm. Geol. Unders. II. RK 96.

Appleby, P.G. and Oldfield, F. (1978). The calculation of lead-210 dates assuming a constant rate of supply of unsupported ^{210}Pb to the sediment. Catena, 5, 1-8.

Arkell, B.P., Leeks, G.J.L., Newson, M.D. and Oldfield, F. Trapping and tracing: some recent observations of supply and transport of coarse sediment from upland Wales. Unpublished manuscript.

Ball, D.F. (1963). The Soils and Land Use of The District Around Bangor and Beaumaris. H.M.S.O. London.

Ball, D.F., Mew, G. and Macphee, W.S.G. (1969). Soils of Snowdon. Fld Stud., 3, 69-107.

Battarbee, R.W. (1978a). Observations on the recent history of Lough Neagh. Phil. Trans. R. Soc. Lond., B, 281, 303-345.

Battarbee, R.W. (1978b). Biostratigraphical evidence for variations in the recent pattern of sediment accumulation in Lough Neagh, Northern Ireland. Verh. Int. Verein, Limnol., 20, 624-629.

Battarbee, R.W. and Digerfeldt, G. (1976). Palaeoecological studies of the recent development of Lake Växjösjön. I. Introduction and chronology. Arch. Hydrobiol., 73, 330-346.

Bengtsson, L. (1975). Phosphorus release from a highly eutrophic lake sediment. Verh. Internat. Verein. Limnol., 19, 1107-1116.

Bengtsson, L. and Persson, T. (1978). Sediment changes in a lake used for sewage reception. Pol. Arch. Hydrobiol., 25, 17-33.

Berglund, B.E. (1973). Pollen dispersal and deposition in an area of Southeastern Sweden - some preliminary results. In Birks, H.J.B. and West, R.G., editors, Quaternary Plant Ecology. Blackwell, Oxford.

Beschta, R.L. (1978). Long-term patterns of sediment production following road construction and logging in the Oregon coast range. Wat. Res. Research, 14, 1001-1016.

Beug, H-J. (1961). Leitpfaden der Pollenbestimmung. Hans Fischer Verlag, Stuttgart.

Birks, H.H. (1972). Studies in the vegetational history of Scotland. II. Two pollen diagrams from the Galloway Hills, Kirkcudbrightshire. J. Ecol., 60, 183-217.

Birks, H.J.B. (1973). Past and Present Vegetation of the Isle of Skye. A Palaeoecological Study. Cambridge University Press, London.

Birks, H.J.B. (1974). Numerical zonations of Flandrian pollen data. New Phytol., 73, 351-358.

Birks, H.J.B. and Birks, H.H. (1980). Quaternary Palaeoecology. Edward Arnold, London.

Birks, H.J.B. and Berglund, B.E. (1973). Holocene pollen stratigraphy of southern Sweden: a reappraisal using numerical methods. Boreas, 8, 257-279.

Birks, H.J.B. and Madsen, B.J. (1979). Flandrian vegetational history of Little Loch Roag, Isle of Lewis, Scotland. J. Ecol., 67, 825-842.

Birks, H.J.B., Thompson Webb III and Berti, A.A. (1975). Numerical analyses of pollen samples from central Canada: a comparison of methods. Rev. Palaeaobot. Palynol., 20, 133-169.

Birks, H.J.B. and West, R.G. (1973). Editors, Quaternary Plant Ecology. Blackwell, Oxford.

Björck, S., Persson, T. and Kristersson, I. (1978). Comparison of two concentration methods for pollen in minerogenic sediments. Geol. For. - Stockh. Forh., 100, 107-111.

Bloemendal, J. (1977). Palaeoecological Studies in a Small Upland Drainage Basin in Caernarvonshire. Unpublished thesis, University of Liverpool.

Bloemendal, J. (in press). Palaeoenvironmental implications of the magnetic characteristics of sediments from DSDP Site 514, Southeast Argentine Basin. Init. Repts. DSDP.

Bonny, A.P. (1976). Recruitment of pollen to the seston and sediment of some Lake District lakes. J. Ecol., 64, 859-887

Bormann, F.H. and Likens, G.E. (1979). Pattern and Process in a Forested Ecosystem. Springer-Verlag, New York.

Bormann, F.H., Likens, G.E., Fisher, D.W. and Pierce, R.S. (1968). Nutrient loss accelerated by clear-cutting of a forested ecosystem. Science (N.Y.), 159, 882-884.

Bormann, F.H., Likens, G.E., Siccama, T.G., Pierce, R.S. and Eaton, J.S. (1974). The export of nutrients and recovery of stable conditions following deforestation at Hubbard Brook. Ecol. Monog., 44, 255-277.

Born, S.M., Smith, S.A. and Stephenson, D.A. (1979). Hydrogeology of glacial terrain lakes, with management and planning applications. J. Hydrol., 43, 7-43.

CALCOMP (1971). GPCP. A General Purpose Contouring Program. California Computer Products, California.

Cambray, R.S., Fisher, E.M.R., Peirson, D.H. and Parker, A. (1972). Radioactive fallout in air and rain. Results to the middle of 1972. A.E.R.E. Report 7245. H.M.S.O., London.

Carroll, D. (1958). Role of clay minerals in the transportation of iron. Geochim. cosmochim. Acta, 14, 21-26.

Clapham, A.R., Tutin, T.G. and Warburg, E.F. (1962). Flora of the British Isles. Cambridge University Press, London.

Coey, J.M.D. (1975). Iron in a Post-glacial sediment core: a Mössbauer effect study. Geochim. cosmochim. Acta, 39, 401-415.

Cooke, R.U. and Doornkamp, J.C. (1973). Geomorphology in Environmental Management. Clarendon Press, Oxford.

Crabtree, K. Late-Quaternary Deposits near Capel Curig, North Wales. Unpublished Ph.D. thesis, University of Bristol.

Csanady, G.T. (1978). Water circulation and dispersal mechanisms. In Lerman, A. Editor, Lakes. Chemistry, Geology, Physics. Springer Verlag, New York.

Currie, R.G. and Bornhold, B.D. The magnetic susceptibility of continental shelf sediments. Unpublished manuscript.

Davies, D.A.B. (1936). Ordovician rocks of the Trefriw district (North Wales). Q.J. Geol. Soc. Lond., 92, 62-90.

Davis, J.C. (1973). Statistics and Data Analysis in Geology. John Wiley and Sons, New York.

Davis, M.B. (1963). On the theory of pollen analysis. Am. J. Sci., 261, 897-912.

Davis, M.B. (1973). Redeposition of pollen grains in lake sediments. Limnol. Oceanogr., 18, 44-52.

Davis, M.B. (1976). Erosion rates and land-use history in southern Michigan. Environ. Conserv., 3, 139-148.

Davis, M.B. and Brubaker, L.B. (1973). Differential sedimentation of pollen grains in lakes. Limnol. Oceanogr., 18, 635-646.

Davis, M.B., Brubaker, L.B. and Thompson Webb III. In Birks, H.J.B. and West, R.G., editors, Quaternary Plant Ecology, Blackwell, Oxford.

Dearing, J.A. (1979). The application of magnetic measurements to the study of particulate flux in lake-watershed ecosystems. Unpublished Ph.D. thesis, University of Liverpool.

Dearing, J.A., Elner, J.K. and Happey-Wood, C.M. (in press). An examination of total sediment flux and erosional processes in a Welsh upland catchment based on magnetic studies of the recent lake sediments. Quat. Res. (N.Y.).

Dearing, J.A. and Flower, R. (in preparation). Some observations on the magnetic properties of trapped seston samples from Lough Neagh, Northern Ireland.

Dendy, F.E. (1968). Sedimentation in the Nation's Reservoirs. J. Soil. Wat. Conserv., 23, 135-137.

Digerfeldt, G. (1969). Kvartargeologiska och paleolimnologiska undersökningar i sjön Trummen. Meddelanden, 25, University of Lund.

Digerfeldt, G. (1972). The Post-glacial development of Lake Trummen. Folia Limnologica Scandinavica, 16.

Digerfeldt, G. (1973). The Post-Glacial Development of the Bay Ranviken, Lake Immeln. III. Paleolimnology. University of Lund, Department of Quaternary Geology. Report 2.

Digerfeldt, G. (1977a). Palaeoecological studies of the recent development of Lake Växjösjön. II Settlement and landscape development. Arch. Hydrobiol., 79, 465-477.

Digerfeldt, G. (1977b). The Flandrian Development of Lake Flarken. Regional Vegetation History and Palaeolimnology, University of Lund, Department of Quaternary Geology. Report 13.

Digerfeldt, G., Battarbee, R.W. and Bengtsson, L. (1975). Report on annually laminated sediment in Lake Järläsjön, Nacka, Stockholm. Geol. For. - Stockh. Forh., 97, 29-40.

Dunlop, D.J. (1972). Magnetite behaviour near the single domain threshold. Science (N.Y.), 176, 41-43.

Dunlop, D.J. (1973). Superparamagnetic and single domain threshold sizes in magnetite. J. Geophys. Res., 78, 1780-1793.

Dyrness, C.T. (1967). Erodibility and erosion potential of forest watersheds. In Sopper, W.E. and Lull, H.W., editors, International Symposium on Forest Hydrology. Pergamon Press, Oxford.

Edwards, K.J. and Rowntree, K.M. (1980). Radiocarbon and palaeo-environmental evidence for changing rates of erosion at a Flandrian stage site in Scotland. In Cullingford, R.A., Davidson, D.A. and Lewin, J., editors, Timescales in Geomorphology. John Wiley and Sons, Chichester.

Emery, F.V. (1969). Wales. Longmans, London.

Faegri, K. and Iversen, J. (1975). Textbook of Pollen Analysis. Blackwell, Oxford.

Fitzpatrick, E.A. (1971). Pedology. A Systematic Approach to Soil Science. Oliver and Boyd, Edinburgh.

Godwin, H. (1975). History of the British Flora. Cambridge University Press, London.

Godwin, H., Walker, D. and Willis, E.H. (1957). Radiocarbon dating and Post-glacial vegetational history: Scaleby Moss. Proc. R. Soc. Lond. B., 147, 352-366.

Gorham, E. and Swaine, D.J. (1965). The influence of oxidising and reducing conditions upon the distribution of some elements in lake sediments. Limnol. Oceanogr., 10, 268-279.

Graf, W.H. and Mortimer, C.H. (1979). Editors, Hydrodynamics of Lakes. Elsevier, Amsterdam.

Gregory, K.J. and Walling, D.E. (1973). Drainage Basin Form and Process. Edward Arnold, London.

Grimes, W.F. (1965). Neolithic Wales. In Foster, I. L ., and Daniel, G., editors, Prehistoric and Early Wales. Routledge, London.

Hansen, N.-E.O. (1979). Effects of boundary layers on mixing in small lakes. In Graf, W.H. and Mortimer, C.H., editors, Hydrodynamics of Lakes. Elsevier, Amsterdam.

Harvey, A.M. (1974). Gully erosion and sediment yield in the Howgill Fells, Westmorland. In Gregory, K.J. and Walling, D.E., editors, Fluvial Processes in Instrumented Watersheds. Alden Press, Oxford.

Hodgson, J.M. (1974). Soil Survey Field Handbook. Soil Survey Technical Monograph No. 5. Harpendon, Harpendon.

Howells, M.F., Francis, E.H., Leveridge, B.E. and Evans, C.D.R. (1978). Classical Areas of British Geology. Capel Curig and Betws-y-Coed. H.M.S.O., London.

Hutchinson, G.E. (1957). A Treatise on Limnology. Volume I. Geography, Physics, and Chemistry. John Wiley and Sons, New York.

Huttunen, P., Merilainen, J. and Tolonen, K. (1978). The history of a small dystrophied forest lake, southern Sweden. Pol. Arch. Hydrobiol., 25, 189-202.

Imeson, A.C. (1971). Heather burning and soil erosion on the North Yorkshire Moors. J. appl. Ecol., 8, 537-542.

Ince, J. (1980). Unpublished Ph.D. thesis, City of London Polytechnical College.

Janssen, C.R. (1966). Recent pollen spectra from the deciduous and coniferous-deciduous forests of Northeastern Minnesota: a study in pollen dispersal. Ecology, 47, 804-825.

Jowsey, P.C. (1966). An improved peat sampler. New Phytol., 65, 245-248.

Kjensmo, J. (1978). Postglacial sediments in Vilbergtjern, a small meromictic kettle lake. Pol. Arch. Hydrobiol., 25, 207-216.

Lamb, H.H. (1965). The history of our climate. In Taylor, J.A., editor, Climate Changes with Special Reference to Wales and its Agriculture. University College of Wales, Aberystwyth. Memo. No. 8. Pergamon Press, Oxford.

Le Borgne, E. (1955). Susceptibilite Magnetique anormale du sol superficiel. Annls. Geophys., 11, 399-419.

Le Borgne, E. (1960). Influence du feu sur les proprietes magnetiques du sol et du granite. Annls. Geophys., 16, 159-195.

Ledger, D.C., Lovell, J.P.B. and McDonald, A.T. (1974). Sediment yield studies in upland catchment areas in southeast Scotland. J. appl. Ecol., 11, 201-206.

Lehman, J.T. (1975). Reconstructing the rate of accumulation of lake sediment: the effect of sediment focussing. Quat. Res. (N.Y.), 5, 541-550.

Leopold, L.B. (1956). Land use and sediment yield. In Thomas, W.L., editor, Man's Role in Changing the Face of the Earth. University of Chicago Press, Chicago.

Levi, S. and Merrill, R.T. (1978). Properties of single-domain, pseudo-single-domain and multidomain magnetite. J. Geophys. Res., 83, 309-323.

Lewin, J., Cryer, R. and Harrison D.I. (1974). Sources for sediments and solutes in mid-Wales. In Gregory, K.J. and Walling, D.E. editors, Fluvial Processes in Instrumented Watersheds. Alden Press, Oxford.

Liddle, M.J. A Survey of Twelve Lakes in the Gwydyr Forest Region of Snowdonia. Unpublished report, University College North Wales.

Likens, G.E. (1972). Eutrophication and aquatic ecosystems. In Likens, G.E., editor, Nutrients and Eutrophication. Special Symposia Vol. 1, Amer. Soc. Limnol. Oceanogr. Lawrence, Kansas.

Likens, G.E. and Bormann, F.H. (1974). Linkages between terrestrial and aquatic ecosystems. Bioscience, 24, 447-456.

Likens, G.E. and Bormann, F.H., Pierce, R.S., Eaton, J.S. and Johnson, N.M. (1977). Bio-Geo-Chemistry of a Forested Ecosystem. Springer-Verlag, New York.

Likens, G.E. and Davis, M.B. (1975). Post-glacial history of Mirror Lake and its watershed in New Hampshire, U.S.A.: an initial report. Verh. Intl. Verein. Limnol., 19, 982-993.

Longworth, G., Becker, L.W., Thompson, R., Oldfield, F., Dearing, J.A. and Rummery, T.A. (1979). Mössbauer effect and magnetic studies of secondary iron oxides in soils. J. Soil Sci., 30, 93-110.

Longworth, G. and Tite, M.S. (1977). Mössbauer and magnetic susceptibility studies of iron oxides in soils from archaeological sites. Archaeometry, 19, 3-14.

Loucks, O.L. (1975). Models linking land-water interactions around Lake Wingra, Wisconsin. In Hasler, A.D., editor, Coupling of Land and Water Systems. Springer-Verlag, New York.

Lowrie, W. and Fuller, M. (1971). On the alternating field demagnetization characteristics of multidomain thermoremanent magnetization in magnetite. J. Geophys. Res., 76, 6339-6349.

Macan, T.T. and Worthington, E.B. (1972). Life in Lakes and Rivers. Collins, London.

Mackereth, F.J.H. (1966). Some chemical observations on Post-glacial lake sediments. Phil. Trans. R. Soc. Lond., B, 250, 165-213.

Mackereth, F.J.H. (1969). A short core sampler for sub-aqueous deposits. Limnol. Oceanogr., 14, 145-151.

Manny, B.A., Wetzel, R.G. and Bailey, R.E. (1978). Paleolimnological sedimentation of organic carbon, nitrogen, phosphorus, fossil pigments, pollen, and diatoms in a hypereutrophic, hard-water lake: a case history of eutrophication. Pol. Arch. Hydrobiol., 25, 243-267.

Mather, P.M. (1976). Computational Methods of Multivariate Analysis in Physical Geography. John Wiley, London.

McElhinny, M.W. (1973). Palaeomagnetism and Plate Tectonics. Cambridge University Press, London.

McKeague, J.A., Damman, A.W.H. and Heringa, P.K. (1968). Iron-manganese and other pans in some soils of Newfoundland. Can. J. Soil Sci., 48, 243-253.

Megahan, W.F. (1975). Sedimentation in relation to logging activities in the mountains of central Idaho. In Present and Prospective Technology for Predicting Sediment Yields and Sources. Proceedings of the Sediment Yield Workshop. Oxford, Miss., U.S. Dept., Agr., Agr. Res. Service, ARS-S-40.

Molyneux, L. (1971). A complete result magnetometer for measuring the remanent magnetisation of rocks. Geophys. J.R. astr. Soc., 32, 429-434.

Molyneux, L. and Thompson, R. (1973). Rapid measurement of the magnetic susceptibility of long cores of sediment. Geophys. J. R. astr. Soc., 32, 479-481.

Moore, P.D. and Chater, E.H. (1969). The changing vegetation of west-central Wales in the light of human history. J. Ecol., 57, 361-379.

Moore, P.D. and Webb, J.A. (1978). An Illustrated Guide to Pollen Analysis. Edward Arnold, London.

Morgan, R.P.C. (1977). Soil Erosion in the United Kingdom: Field Studies in the Silsoe Area, 1973-75. Occasional Paper No. 4. National College of Agricultural Engineering, Cranfield Institute of Technology.

Mortimer, C.H. (1941). The exchange of dissolved substances between mud and water in lakes. J. Ecol., 29, 280-329.

Mothersill, J.S. and Shegelski, R.J. (1973). The formation of iron and manganese-rich layers in the Holocene sediments of Thunder Bay, Lake Superior. Can. J. Earth Sci., 10, 571-576.

Mullins, C.E. (1974). The magnetic properties of the soil and their application to archaeological prospecting. Published Ph.D. thesis in Archeo-Physika, 5, 143-347. Rheinland-Verlag, Bonn.

Mullins, C.E. (1977). Magnetic susceptibility of the soil and its significance in soil science: a review. J. Soil Sci., 28, 223-246.

Mullins, C.E. and Tite, M.S. (1973). Magnetic viscosity, quadrature susceptibility, and frequency dependence of susceptibility in single-domain assemblies of magnetite and maghemite. J. Geophys. Res., 78, 804-809.

Muxworthy, D.T. (1977). A User's Guide to SYMVU. University of Edinburgh Program Library Services No. 24.

Newson, M.D. (1980). The erosion of drainage ditches and its effect on bedload yields in mid-Wales: recconnaissance case studies. Earth Surf. Processes, 5, 275-290.

Oldfield, F. (1970). Some aspects of scale and complexity in pollen-analytically based palaeoecology. Pollen et Spores, 12, 163-171.

Oldfield, F. (1975). Recent Ecological History of Small Drainage Basins in the Western and Southern Highlands of Papua New Guinea. Unpublished report to the Nuffield Foundation.

Oldfield, F. (1977). Lakes and their drainage basins as units of sediment-based ecological study. Prog. Phys. Geogr., 1, 460-504.

Oldfield, F. (1981). Peats and lake sediments: formation, stratigraphy, description and nomenclature. In Goudie, A., editor, Geomorphological Techniques. Allen and Unwin, London.

Oldfield, F., Appleby, P.G. and Battarbee, R.W. (1978c). Alternative ^{210}Pb dating: results from the New Guinea Highlands and Lough Erne. Nature (Lond.)., 271, 339-342.

Oldfield, F., Dearing, J.A., Thompson, R. and Garrett-Jones, S.E. (1978b). Some magnetic properties of lake sediments and their possible links with erosion rates. Pol. Arch. Hydrobiol., 25, 321-331.

Oldfield, F., Rummery, T.A., Thompson, R. and Walling, D.E. (1979a). Identification of suspended sources by means of magnetic measurements: some preliminary results. Wat. Res. Research, 15, 211-218.

Oldfield, F., Thompson, R. and Barber, K.E. (1978a). Changing atmospheric fallout of magnetic particles recorded in recent ombrotrophic peat sections. Science (N.Y.), 199, 679-680.

Oldfield, F., Thompson, R. and Dickson, D.P.E. (1981a). Artificial magnetic enhancement of stream bedload: a hydrological application of superparamagnetism. Phys. Earth Planet. Inter., 26, 107-124.

Oldfield, F., Tolonen, K. and Thompson, R. (1981b). History of particulate atmospheric pollution from magnetic measurements of dated Finnish peat profiles. Ambio., 10, 185-188.

Olsson, I.V. (1974). Some problems in connection with the evaluation of ^{14}C dates. Geol. For.-Stockh. Forh., 96, 311-320.

O'Reilly, W. (1976). Magnetic minerals in the crust of the earth. Rep. Prog. Phys., 39, 857-908.

O'Sullivan, P.E., Oldfield, F. and Battarbee, R.W. (1973). Preliminary studies of Lough Neagh sediments. I. Stratigraphy, chronology and pollen analysis. In Birks, H.J.B. and West, R.G., editors, Quaternary Plant Ecology. Blackwell, Oxford.

Parry, L.G. (1965). Magnetic properties of dispersed magnetite powders. Phil. Mag., 11, 303-312.

Parry, L.G. (1980). Shape-related factors in the magnetization of immobilised magnetite particles. Phys. Earth and Planet. Inter., 22, 144-154.

Peck, R.M. (1973). Pollen budget studies in a small Yorkshire catchment. In Birks, H.J.B. and West, R.G., editors, Quaternary Plant Ecology, Blackwell, Oxford.

Pennington, W. (1973). The recent sediments of Windermere. Freshwat. Biol., 3, 636-382.

Pennington, W. (1979). The origin of pollen in lake sediments: an enclosed lake compared with one receiving inflow streams. New Phytol., 83, 189-213.

Pennington, W., Cambray, R.S., Eakins, J.D. and Harkness, D.D. (1976). Radionuclide dating of the recent sediments of Blelham Tarn. Freshwat. Biol., 6, 317-331.

Pennington, W., Cambray, R.S. and Fisher, E.M. (1973). Observations on lake sediments using fallout ^{137}Cs as a tracer. Nature (Lond.), 242, 324-326.

Pennington, W., Haworth, E.Y., Bonny, A.P. and Lishman,J.P. (1972). Lake sediments in Northern Scotland. Phil. Trans. R. Soc. Lond., B, 264, 191-294.

Pennington, W. and Lishman, J.P. (1971). Iodine in lake sediments in Northern England and Scotland. Biol. Rev., 46, 279-313.

Pennington, W. and Sackin, M.J. (1975). An application of principal components analysis to the zonation of two Late-Devensian profiles. New Phytol., 75, 419-453.

Radhakrishnamurty, C. and Deutsch, E.R. (1974). Magnetic techniques for ascertaining the nature of iron oxide grains in basalts. J. Geophys., 40, 453-465.

Radhakrishnamurty, C., Likhite, S.D., Amin, B.S. and Somayajulu, B.L.K. (1968). Magnetic susceptibility stratigraphy in ocean sediment cores. Earth and Planet. Sci. Lett., 4, 464-468.

Ratcliffe, D.A. (1959). The vegetation of the Carneddau. J. Ecol., 47, 371-403.

Rea, D.K., Owen, R.M. and Meyers, P.A. (1981). Sedimentary processes in the Great Lakes. Rev. Geophys. Space Phys., 19, 635-648.

Rhys, J. (1883). Pennant's Tours in Wales. H. Humphreys.

Ritchie, J.C., Mettenry, J.R. and Gill, A.C. (1973). Dating recent reservoir sediments. Limnol. Oceanogr., 18, 254-263.

Robbins, J.A., Edgington, D.N. and Kemp, A.L.W. (1978). Comparative ^{210}Pb, ^{137}Cs and pollen geochronologies of sediments from Lakes Ontario and Erie. Quat. Res. (N.Y.), 10, 256-278.

Robinson, S. Mineral magnetic properties of cores D10311 and S8/79/7. Unpublished manuscript.

Robinson, M. and Blyth, K. (1982). The effect of forestry drainage operations on upland sediment yields: a case study. Earth Surf. Processes, 7, 85-90.

Rowley, J.R. and Dahl, A.O. (1956). Modifications in the design and use of the Livingstone piston sampler. Ecology, 37, 849-851.

Rummery, T.A. (1981). The Effects of Fire on Soil and Sediment Magnetism. Unpublished Ph.D. thesis, University of Liverpool.

Rummery, T.A., Bloemendal, J., Dearing, J.D., Oldfield, F. and Thompson, R. (1979b). The persistence of fire-induced magnetic oxides in soils and sediments. Annls. Geophys., 35, 103-107.

Rummery, T.A., Oldfield, F., Newson, M. and Thompson, R. (1979a). Magnetic tracing of stream bedload. Geophys. J.R. astr. Soc., 57, 278-279.

Scavia, D. and Robertson, A. (1979). Editors, Perspectives on Lake Ecosystem Modeling. Ann Arbor Science, Michigan.

Schwertmann, V. and Taylor, R.M. (1976). Iron oxides. In Minerals in the Soil Environment. Am. Soc. Agron. Publication.

Scott, R. (1949). The Historical Background. In North, F.J., Campbell, B. and Scott, R., editors, Snowdonia. Collins, London.

Sears, P.B. (1956). The processes of environmental changes by man. In Thomas, W.L., editor, Man's Role in Changing the Face of the Earth. University of Chicago Press, Chicago.

Sly, P.G. (1978). Sedimentary processes in lakes. In Lerman, A., editor, Lakes, Chemistry, Geology, Physics. Springer-Verlag, New York.

Stacey, F.D. and Banerjee, S.K. (1974). The Physical Principles of Rock Magnetism. Elsevier, New York.

Stober, J.C. (1978). Palaeomagnetic secular variation studies on Holocene lake sediments. Unpublished Ph.D. thesis, University of Edinburgh.

Strahler, A.N. (1956). The nature of induced erosion and aggradation. In Thomas, W.L., editor, Man's Role in Changing the Face of the Earth. University of Chicago Press, Chicago.

Tauber, H. (1965). Differential pollen dispersion and the interpretation of pollen diagrams. Danm. Geol. Unders. II. RK 89.

Taylor, R.M. and Schwertmann, U. (1974). Maghemite in soils and its origin. I. Properties and observations on soil maghemites. Clay Minerals, 10, 289-298.

Thompson, R. (1974). Palaeomagnetism. Sci. Prog. Oxf., 61, 349-373.

Thompson, R., Battarbee, R.W., O'Sullivan, P.E. and Oldfield, F. (1975). Magnetic susceptibility of lake sediments. Limnol. Oceanogr., 20, 687-698.

Thompson, R., Bloemendal, J., Dearing, J.A., Oldfield, F., Rummery, T.A., Stober, J.C. and Turner, G.M. (1980). Environmental applications of magnetic measurements. Science (N.Y.), 207, 481-486.

Thompson, R. and Morton, D.J. (1979). Magnetic susceptibility and particle size distribution in recent sediments of the Loch Lomond drainage basin, Scotland. J. Sed. Petrol., 49, 810-812.

Thompson, R. and Waine-Hobson, T. (1979). Palaeomagnetic and stratigraphic study of the Loch Shiel marine regression and overlying gyttja. J. Geol. Soc., 136, 383-388.

Tite, M.S. and Mullins, C.E. (1971). Enhancement of the magnetic susceptibility of soils on archaeological sites. Archaeometry, 13, 209-219.

Toulmin-Smith, L. (1906). The Itinerary in Wales of John Leland in or About the Years 1536-1539. George Bell and Sons, London.

Towler, N.W. (1977). Correlation of Lake Sediments Using Palaeomagnetic Techniques. Unpublished thesis, University of Edinburgh.

Trimble, S.W. (1977). The fallacy of stream equilibrium in contemporary denudation studies. Am. J. Sci., 277, 876-887.

Turner, G.M. (1979). Geomagnetic Investigations of some recent British Lake Sediments. Unpublished Ph.D. thesis, University of Edinburgh.

Turner, G.M. and Thompson, R. (1979). Behaviour of the earth's magnetic field as recorded in the sediment of Loch Lomond. Earth and Planet. Sci. Lett., 42, 412-426.

Turner, G.M. and Thompson, R. (1981). Lake sediment record of the geomagnetic secular variation in Britain during Holocene times. Geophys. J.R. astr. Soc., 65, 703-725.

Turner, J. (1964). The anthropogenic factor in vegetational history. I. Tregaron and Whixall Mosses. New Phytol., 63, 73-90.

Tutin, W. (1969). The usefulness of pollen analyses in the interpretation of stratigraphic horizons, both Late-glacial and Postglacial. Verh. Int. Verein. Limnol., 17, 154-164.

Vadyunina, A.F. and Babanin, V.F. (1972). Magnetic susceptibility of some soils in the U.S.S.R. Soviet Soil Sci., 4, 588-599.

Vernon, R.H. (1961). Magnetic susceptibility as a measure of total iron plus manganese in some ferromagnesian silicate minerals. Am. Mineral., 46, 1141-1153.

Walker, R. (1977). The Late-Quaternary History of the Diatom Flora of High Mountain Tarns in North Wales. Unpublished Ph.D. thesis, Liverpool Polytechnical College.

Walling, D.E., Peart, M.R. and Thompson, R. (1979). Suspended sediment sources identified by magnetic measurements. Nature (Lond.), 281, 110-113.

Wasilewski, P.J. (1973). Magnetic hysteresis in natural materials. Earth and Planet. Sci. Lett., 20, 67-72.

Wedepohl, K.H. (1970). Editor, Handbook of Geochemistry. Springer-Verlag, New York.

West, R.G. (1977). Pleistocene Geology and Biology. Longman, London.

Wetzel, R.G. Limnology. W.B. Saunders Company, Philadelphia.

Wright, R.F. (1976). The impact of forest fires on the nutrient influxes to small lakes in northeastern Minnesota. Ecology, 57, 649-663.

Additional references:-

Dickson, J.H., Thompson, R., Turner, G., Baxter, M.S., Drndarsky, N.D., and Rose, J. (1978). Palynology, palaeomagnetism and radiometric dating of Flandrian marine and freshwater sediments of Loch Lomond. Nature (Lond.), 274, 548-553.

Scollar, I. (1965). A contribution to magnetic prospecting in archaeology. Archaeo-Physika, 1, 21-92. Rheinland Verlag, Bonn.